

**THE POTENTIAL OF BIOLOGICAL SLUDGE AMENDED
COMBUSTION COAL ASH RESIDUES AS ARTIFICIAL PLANT
GROWTH MEDIA: A LABORATORY COLUMN STUDY TO ASSESS
THE INFLUENCE OF WEATHERING ON ELEMENTAL RELEASE**

by

BONOKWAKHE HEZEKIEL SUKATI

**Submitted in partial fulfilment of the requirements for the degree
MSc (Agric) Soil Science
In the Faculty of Natural and Agricultural Sciences
University of Pretoria**

**Supervisor: Mr C. de Jager
Co-supervisor: Prof. J.G. Annandale**

June 2012

DECLARATION

I hereby certify that this thesis is my own original work, except where duly acknowledged. I also certify that no plagiarism was committed in writing this work and has not been previously submitted partly or fully for a degree to any other University.

Signed: _____

Bonokwakhe Hezekiel Sukati

Date: _____

DEDICATION

This work is dedicated to my family especially my parents Mrs Hleziphi N. Sukati and the late Mr Richard M. Sukati who tirelessly prayed and extended support to my success. The work is also dedicated to my children; Sakhiwo, Lindelwa, Mthobisi and Uya Sukati, to my siblings Mbongeni W., Nombulelo N., Thobile F. and Hlengiwe P. Sukati, and to my fiancée Gcinaphi Manana.

ACKNOWLEDGEMENT

First and foremost I wish to extend my sincere gratitude to Sasol Synfuels in Secunda who funded this project and to Professor J.G. Annandale and Mr P.C. De Jager who gave me the opportunity to be part of this work and provided guidance that led to my prestigious MSc (Agric) Soil Science Degree. My appreciation is also due to the laboratory manager Mr Charl D. Hertzog who allowed me to carry out all the experiments in the laboratories and tirelessly helped in the development of the columns and in the analysis of my samples. Thanks to the Departmental Administration and to my colleagues in Soil Science and other disciplines that contributed much to my study.

TABLE OF CONTENTS

DEDICATION.....	ii
ACKNOWLEDGEMENT.....	iii
TABLE OF CONTENTS.....	iv
LIST OF TABLES.....	viii
LIST OF FIGURES.....	x
ABSTRACT.....	xv
1. Introduction.....	1
1.1 Specific objectives.....	6
1.2 Thesis lay out.....	6
CHAPTER 2: LITERATURE REVIEW.....	8
2.1 Fine and gasification ashes characteristics.....	8
2.2 Sources and mobility of macronutrients (N, P, K, Ca and Mg) in coal ash.....	14
2.3 Sources and mobility of micronutrients (Zn, Cu, Mn, Mo, Fe, and B) in coal ash.....	20
2.4 Sludge characteristics.....	22
2.5 Possible benefits of amending coal ash with biological sludge.....	24
2.6 The potential of biological sludge – coal ash mixtures as artificial growth media.....	26
2.7 Unsaturated packed low tension column system.....	27
2.8 Conclusion.....	34
CHAPTER 3: MATERIALS AND METHODS.....	36
3.1 Mixture formulations.....	36
3.2 Calculations involving the packing of the columns.....	38
3.3 Packing of the columns.....	39
3.4 The development of the unsaturated column system, specifications and set up.....	39
3.5 Leaching procedure and collection of leachate.....	40
CHAPTER 4: PARTICLE SIZE DISTRIBUTION AND WATER RETENTION OF BIOLOGICAL SLUDGE – COAL ASH MIXTURES.....	43
4.1 Introduction.....	43
4.2 Materials and Methods.....	46
4.2.1 Particle size analysis.....	46

4.2.2 Assessing water retention characteristics	46
4.3 Results and Discussions	48
4.3.1 Particle size analysis of fine and gasification ash	48
4.3.2 Changes in water holding capacity of fine ash and gasification ash over time	50
4.3.3 The contribution of water locked-up in hydrated minerals to water retention	52
4.3.4 Change in water holding capacity of the mixtures over time	54
4.4 Conclusion.....	56
CHAPTER 5: NITROGEN DYNAMICS IN SLUDGE-COAL ASH MIXTURES AS	
INFLUENCED BY WEATHERING	
5.1 Introduction	58
5.2 Materials and methods	60
5.2.1 Selection of mixtures	60
5.2.2 Determination of inorganic nitrogen (NH_4^+ , NO_3^- and NO_2^-)	62
5.2.3 Determination of ammonium (NH_4^+)	63
5.2.4 Indirect determination of nitrate (NO_3^-)	63
5.2.5 Indirect determination of nitrite (NO_2^-)	64
5.3 Results and discussion	64
5.4 Conclusion.....	71
CHAPTER 6: ELEMENTAL DETERMINATION IN SLUDGE, FINE AND GASIFICATION	
ASHES, ELEMENTAL RELEASE, SALINITY AND pH OF MIXTURES	
6.1 Introduction	72
6.2 Materials and methods	74
6.2.1 Mixture analysis with X-ray Fluorescence Spectroscopy (XRF)	74
6.2.2 Mixture analysis with Inductively coupled plasma mass spectroscopy (ICP-MS).....	75
6.2.3 Phosphorus determination of mixtures	75
6.2.4 Analysis of leachate with Inductively Coupled Plasma Optical Emission Spectrometry (ICP-OES)	75
6.2.5 Salinity and pH determination	77
6.3 Results and discussion	77
6.3.1 pH changes of mixtures as influenced by leaching	77
6.3.2 Electrical Conductivity (EC) changes of mixtures as influenced by leaching	82

6.3.3 Calcium content of Sasol sludge, fine and gasification ashes measured in 2006, 2007, 2008 and 2011.....	85
6.3.4 Calcium content of mixtures.....	87
6.3.5 Calcium leaching from mixtures.....	89
6.3.6 Magnesium content of Sasol sludge, fine and gasification ashes measured in 2006, 2007, 2008 and 2011.....	94
6.3.7 Magnesium content of mixtures.....	96
6.3.8 Magnesium leaching from mixtures.....	97
6.3.9 Potassium content of Sasol sludge, fine and gasification ashes measured in 2006, 2007, 2008 and 2011.....	101
6.3.10 Potassium content in mixtures.....	102
6.3.11 Potassium leaching from mixtures.....	104
6.3.12 Sodium content of Sasol sludge, fine and gasification ashes measured in 2006, 2007, 2008 and 2011.....	106
6.3.13 Sodium content of mixtures.....	107
6.3.14 Soluble sodium released.....	109
6.3.15 Phosphorus content of Sasol sludge, fine and gasification ashes measured in 2006, 2007, 2008 and 2011.....	111
6.3.16 Phosphorus content in mixtures.....	112
6.3.17 Soluble phosphorus released.....	114
6.3.18 Micronutrients.....	116
6.3.19 Iron and manganese in mixtures.....	116
6.3.20 Soluble Fe and Mn.....	117
6.3.21 Zinc and copper.....	120
6.3.22 Solubility of zinc and copper in mixtures.....	120
6.3.23 Boron and molybdenum in mixtures.....	123
6.4 Conclusions.....	125
CHAPTER 7: ASSESSING THE CATION EXCHANGE CAPACITY PROPERTIES OF THE VARIOUS MIXTURES.....	128
7.1 Introduction.....	128
7.2 Materials and methods.....	130

7.2.1 Ammonium acetate procedure for the measurement of CEC for unleached and leached mixtures	130
7.2.2 Lithium chloride procedure for the measurement of CEC for leached mixtures.....	132
7.2.3 Potassium chloride (KCl) method for the measurement of CEC for leached mixtures	133
7.3 Results and discussion	134
7.3.1 Cation exchange capacity (CEC) determination of selected unleached and leached mixtures using ammonium acetate (NH ₄ OA _c) procedure	134
7.3.2 Statistical comparison of CEC (NH ₄ OA _c) of unleached and leached mixtures.....	137
7.3.3 Cation exchange capacity (KCl) of leached mixtures	138
7.3.4 Cation exchange capacity (LiCl) of leached mixtures	138
7.3.5 Statistical comparison CEC (NH ₄ OA _c), CEC (LiCl) and CEC (KCl) procedures.....	141
7.3.6 The contribution of sludge, fine and gasification ashes to cation exchange capacity of the mixtures	143
7.4 Conclusions	146
CHAPTER 8: GENERAL DISCUSSION	147
CHAPTER 9: CONCLUSIONS AND RECOMMENDATIONS.....	152
9.1 Conclusions	152
9.2 Recommendations.....	153
10. References	154
11 Appendices	167

LIST OF TABLES

Table 2. 1: Characterization of Sasol’s biological sludge (using digestion method), fresh gasification and fine ashes (using X-ray Fluorescence Spectroscopy (XRF)) (Sasol Synfuels, 2008)	11
Table 2. 2: Characterization of Sasol sludge (Sasol Synfuel, 2008).....	24
Table 4. 1: Mixtures with highest and lowest water holding capacities (WHC).	54
Table 5.1: Mixtures selected for inorganic nitrogen analysis	61
Table 5.2: pH values in selected mixtures for the 1 st and 10 th eluviation cycles.	66
Table 6.1: ICP – OES theoretical and actual analytical ranges for each element and wavelengths used in the analysis (Essington, 2004)	76
Table 6.2: Standards used to calibrate the ICP - OES.....	77
Table 6.3: The Ca contentfor the Sasol fine and gasification ashes as determined by X-ray Fluorescence Spectroscopy (XRF) measured in 2008 and 2011 by two laboratories.	86
Table 6.4: Comparison of total Ca content determined using acid digestion and XRF in fine and gasification ashes based on 95 % confidence intervals.....	87
Table 6.5: Measured and calculated means for Ca, in selected mixtures using microwave digestion method.....	89
Table 6.6: Magnesium content in Sasol fine and gasification ashes as determined by X-ray Fluorescence Spectroscopy (XRF) measured in 2008 and 2011.	95
Table 6.7: Comparison of total Mg content determined using acid digestion and XRF in fine and gasification ashes based on 95% confidence intervals.....	95
Table 6.8: Measured and calculated means for Mg, in selected mixtures using microwave digestion method.....	97
Table 6.9: Potassium content in Sasol fine and gasification ashes as determined by X-ray Fluorescence Spectroscopy (XRF) measured in 2008 and 2011.	102
Table 6.10: Comparison of total K content determined using acid digestion and XRF in fine and gasification ashes based on 95% confidence intervals.....	102
Table 6.11: Measured and calculated means for K, in selected mixtures using microwave digestion method.....	103
Table 6.12: Sodium content in Sasol fine and gasification ashes as determined by X-ray Fluorescence Spectroscopy (XRF) measured in 2008 and 2011.	107

Table 6.13: Comparison of total Na content determined using acid digestion and XRF in fine and gasification ashes based on 95 % confidence intervals	107
Table 6.14: Measured and calculated means for Na, in selected mixtures using microwave digestion method.....	108
Table 6.15: Phosphorus content in Sasol fine and gasification ashes as determined by X-ray Fluorescence Spectroscopy (XRF) measured in 2008 and 2011.	112
Table 6.16: Comparison of total P content determined using acid digestion and XRF in fine and gasification ashes based on 95 % confidence intervals.....	112
Table 6.17: Measured and calculated means for P, in selected mixtures using microwave digestion method.....	113
Table 6.18: Measured and calculated Cu, Mn, Zn and Fe in selected mixtures	117
Table 7.1: Cations replaced by NH ₄ in step 1 and NH ₄ replaced by K in the minus step.....	138
Table 7.2: Comparing mean CEC of the reference material (kaolinite and illite) included determined by the NH ₄ OA _c , LiCl and KCl procedures to that reported in literature.	143

LIST OF FIGURES

Fig. 3. 1: a) Sludge content in mixtures (wet mass of sludge expressed as a percentage of the total wet mass), b) gasification ash content in mixtures and c) fine ash content in mixtures	37
Fig. 3. 2: a) Side view of column base showing opening to which vacuum was connected, b) Top view of column base showing grooved ‘floor’, drainage outlet and imbedded O-ring, c) Side view of column base showing the imbedded O-ring to ensure a vacuum tight seal between column and base, d) Bottom view of column base showing drainage outlet and threaded opening to which a Schott Duran glass bottle were screwed/fitted.....	41
Fig. 3. 3: a) The transparent polyethylene column (length: 0.3 m, internal diameter: 0.105 m), b) The five layered mesh placed at the outflow boundary of the column or at the base of the column, c) The securing of the mesh by the column in the column base, d) The column assembly consisting of the transparent column, the column base and the Schott bottle.	41
Fig. 3. 4: The low tension column battery on each bench, connected to the vacuum system (blue pipe from column connected to the red main vacuum line) and collection plastic bottles.	42
Fig.4. 1: Particle size distribution of fine and gasification ash. The error bars are standard deviations. The values above the bars are the coefficient of variance (n = 30).....	50
Fig.4. 2: a) Change in gravimetric water content (kg kg ⁻¹) of fine ash from the 1 st to 10 th eluviation cycle, b) Volumetric water content (%) of fine ash from the 1 st to 10 th eluviation cycle, c) Gravimetric water content (kg kg ⁻¹) of gasification ash from 1 st to 10 th eluviation cycle, d) Volumetric water content (%) of gasification ash from the 1 st to 10 th eluviation cycle.	52
Fig.4. 3: a) Assessment of water retention in fine ash (mixture 1), b) Assessment of water retention in gasification ash (mixture 11), c) Assessment of water retention in mixture 46 with 50% fine ash and 50% sludge and d) Assessment of water retention in mixture 51 with 50% gasification ash and 50% sludge	53
Fig.4. 4: a) Gravimetric water content (kg kg ⁻¹) of the various mixtures after the 1 st eluviation cycle, b) Volumetric water content (%) of the various mixtures after the 1 st eluviation cycle, c) Gravimetric water content (kg kg ⁻¹) of the various mixtures after the 10 th eluviation cycle d) Volumetric water content (%) of the various mixtures after the 10 th eluviation cycle. The arrows indicate an increase in fine ash content.....	55
Fig.5. 1: Total inorganic N (NH ₄ ⁺ , NO ₃ ⁻ and NO ₂ ⁻) released by selected mixtures calculated for ten eluviation cycles. The arrows indicate the increasing gradient in fine ash.	65

Fig.5. 2: Inorganic N (NH_4^+ , NO_3^- and NO_2^-) released by selected mixtures calculated for eluviation cycles 1 and 10. The arrows indicate the increasing gradient in fine ash.67

Fig.5. 3: a) Log millimolar $\text{NH}_4^+:\text{NO}_3^-$ ratio based on the ammonium and nitrate released after ten eluviation cycles, b) Log millimolar $\text{NH}_4^+:\text{NO}_2^-$ ratio based on the ammonium and nitrite released after ten eluviation cycles, c) Log millimolar $\text{NO}_3^-:\text{NO}_2^-$ ratio based on the nitrate and nitrite released after ten eluviation cycles.68

Fig.5. 4: NH_4^+ , NO_3^- and NO_2^- release trends for selected eluviation cycles; 1, 5, 8 and 10 in a, b, c and d respectively (expressed as N).70

Fig.6. 1: a) The change in pH of the pore solution upon sludge addition for the first eluviation cycle, b) frequency distribution of the pore solution pH for the first eluviation cycle, c) The change in pH of the pore solution upon sludge addition for the tenth eluviation cycle, and d) frequency distribution of the pore solution pH for the tenth eluviation cycle. The SL in a and c means sludge. The blue rectangles in a and c demarcate proposed optimum pH range suitable for plant growth.81

Fig.6. 2: Salinity comparison for the first and tenth eluviation cycles. The blue rectangle in demarcates proposed optimum salinity range for plant growth.83

Fig.6. 3: a) The change in electrical conductivity of the pore solution upon sludge addition to the various treatment groups (with sludge increasing from 0 to 50%, fine ash decreasing and gasification ash increasing – illustrated in chapter 3) for the first eluviation cycle, b) frequency distribution of the pore solution electrical conductivity for the first eluviation cycle, c) The change in electrical conductivity of the pore solution upon sludge addition for the tenth eluviation cycle and d) frequency distribution of the pore solution electrical conductivity for the tenth eluviation cycle. The SL in a and c means sludge. The blue rectangles in a and c demarcate proposed optimum EC range for plant growth.84

Fig.6. 4: The variation in calcium content of Sasol sludge, fine and gasification ashes based on analyses done in 2006, 2007, 2008 and 2011 (at least 1 sample per year). The method used was acid digestion using hydrofluoric acid (HF) acid and a mixture of perchloric acid (HClO_4) and nitric acid (HNO_3) (as indicated in section 6.2.2).85

Fig.6. 5: Calculated Ca content of the mixtures based on the mean content depicted in Fig 6.3. of sludge, fine and gasification ash to total Ca content of mixtures88

Fig.6. 6: a) Cumulative amount of soluble Ca (mmol kg^{-1}) released after 10 eluviation cycles and b) Cumulative soluble Ca (%) in mixtures released after 10 eluviation cycles. The arrows in a and b indicate the direction of increasing gasification ash content of each sludge treatment group.90

Fig.6. 7: a) Log molar Ca:Mg ratio based on the cumulative calcium and magnesium released after ten eluviation cycles, b) Log molar Ca:K ratio based on the cumulative calcium and potassium released after ten eluviation cycles, c) Log molar Ca:Na ratio based on the cumulative calcium and sodium released after ten eluviation cycles, and d) Log millimolar Ca:P ratio based on the cumulative calcium and phosphorus released after ten eluviation cycles. The SL in a, b, c and d means sludge.93

Fig.6. 8: The variation in magnesium content of the Sasol sludge, fine and gasification ashes based on analysis performed in 2006, 2007, 2008 and 2011 as determined by digestion method.94

Fig.6. 9: Contribution of sludge, fine and gasification ash to Mg content of mixtures96

Fig.6. 10: a) Cumulative amount of Mg (mmol kg^{-1}) released after 10 eluviation cycles and b) Cumulative soluble Mg fraction (%) in mixtures released after 10 eluviation cycles. The arrows in a and b indicate the direction of increasing gasification ash content of each sludge treatment group.....99

Fig.6. 11: a) Log millimolar Mg:K ratio based on the cumulative magnesium and potassium released after ten eluviation cycles, b) Log millimolar Mg:Na ratio based on the cumulative magnesium and sodium released after ten eluviation cycles and c) Log millimolar Mg:P ratio based on the cumulative magnesium and phosphorus released after ten eluviation cycles.100

Fig.6. 12: Potassium content in Sasol sludge, fine and gasification ashes measured in 2006, 2007, 2008 and 2011 as determined by digestion method101

Fig.6. 13: Contribution of sludge, fine and gasification ash to total K content of mixtures.....103

Fig.6. 14: a) Cumulative amount of K (mmol kg^{-1})released after 10 eluviation cycles and b) Cumulative soluble K fraction (%) in mixtures released after 10 eluviation cycles. The arrows in a and b indicate the direction of increasing gasification ash content of each sludge treatment group.....104

Fig.6. 15: a) Log millimolar K:Na ratio based on the cumulative potassium and sodium released after ten eluviation cycles and b) Log millimolar K:P ratio based on the cumulative potassium and phosphorus released after ten eluviation cycles..... 105

Fig.6. 16: Sodium content in Sasol sludge, fine and gasification ashes measured in 2006, 2007, 2008 and 2011 as determined by digestion method..... 106

Fig.6. 17: Contribution of sludge, fine and gasification ash to total Na content of mixtures 108

Fig.6. 18: a) Cumulative amount of Na (mmol kg^{-1}) released after 10 eluviation cycles and b) Cumulative soluble Na fraction (%) in mixtures released after 10 eluviation cycles. The arrows in a and b indicate the direction of increasing gasification ash content of each sludge treatment group..... 110

Fig.6. 19: Phosphorus content in Sasol sludge, fine and gasification ashes measured in 2006, 2007, 2008 and 2011 as determined by digestion method 111

Fig.6. 20: Contribution of sludge, fine and gasification ash to total P content of mixtures 113

Fig.6. 21: a) Cumulative amount of P (mmol kg^{-1}) released after 10 eluviation cycles and b) Cumulative soluble P fraction (%) in mixtures released after 10 eluviation cycles. The arrows in a and b indicate the direction of increasing gasification ash content of each sludge treatment group..... 115

Fig.6. 22: a) Contribution of sludge, fine and gasification ash to total Fe content of mixtures, b) Cumulative amount of Fe (mmol kg^{-1}) released after 10 eluviation cycles, c) Contribution of sludge, fine and gasification ash to total Mn content of mixtures and d) Cumulative amount of Mn (mmol kg^{-1}) released after 10 eluviation cycles. The arrows in b and d indicate the direction of increasing gasification ash content of each sludge treatment group..... 119

Fig.6. 23: a) Contribution of sludge, fine and gasification ash to total Zn content of mixtures, b) Cumulative amount of Zn (mmol kg^{-1}) released after 10 eluviation cycles, c) Contribution of sludge, fine and gasification ash to total Cu content of mixtures and d) Cumulative amount of Cu released after 10 eluviation cycles. The arrows in b and d indicate the direction of increasing gasification ash content of each sludge treatment group..... 122

Fig.6. 24: a) Cumulative amount of B (mmol kg^{-1}) released after 10 eluviation cycles and b) Cumulative amount of Mo (mmol kg^{-1}) released after 10 eluviation cycles. The arrows in a and b indicate the direction of increasing gasification ash content of each sludge treatment group. ... 124

Fig.7. 1: a) Cation exchange capacity means for selected unleached mixtures determined by ammonium acetate (NH_4OA_c) procedure, b) Cation exchange capacity means for selected leached mixtures determined by NH_4OA_c procedure, c) Cation exchange capacity of leached mixtures determined by lithium chloride (LiCl) method and d) cation exchange capacity of leached mixtures determined by potassium chloride (KCl) method. Means with the same letter are not significantly different from each other and means with different letters are significantly different from each other. 140

Fig.7. 2: Comparison of the CEC of selected leached mixtures as measured by NH_4OA_c , LiCl and KCl methods..... 141

Fig.7. 3: a) Sludge and fine ash contribution to CEC for selected mixtures (1, 21, 22, 31, 39 and 46) with sludge content increasing (0 to 50%), fine ash decreasing (100 to 50%), gasification ash content 0%, b) Sludge and gasification ash contribution to CEC for selected mixtures (11, 12, 30, 38, 45 and 51) with sludge content increasing and c) fine and gasification ash contribution to CEC for selected mixtures (1, 6 and 11) without sludge. 145

ABSTRACT

Sasol biological sludge, coal fine and gasification ash were the three waste streams involved in this study. The main concern is that on their own they are not suitable as growth mediums, the ash is alkaline ($\text{pH} > 12$) with high salinity (total dissolved solids of $8000 \text{ mg } \ell^{-1}$). Fine ash is microporous (particle size diameter $< 250 \text{ } \mu\text{m}$) and forms cemented layers that can restrict root growth while, gasification ash is macroporous (most particle size diameter ranged between 1 and 75 mm) and has a low water holding capacity. Sludge is unstable and can inhibit gaseous exchange. However, these wastes potentially, have physical, biological and chemical attributes that make them suitable as hospitable growth medium. Sludge can promote micro-fauna activity and, provide plant available nitrogen (N) as well as phosphorus (P) the ash is poor in. On a short term bases and in the long term it can also contribute to cation exchange capacity (CEC). Fine ash can increase water holding capacity and gasification ash can improve gaseous exchange. It was hypothesized that if the ash was treated with sludge, pH will be reduced to between 5.5 and 8, and weathering will reduce salinity to less than 400 mSm^{-1} , increase CEC and increase plant available N and P. Therefore, the main purpose of this laboratory column study was to establish combinations of these waste streams that hold promise as plant growth media, based on various chemical and physical criteria link to hospitable plant growth media, as well as the influence of weathering on the release of essential plant nutrients. A total of 51 mixtures (each weighing 2.6 kg) were formulated based on wet mass basis and divided into 6 groups based on sludge content (0, 10, 20, 30, 40 and 50%) and packed into columns, subjected to wetting and drying for 1 year (10 wetting and drying cycles) by passing through deionized water equivalent to the pore volume and allowing the mixtures to dry in between. The leachates were analysed using Inductively Coupled Plasma Optical Emission Spectrometry (ICP-OES) and Kjeldahl procedures (for N release). Total elemental analysis was done using X-ray Fluorescence Spectroscopy (XRF) and acid digestion method. Particle size distribution was done using the sieve method. Cation exchange properties were assessed using ammonium acetate (NH_4OAc), lithium chloride (LiCl) and potassium chloride (KCl) methods. Results indicated that sludge was critical for these mixtures, at a minimal content of 10% it increased the water holding capacity of the mixtures. In the mineralization of inorganic N at a lower limit of 20% sludge enabled the production of plant available NH_4^+ and NO_3^- and less NO_2^- . Increasing sludge to 50% further reduced the production of NO_2^- in the mixtures. In terms of elemental release, mixtures without sludge were dominated

by Na and the order of abundance was as follows; Na>K>Ca>Mg>P on mmol kg^{-1} but the introduction of sludge at a lower content limit of 10% changed the abundance of the elements as follows; P>Mg>Ca>Na>K on mmol kg^{-1} . Sludge content as low as 10% reduced the pH of the mixtures to between 7.6 and 8 and EC to less than 400 mSm^{-1} . However, increasing sludge to 50% increased the leachate EC dramatically and kept the EC high (415 mSm^{-1}) till the end. Introduction of sludge at a low limit of 10 % content increased the CEC above $8 \text{ cmol}_c \text{ kg}^{-1}$. The effects of fine ash on the water holding capacity of the mixtures were seen at the 10 % level, for example, mixture 13 with 10% fine ash had 0.3 mg kg^{-1} , while mixture 12 with 0% fine ash had 0.27 mg kg^{-1} . Increasing fine ash content above 40% increased pozzalanic properties, pH (>8), EC (> 400 mSm^{-1}), Na release and reduced CEC. Gasification ash is the biggest waste stream and utilizing these wastes as growth media will mean that it realistically will always dominate these mixtures. This study showed that on its own it will be a challenging environment. However, the amendment with sludge and fine ash resulted in some chemically and physically favourable changes in these media. It can be concluded that the main objective has been achieved and bio assay evaluation of these mixtures is recommended.

Keywords: water holding capacity; nitrogen; elemental release; cation exchange capacity.

CHAPTER 1

1. Introduction

Fine and gasification ashes are byproducts of coal combustion which is a process intended to generate energy and the quantity of ash produced worldwide is estimated to exceed 6×10^8 million tons annually (Jayasinghe *et al.*, 2009). South Africa produces approximately 28 million tons of ash annually (Reynolds *et al.*, 2000) and Sasol Synfuels in Secunda consumes over 45 million tons of low grade, high ash coal (lignite and sub-bituminous coals) annually and produces 4 and 7 million tons of fine and gasification ashes respectively (Ginster & Matjie, 2005 & Mahlaba *et al.*, 2011). According to Jala and Goyal (2006) and Haynes (2009), lignites and sub-bituminous coals tend to have low sulphur (S) contents and are high in calcium (Ca) resulting in alkaline ash. Such coals may also have high moisture content and low ash fusibility (potential to slagging) (Katalambula & Gupta, 2009). Consequently, ash properties depend on the physical and chemical characteristics of the coal gasified, coal particle size and more significantly on the gasification process (Jankowski, *et al.*, 2005).

Sasol fine ash is a combination of about 83% fly ash and the remaining 17% is made up of both gasification ash and bottom ash fines with particles of less than $250 \mu\text{m}$ (Mahlaba *et al.*, 2011). The mineralogy of Sasol fine ash characterized using X-ray diffraction (XRD) technique consists of major phases such as amorphous phase (a phase with non-fixed elemental proportions and has no ordered crystalline structure), mullite ($\text{Al}_6\text{Si}_2\text{O}_{13}$) and quartz (SiO_2) and some minor and trace mineral phases. Physically, fine ash has 60% of particle sizes falling between $5 \mu\text{m}$ and $75 \mu\text{m}$ in diameter. Gasification ash is a combination of red and white fused sintered clinkers with heterogeneous texture varying from fine material to large irregularly shaped aggregates ranging from 4 to 75 mm (Matjie *et al.*, 2008). The mineralogy of gasification ash consists of major oxides like quartz (SiO_2), mullite ($\text{Al}_6\text{Si}_2\text{O}_{13}$) and anorthite ($\text{CaAl}_2\text{Si}_2\text{O}_8$) and some minor oxides (Ginster & Matjie, 2005 & Matjie *et al.*, 2008). Fly ash is generally grey in colour, abrasive, mostly alkaline, and refractory in nature and is generated from the combustion of powdered coal. This type of ash consists of fine particles resulting from fused clay minerals mainly comprising aluminium-silicate ($(\text{AlO})_2\text{SiO}_3$) that gives it pozzolanic properties (cementitious characteristics) and Sasol fly ash is dominated by 59% of silt-sized particles (Ahmaruzzaman, 2010 & Mahlaba *et al.*, 2011). Generally, finer particles of ashes are spherical in

shape and the spheres may be solid, hollow (cenospheres) or encapsulating (plerospheres) (Kopsick & Angino, 1981 & Matjie *et al.*, 2008).

Sasol ashes are alkaline with a pH greater than 12 and have a high salinity of approximately 8000 mg l⁻¹ (Mahlaba *et al.*, 2011). However, coal ash may be rich in non available plant nutrients such as boron (B), but occasionally can supply plant available potassium (K), Ca and magnesium (Mg). Alkaline ash is generally a poor source of plant available nitrogen (N) and phosphorus (P) (Jankowski *et al.*, 2006). These plant nutrients are generally released from the ash minerals by processes of weathering such as hydrolysis, carbonation, oxidation, hydration and dissolution (McConnell, 1998 & Brady & Weil, 2008). Chemical weathering over time induces transformation of the ash components converting alumino-silicate glass (mineral phases) to non-crystalline clay minerals and the formation of these secondary minerals is shown by an increase in cation exchange capacity (CEC) (Zevenbergen *et al.*, 1999). It was envisaged that the increase in CEC during weathering results from aluminium-Silicon rich phases that form during mineral transformation with increased adsorption capability (Gitari *et al.*, 2009).

Deposition and management of ash is a great challenge to energy producing plants since there is pressure on governments from the international community to reduce greenhouse gases and environmental pollution. Ash generally is used in cement and concrete manufacturing, agriculture as soil amendment and in waste stabilization, but if not used, it is generally “land filled” as part of daily management practice or is washed out with water into artificial lagoons (Jala & Goyal 2004, Haynes, 2009 & Gitari *et al.*, 2009). Sasol adopted landfilling as their major daily management practice (Mahlaba *et al.*, 2011). Landfilling degrades soil and can endanger human health and the environment through the release of toxic elements to subsurface aquifers that serve as drinking water supplies close to ash disposal sites (Wang & Wang, 1992, Asokan *et al.*, 2005 & Jankowski *et al.*, 2005).

Sludge is a redundant byproduct of industrial wastewater treatment processes (Wang, 1996) and can be derived from various processes that influence its properties (Snyman & Van der Waals, 2004). Sasol biological sludge is a byproduct of the aerobic activated biosolid treatment process and has a pH of 6.8. Generally, sludge contains mainly organic N, P and high organic matter

(OM) content that makes it a potential source of nutrients for plant growth (Snyman & Van der Waals, 2004, Snyman & Herselman, 2006). Nitrogen and P are contained in appreciable amounts while K content is generally low because most K compounds are water soluble and remain in the sewage effluent or the liquid portion during sludge dewatering (Rehcegl, 1995). Nitrogen is present in sludge mainly in the organic form and needs to be mineralized into inorganic forms (nitrate - NO_3^- , nitrite - NO_2^- and ammonium - NH_4^+). Sludge contains variable quantities of organic N and inorganic N (NO_3^- , NO_2^- and NH_4^+) (Snyman & Van der Waals, 2004).

According to Herselman *et al.* (2005) sludge disposal on land either for beneficial or non beneficial use is the most adopted strategy for sludge management. However, this management strategy increases the risk of environmental pollution. Another least adopted sludge management method is incineration which not only generates carbon dioxide (CO_2), a greenhouse gas, but also numerous flue gases and toxic residues. The ash produced during incineration is even more hazardous, as it contains high concentrations of heavy metals (Moldes *et al.*, 2007).

To minimize the transfer of toxic materials to the environment, Jala and Goyal (2004) and Haynes (2009), suggest that establishment of vegetation and the raising of forests on fly ash basins and landfill sites can stabilize the ash against wind and water erosion and reduce the leaching of metals and metalloids through water loss as evapotranspiration. However, ash and sludge on their own are not suitable as growth mediums. Ash is alkaline and can induce deficiencies of essential plant nutrients such as P and trace elements such as, iron (Fe), manganese (Mn), zinc (Zn) and copper (Cu) (Haynes, 2009). Unweathered alkaline ash can also contain high levels of soluble salts that may induce osmotic stress on plants and microorganisms, creating conditions difficult to assimilate water. This is an important parameter that can limit the suitability of any growth medium to support life if not leached (Brady & Weil, 2008, & Haynes, 2009). Furthermore, in highly alkaline conditions, the dominant inorganic N form is often ammonia (NH_3) which volatilizes, and high NH_3 concentrations have a negative effect on microbial activity (Keen & Prosser, 1987). An important nitrifying bacterium, for example, *Nitrobacter* which converts NO_2^- to NO_3^- , is inhibited by high NH_3 concentrations. *Nitrosomonas*, which convert NH_4^+ to NO_2^- are less sensitive to high pH and therefore alkaline

conditions can also lead to a build-up of NO_2^- , another biotoxic compound (Keen & Prosser, 1987).

Physically, gasification ash has a low water holding capacity and thus will not be able to provide enough water for shallow rooted plants. This is another factor that makes plant establishment difficult, limiting options for vegetative capping. Inversely, too much fine ash can restrict root growth due to the natural compaction of its particles and or formation of solid cemented layers (Haynes, 2009). Unstable sludge, on the other hand, is anaerobic, a condition that inhibits gaseous exchange.

To establish a vegetative cover under such extreme conditions, engineering experts have suggested capping the Sasol ash heaps with topsoil. The philosophy behind capping the ash dump with topsoil was to try and establish a vegetation cover consisting of shallow and deep rooted plants which will help minimize pollutant transfer to the environment and increase water transfer to the atmosphere. Furthermore, established vegetation will also stabilize the ash dump against wind and water erosion (Jala & Goyal, 2004). However, capping the ash dump will require importing a significant amount of valuable and irreplaceable topsoil as growth medium from elsewhere, there by seeking additional enriched inputs. It seems worthwhile, therefore, to investigate the feasibility of combining these waste streams as an alternative or as part of a more integrated waste disposal strategy to transform the outer layers of the ash dump into a suitable growth medium for plants. This follows the fact that these wastes potentially have chemical, physical and biological attributes that make them suitable to engineer a hospitable growth medium for plants.

Sludge can promote the establishment of micro-fauna in the ash as it contains microorganisms such as bacteria, viruses, fungi and yeasts, parasitic worms and protozoa (Snyman & Van der Waals, 2004) that the ash is poor in. There can also be an introduction of bacteria species responsible for N mineralization such as autotrophs, *Nitrosomonas* that convert NH_4^+ to NO_2^- and autotrophs, *Nitrobacter* species that convert NO_2^- to NO_3^- (Dinçer & Kargi, 2000). Sludge will also increase the content of plant available N and P in which the ash is poor in. Moreover, sludge is a source of organic material and humified or stabilized sludge can promote the

establishment of soil micro-flora and fauna, increasing water holding capacity and contribute to CEC (a function of organic matter functional groups) (Brady and Weil, 2008 & Essington, 2004). Therefore, stabilized sludge will generally increase the fertility of the artificial growth medium.

Fine ash consists of fine particles (Jala & Goyal, 2004) that can contribute to the microporosity of the medium and increase the ability to retain water. Conversely, gasification ash is macroporous (Jala & Goyal, 2004), a characteristic that can provide the necessary aeration needed for numerous microbial mediated processes, essential for a functioning soil medium, for example, nitrogen mineralization and nitrification. This characteristic can further ensure rapid infiltration and minimize run-off from the ash dump. The high hydraulic conductivity of the gasification ash will also increase capillary rise resulting in more sustainable transfer of water to the atmosphere and greater cumulative evaporation.

It has been shown that Sasol sludge amended gasification ash can support vegetation. Annandale *et al.* (2004) conducted a preliminary rehabilitation trial on the ash dump in which sludge was surface incorporated as an alternative to importing topsoil as a growth medium to establish a vegetative cap on the ash. In this trial, several perennial grasses and shrubs were screened with the primary objective of establishing which species could adapt to the substrate conditions. Of all the perennial grasses tested, *Chloris gayana* and *Cynadon dactylon* indicated the best establishment, good overall cover, dense stand and best survival. Some of the grasses and shrubs could not survive. It was therefore evident that a better understanding was needed of the chemistry and essential plant nutrient release behaviour of these waste combinations.

In this study it was hypothesised that the incorporated sludge will increase water holding capacity of the ashes, add P and N into the mixtures, increase elemental release, reduce the high pH and salinity in ash to optimum levels suitable for plant growth through dilution effects and also increase the CEC of the mixtures. It was also hypothesized that subjecting the mixtures to wetting and drying cycles (eluviation cycles) will induce weathering processes that can reduce pH, salinity, increase elemental release and increase CEC through the transformation of primary minerals to secondary minerals. The addition of fine ash was expected to increase water holding

capacity of the mixtures. The main purpose of this work was therefore to establish various biological sludge – coal ash combinations that have the potential of supporting plant growth and to assess the release of essential plant nutrients as influenced by weathering under laboratory low tension column system.

1.1 Specific objectives

- i) To establish biological sludge – coal ash combinations suitable to serve as growth media with sufficient available essential plant nutrients, also physically and biologically suitable.
- ii) To assess elemental release as influenced by weathering, physical (particle size distribution and water holding capacity) and biological (nitrogen mineralization) characteristics of the mixtures.
- iii) To assess pH and salinity dynamics in the mixtures as influenced by sludge incorporation and weathering.
- iv) To determine the cation exchange capacity of the mixtures using ammonium acetate (NH_4OAc), potassium chloride (KCl) and lithium chloride (LiCl) as influenced by sludge incorporation and weathering.

1.2 Thesis lay out

The outlay of the thesis included several chapters attempting to achieve the above objectives.

Chapter 2

This section focused on the literature study covering the physical, biological and chemical characteristics of Sasol sludge, fine and gasification ashes; the potential of the individual wastes and the biological sludge-coal ash mixtures in releasing essential plant nutrients and subsequent support of plant growth. It also covered literature on the development and advantages of unsaturated low tension columns.

Chapter 3

Generic materials and methods were covered under this section and these included the development and set up of unsaturated low tension columns, mixture formulations and the

approach followed in packing the columns, carrying out wetting and drying cycles and the collection and preparation of leachates for analysis.

Chapter 4

This section dealt with the physical characteristics of the mixtures and this included particle size distribution and water holding and release capacity of the mixtures.

Chapter 5

The focus in this section was on the biological characteristics of the mixtures. To achieve this microbial mineralized inorganic nitrogen species (NH_4^+ , NO_2^- and NO_3^-) were determined in the leachates.

Chapter 6

This section covered the chemical characteristics of the mixtures that included pH and salinity changes and the release of Ca, Mg, P, K, Na, Mn, Cu, B, Mo, Zn and Fe as influenced by weathering induced by eluviation cycles. It also incorporated work done in 2006, 2007, 2008 and 2011 that covered the characterization of Sasol sludge, fine and gasification ashes.

Chapter 7

This chapter covered the determination of cation exchange capacity (CEC) for fresh mixtures using ammonium acetate (NH_4OAc) method, and the determination of CEC for leached mixtures using NH_4OAc , lithium chloride (LiCl) and potassium chloride (KCl) methods. Basically this section compares the efficiency of these methods in determining CEC in biological sludge-coal ash mixtures and covers the effect of sludge and weathering in the development of negative charges in the mixtures.

Chapter 8

General discussion

Chapter 9

Conclusions and Recommendations of the study.

CHAPTER 2: LITERATURE REVIEW

2.1 Fine and gasification ashes characteristics

Fine and gasification ashes are inevitable co-products of coal gasification process employed by Sasol Synfuels in Secunda to produce synthesis gases (Ginster & Matjie, 2005). Seven million tons of gasification ash is produced annually from the combustion of low grade coal (lignite and sub-bituminous coals) that has low sulphur (S) content and high in calcium (Ca) resulting in basic ash (Ginster & Matjie, 2005, Jala & Goyal, 2006 & Haynes, 2009). The fine ash is a combination of about 83% fly ash and the remaining 17% is made up of both gasification ash and bottom ash fines with particles of less than 250 μm (Mahlaba *et al.*, 2011). Gasification ash is a combination of red and white fused sintered clinkers with heterogenous texture varying from fine material to large irregularly shaped aggregates (Matjie *et al.*, 2008). Fly ash (generally grey in color, abrasive, mostly alkaline, and refractory in nature) is generated from the combustion of powdered coal and has fine particles resulting from fused clay minerals mainly comprising aluminium silicate ($\text{AlO})_2\text{SiO}_3$) giving it the pozzolanic (cementitious characteristics) properties (Ahmaruzzaman, 2010). Sasol fly ash is dominated by 59% of silt-sized particles (Mahlaba *et al.*, 2011).

Coal ash properties generally depend on the physical and chemical characteristics of the coal, the coal particle size distribution and more significantly on the combustion process (Jankowski, *et al.*, 2005). For example, the Ca to S molar ratio of over 2.5 in the feedstock results in the ashes containing not only calcium sulphate (CaSO_4) but also calcium oxide (CaO) (Anthony *et al.*, 2003). The presence of significant amounts of CaO and oxides of iron (Fe), and magnesium (Mg) make the ash basic (Tsai, 1982). The mineralogy of weathered Sasol fine ash was characterized by Mahlaba *et al.* (2011) using X-ray diffraction (XRD) technique and found that it contained major phases; amorphous phase (a phase with non fixed elemental proportions and has no ordered crystalline structure), mullite ($\text{Al}_6\text{Si}_2\text{O}_{13}$) and quartz (SiO_2), minor phases; calcite (CaO_3), magnetite (FeFe_2O_4), ettringite ($\text{Ca}_6\text{Al}_2(\text{SO}_4)_3(\text{OH})_{12}\cdot 26\text{H}_2\text{O}$) and sillimanite (Al_2SiO_5), trace mineral phases; pyrrhotite (Fe_9S_{10}), and analcime ($\text{NaAlSi}_2\text{O}_6\cdot\text{H}_2\text{O}$), periclase (MgO) and hematite (Fe_2O_3). Sasol fresh gasification ash contains of major oxides; quartz (SiO_2), mullite ($\text{Al}_6\text{Si}_2\text{O}_{13}$) and anorthite ($\text{CaAl}_2\text{Si}_2\text{O}_8$); minor oxides; diopside ($\text{CaMgSi}_2\text{O}_6$), hematite (Fe_2O_3), cristobalite (SiO_2) and anhydrite (CaSO_4) (Ginster & Matjie, 2005 & Matjie *et al.*, 2008).

Sasol fine ash contains 60% of the amorphous phase (Mahlaba *et al.*, 2011) that represents the pozzolanic nature of the ash. A pozzolan can be described as a siliceous - aluminous material that is formed, when calcium hydroxide ($\text{Ca}(\text{OH})_2$) chemically reacts with silicic acid (H_4SiO_4 , or $\text{Si}(\text{OH})_4$). The resultant products formed include calcium silicate hydrate ($\text{Ca}_9\text{Si}_6\text{O}_{18}(\text{OH})_6 \cdot 8(\text{H}_2\text{O})$) and Strätlingite ($\text{Ca}_2\text{Al}_2\text{SiO}_2(\text{OH})_{10} \cdot 3\text{H}_2\text{O}$) (Matschei *et al.*, 2007) depending on the presence of Ca, Al and Si in the ash. These pozzolans have a cementitious characteristic that they acquire after addition of lime during the combustion process. Basically the Ca, aluminium (Al) and silicon (Si) in ash react with the free lime in the presence of water to form these cementitious materials (Haynes, 2009). The pozzolans in the ash are important as adsorption sites for pollutants such as chloride and can possibly increase water holding capacity (Mahlaba *et al.*, 2011).

Physically, gasification ash is the coarse grained material that consists of agglomerated dark grey granular particles with a very porous surface texture (Kopsick & Angino, 1981, Jala & Goyal, 2004 & Cheng, 2005). Sasol gasification ash has fine to large irregularly shaped aggregates of sizes ranging from 4 to 75 μm (Matjie *et al.*, 2008). In characterizing Sasol fine ash Mahlaba *et al.* (2011) found that particles falling between 5 μm and 75 μm constituted 60%. This percentage was greater than particles that fell between 1 – 5 μm (16%) and between 75 – 425 μm (30%). Generally, finer particles of ashes are spherical in shape showing a complete melting of silicates which occurs during combustion at temperatures above 1350 °C and pressures greater than 2000 kPa (Matjie *et al.*, 2008). The spheres of both ashes may be solid, hollow (cenospheres) or encapsulating (plerospheres) (Kopsick & Angino, 1981). Micrographic evidence indicated that most of the particles in fine ash occur as solid spheres of amorphous glass that forms during cooling of the melt phase (Tishmack & Burns, 2004). In addition, only a few hollow spheres and some spheres packed with other numerous small spheres or crystals of minerals, may be present (Trivedi & Sud, 2002). The crystals of minerals formed are a result of cooling of the minerals and non-mineral inorganic elements in the coal mineral matter that melt and form liquid phases during the gasification process (Matjie *et al.*, 2008). Fine ash has a low particle density, a high surface area and light grey particles (Asokan *et al.*, 2005 & Jala & Goyal, 2006).

Coal ash is generally rich in elements such as Ca, Mg, sodium (Na), potassium (K), phosphorus (P), boron (B) and minor elements (Jankowski *et al.*, 2005). However, sulphate (SO_4), (K), and Ca total content generally increase with decrease in particle sizes (Bendz *et al.*, 2007). Sasol fresh fly and fine ashes together with weathered fine ash contain elements which are classified as major ($> 1\%$) in coal ash and include; Si, Al, Ca, Fe, Mg and Na, also contains minor (0.1 – 1%) elements that include; K, S and P, characterized by (Mahlaba *et al.*, 2011) using X-ray Fluorescence (XRF). Calcium is generally a dominant cation in fine ash followed by Mg, Na and K (Maiti *et al.*, 1990). However, these claims differed slightly when compared to cation dominance in Sasol fine and gasification ashes; the Ca was the most dominant cation followed by Mg, K and Na (Table 2.1). A major portion of K is localized in the interior glassy matrix (principally an alumino-silicate glass containing elements such as; Ca, Fe, Mg and P and is derived from crystallized minerals) the external glass is enriched with Mg (Matjie, *et al.*, 2005 & Jala & Goyal, 2006). A number of metals and metalloids may also be present as carbonates, oxides, hydroxides, and sulphates, including; cadmium (Cd), arsenic (As), selenium (Se), lead (Pb), nickel (Ni), copper (Cu), chromium (Cr), cobalt (Co), molybdenum (Mo), beryllium (Be) in lower but still significant concentrations (Jankowski *et al.*, 2005).

As discussed earlier, coal ash can be acidic or alkaline depending on the S content of the feed stock used for combustion (Carlson & Adriano, 1993). Sulphur in coal exists as pyritic sulphur (FeS_2), sulphate sulphur (SO_4), organic sulphur, and as elemental sulphur (S). During combustion S is oxidized to SO_2 , SO_3 then eventually to sulphuric acid (H_2SO_4) when it reacts with water molecules that make the ash acidic (Chatterjee, 1940 & Ryan, 1997). According to Jala & Goyal (2006), anthracite coals (highest ranked coal that has the highest heating value of 13600 British thermal unit per pound of coal² and contains 94% carbon) are generally high in S and produce acidic ash while lignite coals (lowest ranked coal that has a heating value of 7000 British thermal unit per pound of coal² and contains 72% carbon) tend to be lower in S but higher in Ca content and produce alkaline ash. Some of the alkaline ashes can have pH values exceeding 12 (Edmunds, 2002 & Haynes, 2009). As indicated earlier on that the feed stock for Sasol is low grade coal (lignite and sub-bituminous coals) that has low S content and high in Ca increase the pH for both fine and gasification ashes to above 12 (table 2.1). The pH for fine ash is

mostly contributed by fly ash that forms 83% of fine ash and has a pH value of 12.5 (Mahlaba *et al.*, 2011). The presence and high concentrations of soluble salts (Na^+ , K^+ , Mg^{2+} Ca^{2+} and Cl^-) in alkaline and unweathered ash give the ash a saline status and a high electrical conductivity (EC) of 1300 mSm^{-1} (Haynes, 2009).

Table 2.1: Characterization of Sasol's biological sludge (using digestion method), fresh gasification and fine ashes (using X-ray Fluorescence Spectroscopy (XRF)) (Sasol Synfuels, 2008)

Parameter	Gasification Ash	Fine ash	Units
pH	10.80	> 12	Unit less
Volatile Matter	4.6	16.9	%
Total N	< 0.04	0.04	%
Total C	5.7	2.67	%
C/N Ratio	N was below detection	66.75	Unit less
Ca	5.75	5.07	%
Mg	0.973	0.954	%
P	0.251	0.229	%
K	0.904	0.230	%
Na	0.383	0.143	%
Fe	1.93	0.56	%
Cu	246	17.4	mg kg^{-1}
Mn	200	316	mg kg^{-1}
Zn	220	20	mg kg^{-1}
Al	Below detection	2.029	%
S	Below detection	0.123	%

The leaching of these chemical constituents from the ash depends on several factors such as the nature of the mineral phases present, patterns and speciation of the chemical constituents existing in the ash and elements combined with the glass phases are more resistant to leachate solutions. The presence of a non porous continuous outer surface and a dense particle interior (in fly and fine ash) restricts metal leachability from residues. Other physicochemical factors that also influence leaching include; the type of the leaching medium (considering the particle size distribution), pH, the complexing agents (functional groups) present in the solid sample and various reaction kinetics (Van der Sloot *et al.*, 1981, Anthony *et al.*, 2003 & Saikia, 2006).

Kopsik & Angino (1981), conducted a laboratory based column study on the leaching of Ca, Mg, Na, K, Fe, Mn, Zn and Cu from six fly ash samples (collected from six different places) and

three bottom ash samples (collected from three different places) separately using distilled water and to assess pH change. Column specifications used; 1.0 m in length and 0.05 m internal diameter. Fly ashes had finer sized particles ranging from 0.5 to 100 μm , while bottom ashes were coarse grained with particle sizes above 100 μm . The samples were packed to a height of 0.46 m. Distilled water was passed from the bottom to prevent preferential flow and the columns were kept saturated between leachings. Three leaching patterns were observed in their work. The most prevalent trend was characterized by a large initial release of all elements except for Ca in both fly and bottom ash samples and leveling off of concentrations later in the leaching process. The next trend observed was that there was a constant release pattern for Ca in all ashes and subsequent leaching did not lower its concentration. This was explained by the presence of soluble Ca-sulfates and oxide in the ash that represented a constant source of Ca for release.

The final trend involved a delayed release curve (in fly ash) in which a short period of time elapsed before the maximum concentration in the leachate was observed. Their explanation was that the leaching behavior was related to the morphology of the fly ash. The delay in elemental release was because of the large total surface (due to small particle size diameter) available for the reaction with the leaching solution. Because of the aluminosilicate material in fly ash the leaching water initiated pozzolanic reactions that developed an impermeable layer delaying leaching of the elements more especially iron (Fe), manganese (Mn), zinc (Zn) and copper (Cu). Iron concentration was the lowest in the leachates of all samples and the reason given was that it occurred in the matrix or as extraneous sulphide material that is not susceptible to leaching. In the beginning of the experiment one bottom ash and two fly ashes were acidic (pH 3-5); four fly ashes and two bottom ashes were alkaline (pH 9.1-11.8). The pH remained approximately the same after the study for most of the samples. This period (two weeks) was not enough to realize significant changes in pH.

Clearly coal ash can serve as a source of plant available Ca and Mg but is a poor source of N or plant available P and can only occasionally supply plant available K (Jankowski *et al.*, 2006). Some studies show that only 1-3% fine ash material is soluble in water and if the water extracts are analysed they indicate Ca and Na as the principal cations extracted. However, the concentration of ions in leachates is controlled by the solubility of particular minerals present in

the ash (Iyer, 2002). The controlling minerals include CaCO_3 , dolomite ($\text{CaMg}(\text{CO}_3)_2$) and MgO amongst others (Jankowski *et al.*, 2006). The susceptibility of these minerals to hydrolysis depends on the surface area of the ash, reaction time and water/solid ratio. However, pH still remains the major factor controlling the extractability of a number of elements including essential plant nutrients (Iyer, 2002).

Weathering processes are the only factors that influence elemental leaching and the formation of secondary minerals and subsequent release of elements in ash. Processes involved in the weathering include; hydrolysis, carbonation, oxidation, hydration and dissolution (McConnell, 1998 & Brady & Weil, 2008). Basically hydrolysis in this context refers to the ionization of carbonic acid into hydrogen (H^+) and bicarbonate (HCO_3^-). The free H^+ replaces other ions in a mineral's atomic structure altering its chemical composition into a weaker secondary mineral. The oxidation process involves the reaction of oxygen (O_2) with iron (Fe) in a mineral to form an iron oxide mineral, for example, hematite may be formed and this mineral is insoluble (McConnell, 1998). The hydration process involves the chemical union of a mineral with one or more water molecules (Brady and Weil, 2008).

McConnell (1998) and Brady and Weil (2008) describe dissolution as a process by which a gas, solid or another liquid dissolve in a solvent. In the case of carbonation process, CO_2 diffuses into moist ash and reacts with water (H_2O) producing a carbonic acid (H_2CO_3) which eventually dissolves minerals during weathering. Dissolution rates differ from mineral to mineral, hence the rates decrease in this order; Ca-plagioclase > Na-Plagioclase > K-feldspar > quartz (Kump *et al.*, 2000). In ash, chemical weathering over time effects an alteration of the ash components and the aluminosilicate glass property to non-crystalline clay minerals. The formation of the clay mineral is generally indicated by an increase in CEC (Zevenbergen *et al.*, 1999). Gitari *et al.*, (2009) suggest that the increase in CEC is attributable to the Al-Si rich phases that form during mineral transformation with increased adsorption capability.

The rate of weathering processes depend on mineralogy of the ash components exposed, the reactive surface area of these minerals, the supply of water, its residence time in the ash and initial pH, the abundance of organic acids, and the temperature of ash solutions (Kump *et al.*,

2000). Most of the elements are released after long equilibration times when the alkalinity of the ash is significantly depleted and pH of the leachate approaches circum-neutral or acidic levels (Gitari *et al.*, 2009). The reduction of pH is the result of carbonation.

Management of ash is a great challenge to the energy producing plants since there is pressure on governments to reduce green house gases and environmental pollution. Ash generally used in cement and concrete manufacturing, agriculture as soil amendment and in waste stabilization, but if not used, it is generally “land filled” as part of daily management practice or is washed out with water into artificial lagoons (Jala & Goyal 2004, Haynes, 2009 & Gitari *et al.*, 2009). Sasol adopted landfilling as their daily management practice.

The contamination of the environment could be through the release of toxic constituents to subsurface aquifers that serve as drinking water supplies nearby the disposal area (Wang & Wang, 1992, Asokan *et al.*, 2005 & Jankowski *et al.*, 2005). As remediation strategy to reduce environmental contamination Jala and Goyal (2004) and Haynes (2009), suggested that establishment of vegetation and the raising of forests on ash basins and landfill site can serve a variety of functions like stabilizing the ash against wind and water erosion and reduction of the leaching of the metals and metalloids through water loss as evapotranspiration.

2.2 Sources and mobility of macronutrients (N, P, K, Ca and Mg) in coal ash

Potassium is localized in the interior glassy matrix in ash (Jala & Goyal, 2006). Generally, K can exist as; water – soluble, exchangeable, fixed and structural forms. Hence the order of K forms availability to plants is as follows: water – soluble > exchangeable > non-exchangeable > mineral K. The availability of any of these K forms to plants is related to the structural and surface chemistry of the minerals (Huang *et al.*, 2005 & Huo-Yan *et al.*, 2010). The water-soluble K is the K^+ in solution immediately available to plants and potentially subject to leaching. The balance between water-soluble K and exchangeable K depends on factors such as pH, CEC and clay mineralogy and could be influenced by the alteration of ions in soil solution and the total concentration of soluble anions (Huo-Yan *et al.*, 2010). Exchangeable K is the portion of the K that is electrostatically bound / adsorbed as an outer-sphere complex to the surfaces of minerals and organic matter. Potassium in this form is readily exchanged with other cations. The non-

exchangeable K is slowly available and does not only become adsorbed but fits in between layers of swelling minerals and become an integral part of the crystal, while mineral K is relatively unavailable and is in the crystal structure of the minerals (Huang *et al.*, 2005 & Brady & Weil, 2008).

Mineral dissolution, precipitation, sorption and desorption of chemical species are responsible for the release and/or sequestration of essential elements such as K (Brown *et al.*, 1999). Slow dissolution of minerals in ash is a dominating mechanism for the non-exchangeable and mineral K release. The release may also proceed via selective exchange of interlayer K. Other factors that influence K release include particle size and chemical composition. For example, minerals with finest particles may undergo 'layer weathering' implying a rapid initial release which results in mixed-layer clays that strongly retain the remaining K (Simonsson *et al.*, 2009). Larger particles release K through 'edge weathering' (Murashkina *et al.*, 2007). Redox processes and formation of hydroxyaluminium interlayers also affect K release. The reduction of structural Fe^{3+} to Fe^{2+} promotes fixation of interlayer cations like K (Simonsson *et al.*, 2009). An increase in pH as well may enhance the fixation of K probably as an indirect result of a reduction in hydroxyaluminium interlayering of minerals. However, K release or leachability from the interior glassy matrix in ash may be observed at pH 6 to above 10 (Jala & Goyal, 2006 & Simonsson *et al.*, 2009).

Alternate wetting and drying of these minerals may aid in slow release of fixed potassium (Sharma *et al.*, 2010). This is made possible by the chemical weathering processes that are initiated by the introduction of water. Water also leaches out the soluble K in solution. The dissolution of calcite and gypsum in ash increases the concentration of Ca^{2+} and Mg^{2+} which further increase K desorption by replacing it from the exchange site (Kolahchi & Jalali, 2007). The K in the inter layers can be exchanged by Ca^{2+} and H^+ enhancing its release (Rahmatullah & Mengel *et al.*, 2000).

Phosphorus fractions include non-occluded inorganic phosphate (phosphate in solution, phosphate adsorbed to mineral surfaces and some phosphate in minerals) and occluded phosphate (Phosphate fractions held by Fe, Al and Ca) (Mengel *et al.*, 2001). Phosphorus release is dependent on pH which is a function of Ca compounds (carbonates and phosphates) in alkaline

conditions like in ash. The weathering degree of occluded P in Ca compounds is high (Peltovuori *et al.*, 2002). The solubility of P may also be controlled by chemisorption (chemical bonding to surface) of P on calcite (CaCO_3). A surface complex of calcium carbonate P with a well defined chemical composition may form on the calcite (Pizzeghello *et al.*, 2011). An increase in pH desorbs the P from the Ca-P compounds by increasing competition between hydroxyl ions and the adsorbed P (Jin *et al.*, 2006). The depletion of non-occluded P through leaching creates a gradient that accelerates P release from the exchange site and from the Ca-P compounds. In this study it is also expected that as weathering progresses P will increasingly be associated with Ca.

The initial P release in ash is generally rapid until equilibrium is reached. Based on modelling, the fast, intermediate and slow P release is attributed to; the dissolution of poorly crystalline metastable calcium phosphates converting to hydroxyapatite, desorption of adsorbed P from carbonate surfaces and dissolution of calcium hydroxyapatite respectively. A combination of desorption and diffusion-dissolution reactions control the initial fast and final slow release of P (Shuriatmadari *et al.*, 2006). The P forms released include species such as HPO_4^{2-} and H_2PO_4^- with HPO_4^{2-} dominating under alkaline conditions (Brady and Weil, 2008).

Calcium occurs in primary minerals such as Ca phosphates and Ca carbonates (present as calcite or dolomite) in alkaline conditions (Mengel *et al.*, 2001). In Sasol ashes Ca is contained in CaCO_3 , $\text{Ca}_6\text{Al}_2(\text{SO}_4)_3(\text{OH})_{12} \cdot 26\text{H}_2\text{O}$ and in lime (CaO) (Mahlaba *et al.*, 2011). Calcite in ash also remains as the main source of Ca (Kolahchi & Jalali, 2007). This cation (Ca^{2+}) generally competes strongly with metals for adsorption sites on the exchange complex. The adsorption of Ni, Cd, Pb and Zn that are also present in ash is reduced by the presence of Ca (Wang, 1997). The retention of calcium on the exchange site is determined by factors such as; valence, hydration size and/or the relative energies of hydration of various cations and clay mineralogy (Agbenin, 2006).

The release of Ca cations from the minerals is initiated by hydrogen ions (H^+) and also chelating agents causing dissolution of the minerals. The rate of Ca leaching increases with an increase in the addition of water and with the content of Ca bearing minerals. The diffusion of CO_2 into moist ash causes the carbonation and the transformation of Ca to CaCO_3 which in turn dissolves to

form aqueous forms of $\text{Ca}(\text{HCO}_3)_2$ which is more water soluble and this is an important means by which Ca leaching takes place.

Magnesium (Mg) in ash is localized in the external glassy matrix (Jala & Goyal, 2006) and is present in the divalent, Mg^{2+} , form in nature. Sasol ash contains MgO as the main source of Mg (Mahlaba *et al.*, 2011). However, Kolahchi and Jalali (2007) claimed that gypsum ($\text{CaSO}_4 \cdot 2(\text{H}_2\text{O})$) in ash remains the main source of Mg in ash. There are generally two pools of Mg; non exchangeable (Mg located in minerals), exchangeable (Mg associated with cation exchange sites on clay surfaces) and soluble Mg (Brady & Weil, 2008 & Mikkelsen, 2010).

The release of non exchangeable Mg is gradual from the minerals and is through the processes of weathering. But Mg naturally adsorbed on the exchange sites is generally replaced by cations present in the soil solution such as K. In this case 2 K^+ ions are required to replace 1 Mg^{2+} ion which then becomes soluble. The behavior of Mg is thus similar to that of Ca ions in the exchange site, but the adsorption of Ca is much stronger than the adsorption of Mg. This is due to the fact that Mg has a much larger hydrated radius than Ca cations (Mikkelsen, 2010).

Sodium silicate and halite (NaCl) are sources of Na in ash. Other Na sources may include Trona ($\text{Na}_2\text{CO}_3 \cdot \text{NaHCO}_3 \cdot 2\text{H}_2\text{O}$), Nahcolite (NaHCO_3) and Soda ($\text{Na}_2\text{CO}_3 \cdot 10\text{H}_2\text{O}$) that generally occur in very dry and alkaline soil and soda pans (Dijkistra *et al.*, 2006). In Sasol ashes Na is contained in $\text{NaAlSi}_2\text{O}_6 \cdot \text{H}_2\text{O}$ (Mahlaba *et al.*, 2011). Generally Na^+ together with other cations (Ca^{2+} , Mg^{2+} , and K^+) are important in defining the status of salt affected soil media as saline, sodic and sodic-saline. Brady and weil (2008) defined saline soils as containing sufficient salinity to give effective electrical conductivity (EC_e) values greater than 4.0 mS/m but have an exchangeable sodium percentage (ESP) less than 15 or sodium adsorption ratio (SAR) of less than 13. The pH of saline soils is below 8.5. While sodic soils have low soluble salts (EC_e less than 4.0 mS/m) but with ESP and SAR values above 15 and 13 respectively. The pH of such soil media exceeds 8.5. Saline-sodic soils on the other hand have EC_e greater than 4.0 mS/m and ESP greater than 15 or SAR greater than 13. Alkaline coal ash is not an exception to saline-sodic conditions since it has a pH of greater than 12 and an EC_e of more than 4.0 mS/m (Haynes, 2009). Based on sodium

effect on the status of alkaline soil media it is important to understand its sorption and desorption processes that influence the status of ash.

Sodium competes with other exchangeable cations (Ca^{2+} , Mg^{2+} , and K^+) for the adsorption site on clay minerals. A closer competitor seems to be Ca^{2+} . The adsorption selectivity of either Na^+ or Ca^{2+} depends on both ionic strength and clay mineralogy. Both the latter and the former adsorption parameters effect changes to the electrical potential of the diffuse double layer (DDL) which further influences the selectivity. A decrease in electric potential increases preference for Na^+ while an increase in electric potential increases preference for Ca^+ . The affinity of the external surfaces of the clay minerals for Ca^+ increases with an increase in solution ionic strength. As ESP decreases (exchangeable Ca^{2+} increases) preference for Na^+ increases due to a decrease in the electric potential (Kopittke *et al.*, 2006). Calcium ions have a larger interaction with mineral surfaces than Na^+ due to the fact that Ca^{2+} forms monodentate inner sphere complex. Sodium ions have a weak interaction with the mineral surfaces forming outer sphere complexes (Rahnemaie *et al.*, 2006). Therefore, the removal of excess Na^+ is effected by the introduction of Ca^{2+} . A significant supply of soluble sources of Ca^{2+} in the solution helps in the dissolution rate of the mineral and in replacing the Na^+ from the exchange site. This replaced Na^+ becomes available for plant uptake or leached out (Qadir *et al.*, 2005). The dissolution of soluble salts as well such as halite release Na. However, the release is relatively slow as a result of kinetically controlled dissolution of less soluble mineral phases (Dijkstra *et al.*, 2006).

Nitrogen amongst macronutrients is the most limiting nutrient to plant growth (Yuan *et al.*, 2008) and is contained by amino acids, for example, lysine and alanine which are the building blocks of proteins contained in organic matter (OM). Amino acids are the major sources of organic N and precursor of ammonium (NH_4^+) production (Pietri & Brookes, 2008). Organic matter largely of biological origin is present in Sasol ash in relatively low levels (4.6 – 16.9%) as a source of organic N (Sasol Synfuels, 2008).

Generally, during N mineralization process, microorganisms attack humic compounds and in the process amino compounds (R-NH_2) are formed that are further hydrolyzed producing N as NH_4^+ (Brady and Weil, 2008). Microbial mineralization of NH_4^+ from soil organic matter forms the

principal source of plant available N. The processes of ammonification (microbial transformation of organic N to NH_4^+) and nitrification (the oxidation of NH_4^+ to nitrate (NO_3^-)) make the inorganic N species available to plants and microbes and further make N susceptible to leaching, volatilization and denitrification losses (Vernimmen *et al.*, 2007). Understanding the individual processes helps in conceptualizing the N speciation. Nitrification is an aerobic and autotrophic process that converts NH_4^+ to nitrite (NO_2^-) by autotrophs, *Nitrosomonas* bacteria species as the first step and then the NO_2^- is converted to NO_3^- by autotrophs, *Nitrobacter* species as the second step (Dinçer & Kargi, 2000). Nitrification can also be reversed by anaerobic bacteria in a dissimilatory nitrate reduction to ammonium (DNRA), reducing NO_3^- to NO_2^- and then to NH_4^+ . Mineralization as well can be reversed by the immobilization (at high carbon/nitrogen (C/N) ratio) process converting NO_3^- and NH_4^+ into organic forms (Brady & Weil, 2008). Denitrification process on the other hand is an anoxic, heterotrophic process that converts NO_3^- to nitrogen gas (N_2O , NO and N_2) by nitrifying organisms (Dinçer & Kargi, 2000). Another contributing process to N loss is volatilization which occurs mainly at high pH (alkaline conditions) where NH_4^+ is converted to ammonia (NH_3) N gas (Brady & Weil, 2008).

The mineralization process of N depends on several factors such as; pH, temperature, aeration, soil type, moisture, type of organic matter, and the supply of essential nutrients like P (Serna & Pomares, 1992 & Vernimmen *et al.*, 2007). However, the main focus is on pH which is the master variable affecting most N speciation in soil (Mørkved *et al.*, 2007), temperature and aeration.

Generally, the optimum pH for nitrification ranges between 8 and 9 and some researchers have reported that at pH between 5 and 5.5 nitrification ceases. It has also been reported that the optimum pH for *Nitrosomonas* is 8.5 to 8.8 and that for *Nitrobacter* is 8.3 to 9.3. In contrast some studies have indicated that the optimum pH for *Nitrobacter* is 7.7. The activities of *Nitrosomonas* cease at pH 9.6 (Shammas, 1986). Pietri and Brookes (2008) reported that the optimum pH for ammonification ranges from 6.0 to 8.0 and for nitrification ranges from 7.5 to 8.0. Mørkved *et al.*, (2007) reported that nitrification is generally detected in soils with pH greater or equal to 4. In terms of pH it is clear that ammonification dominates at higher pH values than nitrification. However, denitrification (N_2O emission) occurs mainly under anaerobic and

slightly acidic conditions. DinÇer & Kargi, (2000) reported that denitrifying organisms can tolerate pH values between 6 and 9 while an optimum pH ranges between 7 and 8.

From this discussion it can be deduced that a reduction in pH and anaerobic conditions lead to N losses through denitrification as N_2O , NO and N_2 . An increase in aeration combined with reduced pH produces NO_3^- ions than NH_4^+ ions. The former N ions are susceptible to leaching. Higher pH values at the same time increase N losses through volatilization as NH_3 . In contrast to N losses, NH_4^+ ions are further adsorbed to negatively charged clay minerals as exchangeable forms or sometimes entrapped in the interlayers of clay minerals as nonexchangeable (Brady & Weil, 2008).

According to Shammas (1986) the nitrification rate is a function of temperature within the range of 5 to 35° C while the maximum rate occurring at 30 °C. Other researchers have reported 26°C and some reported 27°C as the optimum temperature. At temperatures below 15° C nitrification drops sharply and is reduced by 50% at 12 °C. The formation of both NO_2^- and NO_3^- is strongly inhibited at temperatures of 10°C or less. At low temperatures biostatic effect affects the activities of nitrifiers (Sierra, 2002). It is clear that temperatures between 26 to 30 °C can maximize nitrification increasing N availability to plants.

2.3 Sources and mobility of micronutrients (Zn, Cu, Mn, Mo, Fe, and B) in coal ash

Gupta *et al.* (2008) described micronutrients as trace elements or trace minerals that are required by plants in extremely small quantities and they include; Zn, Cu, Mn, Mo, Fe, Cl, and B (Fageria *et al.* 2002 & Brady & Weil, 2008). Some minerals contain micronutrients which define their amounts and distribution. Boron in ash occurs in borax, Mg hydroxides, Ca carbonates. Organic matter also adsorbs significant amounts of B (Rahnemaie *et al.*, 2006). Copper occurs in carbonates under alkaline conditions. Iron is contained in ferromagnesium silicates and precipitates as Fe oxides or hydroxides during weathering. In Sasol ash Fe occurs in $FeFe_2O_4$, Fe_2O_3 and in Fe_9S_{10} (Mahlaba *et al.*, 2011). Molybdenum is a constituent of oxides, molybdates and sulfides and has a similar chemistry as P, thus it can associate with Ca. Manganese occurs in carbonates (rhodochrosite - $MnCO_3$), silicates (rhodanate - $NaSCN$), simple oxides (manganite - $MnO(OH)$) and complex oxides (braunite - $Mn^{2+}Mn^{3+}_6[O_8|SiO_4]$). Zinc as well is a constituent of

carbonates (smithsonite - ZnCO_3), sulfides (sphalerite-(Zn,Fe)S) and silicates (hemimorphite - $\text{Zn}_4\text{Si}_2\text{O}_7(\text{OH})_2 \cdot (\text{H}_2\text{O})$) (Fageria *et al.* 2002).

The release of micronutrients is controlled by sorption-desorption processes which further depend on several factors such as; pH, redox potential, nature of the mineral, organic matter, CaCO_3 , ionic strength, simultaneous presence of competing metals, soil temperature and moisture content (White & Zasoski, 1999, Fageria *et al.* 2002, Wei *et al.* 2006, Singh *et al.* 2006, Jalali & Moharrami, 2007). Boron availability is highest at pH 5.5 – 7.5 and adsorption increases above and below this range on clay and Al and Fe hydroxyl surfaces. Calcium carbonate also adsorbs B at higher pH levels. Copper adsorption increases as pH increases from 4 – 7, however, pH levels above 6 induce hydrolysis of hydrated Cu which then increases its adsorption to clay minerals and organic matter (Fageria *et al.* 2002). Copper precipitates as carbonate of hydroxides (Malachite – $\text{Cu}_2\text{CO}_3(\text{OH})_2$ and Azurite - $\text{Cu}_3(\text{CO}_3)_2(\text{OH})_2$) at higher pH and forms strong bond with soil organic matter (Wei *et al.*, 2006). Iron solubility decreases as the pH increases from 4 – 9. As pH increases to above 5, Fe^0 (metallic) oxidizes to Fe^{2+} (ferrous) and Fe^{2+} oxidizes to Fe^{3+} (ferric). The ferric iron is reduced to ferrous which becomes readily available in acidic conditions and precipitates in alkaline conditions. Under aerated conditions Fe solubility is controlled by dissolution and precipitation of Fe^{3+} forming secondary minerals such as Goethite - $\text{FeO}(\text{OH})$ and Haematite - Fe_2O_3 . Manganese solubility increases as soil pH decreases and the reduction of Mn^{4+} to Mn^{3+} and Mn^{2+} at pH lower than 5. At higher pH levels Mn adsorption increases on organic colloids (Fageria *et al.* 2002). Addition of organic matter increases Mn availability through complexation and can supply electrons for the reduction of Mn oxides hence increasing its availability (Wei *et al.*, 2006). Molybdenum solubility increases with increase in pH with less adsorption on $\text{pH} > 5$. The Mo form, MoO_4^{2-} , polymerizes in solution under acidic conditions ($\text{pH} < 5$) and sorption on Fe oxides increases, decreasing Mo availability. The adsorption of Zn on hydrous oxides of Al, Fe and Mn increases as pH increases above 5.5. But at pH above 7, Zn solubility increases due to solubilization of organic matter and also forms $\text{Zn}(\text{OH})^+$ and increased complexation of Zn with lower positive charge (Fageria *et al.* 2002). Possible secondary zinc minerals that can form under alkaline conditions include: smithsonite (ZnCO_3), hydrozincite [$\text{Zn}_5(\text{OH})_6(\text{CO}_3)_2$], willemite (Zn_2SiO_4) Franklinite, (hopeite [$\text{Zn}_3(\text{PO}_4)_2 \cdot 4\text{H}_2\text{O}$] (Essington. 2004).

Organic matter during humification produces water insoluble (humic acids or humin) and water soluble (fulvic acids) compounds that react and form complexes with cations (Fageria *et al.* 2002). Organic matter therefore, has a strong ability to dissolve and complex with non-available elements such as Fe, Zn and Mn and increases their solubility and availability (Wei, 2006). Organic matter is the main source of B an increase in organic matter and pH, increases B availability. Copper as well is highly bound by organic matter more especially at soil pH 6.5. Iron forms complexes with organic acids and such complexes enhance Fe solubility. Organic matter also reduces Mo availability through the formation of complexes (Fageria *et al.* 2002).

2.4 Sludge characteristics

Sludge is an unwanted by-product of wastewater treatment process (Wang, 1997) and is derived from various processes that influence its characteristics (Snyman & Van der Waals, 2004). Sasol biological sludge is a byproduct of the aerobic activated biosolid treatment process. According to Gray (1990) this process consists of two phases; aeration and sludge settlement. In the aeration phase waste water is added to the aeration compartment that contains mixed microbial populations (heterotrophic bacteria and autotrophic microorganisms) and air is added to oxygen for the respiration of the organisms. There is continuous agitation to ensure adequate food and maximize oxygen concentration gradient to enhance mass transfer and to help disperse metabolic end products from within the floc. As the settled waste water enters the aeration tank it displaces the mixed liquor into a sedimentation reservoir. In phase two the flocculated biomass settles rapidly out of suspension to form sludge with the clarified effluent, which is almost free from solids, subsequently discharged as the final effluent. The added microorganisms use organic matter as food source to produce more microorganisms which are eventually settled out; CO₂ is dispersed to the atmosphere; water (H₂O) leaves as part of final effluent; energy is used by the microorganisms to maintain their life systems. The process requires an adjusted pH for the well being and operation of the microorganisms. The pH of a well digested sludge is on the acidic side usually pH 6 or less. Sasol sludge has a pH of 6.8 (Sasol Synfuel, 2008). During digestion CO₂ forms carbonic acid (H₂CO₃) (if it is oxic and suboxic but under redoxic conditions, for example, anaerobic digestors it will be methane (CH₄)) when mixed with water and tends to drive the pH of the wastewater down if the wastewater does not have sufficient alkalinity to buffer the acid formation (Junkins *et al.*, 1983).

Similarly, Sasol sludge contains significant levels of plant nutrients and organic matter (82.4%) that make it possible to use in agriculture (Table 2.2). Total N (7.1%) and P (0.451%) are contained in appreciable amounts while K content is generally low (0.262%) (Table 2.2). The K content is generally low in Sasol sludge, because most K compounds are water soluble and remain in the sewage effluent or the aqueous fraction during sludge dewatering (Rehcigl, 1995). Nitrogen is present mainly in the organic form that must be mineralized before made available to plants (Snyman & Van der Waals, 2004). However, Rehcigl (1995) claimed that a proportion of inorganic N by far is the largest fraction (50 to 90%) of the total N in any sludge and only 10 to 30% of the total P in anaerobic sludges is organic P. This may depend on the source of the wastewater and the processing that determines the type of the sludge. In South Africa both municipal wastewater and sludge contain variable amounts of organic N, nitrate (NO_3^-), nitrite (NO_2^-) and ammonium (NH_4^+) (Snyman & Van der Waals, 2004) that makes it difficult to rule out which of them dominates.

There are several disposal methods that are used in the management of sludge. Sludge disposal on land for beneficial or non beneficial use is the most used strategy for sludge management (Herselmen *et al.*, 2009). However this management strategy increases the risk of environmental pollution. Another method of sludge disposal is incineration. This management strategy does not only generate carbon dioxide (CO_2), a greenhouse gas, but also possibly a myriad of flue gases and toxic residues (Moldes *et al.*, 2007). The ash produced during incineration is more hazardous as well since it contains high concentrations of heavy metals. Therefore, in South Africa the annual produced dry sludge that amounts to 310000 tons, 30% is used in agriculture, 67% land filled, 3% other and non is incinerated (Herselmen *et al.*, 2009).

There are some risks associated with the use of sewage sludge in agriculture. There is a possibility of ground water and surface water nitrate and phosphate contamination. Heavy metals such as Cu and Zn that mainly comes from domestic sources, Cd and Pd mainly from industrial sources may as well contaminate both ground water and surface water (Snyman & Van der Waals, 2004). A decrease in pH of the medium treated with sludge increases the mobility of these heavy metals. Zinc and Cu are important plant micronutrients that sludge can supply but concentrations of 150 to 200 mg kg^{-1} Zinc and 21 mg kg^{-1} Cu in dry matter of tissues are

considered toxic to plants. (Mengel *et al.*, 2001, Snyman & Van der Waals, 2004). Another risk of sludge usage in agriculture is that it contains pathogenic organisms such as bacteria, viruses, fungi and yeasts, parasitic worms and protozoa. If humans or animals are exposed to some of these pathogenic organisms in the environment or in agriculture can contract diseases (Snyman & Van der Waals, 2004).

Table 2.2: Characterization of Sasol sludge (Sasol Synfuel, 2008)

Parameter	Sludge	Units
pH	6.8	Unit less
Moisture (A.D.)	13.1	%
Moisture Loss	77.7	%
Tot. Moisture	80.7	%
Solids(A.D.)	86.9	%
Ash (A.D.)	4.5	%
Volatile solids	82.4	%
Ash: Dry	5.2	%
Total N	7.9	%
Total C	56.3	%
C/N Ratio	7.1	Unit less
Ca	0.4	%
Mg	0.1	%
P	0.5	%
K	0.3	%
Na	0.2	%
Fe	0.5	%
Cu	100	mg kg ⁻¹
Mn	97	mg kg ⁻¹
Zn	113	mg kg ⁻¹

2.5 Possible benefits of amending coal ash with biological sludge

Sludge incorporated in ash is more likely to increase the contents of plant available N and P in which the ash is poor in as characterized by Sasol Synfuel (2008). But the ash may be rich in non available essential plant nutrients such as Na, B, and SO₄ but occasionally can supply plant available K, Ca and Mg (Jankowski *et al.*, 2006). As discussed above these plant nutrients are generally released from the minerals by the processes of weathering (McConnell, 1998 & Brady & Weil, 2008) and the controlling minerals in ash include CaCO₃, CaMg(CO₃)₂ and MgO (Jankowski *et al.*, 2006). The susceptibility to hydrolysis depends on the surface area of the ash,

reaction time and water/solid ratio. The high levels of calcium oxide (CaO) and magnesium oxide (MgO) in ash also play a major role of precipitating heavy metals in sludge and thus reducing their toxicity to plants which may be growing in an ash-sludge medium (Fang *et al.*, 1999).

The clay minerals in the ash contribute to CEC through inorganic functional groups (Essington, 2004). Chemical weathering over time effects an alteration of the ash components and aluminosilicate glass to non-crystalline clay minerals. The formation of these clay minerals is generally indicated by an increase in CEC (Zevenbergen *et al.*, 1999). It is envisaged that the increase in CEC is attributable to the aluminium-silicon rich phases that form during mineral transformation with increased adsorption capability (Gitari *et al.*, (2009).

The release of trace elements may also be accelerated by the presence of soluble organic matter from sludge which forms soluble metal organic complexes. If the presence of insoluble organic matter is significantly high it can reduce the bioavailability of trace elements (Singh & Agrawal, 2008). But Li and Shuman (1996) maintain that the addition of sludge retains heavy metals due to creation of new sorbing surfaces (increased CEC) by the sorption of organic ligands. Organic matter increases CEC through its deprotonated functional groups such as carboxylic and phenolic groups (Essington, 2004). Soluble organic matter can also reduce soluble salt concentration which is high in unweathered ash deposits with electrical conductivity (EC) of $>13 \text{ dSm}^{-1}$ (Haynes, 2009).

Sludge can also promote the establishment of micro-fauna in the ash as it contains microorganisms such as bacteria, viruses, fungi and yeasts, parasitic worms and protozoa (Snyman & Van der Waals, 2004) that the ash is poor in. Furthermore, there is introduction of bacteria species responsible for N mineralization such as autotrophs, *Nitrosomonas* that converts NH_4^+ -N to NO_2 -N and autotrophs, *Nitrobacter* species that converts NO_2 -N to NO_3^- -N (Dinçer & Kargi, 2000).

Physically, Sasol fine ash consists of fine particles with an average diameter of less than $250 \mu\text{m}$ (Mahlaba *et al.*, 2011). This characteristic of fine ash can contribute to the microporosity of the

medium and increase the ability to retain water. Inversely gasification ash is macroporous with average particle sizes ranging from 4 to 75 μm (Matjie *et al.*, 2008) that can provide the necessary aeration needed for numerous microbial mediated processes, essential for a functioning growth medium, e.g. mineralization and nitrification. This characteristic also ensures rapid infiltration and minimize run-off from the ash dump. The increased unsaturated hydraulic conductivity will also increase capillary rise resulting in more sustainable transfer of water to the atmosphere and greater cumulative evaporation. The addition of sludge in fine ash increases its organic matter content that further increases water infiltration (Snyman & Van der Waals, 2004), while, in gasification ash it may increase the retention of water.

2.6 The potential of biological sludge – coal ash mixtures as artificial growth media

Saikia *et al.* (2006) conducted a laboratory study in columns (0.018 m internal diameter) in a mixture of fly ash, municipal solid waste (all waste generated by a community excluding industrial and agricultural process waste) and sewage sludge incinerator ash. They observed that there was a rapid initial pH increase which became approximately constant or decreased. The explanation given was that the initial sharp rising of the pH values was due to the solubility of alkaline materials like carbonates, which neutralize leachants acidities coming from the ash. Saikia *et al.* (2006), observed high concentrations of mobile metal species like; Pb, chromium (Cr), selenium (Se), arsenic (As), molybdenum (Mo), cadmium (Cd) and B) in the leachants as the pH was decreasing. The decrease in pH of the leachant in the subsequent leaching favored the formation of mobile metal species and decreased the ability of metal ions to form surface complexes with hydrous oxides and silicates present in the residues.

Recently, Annandale *et al.* (2004) conducted an onsite rehabilitation trial on the Sasol ash dump by amending combustion coal ash with industrial sludge, as an alternative to importing top soil as a growth medium to establish vegetative cap on the ash dump. Substrates of ash alone and ash amended with sludge were developed. In this trial several perennial grasses and shrubs were screened with the primary objective of establishing which species could adapt to the climate and substrate conditions. Of all the perennial grasses germinated on the sludge treated ash, *Chloris gayana* and *Cynodon dactylon* indicated the best establishment, good overall cover, dense stand and best survival. Some of the grasses and shrubs could not survive. This trial was provided the

basic needed information on the functionality of the waste combinations as artificial growth media. It was therefore evident that the physical and essential plant nutrient release behavior of these waste combinations needed to be elucidated and quantified, using appropriate column system in order to gain predictive capability on the most suitable growth medium combinations. Based on the research done by Annandale et al. (2004) it is clear that both ash and sludge have physical, biological and chemical attributes that provide the potential to support plant growth. Most of the work in the literature has been done in the field and plants planted are used as indicators of elemental release by the mixtures. The treatment of ash with sludge is usually done with the objective of increasing the fertility of the media. The soils and plant biomass are analyzed to quantify available/released essential plant nutrients. Such analysis poorly represents the chemical dynamics of the mixtures, that is, it does not give information on the retention and release mechanisms responsible.

2.7 Unsaturated packed low tension column system

Soil columns have been used for more than three centuries with early investigations appearing in 1703 and can be described as discrete blocks of soil located either outdoors or in a laboratory (Goss *et al.*, 2010 & Lewis & Sjoström, 2010). This is generally achieved by encasing the soil column in a rigid and impermeable shell material, both for structural reasons and to prevent fluid loss, but, the technical approach adopted in constructing columns is not standard, as a result, the smallest column ever reported measured 0.01 m in diameter and 0.014 m in length and was used to investigate the release of heavy metals from contaminated soils (Voegelin *et al.*, 2003) while the largest measured up to 2 m x 2 m x 5 m (Mali *et al.*, 2007). Due to the differences in design, soil columns can be operated under saturated and unsaturated regimes. Columns can further be classified into two broad categories; packed columns that use disturbed material and monolithic columns that use undisturbed material (Lewis & Sjoström, 2010). However, for this discussion focus is on packed unsaturated columns.

Packed soil columns, are built using disturbed material packed into a rigid container and compacted. The objective of packing is to produce a homogenous soil column having a bulk density similar to that observed naturally and avoiding the formation of stratifying layers or preferential flow pathways (Lewis & Sjoström, 2010). Such columns tend to lack macropores,

channeling, and native soil structure due to the packing and compaction (Singh *et al.*, 2002). Macropores and channeling are difficult to eliminate but can easily be minimized by ensuring that the column diameter is thirty times as large as the maximum particle size of the material used to pack the column (Bi *et al.*, 2010). During packing and compaction it is a challenge to pack the whole column at the same field bulk density. Hence various effective packing methods have been successfully used to achieve the desired density but the focus is on dry or damp method.

The dry and damp packing technique involves loading small discrete amounts of dry or damp soil into the column (Lewis & Sjoström, 2010) ensuring close contact of the particles of the packed material allowing elimination of macropores. However, Bi *et al.* (2010) argues that this method is tedious and usually results in layering of the soil, results in stratification and defies reproducibility of the soil column. But they further suggested that the sample can be loaded into the column with the help of a stainless steel spatula depositing the material in layers thinner than 0.01 m and in some cases at 0.15 m and then mechanically packing it either by hand or with some type of ram (Lewis & Sjoström, 2010). The material packed also needs to be homogenized if large particles exist by grinding manually using a pestle and mortar to smaller particles to ensure reproducible column packing (Bi *et al.*, 2010). To minimize layering and ensure hydraulic connectivity the surface of the soil is slightly scarified after compaction before the addition of another layer (Lewis & Sjoström, 2010).

One other successful technique used for packing in smaller soil columns is vibration which depends on power (Lewis & Sjoström, 2010). Small soil columns can also be compacted by slightly taping the column side wall with an object if the bulk density is not very high (Bi *et al.*, 2010 & Schwab *et al.*, 2008) and variation in density can also be controlled by dropping the soil column from a height of 0.03 m consecutively for three times on a hard surface (Hansen, 2010), but this method is very arbitrary because the 0.03 m height and frequency of dropping may achieve a density lower or higher than field bulk density for some columns.

This packing method has the advantage of reproducibility, that is, the lack of heterogeneities and macropores should lead to reproducible bulk densities and dispersivities (Lewis &

Sjoström, 2010). However, sidewall flow is a preferential flow which is a concern with packed unsaturated column. To minimize this some methods have been proposed and tried. Suggested successfully used methods include; roughening the sidewall by gluing sand to it (Sentenac *et al.*, 2001) confining the soil column with a flexible latex membrane to overcome side wall flow (Charbeneau, 2000) and wetting the inside of the column then packing it with a swelling clay such as montmorillonite (Lewis & Sjoström, 2010). In the latter approach, the excess (dry) clay is allowed to fall out of the column while the hydrated clay forms a liner on the column wall. However, there is a possibility to have a flow at the soil - membrane boundary and the clay mineral is highly reactive and will participate in chemical reactions.

The sidewall can also be coated with paraffin and extra paraffin should be added along the soil tube interface to prevent preferential flow (Shan *et al.*, 2005). Goss *et al.* (2010) suggested that injecting petroleum between the casing and the soil can reduce preferential flow. This was supported by Steiner *et al.* (2010) that petroleum jelly can seal the gap between the soil column and the casing around it in order to prevent edge-flow effects. However, the application of petroleum can negatively affect the solution chemistry.

Other undesirable forms of preferential flow include macropore flow or fingering in packed soil columns (Lewis & Sjoström, 2010). Macropore flow refers to any flow which takes place outside of the normal pore structure of the soil, such as in wormholes or decayed roots. While these may play a more significant role in monolith-type soil columns, macropores still exist in apparently homogeneous packed soil columns on account of the heterogeneity of the soil grains themselves (Cortis & Berkowitz, 2004 & Oswald *et al.*, 1997). Fingering also occurs when instability develops in the wetting front as it moves through coarse unsaturated soils such as sands and is a function of the soil grain size, with silts having fingers on the order of 1 m in diameter and coarse sands having fingers on the order of 1 cm. Fingering can persist until the soil has either been fully dried or fully saturated and is most likely to occur when the soil being infiltrated is initially extremely dry (Lewis & Sjoström, 2010). This is not necessarily bad if the purpose is to simulate field conditions.

Suction is needed in unsaturated soil columns in order to extract the pore water and maintain the column under unsaturated condition. However, Lewis and Sjoström (2010) argues that attempting to sample pore water by applying suction to an open ended pipe attached to the base of a soil column normally fails because only air is drawn in. But this is normally not the case; it depends on how close the columns are to saturation. For this reason, rigid porous materials are used as an interface between the sampling device and the soil to ensure that pore liquids in the soil are in hydraulic contact with liquid within the sampling device (Plummer *et al.*, 2004, Chu *et al.*, 2003, Hutchison *et al.*, 2003, Magesan *et al.*, 2003, Powelson & Mills, 2001 & Vogeler, 2001). Rigid porous materials that are used in soil columns installed with a suction device include; ceramic, porous polytetrafluoroethylene (PTFE), fritted glass, porous stainless steel, porous plastic and fibreglass wicks and to help in choosing a rigid porous material for an experimental apparatus, the bubbling pressure (air entry pressure - the pressure where the largest pores that can retain water against gravity evacuates) of the material must be considered.

Mechanical dispersion and molecular diffusion occurs in unsaturated columns and may affect the results. This is caused by deviations in the microscopic fluid velocity caused by differences in pore sizes and geometries, creating localized dilutions (Lewis & Sjoström, 2010). Mechanical dispersion is a linear function of the dispersivity – which is a property of the soil – and the fluid velocity. However, this is a function of pore size distribution. Molecular diffusion in contrast is driven by concentration gradients (Fick's law) and will occur regardless of whether the fluid is moving. Unless the fluid is nearly immobile, mechanical dispersion dominates and molecular diffusion effects can often be neglected (Leij & van Genuchten, 2002). The dispersivity of unsaturated soils is inversely related to the soil moisture content (Lewis & Sjoström, 2010) and may be nearly an order of magnitude higher in unsaturated soil than that of an identical saturated soil. The flux density also appears to have a lesser effect on the dispersivity in unsaturated soil (Toride *et al.*, 2003).

There is a significant relationship between the diameter of a column and the measured dispersivity. Larger column diameters (≥ 0.076 m) tend to produce greater experimental dispersivities than columns with diameters < 0.076 m, which may be on account of the greater difficulty in uniformly packing larger columns (Bromly *et al.*, 2007). However, there is less relationship between the column length and dispersivity. Dispersivities in larger columns having

diameters ≥ 0.076 m can be grouped according to their lengths. Columns longer than 0.107 m produced greater dispersivities than columns < 0.107 m (Bromly *et al.*, 2007). By extension, once the fluid flow in a saturated soil column is forced to a value that is approximately an order of magnitude higher than that of the unsaturated regime, the saturated hydrodynamic dispersion can be expected to overtake the unsaturated dispersion. Pressure differentials in a saturated soil column between the upper and lower boundaries may be much lower than those of an unsaturated soil column, leading to potentially higher fluid flow velocities since macropores are less resistant against flow and consequently higher hydrodynamic dispersions (Lewis & Sjoström, 2010).

The draining system may be designed to prevent saturated conditions in the bottom of the column or to create a water table within the column depending on the purpose of the experiment (Hansen *et al.*, 2000). At the bottom of the column a peristaltic pump can be connected to continuously collect leachate by applying constant suction (Zhao, 2009). In circular soil columns the draining system is often formed as a funnel and typically consists of different layers of sand with varying particle size, or it simply consists of a filter placed on a perforated platform, possibly combined with a thin layer of sand (Hansen *et al.*, 2000). A similar structure was constructed by Shan *et al.* (2005) using small polyvinyl chloride (PVC) tubes with an open strip facing up filled with quartz sand to collect leachate from the soil column. In large-scale lysimeters, which are often used for waste products, the bottom of the lysimeter is often lined with an impervious material with a draining layer placed above such as geotextile with a fixed synthetic draining layer to prevent particles from entering the leachate collecting system (Hansen *et al.*, 2000).

According to Hansen *et al.* (2000) a low suction can be applied constantly or periodically to the draining system and a zero-tension lysimeter allows the soil solution to drain freely through the test material while with low-tension lysimeter and the equilibrium-tension lysimeter, suction is applied. In a low tension lysimeter and in an equilibrium-tension lysimeter, soil solution can be extracted from finer pores also by establishing good contact between the sampling point and the test material and applying suction. Draining from the test materials differs in quantity when

vacuum is applied or not applied, and when vacuum is applied at fixed or variable levels (Hansen *et al.*, 2000).

Static tension refers to the fact that the columns are connected to a vacuum system and a static tension of approximately -10 kPa can be applied at the base of the columns. This enables the removal of saturated environments within the packed material. Therefore, static tension systems are arguably a better approach compared to free draining systems to simulating release and sequestering dynamics of unsaturated porous systems. Firstly, in free draining columns water perching or ponding occurs at the outflow boundary resulting in artificially wetter conditions at best and potentially anaerobic conditions at worst, compared to unconfined porous medium. Secondly, applying tension at the base of the columns helps to minimize these boundary conditions and ensure that the columns drain better ensuring conditions closer to that of unconfined porous media. Thirdly, the ability to apply vacuum allows better control of the water content and aeration of the columns. Different tensions can be applied to simulate different aeration scenarios if needed and wetting and drying cycles under laboratory condition can be accelerated through vacuum drying or force aeration of the columns. Lastly, pore solution chemistry can be investigated directly and residence time can be controlled.

In free draining systems the only means to gain any insight into pore solution chemistry is through the analysis of the free drainage collected. Little control over the residence time of solution in free draining steady state flow systems exists. In order to interpret data in context the assumption must be made that the chemistry of the free drainage more or less mirrors pore solution chemistry. A better approach is to approximate the nearness of the residence time to “equilibrated” or more correctly steady state. This is done by using, for example, the Damköhler number:

$$(Da) = R.K.L.V^{-1} \quad (\text{Eq. 2.1})$$

Where R is the retardation coefficient of the element of interest, L is the column length, V the pore velocity (ms^{-1}) and K kinetic constant based on the rate of elution (Andrés & Fransisco, 2008). Preferential flow paths can develop in any artificially packed system. This will decrease tortuosity resulting in shorter residence times and less contact of the percolating solution with the

total surface area of the medium, this will also influence pore velocity calculations. All conclusions made and recommendation forwarded about nearness to equilibrium, solution composition, ion concentration and ion activities are, therefore, transport and pathway dependent. The advantage of a constant tension system is that entrained pore solutions, in pores that can retain water against gravity, can be sampled directly after it was allowed to equilibrate for a specific time. The intricacies of relating the chemistry of the free drainage to pore solution chemistry and the nearness to equilibrium are circumvented. This allows the comparison of pore solution chemistry of different residence times to that of free drainage.

Soil column studies therefore allow for the assessment of elemental transport, the evaluation of transport models, monitoring the fate and mobility of contaminants in the soil (Lewis & Sjoström, 2010). To achieve this, column techniques incorporate the use of models, equations and break through curves (Mahmood-Ul-Hassan *et al.*, 2008). Such experiments involve packing the relevant soil material into columns where the transport, mobility, bioavailability and chemical behavior of contaminants in the soil matrix is to be quantified (Wang *et al.*, 2009).

Secondly, columns enable hydraulic conductivity studies. Early investigations (1703) that introduced soil column technology concentrated on identification of the components of water balance and this was aimed at determining the proportion of natural precipitation leaving the soil as a result of deep drainage and surface runoff (Goss *et al.*, 2010). Preferential flow in macropores is an important component since it can lead to rapid transport of surface applied contaminants to the subsurface and make difficult agricultural water management. In addition wetting fronts propagate in macropores to significant depths and bypass the soil matrix pore space (Akay & Fox, 2007). Field studies using hydrometric methods and/or natural and artificial tracers enable assessing macropore flow under field conditions, but face climatic variability complexities and difficulties associated with field assessment of hydraulic properties. Thus hydraulic conductivity is better assessed using small undisturbed soil columns under laboratory conditions (Lamy *et al.*, 2009).

Lastly columns enable the study of the influence of organic acids on mobility of heavy metals. Dissolved organic matter could contribute effective organic ligands to form complexes

with heavy metals in the soil. The soluble complexes with heavy metals can be transported downward and possibly deteriorate ground water quality. The addition of soluble organic ligands has been found to decrease the sorption of trace metals by soils because they form soluble complexes with heavy metals (Li & Shuman, 1997).

2.8 Conclusion

This review shows the potential of combining ash and sludge can be a better utilization management tool which can create a more conducive environment to establish a vegetative cap. Sludge has high levels of available inorganic N and P that ash is poor in and also contains both soluble and insoluble organic matter, with the former complexing trace elements increasing their mobility and the latter contributing to the retention of elements. Thus sludge can contribute to CEC of the medium and can provide C, a source of energy to microorganisms responsible for essential processes such as N mineralization and nitrification. Introduction of sludge can also introduce important bacterial microorganisms that decompose organic material. Ash as well contains plant nutrients such as Ca, Mg, K and Na that sludge is poor in. Physically gasification ash is macroporous and this characteristic can provide the necessary aeration needed for numerous microbially mediated processes essential for a functioning growth medium, e.g. mineralization and nitrification. The increased hydraulic conductivity can also increase capillary rise resulting in more sustainable transfer of water to the atmosphere and greater cumulative evaporation. This characteristic can ensure rapid infiltration and minimize run-off from the ash dump. Fine ash, on the other hand is micro porous and this characteristic can contribute to the micro porosity of the medium and increase the ability to retain water. The production of C, humic and fulvic acids by sludge during decomposition can contribute to the reduction of the high pH of the ash.

Weathering processes such as dissolution, hydrolysis, oxidation and hydration can help in the release of the elements from the clay minerals that contain them. Other factors such as pH, ionic strength, electric potential, concentrations of ions in the solution, temperature, affinity of adsorption by the exchange surfaces, type of clay mineral, point of zero charge, cation exchange capacity and carbon-nitrogen ratio govern the absorption and release of the plant nutrients.

However, pH remains the master variable in control of adsorption and desorption of micro- and macro-nutrients in soils and artificial soil materials like coal ash-industrial sludge mixtures.

A more realistic combination of ash and sludge was evident with on-site rehabilitation trial which was conducted by Annandale *et al.* (2004), where substrates of ash alone and ash amended with sludge were developed. Several perennial grasses and shrubs were screened with the primary objective of establishing which species could adapt to the climate and substrate conditions. *Chloris gayana* and *Cynodon dactylon* established the best, with a dense stand and best survival. However, some of the grasses and shrubs could not survive on certain substrates. This trial was used as a precursor to the functionality of the waste combinations as growth media. It was therefore evident that the physical and essential plant nutrient release behaviour of these waste combinations needed to be elucidated and quantified. Sometimes, plant biomass is analyzed to estimate available essential plant available nutrients. Generally, such an analysis poorly represents the chemical dynamics of growth media, that is, it does not give information on the retention and release mechanisms responsible. This can only be done under laboratory conditions using appropriate methods using carefully designed column systems. Packed unsaturated low tension columns set-up in a laboratory can improve aeration and oxidation; they can also enable the study of the medium's hydraulic conductivity and nutrient retention and release. Such columns can also give one predictive capability into the most suitable growth media combinations. However, various options may be expected since no one combination will always be better than others.

CHAPTER 3: MATERIALS AND METHODS

The materials and methods covered in this section included: mixture formulation technique, components of each mixture, calculations involving packing of columns, the development of the low tension column system and leaching procedure. Materials and methods regarding analysis of elements (macro and micronutrients), pH and salinity, particle size distribution and cation exchange capacity (CEC) are dealt with under their respective chapters.

3.1 Mixture formulations

Biological sludge, fine and gasification ashes were collected from Sasol Synfuels in Secunda. Each waste stream was randomly collected from its source to ensure correct representation of the site. Both gasification and fine ash were collected from freshly dumped heap and fresh fine ash dam respectively. Freshly processed sludge was collected directly from the final point (at stage of disposal) of the plant. For each of the wastes 300 kg was collected and transferred into a tightly closing plastic container. The plastic containers with samples were later, during the same day, enclosed in a cold room at 4 °C to minimize chemical reactions and biological activities that may occur.

The general approach followed in developing the mixtures are illustrated in Fig. 3.1 a, b and c). The mixtures were expressed on a wet mass basis. The sludge was viewed as a suspension and mixtures containing 10, 20, 30, 40, 50% (Fig 3.1 a) represented the amount of the sludge suspension added relative to the two solid phases. A previous approach revealed that sludge as a solid and base sludge additions on a dry mass bases proved to be unpractical. In a preliminary trial it was evident that the high liquid content(10 – 13% solids) of the sludge resulted in the final volumes of mixtures containing greater than 60% sludge to be more than the volume of the columns.

The fine and gasification ash are similar to soil, the liquid phase is a minor component (12 – 13% moisture) of the natural mass in their ‘natural state’. The gasification and fine ash content in the mixtures are represented in Fig. 3.1 b and c respectively.

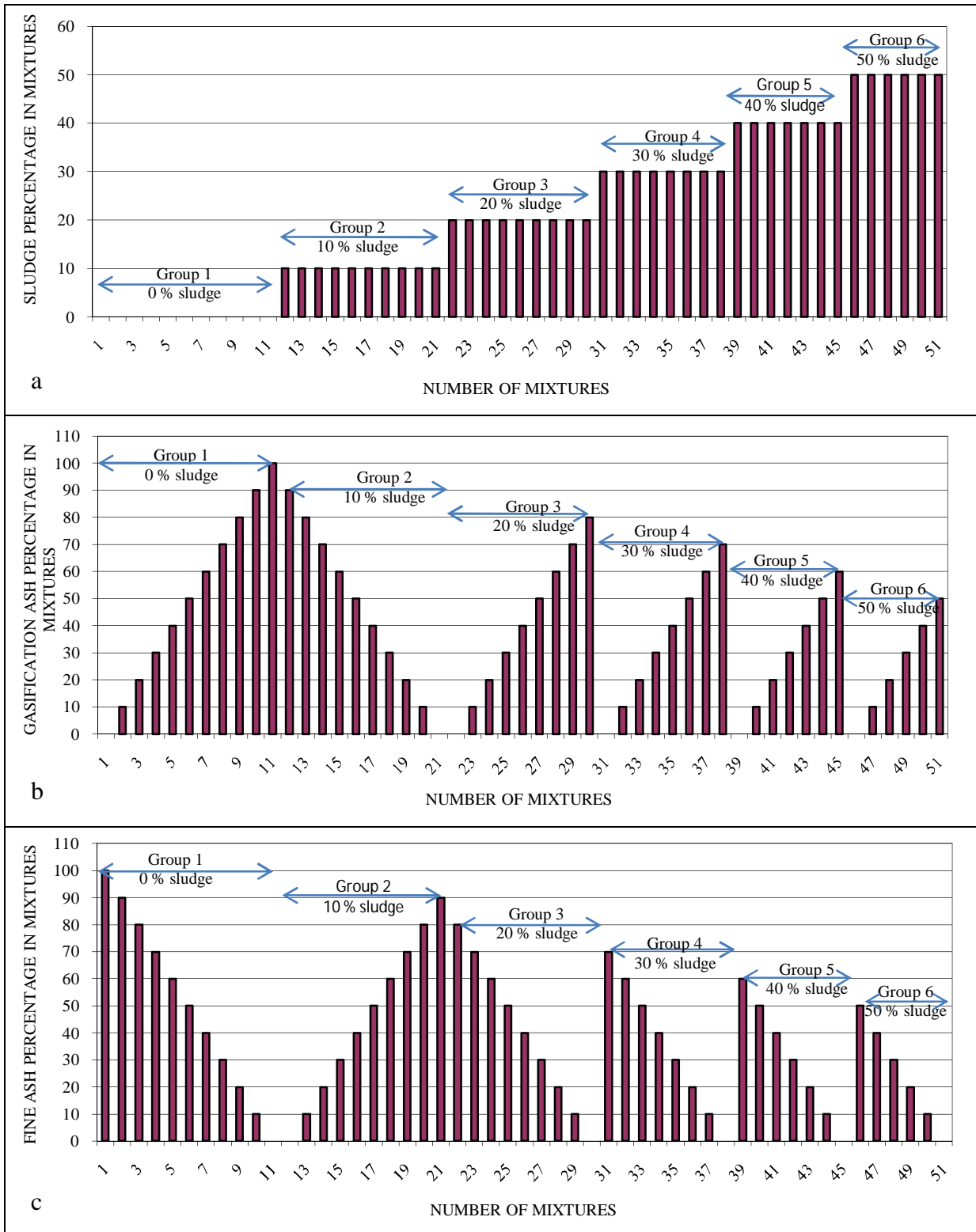


Fig. 3.1: a) Sludge content in mixtures (wet mass of sludge expressed as a percentage of the total wet mass), b) gasification ash content in mixtures and c) fine ash content in mixtures

A total of 51 mixtures (hand mixed) were formulated containing varying amounts of sludge, fine and gasification ashes. There were no replications included because of the gradient in sludge, gasification ash and fine ash content represented by the various mixtures. The mixtures were conveniently divided into 6 groups based on sludge content (Fig 3.1 a, b and c). Group 1 (mixtures 1 – 11) represented treatments that received no sludge while fine ash content was reduced (100 – 0%) and gasification ash content increased (0 – 100%). Group 2 (mixtures 12 – 21) represented treatments that received 10% sludge while fine ash content was increased and gasification ash content was reduced. Group 3 (mixtures 22 – 30), group 4 (31 – 38), group 5 (39 – 45) and group 6 (46 – 51) received 20, 30, 40 and 50% sludge respectively while the fine ash decreased and gasification ash increased.

3.2 Calculations involving the packing of the columns

The columns were packed at a wet bulk density ($\rho_b = M_{\text{total}} / V_{\text{total}}$) of approximately 1200 kg m⁻³. In order to leave adequate space for the addition of deionized water to the mixture only 0.25 m of the column height was considered for total volume calculation. Based on this, the mass of mixture that was prepared to be packed in each column was calculated:

$$\text{Volume} = \Pi r^2 h \quad (3.1)$$

Where r is the radius and h is the height

$$\begin{aligned} \text{Column volume (cm}^3\text{)} &= \Pi \times (5.25 \text{ cm})^2 \times 25 \text{ cm} \\ &= 2164.75 \text{ cm}^3 \end{aligned}$$

$$\begin{aligned} \text{Total mass of mixture} &= \text{bulk density} \times \text{volume} \\ &= 1.2 \text{ g/cm}^3 \times 2164.75 \text{ cm}^3 \\ &= 2597.7 \text{ g} = 2.6 \text{ kg} \end{aligned} \quad (3.2)$$

The amount of deionized water that must be added to each mixture was approximated by calculating the pore volume of the mixture (Tan, 2005, Lal & Shukla, 2004).

$$\text{Total porosity} = 1 - \rho_b / \rho_s \quad (3.3)$$

Where:

$$\text{Dry bulk density } (\rho_b) = M_{\text{solids}} / V_{\text{total}} \quad (3.4)$$

$$\text{Particle size density } (\rho_s) = M_{\text{solids}} / V_{\text{solids}} \quad (3.5)$$

$$\text{Pore volume} = (1 - \rho_b / \rho_s) \times V_{\text{total}} \quad (3.6)$$

To estimate the porosity and pore volume, the equivalent dry bulk density or more specifically the dry mass of the mixtures were needed. The particle density was taken as 2650 kg m^{-3} . Sub samples (100 g) of the mixtures were prepared, weighed off in duplicate into pre-weighed beakers and the oven dried at 105°C for 24 hours. The beakers with their content were then cooled in a desiccator, and afterwards the dry mass percentage of each treatment was determined directly (Eq. 3. 7) (Tan, 2005). The pore volume (Eq. 3.6) was estimated for all samples/mixtures and was found to be 1.1 L (1101.86 cm^3).

$$\text{Dry mass of sample (\%)} = 100 \times [\text{wet mass (g)} - \text{oven dry mass (g)}] / [\text{dry mass (g)}] \quad (3.7)$$

3.3 Packing of the columns

Small discrete amounts of the wet mixture were loaded into the column to ensure close contact of the particles of the packed material and to eliminate macropores. The loading of the material into the column was carried out on increments of 0.1 kg. The material was deposited in layers of about 0.09 m high equivalent to 0.9 kg of the sample in mass. After each layer the material was then mechanically packed using a vibrating table for about 15 seconds. To minimize layering and ensure hydraulic connectivity the surface of the material was slightly scarified after compaction before the addition of the next layer.

3.4 The development of the unsaturated column system, specifications and set up

A static low tension column set up was developed in order to investigate the interaction of sludge, fine and gasification ashes mixtures and the result elemental release in an aerobic environment under alternating wetting and drying conditions. Static tension under these conditions referred to columns connected to a vacuum system and a static tension of approximately -10 kPa that could be applied at the base of the columns. This was done to prevent the accumulation of moisture at the base of the column and encourage aeration.

The column ensemble consisted of the following:

- 1) A column base cut from polypropylene with an internal diameter of 0.11 m (out rim with a 0.01 m thickness) the depth of the base was 0.045 m (Fig 3.2 a – d),

- 2) An O-ring about 0.004 m diameter (Fig 3.2 b and c) was fitted prior in the column bases to ensure vacuum tight seal with column,
- 3) A 0.3 m long transparent polyethylene column, with an internal diameter of 0.105 m (Fig 3.3 a) fitted on the base,
- 4) A 'depth filter' placed at the base of the column consisting of five layers of filtering material (Fig 3.3 c). The filtering material were placed in an order of decreasing pore size: The first layer directly in contact with the mixture was a polypropylene mesh with a pore size of 0.002 m, followed by three nylon meshes with a decreasing pore size of 25, 10 and 5 μm (Fig 3.3 b). The last mesh at the outflow boundary was again a 0.002 m polypropylene mesh and
- 5) A 0.0005 m³ Schott Duran glass bottle that can screw in at the bottom of the column bases (Fig 3.3 d). The column bases were connected to the vacuum system as illustrated in Fig 3.4. A main vacuum line, connected to a vacuum regulator on the bench, serviced eight columns. In total, two rows of 24 columns were mounted back-to-back on one bench (Fig 3.4).

3.5 Leaching procedure and collection of leachate

The approach followed was to simulate wetting and drying cycles. A total of ten wetting and drying cycles were simulated in a period of 12 months starting in January 2010 and ending in December 2010 and in each eluviation cycle the amount of deionized water (1.1 L) estimated based on the calculated porosity and pore volume of the media was added to the columns. This amount of deionized water that passed through the columns was equivalent to approximately one pore volume. The free drained leachates that collected in Schott bottles, shown in Fig 3.4, were removed after free drainage stopped. Clean Schott bottles were then connected to the column bases and a vacuum of -10 kPa was applied in order to collect the pore solution that was allowed to equilibrate with the mixtures for 24 hours. The volume and the mass of the collected solutions were determined for mass balance purposes. Solution pH and electrical conductivity (EC) of both the free drained and pore solutions were immediately determined. Inorganic nitrogen analysis as well was carried out within 24 hours after each leaching to avoid volatilization and denitrification. After inorganic nitrogen analysis, pH and EC determination the leachates were



Fig. 3.2: a) Side view of column base showing opening to which vacuum was connected, b) Top view of column base showing grooved ‘floor’, drainage outlet and imbedded O-ring, c) Side view of column base showing the imbedded O-ring to ensure a vacuum tight seal between column and base, d) Bottom view of column base showing drainage outlet and threaded opening to which a Schott Duran glass bottle were screwed/fitted.

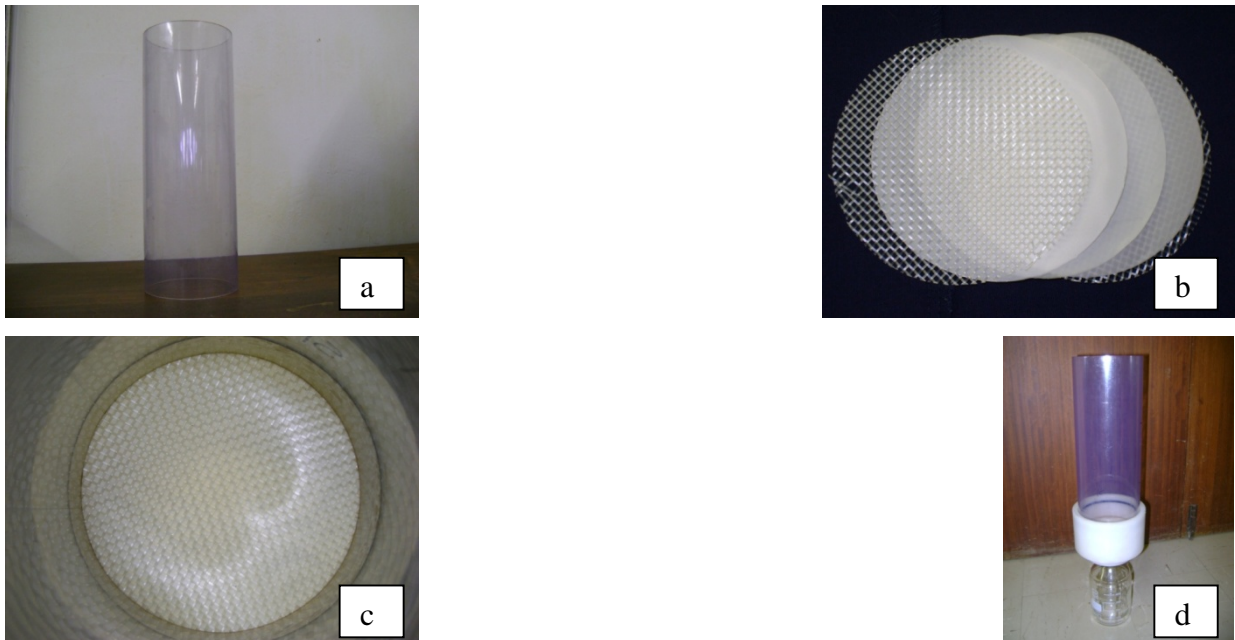


Fig. 3.3: a) The transparent polyethylene column (length: 0.3 m, internal diameter: 0.105 m), b) The five layered mesh placed at the outflow boundary of the column or at the base of the column, c) The securing of the mesh by the column in the column base, d) The column assembly consisting of the transparent column, the column base and the Schott bottle.



Fig. 3.4: The low tension column battery on each bench, connected to the vacuum system (blue pipe from column connected to the red main vacuum line) and collection plastic bottles.

refrigerated at 4 °C to minimize chemical and biological activities that could occur before further analysis.

CHAPTER 4: PARTICLE SIZE DISTRIBUTION AND WATER RETENTION OF BIOLOGICAL SLUDGE – COAL ASH MIXTURES

4.1 Introduction

Sasol gasification ash had large irregularly shaped aggregates of sizes ranging from 4 to 75 mm as characterized by Matjie *et al.*, (2008) while fine ash consisted of particles that fell between 5µm and 75 µm and constitute about 60%. This percentage was greater than particles that fell between 1 – 5 µm (16%) and between 75 – 425µm (30%) as characterized by Mahlaba *et al.* (2011).

Generally, finer particles of ashes are spherical in shape showing a complete melting of silicates which occurs during combustion at temperatures above 1350 °C and pressures greater than 2000kPa (Matjie *et al.*, 2008). The spheres of both ashes may be solid, hollow or encapsulating (Kopsick & Angino, 1981). Micrographic evidence indicated that most of the particles in fine ash occur as solid spheres of amorphous glass that form during cooling of the melt phase (Tishmack & Burns, 2004). In addition, only a few hollow spheres and some spheres packed with other numerous small spheres or crystals of minerals, may be present (Trivedi & Sud, 2002). The crystals of minerals formed are a result of cooling of the minerals and non-mineral inorganic elements in the coal mineral matter that melt and form liquid phases during the gasification process (Matjie *et al.*, 2008). Fine ash has a low particle density, a high surface area and light grey particles (Asokan *et al.*, 2005 & Jala & Goyal, 2006).

Sasol gasification ash was characterized by Matjie *et al.* (2008) and found that it contained minerals (contribute to water retention through hydration during weathering) by weight such as; quartz (10.7%), anorthite (13.1 %), mullite (17.7%), cristobalite (1.8%) and diopside (0.7%). While for weathered Sasol fine ash Mahlaba *et al.* (2011) found that it contained mullite (18 %) and quartz (10 %) as major mineral phases and magnetite (2%), attringite (3%), calcite (3%) and sillimanite (Al_2SiO_5) (1.5%) as minor phases. Periclase (0.75%), analcime ($\text{NaAlSi}_2\text{O}_6 \cdot \text{H}_2\text{O}$) (0.75%), pyrrhotite (0.3%) and hematite (0.5%) were found as trace mineral phases. Mahlaba *et al.* (2011) characterized weathered Sasol fine ash as having a high water holding capacity (moisture content ranging between 27 and 37%) that can sustain hydration

reactions. These minerals together with the physical and pozzolanic properties can contribute to CEC through surface charge development and to water holding capacity.

A pozzolan is a siliceous and aluminous material that is formed, for example, when calcium hydroxide ($\text{Ca}(\text{OH})_2$) chemically reacts with silicic acid (H_4SiO_4 , or $\text{Si}(\text{OH})_4$). The resultant products formed include calcium silicate hydrate ($\text{Ca}_9\text{Si}_6\text{O}_{18}(\text{OH})_6 \cdot 8(\text{H}_2\text{O})$) and Strätlingite ($\text{Ca}_2\text{Al}_2\text{SiO}_2(\text{OH})_{10} \cdot 3\text{H}_2\text{O}$) (Matschei *et al.*, 2007) depending on the presence of Ca, Al and Si in the ash. These pozzolans have a cementitious characteristic that they acquire after addition of lime during the combustion process. Basically the Ca, Al and Si in ash react with the free lime in the presence of water to form these cementitious materials (Haynes, 2009). The pozzolans in the ash are important as adsorption sites for pollutants such as chloride and can possibly increase water holding capacity (Mahlaba *et al.*, 2011).

Sasol sludge contains a significant amount of organic matter (82.4%) as characterized by Sasol Synfuel (2008). The organic matter in sludge can contribute to water holding capacity if combined with coarse grained medium like gasification ash and may increase water infiltration rate, hence reduces runoff and erosion when combined with fine ash (Snyman & Van der Waals, 2004). Sasol sludge also contains 80.7% moisture (Sasol Synfuel, 2008) a characteristic that inhibits gaseous exchange making it difficult to use as artificial soil medium. However, this is a transient property and can dry out under conditions of high atmospheric demand.

Particle size distribution does not only predict water holding capacity but also total pore space, pore size distribution, bulk density and air filled porosity (Benito *et al.*, 2005). Gasification ash is macroporous, therefore, can provide the necessary aeration needed for numerous microbial mediated processes, essential for functioning of a growth medium. It can also ensure rapid infiltration and minimize run-off from the ash dump. However, a rapid water percolation can increase the rate of loss of nutrients and increase the transportation heavy metals that end up contaminating both the environment and ground water (Brady & Weil 2008). It is clear that gasification ash has a low capacity to hold water and nutrients. The microporosity of fine ash can contribute to the microporosity of the medium, increase the ability to retain water and increase

the release of nutrients. Some of the minerals present in the ash through hydration and humified or stabilized sludge can also increase water holding capacity of an artificial soil medium. However, the pozzolanic nature of the fine ash can increase hydration of minerals and cause hardness of the growth medium and physical compaction.

According to Handreck and Black (1984) and Jayasinghe *et al.*, (2009) an ideal artificial soil medium must generally have a medium to coarse texture, equivalent to a particle-size distribution between 200 and 3000 μm . However, an ideal artificial growth medium must have 20% of its particle size in the range between 100 and 250 μm to be able to have a good balance between airfilled porosity and ability to supply readily available water (Handreck & Black, 1984). Clearly, ranges lower than 0.1 mm can clog pores, increase non plant available water and decrease airfilled porosity (Benito *et al.*, 2005). None of these wastes has a particle size distribution that nicely fits in this range, but it is highly possible to achieve it when the wastes are combined. A pore space of about 50% in a soil medium can be shared equally by air and water (Brady & Weil, 2008). Neither gasification nor fine ash has a pore space of 50%. Gasification ash has a pore space of greater than 50% and fine ash has a pore space of less than 50%. An artificial medium must also have a bulk density of less than 400 kg m^{-3} (Jayasinghe *et al.*, 2009), but this density is much lower than the bulk density of an unconfined medium that ranges between 1000 to 1800 kg m^{-3} (Brady and Weil, 2008). The bulk density range of fine ash is similar to the density of an unconfined medium, it ranges between 1000 and 1800 kg m^{-3} , which is far above the optimum bulk density (400 kg m^{-3}) of an artificial soil medium suggested by Jayasinghe *et al.*, 2009.

A measurement of particle size distribution can help in better understanding the interaction between chemical, physical and biological parameters of the mixtures. It was hypothesized that an increase in fine ash content will increase water holding capacities of the mixtures by ensuring a particle size distribution of between 0.1 and 0.25 mm in the mixtures. Conversely, it was hypothesised that the incorporation and increase of gasification ash content will reduce water holding capacities of the mixtures. Further, it was also hypothesized that the incorporation and increase in sludge content will increase the water holding capacities of the mixtures. Therefore the main aim of this chapter was to assess variation in particle size distribution of the mixtures

and the influence each waste has on water holding capacity when combined as artificial soil medium. This is a laboratory based study where packed unsaturated low tension columns will be used, a system that can allow the study of the ability of the various media to retain water against the application of vacuum. This can be a useful predictor and predictive capability on the most suitable combinations with respect to potential water holding capacity.

4.2 Materials and Methods

4.2.1 Particle size analysis

The sieve method described by Soil Science Society of South Africa (1990) and Smith and Mullins, (1991) was used. From the bulk samples collected at Secunda, 200 g samples of each of the materials (gasification and fine ash) were collected. In total thirty replicates were collected from both gasification and fine ash for particle size analysis. Nine sieves (woven wire) were arranged in descending order of their apertures as follows; 8, 4, 2, 1, 0.5, 0.25, 0.1, 0.05 mm-pan. The 200 g sample of each of the wastes was transferred to the top sieve (8 mm) then washed with distilled water through the sieves while shaking and slightly tapping the column of sieves. Wet-sieving was necessary to help force finer particles (finer particles aggregate and block the sieve apertures) through the sieve apertures. To determine the dry mass of each sample the contents of each sieve was transferred into a pre-weighed beaker and oven dried at 105°C for 24 hours. The oven dried samples in each sieve was then expressed as a percentage of the total oven dried sample. The percent particles collected from each sieve was used to estimate the particle size distribution of the different mixtures. This approach helped to establish the range upon which the optimum particle size distribution falls.

4.2.2 Assessing water retention characteristics

In total 51 different mixtures were formulated containing varying amounts of gasification ash, fine ash and sludge. The general approach followed in developing the mixtures were illustrated in Fig. 3.1 a, b and c in chapter 3. The approach followed was to simulate natural wetting and drying cycles. A total of ten wetting and drying cycles were simulated in a period of 12 months. In each eluviation cycle the amount of distilled water (1.1 L) estimated based on the calculated porosity and pore volume (Eq. 3.3 and 3.6) of the media was added to the columns. This amount of distilled water that passed through the columns was equivalent to approximately one pore

volume and the system was allowed to equilibrate for 24 hours. The free drained leachates that collected in Schott bottles were removed after 24 hours. Clean Schott bottles were then connected to the column bases and a vacuum of -10 kPa was applied in order to collect the pore solution. This matric potential was selected to ensure attainment of field capacity in the mixtures and to ensure minimal removal of finer particles during vacuum application. The volume, as well as the mass of the collected solution, was determined for mass balance purposes. The water holding capacities of the mixtures were taken as the amount of water retained by the mixtures after the free drainage took place and the pore solution, extractable with vacuum of -10 kPa, was removed.

The water content of the mixtures was then expressed on both a gravimetric and volumetric basis. Gravimetrically, the water content was calculated as the ratio between the mass of water (M_w) that remained in the mixtures after the application of a static tension of - 10 kPa and the oven dry mass (M_s) of the mixtures (Eq. 4.1). Volumetrically, the water content was calculated as the ratio between the volume of water (M_w) that remained in the mixtures after the application of a static tension of - 10 kPa and the volume (V_T) occupied by mixtures (Eq. 4.3).

Some of the water retained after the application of vacuum was not necessarily water that resided in micro pores or adsorbed on surfaces, that can easily be removed by normal oven drying at 105 °C. It was expected that some of the water retained was trapped by hydrated minerals and therefore chemically bound (crystal water). This type of water is at a very low energy state and have low propensity to change phase. It was not expected that the energy applied when drying at 105 °C would be enough to liberate crystal water. With the oven drying method it will not be possible to distinguish between water retained and potential plant available and chemically bound water. Equation 4.3 calculates the volumetric water content (in percentage) of the mixtures by expressing the volume of water retained as a fraction of the total volume of the initial mixture.

$$\theta = \frac{M_w}{M_s} \quad (\text{Eq.4.1})$$

$$\theta = \frac{M_w}{M_T} \times 100 \quad (\text{Eq. 4.2})$$

$$\theta = \frac{V_w}{V_T} \times 100 \quad (\text{Eq. 4.3})$$

Where: $M_T = M_w + M_s + M_g$ (Eq. 4.4)

$$V_T = V_w + V_s + V_g \quad (\text{Eq. 4.5})$$

M_w : mass of water retained (kg)

M_s : mass of solids (kg)

M_g : mass of gas (kg)

M_T : Total mass of mixture (kg)

V_w : volume of water retained (m³)

V_s : volume of solids (m³)

V_g : Volume of gas (m³)

(Radcliffe & Šimůnek, 2010)

A separate experiment was also set-up to investigate the pozzolanic nature of the mixtures caused by hydration. A sample of 200 g (replicated 3 times) of each mixture was oven dried at 105 °C for 24 hours and then reweighed to determine water content. The same mixture was further saturated with distilled water, oven dried at 105 °C for 24 hours and then reweighed to determine water content. The saturation with distilled water, oven drying at 105 °C for 24 hours and reweighing to determine water content was carried out five times (this was done assess the locking up of water by hydration). After these wetting and drying cycles the mixture was then dried at 120 °C for 24 hours and then reweighed to determine water content. Further drying was carried out by increasing the temperature by 10 units, that is to 130, 140, 150 and 160 °C. Increasing the temperature was an attempt to forcefully remove all the water added in the mixtures including water molecules involved in hydration.

4.3 Results and Discussions

4.3.1 Particle size analysis of fine and gasification ash

Fine ash generally did not have a diverse particle size distribution (Fig. 4.1). Particles ranging between 100 - 250 μm were consistently the dominant fraction of fine ash (CV = 9.2%). Particles greater than 250 μm were less than 10% of the total oven dry mass and the contribution of these

particles was more variable. Particles ranging between 50 – 100 μm constituted 34.6% (CV = 15.1) of the total oven dry mass. These results slightly differed from Mahlaba *et al.* (2011) findings, who established that particles falling between 5 μm and 75 μm were the dominant fraction (60%) of fine ash. These authors further found that particles that fell between 1 – 5 μm and 75 – 425 μm constituted 16 and 30% respectively.

Particles greater than 1 mm dominated the particle size distribution of the gasification ash (Fig. 4.1). On average particles greater than 1 mm constituted more than 75 % of the total oven dry mass. These results were in agreement with Matjie *et al.* (2008) who found that gasification ash particles are heterogenous varying from 4 to 75 mm. The contribution of particles greater than 1 mm to the total mass was also consistent and the variation between the 30 replicates in the end exhibited a variation of only 6.6%. The contribution of particles less than 1 mm was variable and repeated analyses of these fractions yielded CV values greater than 34% for the size fraction smaller than 1 mm. Particles less than 2 mm was on average 36.2% of the total mass of the gasification ash and the replicates exhibited a 12% variation.

It was clear from the results (Fig. 4.1) that none of the ashes alone are ideal growth media with respect to having readily available water and maintaining adequate aeration. Fine ash constitutes finer particles that are capable of increasing water holding capacity through smaller pore spaces and a larger surface, while gasification ash seemed to be macroporous a property that is weak in holding water against gravity.

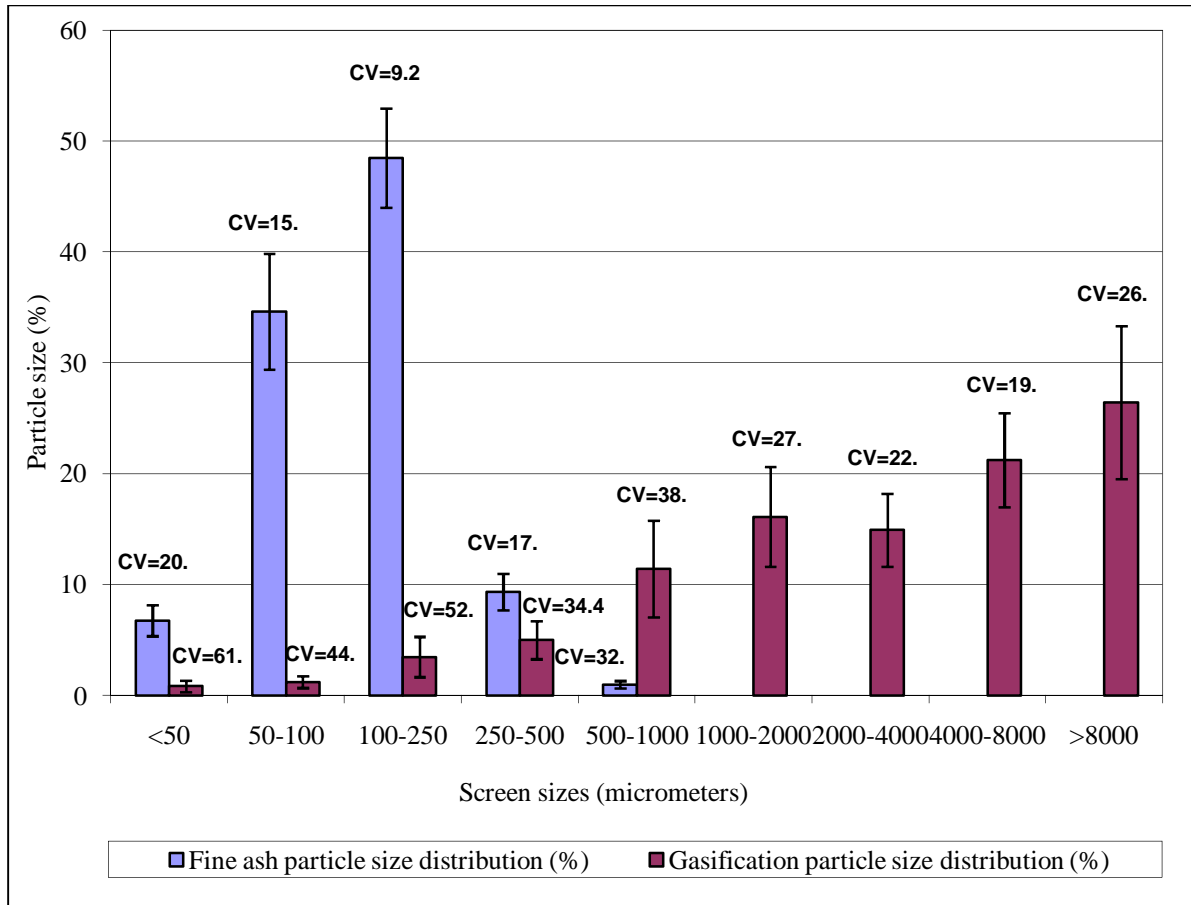


Fig.4. 1: Particle size distribution of fine and gasification ash. The error bars are standard deviations. The values above the bars are the coefficient of variance (n = 30).

4.3.2 Changes in water holding capacity of fine ash and gasification ash over time

The water holding capacity, as reflected by the gravimetric and volumetric water content of the fine ash after free drainage and vacuum extraction, increased from eluviation cycles 1 to 5 by 8.09% (calculated by dividing the difference between the water contents of the 1st and 5th eluviation cycles by the water content of the 1st eluviation cycle and multiply by 100%), gradually decreased by 10.9% (calculated by dividing the difference between the water contents of the 6th and 10th eluviation cycles by the water content of the 6th eluviation cycle and multiply by 100%) from eluviation cycles 6 to 10 (Fig. 4.2 a and b). The overall decrease in water retention over 10 eluviation cycles was 3.78% (calculated by dividing the difference between the water contents of the 1st and 10th eluviation cycles by the water content of the 1st eluviation cycle and multiply by 100%). This difference was quit small because the material maybe just settled,

initially the hydration was more significant and masked the settling of particles and decrease in overall pore volume.

The overall water holding capacity of fine ash was significantly higher than in gasification ash (Table 4.3). In this study it was attributed to the dominant 50 - 250 μm particle range which was lacking in the gasification ash. Gasification is dominated by particles larger than 1 mm (Fig. 4.1) Jala & Goyal, (2004). Attributable water retention by fine ash to the fine particles of the material with an average diameter of less than 200 μm . Furthermore fine ash contains pozzolanic materials like calcium silicate hydrate ($\text{Ca}_9\text{Si}_6\text{O}_{18}(\text{OH})_6 \cdot 8(\text{H}_2\text{O})$) and Strätlingite ($\text{Ca}_2\text{Al}_2\text{SiO}_2(\text{OH})_{10} \cdot 3\text{H}_2\text{O}$). From the chemical formula it is clear that water will be locked up by these minerals that formed resulting in the retention of water molecules (Haynes, 2009). The contribution of hydration on water retention is further discussed in section 4.3.3.

Variable but gradual increased by 10.61% (calculated by dividing the difference between the water contents of the 1st and 7th eluviation cycles by the water content of the 1st eluviation cycle and multiply by 100%) in gravimetric water content was observed with gasification ash from eluviation cycles 1 to 7 and a rapid drop by 15.91% (calculated by dividing the difference between the water contents of the 8th and 10th eluviation cycles by the water content of the 8th eluviation cycle and multiply by 100%) during cycles 8 to 10 (Fig. 4.2c and d) without a definite decrease in the volume of the material. The overall decrease in water retention over 10 eluviation cycles was 7.0%. The gasification ash therefore settled more over time and resulted in a greater decrease in water retention over time. The difference between the overall drop in water content between the fine and gasification was 3.22%. Gasification ash particles contain a large number of completely empty spheres and spheres packed with other numerous small spheres or crystals (Trivedi & Sud, 2002) that may retain water to a certain extent.

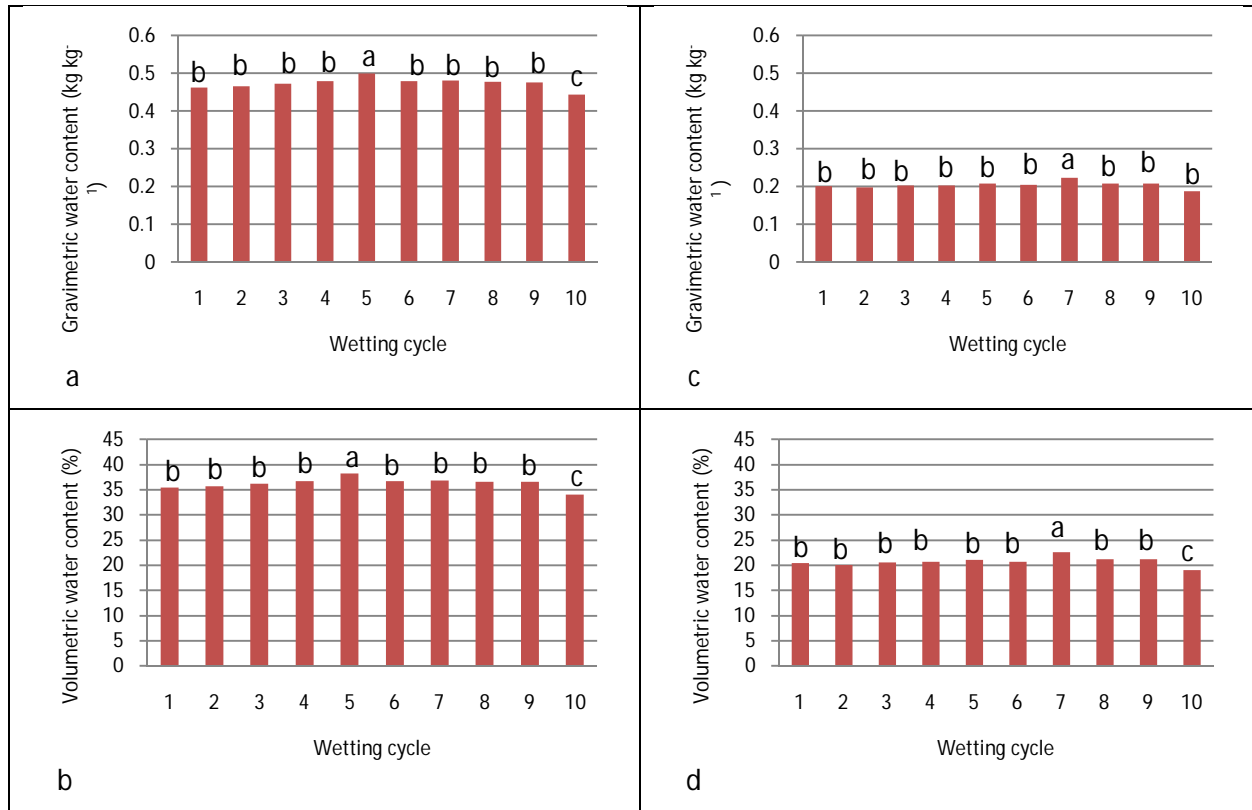


Fig.4. 2: a) Change in gravimetric water content (kg kg⁻¹) of fine ash from the 1st to 10th eluviation cycle, b) Volumetric water content (%) of fine ash from the 1st to 10th eluviation cycle, c) Gravimetric water content (kg kg⁻¹) of gasification ash from 1st to 10th eluviation cycle, d) Volumetric water content (%) of gasification ash from the 1st to 10th eluviation cycle.

4.3.3 The contribution of water locked-up in hydrated minerals to water retention

The mass of fine ash gradually increased from 82.5 to 84.9 g (2.9% increase) with repeated saturation with distilled water followed by oven drying at 105 °C (Fig. 4.3 a). The increase in water holding capacity was attributed to the hydration of minerals present in the ash. Possible hydrated solid phases are calcium silicate hydrate (Ca₉Si₆O₁₈(OH)₆·8(H₂O)), Strätlingite (Ca₂Al₂SiO₂(OH)₁₀·3H₂O) and ettringite (Ca₆Al₂(SO₄)₃(OH)₁₂·26(H₂O))(Matschei *et al.*, 2007). Attempting to remove this water through oven drying by increasing the temperature from 120 to 160 °C was slightly successful. The mass reduced from 84.9 to 82.6 g (2.7% reduction). The mass at 105 °C increased from 82.5 to 84.9 g and this was 2.9% increase and only 0.2% remained in the mixture (100% fine ash) due to pozzalinity. The addition of sludge gradually enhanced the loss of water in fine ash despite the continuous saturation. For example, the addition of sludge in mixture 46 (50% fine ash, 0% gasification ash and 50% sludge) increased water loss, the mass of the mixture reduced from 83.7 to 77.5 g (7.4% reduction) (Fig. 4.4 c) and

this was caused by loss of water held up by the sludge when the temperature was increased (this was result of combustion).

With gasification ash the mass varied but did not change significantly despite continuous saturation and temperature increase (Fig. 4.3 b) and this was because of the combustion. The bottom line here was that gasification ash had no pozzalanic effect. The addition of water increased the mass of the mixture from 108.0 to 108.3 g (0.3 % increase) and oven drying reduced the mass from 108.3 to 107.8 g (0.5% reduction) (Fig. 4.3 b) The addition of sludge significantly increased water loss, for example, mixture 51 had its mass reducing from 19.0 to 14.2 g (25% decrease) despite continuous addition of water (Fig 4.3 d). The drastic reduction in the mass of the mixture could be caused by loss of water held up by the sludge when the temperature was increased (The material volatilized as CO₂ at these high temperatures).

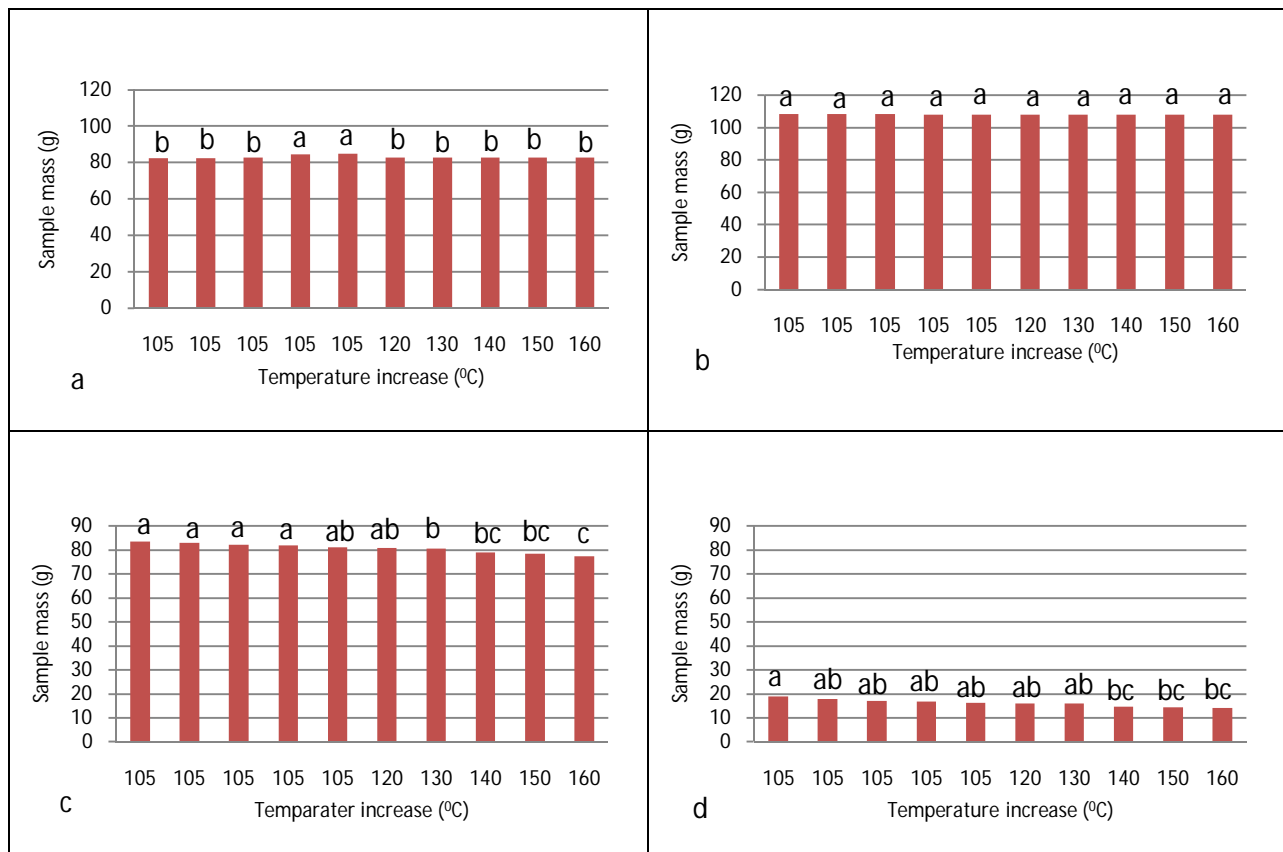


Fig.4. 3: a) Assessment of water retention in fine ash (mixture 1), b) Assessment of water retention in gasification ash (mixture 11), c) Assessment of water retention in mixture 46 with 50% fine ash and 50% sludge and d) Assessment of water retention in mixture 51 with 50% gasification ash and 50% sludge

4.3.4 Change in water holding capacity of the mixtures over time

Seemingly, a combined increase of fine ash and sludge from 10 to 50% content increased water holding capacity of the mixtures (Fig.4.4 a and b). An addition of 50% sludge to 50% fine ash (mixture 46) appreciably increased the water content of the mixture after the first eluviation cycle. The addition of the same amount of sludge (50%) to 50% gasification ash (mixture 51) increased water retention but the increase was less than in mixture 46. Mixture 46 (50% fine ash and 50% sludge) retained the highest water over all combinations and mixture number 11 (100% gasification ash) had the least water holding capacity after the first eluviation cycle. Other mixtures without sludge (mixtures 1 to 10) showed a constant decrease in water retention with an increase in gasification ash and a decrease in fine ash content.

After the tenth eluviation cycle water holding capacity of mixture 51 (50% gasification ash and 50% sludge) decreased significantly from the first eluviation cycle and remained the mixture to hold the least water, followed by mixtures 11 (100% gasification ash), 12 (90% gasification ash and 10% sludge), 30 (80% gasification ash and 20% sludge), 38 (70% gasification ash and 30% sludge) and 45 (60% gasification ash and 40% sludge) after the tenth eluviation cycle (Table 4.1, Fig. 4.4 c and d). This indicated that Sludge addition does not increase the water holding capacity of the gasification ash much. Mixture 46 (50% fine ash and 50% sludge) lost

Table 4.1: Mixtures with highest and lowest water holding capacities (WHC).

Mixtures with highest WHC	Description of mixtures	WHC after eluviation cycle 1 (kg kg ⁻¹)	WHC after eluviation cycle 10 (kg kg ⁻¹)	Mixtures with lowest WHC	Description of mixtures	WHC after eluviation cycle 1 (kg kg ⁻¹)	WHC after eluviation cycle 10 (kg kg ⁻¹)
1	100% FA, 0% GA & 0% SL	0.46	0.44	11	0% FA, 100% GA & 0% SL	0.20	0.19
22	80% FA, 0% GA & 20% SL	0.71	0.55	12	0% FA, 90% GA & 10% SL	0.27	0.20
31	70% FA, 0% GA & 30% SL	0.88	0.65	30	0% FA, 80% GA & 20% SL	0.37	0.22
39	60% FA, 0% GA & 40% SL	0.98	0.65	38	0% FA, 70% GA & 30% SL	0.51	0.24
40	50% FA, 10% GA & 40% SL	0.96	0.62	45	0% FA, 60% GA & 0% SL	0.61	0.26
46	50% FA, 0% GA & 50% SL	0.99	0.63	51	0% FA, 40% GA & 0% SL	0.80	0.31

Note: FA = fine ash, GA = gasification ash and SL = sludge

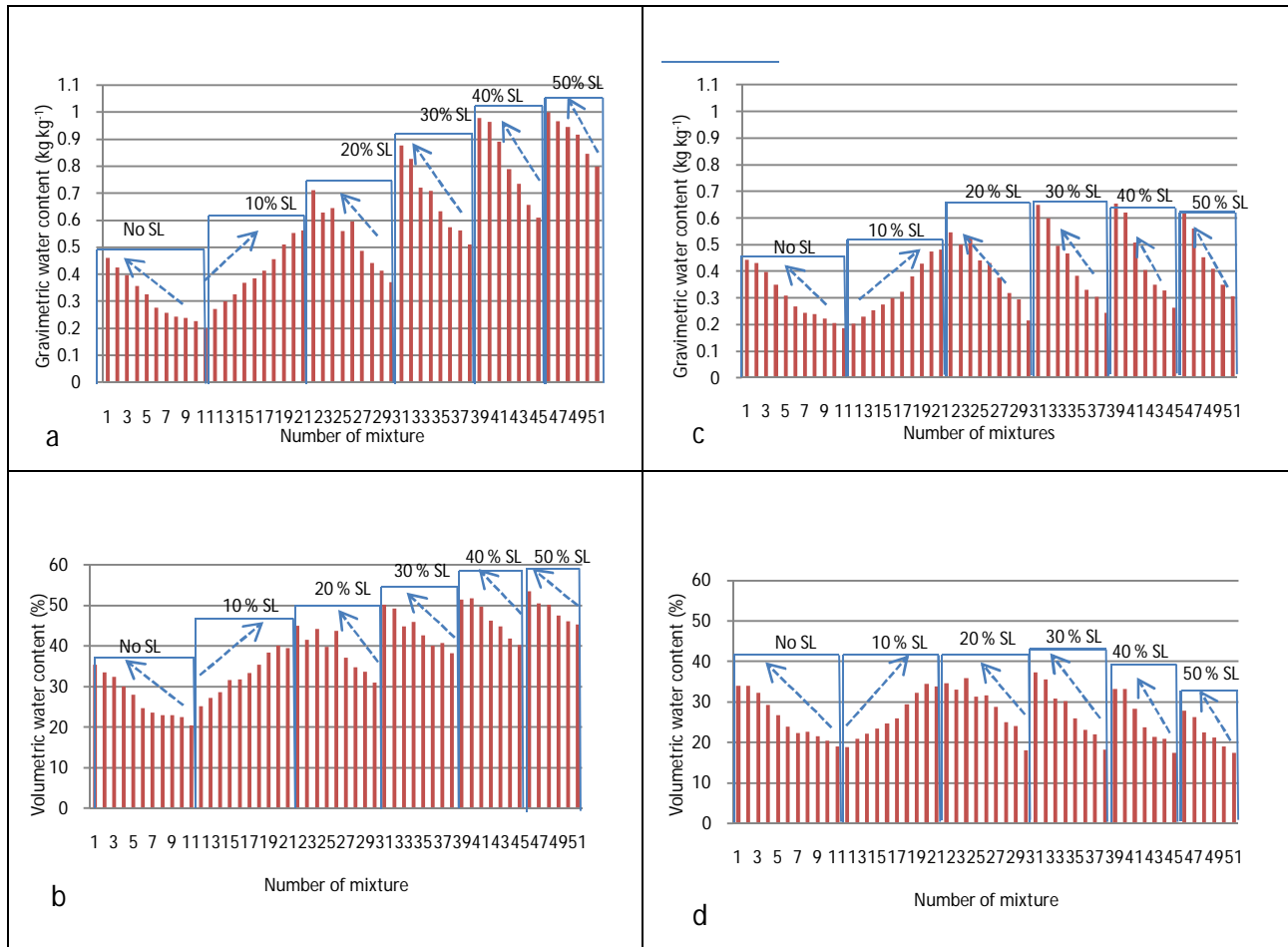


Fig.4. 4: a) Gravimetric water content (kg kg^{-1}) of the various mixtures after the 1st eluviation cycle, b) Volumetric water content (%) of the various mixtures after the 1st eluviation cycle, c) Gravimetric water content (kg kg^{-1}) of the various mixtures after the 10th eluviation cycle d) Volumetric water content (%) of the various mixtures after the 10th eluviation cycle. The arrows indicate an increase in fine ash content.

its moisture content significantly after the tenth eluviation cycle (Fig. 4. d, e and f). Mixtures 31, 39, 40 and 46 maintained their gravimetric water content above 0.6 kg kg^{-1} even after the tenth eluviation cycle; while all other mixtures had their moisture content falling lower than 0.6 kg kg^{-1} (Table 4.1, Fig. 4.4 c and d). Mixture 31 (70% fine ash and 30% sludge) remained with the highest percent gravimetric and volumetric water holding capacity after the tenth eluviation cycle followed by mixtures 24 (60% fine ash, 20% gasification ash and 20 % sludge) and 32 (60% fine ash, 10% gasification ash and 30% sludge). Mixtures without sludge and dominated by by gasification ash, 5 to 11 generally maintained almost the same gravimetric and volumetric water content even after the tenth eluviation cycle.

It was evident that adding sludge to both fine and gasification ash increased both gravimetric and volumetric water content of the ashes, but a mixture of 50% gasification ash and 50% sludge retains less water compared to a similar mixture of 50% fine ash and 50% sludge after the first eluviation cycle. The former (gasification – sludge mixture) lost more water than the latter (fine ash – sludge mixture) after the tenth eluviation cycle.

The increase in water retention in the mixtures of fine ash was an attribute of fine ash particles contributing to microporosity of the medium, the pozzolanic nature and hydration of minerals present such as phyllosilicates and other hydrated minerals (layered double hydroxides) (Zevenbergen *et al.*, 1999, Dermatas & Meng, 2003). Furthermore, weathering of ash to secondary minerals by the wetting and drying cycles exposed new mineral phases and increased the reactive surface area that played an important role in the development of CEC and AEC. The reactive surfaces contributed not only to cation and anion exchange but also to water holding capacity (Zevenbergen *et al.*, 1999). Sludge amendment greater than 20%, did not drastically improve the water holding capacity of the mixtures. This is because humified or stabilized sludge generally contributes more to CEC than acting as a surface for water retention. The negative effect of gasification ash on water holding capacity was due to the fact that gasification ash is macroporous in nature with an average particle size of greater than 1 mm dominant.

4.4 Conclusion

Gasification ash was found to be macroporous with average particle sizes of greater than 1 mm dominating and fine ash was dominated by particle sizes between 100 and 250 μm . The addition of sludge (10 to 50%) significantly increased water content of the mixtures (mixtures 12 to 51 described in chapter 3). Increasing fine ash (10 to 100%) as well increased the water holding capacities of mixtures 22(80% fine ash, 0% gasification ash and 20% sludge), 31(70% fine ash, 0% gasification ash and 30% sludge), 39(60% fine ash, 0% gasification ash and 40% sludge) and 46(50% fine ash, 0% gasification ash and 50% sludge) (dominated by particles between 100 and 250 μm) for the first eluviation cycle. Alternatively, increasing gasification ash drastically reduced the water holding capacity of mixtures 11(0% fine ash, 100% gasification ash and 0% sludge), 12(0% fine ash, 90% gasification ash and 10% sludge), 30(0% fine ash, 80% gasification ash and 20% sludge), 38(0% fine ash, 70% gasification ash and 30% sludge), 45(0% fine ash, 60% gasification ash and 40% sludge) and 51(0% fine ash, 50% gasification ash and

50% sludge) dominated by particles greater than 8mm after the first eluviation cycle. After the tenth eluviation cycle mixture 31 retained the highest volumetric water content (37.2 %) followed by mixtures 24 (60% fine ash, 20% gasification ash and 20% sludge) with 35.9 % and 32 (60% fine ash, 10% gasification ash and 30% sludge) with 35.6 % volumetric water content. With gravimetric water content mixtures 31 and 39 retained the highest water followed by mixtures 32, 40 (50% fine ash, 10% gasification ash and 40% sludge) and 46. Mixtures 11, 12, 30, 38, 45 and 51 exhibited the lowest water holding capacities even after the tenth eluviation cycle. Mixtures 1 to 5 (described in chapter 3) had increased gravimetric and volumetric water content after the tenth eluviation cycle due to the dominant particles between 100 and 250 μm and pozzolanic nature through the hydration of the siliceous and aluminous material like calcium silicate hydrate ($\text{Ca}_9\text{Si}_6\text{O}_{18}(\text{OH})_6 \cdot 8(\text{H}_2\text{O})$) and Strätlingite ($\text{Ca}_2\text{Al}_2\text{SiO}_2(\text{OH})_{10} \cdot 3\text{H}_2\text{O}$), while mixtures 6 (50% fine ash, 50% gasification ash and 0% sludge) to 11 (dominated by particles greater than 8 mm) had reduced water holding water capacity. It was evident that mixtures; 17, 18, 19, 20, 21, 22, 23, 24, 25, 31, 32, 33, 39, 40 and 46 (described in chapter 3) with 50 to 80% fine ash, 0 to 40% gasification ash and 10 to 50 % sludge were dominated by particle diameters between 0.1 to 0.250 mm can provide plant available water.

CHAPTER 5: NITROGEN DYNAMICS IN SLUDGE-COAL ASH MIXTURES AS INFLUENCED BY WEATHERING

5.1 Introduction

Sasol fine and gasification ash contain lower total nitrogen (less than 0.04%) content relative to the N content for sludge (7.9%) as characterized by Sasol (2008). South African municipal wastewater and sludge contain variable amounts of organic N, nitrate (NO_3^-), nitrite (NO_2^-) and ammonium (NH_4^+) but the organic form of N in sludge is dominant and needs to be mineralized before it becomes available to plants (Snyman & Van der Waals, 2004). Mineralization can be described as the conversion of organic nitrogen into plant available inorganic forms (NH_4^+ and NO_3^-) with the help of microbial activities (Deenik, 2006). Essential processes involved in mineralization such as ammonification (the transformation of organic N to NH_4^+) and nitrification (the oxidation of NH_4^+ to NO_3^-) liberate N from organic matter and make it available to plants and microbes. However, mineralized N is also subjected to leaching and denitrification losses (Vernimmen *et al.*, 2007). Sasol biological sludge contains 82.4 % organic matter as characterized by Sasol (2008) that can be subjected to mineralization.

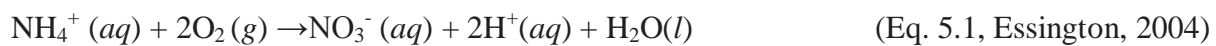
Ammonification process

Amino acids are the major sources of organic N and precursor of ammonium (NH_4^+) production (Pietri & Brookes, 2008). During N mineralization process, microorganisms (*Bacillus*, *Clostridium*, *Proteus*, *Pseudomonas*, and *Streptomyces*) attack humic compounds and in the process amino compounds (R-NH_2) are formed and further hydrolyzed producing N as NH_4^+ . This microbial transformation of organic N to NH_4^+ is termed as ammonification (Brady and Weil, 2008). This process is affected by pH. Pietri and Brookes (2008) reported that the optimum pH for ammonification ranges from 6.0 to 8.0.

Nitrification process

This process occurs under aerobic conditions and oxidizes NH_4^+ to NO_3^- (summarized in Eq. 5.1) Nitrate results from the oxidation of nitrite (NO_2^-) which in turn is a product of NH_4^+ oxidation (Kieber *et al.*, 2005). The conversion of NH_4^+ to NO_2^- is facilitated strictly by aerobic autotrophic bacteria (*Nitrosomonas*, *Nitrosolobus* and *Nitrospira*) and the formation of NO_3^- from NO_2^- is made possible by another group of autotrophs, *Nitrobacter* (Mengel and Kirkby, 2001 & Brady

& Weil, 2008). The process is catalyzed by enzymes contained in the microorganisms. The bacteria contain the enzyme ammonium monooxygenase that oxidizes NH_4^+ to hydroxylamine which then is oxidized to NO_2^- by hydroxylamine oxydoreductase and eventually the NO_2^- is oxidized to NO_3^- by nitrite oxydoreductase (Canfield, *et al.*, 2010). Nitrate can also be formed by the oxidation of ammonia (NH_3) by autotrophic bacteria. In this case NH_3 is initially oxidized to NO_2^- then to hydroxylamine (NH_2OH) and eventually to NO_3^- . Heterotrophic microorganisms can also produce NO_3^- by using NH_3 as an electron donor. This enables them to oxidize NH_3 to NO_3^- (Mengel and Kirkby, 2001).



During nitrification, pH remains as one of the factors that control this process (Vernimmen *et al.*, 2007). pH conditions that are slightly acidic to neutral are preferred by the nitrifying bacteria (Mengel and Kirkby, 2001). Shamma, (1986) reported that the optimum pH for *Nitrosomonas* is 8.5 to 8.8 and that for *Nitrobacter* is 8.3 to 9.3. The activities of *Nitrosomonas* cease at pH 9.6. Under highly alkaline conditions, NH_3 becomes a dominant inorganic N species and at high concentrations it has a negative effect on microbial activity and basically poisons these systems. For example, important nitrifying bacteria, *Nitrobacter*, are inhibited by high NH_3 concentrations. Temperature also affects nitrification; Shamma (1986) stated that nitrification rate is a function of temperature within the range of 5 to 35° C while the maximum rate occurring at 30 °C. However, Sierra, (2002) claimed that the formation of both NO_2^- and NO_3^- is strongly inhibited at temperatures of 10°C or less because at low temperatures biostatic effect affects the activities of nitrifiers. Redox reactions also affect the formation of NH_4^+ , NO_3^- and NO_2^- . Carbon (C) contained in organic matter is an excellent donor of electrons while NO_3^- is an electron acceptor. An abundance of electrons reduces NO_3^- to NH_4^+ (Reddy *et al.*, 2000). In this case a low C/N ratio would favour mineralization (Mengel & Kirkby, 2001).

Immobilization process

This process refers to the assimilation of inorganic N. It involves the transformation of NO_3^- to NH_4^+ and then to organic forms. Causes of this process include high C/N ratio that encourages reduction of NO_3^- to NH_4^+ and when there is short supply of N by organic matter forcing the

microbes to search for NO_3^- to NH_4^+ from soil solution. Immobilization and mineralization occur simultaneously (Mengel & Kirkby, 2001 & Brady & Weil, 2008).

Denitrification process

Denitrification is an anaerobic process by which heterotrophic bacteria reduce NO_3^- to gases such as NO , NO_2 and N_2 . Another contributing process to N loss is volatilization which occurs mainly at high pH (alkaline conditions) where NH_4^+ is transformed to NH_3 (Eq. 5.2) (DinÇer & Kargi, 2000 & Brady & Weil, 2008).



In this chapter it was hypothesized that the ashes will not provide any species of nitrogen and sludge will provide all the plant inorganic nitrogen (NH_4^+ , NO_3^- and NO_2^-) in the mixtures. The main purpose therefore was to assess the contribution of Sasol sludge, fine and gasification ashes to the production of NH_4^+ , NO_3^- and NO_2^- in sludge ash mixtures as influenced by weathering. It was envisaged that all the processes involved in N mineralization would occur due to the conducive conditions brought about by sludge and created aerated conditions. Further, the production of these N species would provide insight to microbial activities.

5.2 Materials and methods

5.2.1 Selection of mixtures

The fifty-one sludge-coal ash mixtures were divided into six groups based on sludge content (described in chapter 3, Fig. 3.1-3.3). From each group three mixtures were selected based on fine and gasification ash content. In this case all three mixtures had the same sludge content but varying quantities of both fine and gasification ashes (Table 5.1). The purpose was to select samples that represented the various treatments the best. The analysis in these samples was done to assess the measured inorganic N (ammonium + nitrate + nitrite) and individual N species; ammonium (NH_4^+), nitrate (NO_3^-) and nitrite (NO_2^-) to calculated total inorganic N and NH_4^+ , NO_3^- and NO_2^- species in non selected mixtures. The calculation of total inorganic N and individual N species content in a mixture was based on the N contribution of the individual waste components; sludge, fine and gasification ashes. To calculate total inorganic N content in a

particular mixture, for example, the measured total inorganic N content of fine ash alone was multiplied by the percent content of fine ash in that mixture. Similarly the measured total inorganic N content of gasification ash alone was multiplied by the percent content of gasification ash in that mixture. The same procedure was followed to calculate the sludge contribution to inorganic N species content in the mixture. The calculated total inorganic N species content of that particular mixture was then obtained by summing the three products.

Table 5.1: Mixtures selected for inorganic nitrogen analysis

Group number	Selected mixtures	Fine ash content (%)	Gasification ash content (%)	Sludge content (%)
1 (0% sludge)	1	100	0	0
	6	50	50	0
	11	0	100	0
2 (10% sludge)	12	0	90	10
	17	50	40	10
	21	90	0	10
3 (20% sludge)	22	80	0	20
	26	40	40	20
	30	0	80	20
4 (30% sludge)	31	70	0	30
	35	30	40	30
	38	0	70	30
5 (40% sludge)	39	60	0	40
	42	30	30	40
	45	0	60	40
6 (50% sludge)	46	50	0	50
	48	30	20	50
	51	0	50	50

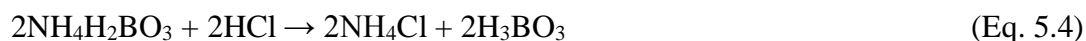
The total inorganic N and NH_4^+ , NO_3^- and NO_2^- were determined on selected pore volume solutions. These solutions were collected from the mixtures by applying vacuum of -10 kPa at the base of each column to remove some of interstitial water that remained in the mixtures after free drainage took place. The pore solutions were sampled 24 hours after free drainage stopped (Chapter 3, section 3.5). The pore volume solution was preferred to clean information about the N dynamics of the various mixtures because this solution has been in contact with the mixtures for longer time cover free drained solution because it was exposed to several chemical reactions for 24 hours before removal.

5.2.2 Determination of inorganic nitrogen (NH_4^+ , NO_3^- and NO_2^-)

The inorganic nitrogen was determined by means of Kjeldahl distillation described by Bremner (1965) and Tan (2005). A 5 ml aliquot of the solution was pipetted into a distillation flask and diluted with 20 ml of de-ionized water to a total volume of 25 ml. Twenty five millimeters of a strong alkali, 50 % sodium hydroxide (NaOH) freshly prepared on a mass bases was pipetted into the same distillation flask containing the diluted aliquot making a total volume of 50 ml. The NaOH was added to convert ammonium (NH_4^+) to ammonia (NH_3). The sample was swirled for a few seconds before 2 g of Devardas Alloy was added to reduce nitrate (NO_3^-) and nitrite (NO_2^-) to NH_3 . After the addition of the Devardas Alloy the flask was immediately connected to a Büchi 321 Kjeldahl distiller (Manufacturer – LABEQUIP Ontario, Canada) and distilled for six min into a 500 ml beaker containing 25 ml of 0.6 M boric acid (H_3BO_3) to collect NH_3 . The 0.6 M H_3BO_3 was prepared by dissolving 200 g using 3000 ml of deionised water and added a combination of 57 ml methylene blue ($\text{C}_{16}\text{H}_{18}\text{ClN}_3\text{S}$) and 117 ml methyl red ($\text{C}_{15}\text{H}_{15}\text{N}_3\text{O}_2$) as indicator then made up to volume (5000 ml). The NH_3 plus H_3BO_3 during distillation formed ammonium borate ($\text{NH}_4^+ + \text{H}_2\text{BO}_3^-$).



The indicator changed to a green colour indicating the completion of NH_3 distillation. The 6 min elapsed when the beaker was almost half full (approximately 230 ml). A measuring cylinder was used to determine the volume of the distilled solution. To estimate total N the ammonium borate was back titrated using 0.01 M hydrochloric acid (HCl) to H_3BO_3 .



The colour changed at the end point of the titration from green to permanent faint pink (the colour of the H_3BO_3). To calculate total inorganic N in solution the volume (L) of HCl used to titrate the ammonium borate was multiplied by the H^+ (mol) added divided by the volume of aliquot (L), the outcome was multiplied by the volume of aliquot (L) and the product (mol L^{-1}) was divided by the dry mass (kg) of the mixture. The outcome ($\text{mol L}^{-1}/\text{kg mix}$) was multiplied

by N molar mass ($14.007 \text{ g mol}^{-1}$) then divided the product by 1000 g to convert the N to mg kg^{-1} .

5.2.3 Determination of ammonium (NH_4^+)

To determine NH_4^+ , a 5 ml aliquot of the same solution was pipetted into the distillation flask and diluted with 20 ml of de-ionized water pushing up to a total volume of 25 ml. The difference with the previous step was that no electron donor (reducing agent) was added (Devarda's alloy) to convert oxidized N to NH_3 . Twenty five millimeters of a 50 % NaOH solution (prepared on a mass bases) was pipetted into the same flask with the diluted aliquot to obtain a final volume of 50 ml. The flask was swirled for a few seconds to enhance chemical reaction. The NaOH was added to convert NH_4^+ to NH_3 . The flask was connected to the Büchi 321 Kjeldahl distiller and distilled for 6 min into a 500 ml beaker containing 25 ml of 0.6 M H_3BO_3 prepared as described above including the methylene blue and methyl red indicators. From this point, to determine NH_4 in the sample the same procedure described in section 5.2.2 was followed.

5.2.4 Indirect determination of nitrate (NO_3^-)

After the determination of NH_4^+ the flask with the aliquot was cooled to prepare for the determination of $\text{NO}_3^- + \text{NO}_2^-$ left in the aliquot. Two grams of the Devarda's Alloy was added into the same flask to convert the NO_3^- and NO_2^- to NH_4 and immediately connected to the Büchi 321 Kjeldahl distiller. The Büchi was turned on for the solution to start boiling and then switched off to recede, after which the distillation continued for 6 min into a 500 ml beaker containing 25 ml of 0.6 M H_3BO_3 prepared as described above including the methylene blue and methyl red indicators. A measuring cylinder was used to determine the volume of the distilled solution. The NH_4^+ accumulating plus H_3BO_3 during distillation formed ammonium borate which changed to a green colour indicating the completion of NH_4^+ distillation. A measuring cylinder was used to determine the volume of the distilled solution. To determine NH_4 the ammonium borate was back titrated using 0.01 M HCl. The colour changed at the end point of the titration from green to permanent faint pink which was the colour of the 0.6 M H_3BO_3 . To estimate $\text{NO}_3^- + \text{NO}_2^-$ represented by NH_4^+ the volume (L) of HCl used to titrate the ammonium borate was multiplied by the H^+ (mol) added divided by the volume of aliquot (L), the outcome was multiplied by the volume of aliquot (L) and the product (mol L^{-1}) was divided by the dry mass (kg) of the mixture.

The outcome ($\text{mol L}^{-1}/\text{kg mix}$) was multiplied by N molar mass ($14.007 \text{ g mol}^{-1}$) then divided the product by 1000 g to convert the NH_4^+ to mg kg^{-1} .

5.2.5 Indirect determination of nitrite (NO_2^-)

In this procedure $\text{NH}_4^+ + \text{NO}_3^-$ were determined (to subtracted from total inorganic N and remain with NO_2^-) by pipetting a separate 5 ml of aliquot into a distillation flask and diluted with 20 ml of de-ionized water increasing the volume to a total of 25 ml. Sulfamic acid (1 ml) was also pipetted into the same flask with diluted aliquot, swirled the flask for a few seconds to reduce NO_2^- to N_2 . After swirling only $\text{NH}_4^+ + \text{NO}_3^-$ were left. The Devarda's Alloy (2 g) was added to reduce the NO_3^- to NH_4^+ and 2 g of MgO was added to convert the NH_4^+ to NH_3 . The flask was then immediately connected to the Büchi and distilled to a volume of 50 ml into a 50 ml conical flask containing 10 ml of 0.6 M H_3BO_3 prepared as described above including the methylene blue and methyl red indicators. A measuring cylinder was used to determine the volume of the distilled solution. The NH_3 accumulating plus H_3BO_3 during distillation formed ammonium borate which changed to a green colour indicating the completion of NH_4^+ distillation. A measuring cylinder was used to determine the volume of the distilled solution. To determine NH_3 the ammonium borate was back titrated using $0.0025 \text{ mol L}^{-1}$ sulphuric acid (H_2SO_4). The colour changed at the end point of the titration from green to permanent faint pink which was the colour of the 0.6 M H_3BO_3 . To estimate $\text{NH}_4^+ + \text{NO}_3^-$ represented by NH_4^+ the volume (L) of HCl used to titrate the ammonium borate was multiplied by the H^+ (mol) added divided by the volume of aliquot (L), the outcome was multiplied by the volume of aliquot (L) and the product (mol L^{-1}) was divided by the dry mass (kg) of the mixture. The outcome ($\text{mol L}^{-1}/\text{kg mix}$) was multiplied by N molar mass ($14.007 \text{ g mol}^{-1}$) then divided the product by 1000 g to convert the NH_4 to mg kg^{-1} . Finally, NO_2^- concentration was calculated as the difference between total inorganic N ($\text{NH}_4^+ + \text{NO}_3^- + \text{NO}_2^-$) and the combination of ammonium and nitrate ($\text{NH}_4^+ + \text{NO}_3^-$).

5.3 Results and discussion

Generally, the inorganic N species, NH_4^+ and NO_2^- were detected in all selected mixtures (1 to 51) while NO_3^- was detected in mixtures 22 to 51 (Fig 5.1). The detection of only NH_4^+ and NO_2^- in all mixtures with no or low sludge content (0 to 10%) indicated that ammonification and the first part of oxidation (conversion of NH_4^+ to NO_2^-) occurred (Fig. 5.1)

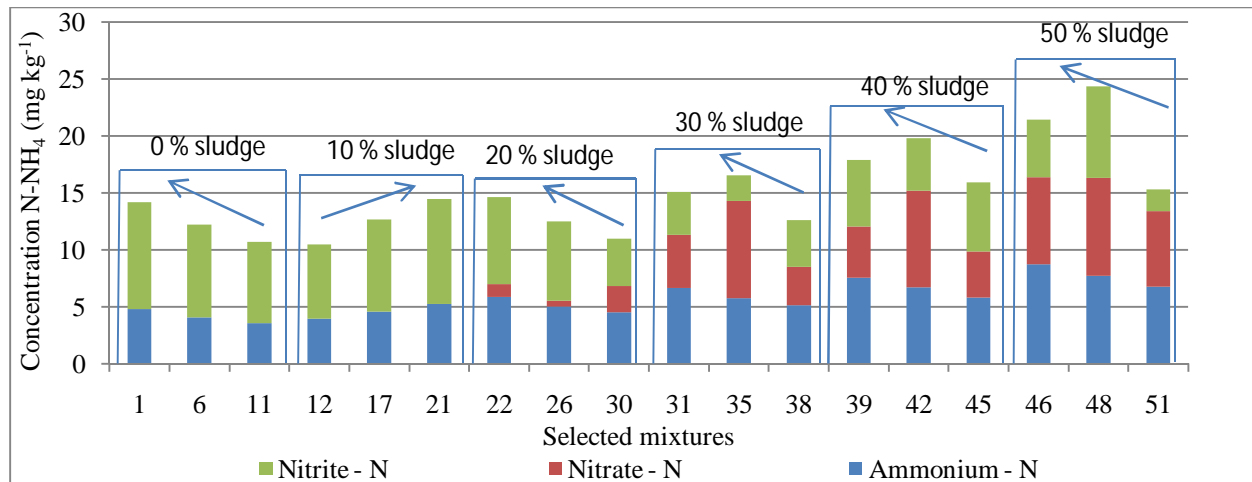


Fig.5. 1: Total inorganic N (NH_4^+ , NO_3^- and NO_2^-) released by selected mixtures calculated for ten eluviation cycles. The arrows indicate the increasing gradient in fine ash.

However, it seems that the second step of nitrification was inhibited in these mixtures. The initial high pH range of 9.4 to 11.7 of the mixtures, were above the optimum pH for microbially mediated ammonification (between 6.0 and 8.0) and for nitrification (between 7.5 to 8.0) generally reported (Pietri & Brookes 2008). From this it was deduced that the ammonifying bacteria (*Bacillus*, *Clostridium*, *Proteus*, *Pseudomonas*, and *Streptomyces*) and the *Nitrosomonas* bacteria potentially present were quite resilient and not severely inhibited / less affected by the extreme conditions (high pH and salinity). Under these conditions NO_3^- produced was close to zero (Fig. 5.1, mixtures) which indicates that *Nitrobacter* bacteria (converting NO_2^- to NO_3^-) were more sensitive and their activity inhibited. It could also be possible that denitrification of NO_3^- could have occurred resulting to low levels of the NO_3^- as a result of high pH and volatilization could also occur since the pH of the ash was close to the pKa (9.2) of $\text{NH}_4^+/\text{NH}_3$. Another reason why especial NO_2^- was detected in the mixtures with low sludge content was that Sasol inject significant amount of NH_3 into the electrostatic precipitators (in the steam plant) to assist in with the removal of fly ash (personal communication with Sasol). The ash is alkaline and it is expected that much would have volatilize, however, it is reasonable to expect that some nitrogen remained in the fly ash and transferred to fine ash since fine ash is made of 83% fly ash and 17% gasification ash and fine particles less than 250 μm (Mahlaba *et al.*, 2011). The NH_3 was converted by autotrophic bacteria into NO_3^- by initially oxidizing the NH_3 to NH_2OH then NO_2^- and finally to NO_3^- , however, conditions were not conducive (high pH 9.4 - 11.7) for the *Nitrobacter* bacteria to swiftly convert the NO_2^- to NO_3^- .

Nitrate was detected in mixtures containing 20 to 50% sludge (Fig. 5.1) because the sludge played a role in buffering the pH and the enrichment of ash with organic N increased mineralization and propensity for NO_3^- to be generated. The pH was reduced from a high and narrow range 11.3 - 11.7 to a lower and wider range 9.0 - 10.3 for the mixtures without sludge and from pH range; 9.4 – 10.0 to 7.7 – 8.2 for mixtures with sludge after the tenth eluviations cycle (Table 5.2). Such conditions were expected to be more conducive for higher *Nitrobacter* bacteria activity responsible for the formation of nitrate. However, a reduction in NO_2^- species (Fig. 5.1) was observed in mixtures containing 20 to 50% sludge and a gradually increase in the NH_4^+ and NO_3^- species. The increase in NH_4^+ and NO_3^- was a result of more N which was available for mineralization and suitable conditions for both ammonifying and the nitrification bacteria created by the reduction in pH and salinity over time. Hence the activities of microorganisms resulted to the quantities of NH_4^+ species in mixtures 35, 42, 46, 48 and 51 becoming equivalent on average to the quantities of NO_3^- species (Fig. 5.1). The reduction of NO_2^- , evident in mixtures 35 and 51 (Fig. 5.1), was due to high oxidation rate of NO_2^- to NO_3^- by *Nitrobacter*. Mixture 48 had the highest mineralized total N (24.4 mg kg^{-1}) than any other mixture and mixture number 12 had the least (10.5 mg kg^{-1}) for all the ten eluviation cycles. Mixtures with high percent gasification ash content, 11, 12, 30, 38, 45 and 51, had the least mineralized total N within their groups (0 to 50% sludge) due to the fact that it maintained a higher pH (11.7) which negatively impacted mineralization (Table 5.2).

Table 5.2: pH values in selected mixtures for the 1st and 10th eluviation cycles.

Eluviation cycle no.	Selected mixtures													
	1	11	12	17	22	30	35	38	39	42	45	46	48	51
1 (pH)	11.3	11.7	9.4	9.6	9.8	9.9	9.9	9.5	10.0	9.8	9.6	9.8	9.6	9.4
10 (pH)	9.6	9.0	8.2	8.3	8.1	8.0	8.0	8.1	7.7	7.7	7.8	7.8	7.7	7.8
1 (EC- mSm^{-1})	580	527	319	520	455	540	505	463	511	551	533	536	549	622
10 (EC- mSm^{-1})	118	88	140	122	222	148	227	191	319	302	243	284	329	220

Note: EC – electrical conductivity

Total inorganic N for the first eluviation cycle was significantly lower than the total inorganic N for the tenth eluviation cycle and this was evident in mixtures (12 to 51) with sludge (10 to 50%) (Fig. 5.2). The high inorganic N for the tenth eluviation cycle was due to the reduction in pH (9.4

– 10.0 to 7.7 – 8.3) of the mixtures over time and an increase in N mineralization. This pH range (7.7 – 8.3) was suitable for both ammonification and nitrification processes (Pietri & Brookes 2008). However, at this stage NO_3^- was close to zero (due to leaching) in all mixtures and the total inorganic N was made up of only NH_4^+ and NO_2^- . The lower total inorganic N for the first eluviation cycle was due to high pH (11.3 – 11.7) which created an overall non conducive environment for all the microbes. However, NH_4^+ and NO_3^- were mineralized more than NO_2^- at this stage due to high oxidation rate of NO_2^- to NO_3^- .

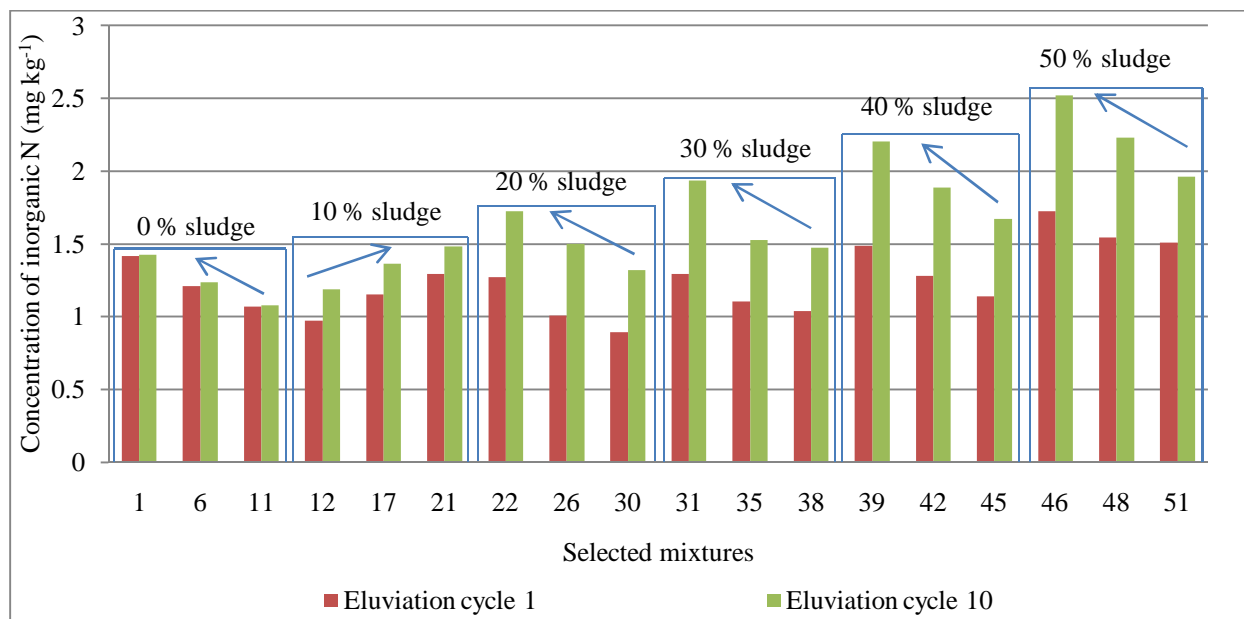


Fig.5.2: Inorganic N (NH_4^+ , NO_3^- and NO_2^-) released by selected mixtures calculated for eluviation cycles 1 and 10. The arrows indicate the increasing gradient in fine ash.

The total inorganic N for the first and the tenth eluviation cycles did not differ much in mixtures without sludge (Fig. 5.2). This was because of the small change in pH range (from 11.3 - 11.7 to 9.6 – 10.3) that inhibited mineralization. As discussed earlier on mixture 46 (50% fine ash and 50% sludge) appeared to have the highest mineralized total N compared to all mixtures for both the first and the tenth eluviation cycles, mixtures 11 (100% gasification ash) and 12 (0% fine ash, 90% gasification ash and 10% sludge) had the least total N for the tenth eluviation cycle and the first eluviations cycle respectively (Fig 5.2). For the first eluviation cycle mixtures 46 and 12 had 1.7 and 0.97 mg kg⁻¹ respectively while for the tenth eluviation cycle mixture 46 had 2.5 mg kg⁻¹ and mixture 11 had 1.1 mg kg⁻¹.

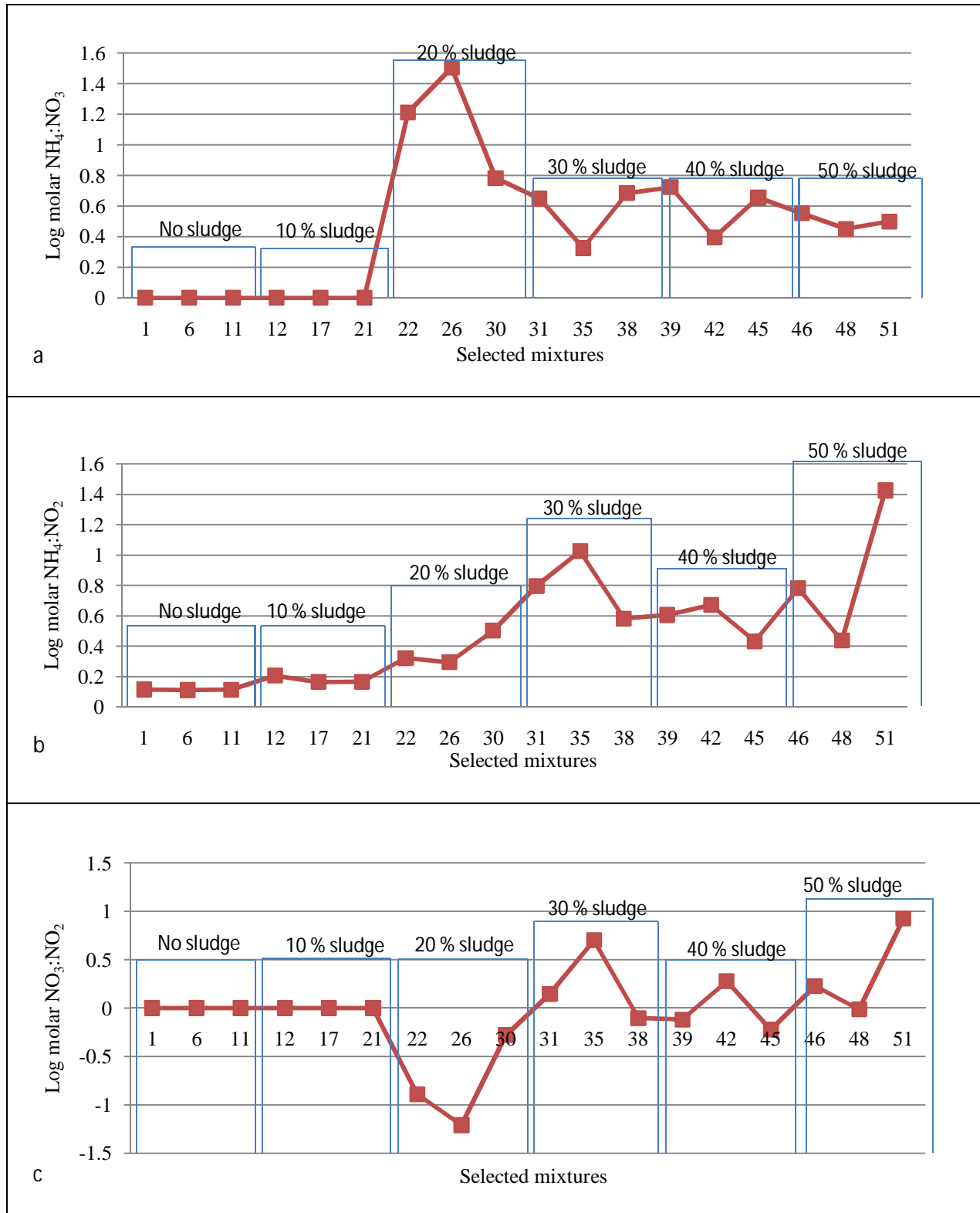


Fig.5. 3: a) Log molar $\text{NH}_4^+:\text{NO}_3^-$ ratio based on the ammonium and nitrate released after ten eluviation cycles, b) Log millimolar $\text{NH}_4^+:\text{NO}_2^-$ ratio based on the ammonium and nitrite released after ten eluviation cycles, c) Log millimolar $\text{NO}_3^-:\text{NO}_2^-$ ratio based on the nitrate and nitrite released after ten eluviation cycles.

The release of each N species was also viewed in relation to the release of the other species. The release of NH_4^+ was more favoured over the release of NO_2^- in all mixture over all eluviation cycles (Fig.5.3 b). This indicates that the conversion rate of NH_4^+ to NO_2^- was low. The release of NH_4^+ was more favoured over the release of NO_3^- in mixtures with 20% sludge but reduced in mixtures with 30 to 50% sludge slightly favouring NO_3^- due to the introduction of sludge that helped to reduce pH and salinity. At this stage the environment was conducive for bacteria converting NO_2^- to NO_3^- (Fig.5.3 a). The release of NO_3^- was favoured only in mixtures with 20% sludge and then fluctuated in mixtures with 30 to 50% sludge (Fig.5.3 c).

To assess the release trends of NH_4^+ , NO_3^- and NO_2^- eluviation cycles 1, 5, 8 and 10 marked as a, b, c and d respectively were selected based on changes they showed on the trends (Fig. 5.4). The mineralization of NH_4^+ seemed not to change much for all the eluviation cycles but increased with increase in sludge content. Nitrate in eluviation cycles 1 and 5 increased with increase in sludge due to a decrease in pH and an increase in the oxidation of NO_2^- to NO_3^- . The saw tooth characteristics for leaching 5 was mixtures dominated with gasification ash. It also seemed that there was flush or pulse of nitrate production during leaching 4 – 5. This lead to a decrease in NO_2^- for the first and the fifth eluviation cycles. An increase in NO_2^- was shown by the 8th and the 10th eluviation cycles. At this stage NO_3^- was reducing to lower levels. The rate of oxidizing NH_4^+ to NO_2^- was higher than the rate at which NO_2^- was converted to NO_3^- or most of the NO_3^- was leached at this point (this seemed that NO_3^- had flushed out).

The reduction in pH could be the result of carbonation where carbon dioxide (CO_2) liberated from the breakdown of the sludge formed carbonic acid (H_2CO_3) and The oxidation of NH_4 results in an increase in the concentration of NO_3^- and 2 moles of H^+ in the solution (Essington, 2004 & Brady & Weil, 2008). The biodegradation of sludge released dissolved organic carbon (DOC) that contained humified compounds such as fulvic acid (FA) and humic acid (HA) (Mulder & Cresser, 1994 & Singh & Agrawal, 2010) which also contributed to a reduction in the pH. The reduction in salinity for all the mixtures could be attributable to the leaching of the salts (Na^+ , K^+ , Ca^{2+} , Mg^{2+} , Cl^- , SO_4^{2-} , HCO_3^- , CO_3^{2-} , and NO_3^-) from the first to the tenth eluviation cycles (Mulder & Cresser, 1994, Li & Shuman 1997 & Sparks 2004). Electrical conductivity (EC) and elemental release will be discussed in the following chapter (chapter 6).

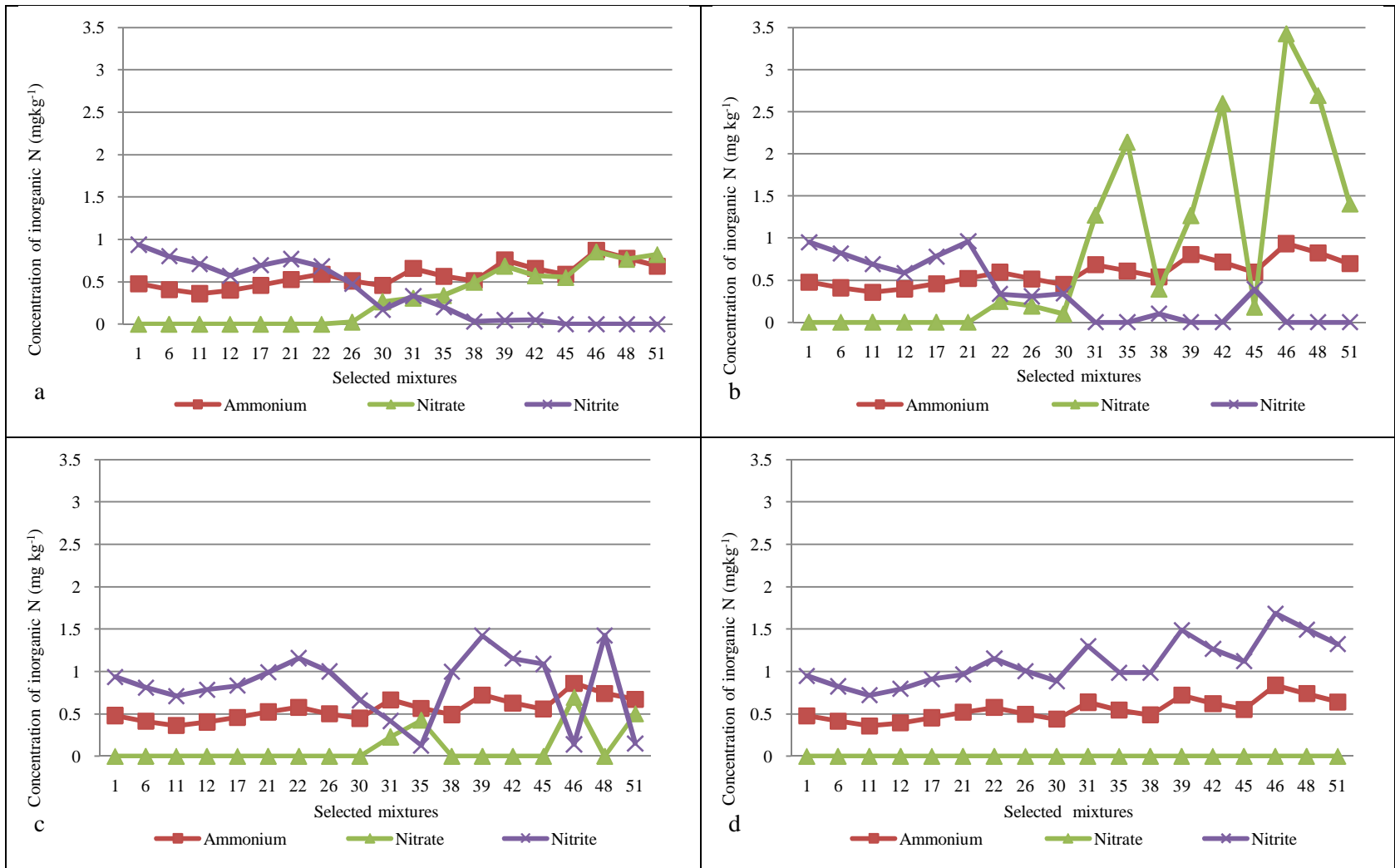


Fig.5. 4: NH_4^+ , NO_3^- and NO_2^- release trends for selected eluviation cycles; 1, 5, 8 and 10 in a, b, c and d respectively (expressed as N).

5.4 Conclusion

The extreme conditions (caused by high pH and salinity) of mixtures with zero and 10% sludge (mixtures 1 to 21 described in chapter 3) negatively affected the nitrifying bacteria (*Nitrobacter*) and as a result only NH_4^+ and NO_2^- nitrogen species were detected and no nitrate. The addition of sludge moderated these ash extreme conditions by reducing the pH from a higher range (11.7-8.3) to a lower range (10.3-7.6) and salinity from a higher range ($622\text{-}95\text{ mSm}^{-1}$) to a lower range ($415\text{-}88\text{ mSm}^{-1}$) of all mixtures (chapter 6) with 20 to 50% sludge. The lower pH range increased the oxidation of NO_2^- to NO_3^- . The NO_3^- and NH_4^+ species were mostly contributed by sludge while fine ash contributed more to the NO_2^- species. This was because the purposely added NH_3 by Sasol to enhance the removal of fly ash in the processing plant was converted to NO_2^- and the oxidation rate of this species to NO_3^- was minimal due to the extreme conditions caused by high pH and salinity. Mixtures 35 (30% fine ash, 40% gasification ash and 30% sludge), 42 (30% fine ash, 30% gasification ash and 40% sludge), 46 (50% fine ash, 0% gasification ash and 50% sludge), 48 (30% fine ash, 20% gasification ash and 50% sludge) and 51 (0% fine ash, 50% gasification ash and 50% sludge) had high amounts of NH_4^+ and NO_3^- and relatively little NO_2^- . These mixtures provided plant available NH_4^+ and NO_3^- desired in a functional growth media. Mixture 48 had the highest mineralized total inorganic N (24.4 mg kg^{-1}) compared to all mixtures and for all eluviation cycles, while mixture 12 (0% fine ash, 90% gasification ash and 10% sludge) exhibited the least (10.5 mg kg^{-1}). Mixtures 11 (0% fine ash, 100% gasification ash and 0% sludge), 12 (0% fine ash, 90% gasification ash and 10% sludge), 30 (0% fine ash, 80% gasification ash and 20% sludge), 38 (0% fine ash, 70% gasification ash and 30% sludge), 45 (0% fine ash, 60% gasification ash and 40% sludge), 51 (0% fine ash, 50% gasification ash and 50% sludge) had the lowest inorganic N within their groups due to high gasification content.

CHAPTER 6: ELEMENTAL DETERMINATION IN SLUDGE, FINE AND GASIFICATION ASHES, ELEMENTAL RELEASE, SALINITY AND pH OF MIXTURES

6.1 Introduction

Industrial sludge contains a significant amount of organic nitrogen (N), phosphorus (P), calcium (Ca), magnesium (Mg), potassium (K), sulphur (S) and trace elements which makes it a good source of nutrients for plants (Rechcigl, 1995 & Wong & Su, 1997). Ash as well is rich in essential plant nutrients listed for sludge, sodium (Na), boron (B), aluminium (Al), silicon (Si) and numerous trace elements as residues from the coal source (Zevenbergen *et al.*, 1999, Dermatas & Meng, 2003, Junkowski *et al.*, 2006, Bendz *et al.*, 2007.). The Al and Si are the basic building blocks necessary for the formation of clay minerals (phyllo silicates) and other hydrated minerals, for example, layered double hydroxides (Zevenbergen *et al.*, 1999, Dermatas & Meng, 2003) that contribute to chemical reactivity and fertility of the ash. While sludge has a high content of organic carbon that ash is poor in and also provides plant available N and P (Snyman & Van der Waals, 2004, Snyman & Herselman, 2006). Therefore, amending ash with sludge does not only alter the adverse properties it has but also build a soil-like matrix that is capable of providing plant available nutrients in correct quantities (Rendell & McGinty, 2010).

The release of the elements from the sludge-ash matrix is important for plant uptake but there are several factors that control their release. Amongst them pH remains the master variable that governs elemental mobility processes (Bendz *et al.*, 2007). In soils the optimum pH for the maximum release of nutrients is between 5.5 and 6.5 (Brady and Weil, 2008). However, Handreck and Black (1984) earlier on claimed that at pH 6 to 7.5 most nutrients are reasonably available to plants but maximum availability occurs between pH 6 and 7 in artificial soil media. Other than pH, elemental release also depends on the mineralogy of the ash components exposed, the reactive surface area of these minerals, the supply of water and its residence time in the ash and initial pH, the abundance of organic acids, and the temperature of ash solutions (Kump *et al.*, 2000). Most of the elements are released after long equilibration times when the alkalinity of the ash is significantly depleted and pH of the leachate approaches circum-neutral or acidic levels (Gitari *et al.*, 2009). Elemental release also depends on the extent of carbonation,

dissolution of the minerals or flushing of the soluble salts as a function of the degree of saturation.

Particle size distribution is another important factor that contributes to elemental release. Chemical reactivity is generally confined to the clay-sized particles and results from the combined reactive surface functional groups and specific surface area (Essington 2004 & Brady and Weil, 2008). More functional groups are expected and charge development will occur as weathering progress and secondary minerals starts to form (charge development will be discussed later). Therefore the incorporation of fine particles definitely enhances chemical reactivities that result in the release of elements and the addition of sludge contributes to the reduction of not only pH but also to the salinity of the medium.

Subjecting the ash – sludge mixtures to wetting and drying cycles induces change in pH and salinity of the mixtures and the addition of water enhance chemical reactions and increases the mobility/leaching of the elements. It is imperative therefore to carry out elemental analysis in fresh samples/mixtures and in both pore and free drained leachates. The analysis of fresh samples could be done using X-ray Fluorescence Spectroscopy (XRF) analytical technique that is capable of analyzing elements in a press powder from fluorine (with atomic number 9) to uranium (with atomic number 92) in the periodic table with detection limits varying from 0.5 ppm for heavier elements to 100 ppm for the lightest elements (Loubser & Verryin, 2008). For lighter elements the XRF technique may not be as reliable so the acid digestion method could be used coupled with Inductively coupled plasma mass spectroscopy (ICP-MS). The digestion technique analyses both macro and trace elements accurately. To analyze the pore and free drained leachates for both macro and trace elements the Inductively Coupled Plasma Optical Emission Spectrometry (ICP-OES) could be used. All samples were subjected to membrane filtration (0.45 μm) to reduce colloidal interference.

In this study it was hypothesised that the addition of sludge and weathering processes brought about by eluviation cycles will reduce the high pH to between 5.5 and 8 and salinity to less than 400 mSm^{-1} of the mixtures to optimum levels suitable for plant growth and further increase the

solubility of major and trace elements. Therefore, the main purpose of this chapter was to assess;change in pH, salinity and elemental release as influenced by eluviation cycles.

6.2 Materials and methods

6.2.1 Mixture analysis with X-ray Fluorescence Spectroscopy (XRF)

X-ray Fluorescence Spectroscopy (XRF) analytical technique was used to measure the total chemical composition of the solid samples. The technique relies on the software (UniQuant) that enables it to analyses raw spectral data qualitatively and quantitatively. It is capable of analyzing elements from fluorine (with atomic number 9) to uranium (with atomic number 92) in the periodic table with detection limits varying from 0.5 ppm for heavier elements to 100 ppm for the lightest elements. However, specific detection limits for MnO, MgO, CaO, Na₂O, K₂O, P₂O₅, Cu, Zn and Fe₂O₃ were 13, 118, 100, 265, 50, 100, 2, 4 and 97 ppm respectively (Loubser & Verryin, 2008). Seemingly, these detection limits were above the lower limit (0.5 ppm) and some like 118 and 265 were even higher than the miximum limit (100 ppm).

In preparation for the press powder analysis each sample was milled in a tungsten carbide milling pot (with insignificant sample contamination) such that at least 80 % of the particles fell below 75µm. A small amount (20 g) of each sample was transferred into a plastic zip-lock bag, added 5 drops of polyvinyl alcohol (used as a binder) then thoroughly mixed between thumbs. The mixed sample was then pressed at a pressure of 20 ton/cm² for two min in collapsible aluminium holders for mechanical support, using a polished piston. The sample was then dried at 110 °C before analysis. During the analysis radiation with sufficient energy was emitted by the x-ray tube and illuminated the sample hence exciting the atom of the element by ejecting one or more strongly held electrons in the inner orbital. Electrons held at an outer or higher orbital replaced the ejected electron and in the process fluorescence secondary photons were emitted to the detector that converted the photons to pulses. The pulses were further processed by a Multi-channel Analyser interpreting its characteristics that relate to the atoms present in the sample (Loubser & Verryin, 2008). The fused beads technique (for the analysis of major elements) requiring high temperatures (1000 °C) in the muffle furnace could not be executed because the samples contained significant amounts of organic matter (sludge) that ignited in the furnace. To validate the results coming from this technique the digestion method was then carried out.

6.2.2 Mixture analysis with Inductively coupled plasma mass spectroscopy (ICP-MS)

This is generally a three acid digestion method standard for soils. A sample of 0.2 g was digested with hydrofluoric acid (HF) acid. It was further digested with a mixture of perchloric acid (HClO_4) and nitric acid (HNO_3) in a ratio of 1:3 to dryness. The sample was then dissolved in a 20% hydrochloric acid and finally analysed by ICP-MS. For the mass spectroscopy 0.5 g of sample was digested by the HF acid and then digested with a mixture of HClO_4 and nitric acid in a ratio of 1:3 to dryness as well. The sample was then dissolved in a 20% HNO_3 acid and analysed by ICP-MS.

6.2.3 Phosphorus determination of mixtures

A portion of sample was fused with a sodium peroxide (Na_2O_2)/ sodium carbonate (Na_2CO_3) mixture, then leached with nitric acid (HNO_3) and deionised water. Ferric solution was added, and an excess of ammonia (NH_3) was added. The solution was filtered, and the residue was further digested with HNO_3 and HClO_4 acids. If necessary, the sample was treated to remove any As or Si, and then diluted to a known volume. An aliquot of an ammonium molybdate ($(\text{NH}_4)_2\text{MoO}_4$) / vanadate (NH_4VO_3) solution was added to a portion of the solution and transferred to a separating funnel. This reagent complexed with the P and turned to a yellow colour - the intensity of the colour was proportional to the P concentration. An aliquot of Methyl isobutyl ketone (MIBK-organic compound $(\text{CH}_3)_2\text{CHCH}_2\text{COCH}_3$) was added to extract the P from the reagent, and then the funnel was shaken well. The phosphorus, complexed with the $(\text{NH}_4)_2\text{MoO}_4$ / NH_4VO_3 reagent was extracted into the MIBK, which was separated from the aqueous phase. Calibration standards were prepared similarly. The standards and samples were read by UV/visible spectrometry, and the P concentration calculated.

6.2.4 Analysis of leachate with Inductively Coupled Plasma Optical Emission Spectrometry (ICP-OES)

An axially viewed Inductively Coupled Plasma Optical Emission Spectrometry (ICP-OES) was used to determine soluble elements (Mg, Ca, Na, K, P, Fe, Zn, Cu, B, Mo and Mn) in the leachates at different wave lengths (Table 6.1). Prior to analysis 20 ml aliquots were vacuum filtered through 0.45 μm membrane filters using a vacuum pump (vacuum was equal to approximately -60 kPa) to remove colloidal particles. The membrane filtered leachates were

allowed to collect in 20 ml polyethylene tubes fitted underneath. The polyethylene tubes were then transferred into plastic trays accommodating 55 tubes at a time and covered with parafilm(Parafilm[®] M Barrier Film)and enclosed in an air tight plastic container to prevent possible evaporation. Method blanks (deionized water treated the same way as the samples) and instrument blanks (deionized water) were also prepared in order to isolate and correct for contamination emanating from the membrane equipment, membranes, glass ware or from the deionized water. Before analysis the ICP-OES was calibrated using standards (MERCK CertiPUR[®] grade standards – Table 6.2) with ranges specific to the elements (Table 6.1). Elemental analysis was performed both in the samples and in blanks with the ICP-OES. The elemental analysis of the blanks was subtracted from the elemental analysis of the mixtures to obtain the quantity of elements contributed by the mixtures alone. Cumulative elemental concentrations in each mixture were calculated by summing up concentrations leached per eluviation cycle.

Table 6.1: ICP – OES theoretical and actual analytical ranges for each element and wavelengths used in the analysis (Essington, 2004)

Element	Theoretical Wavelength (nm)	Theoretical Analytical ranges (mg L ⁻¹)	Actual Wavelengths (nm)	Actual Analytical ranges (mg L ⁻¹)
P	214.9	0.1 – 1000	178.3	0.0 – 120
K	766.5	0.4 – 1000	766.5	0.0 – 120
Ca	317.9	0.0 – 1000	315.9	0.0 – 600
Mg	279.1	0.0 – 1000	279.1	0.0 – 120
Na	589.0	0.0 – 500	330.3	0.0 – 120
Mn	257.6	0.0 – 100	260.6	0.0 – 120
Cu	324.8	0.0 – 200	324.8	0.0 – 300
Fe	259.9	0.0 – 500	259.9	0.0 – 60
Zn	213.9	0.0 – 200	213.9	0.0 – 3
Mo	202.1	0.0 – 500	202.1	0.0 – 6
B	249.7	0.0 – 200	249.7	0.0 – 3

Table 6.2: Standards used to calibrate the ICP - OES

Standard	Grade	Concentration mg L ⁻¹	Catalog number
Na	MERCK CertiPUR [®]	10000	170881
Ca	MERCK CertiPUR [®]	10000	170308
K	MERCK CertiPUR [®]	10000	170342
Mg	MERCK CertiPUR [®]	10000	170331
P	MERCK CertiPUR [®]	10000	170340
Multi element standard solution for Cu, Zn, Mn, Mo, Fe & B	MERCK CertiPUR [®]	100	109487

6.2.5 Salinity and pH determination

Solution pH and electrical conductivity (EC) for both the free drained and pore solutions were immediately (within 24 hours) determined to avoid chemical changes. A multi-parameter analyser (Consort C830) with a 0.01 pH resolution coupled with epoxy electrode was used. The pH meter was initially calibrated using buffer solutions pH 7.0 (potassium dihydrogen phosphate/di-sodium hydrogen phosphate, CertiPUR[®] from MERCK, catalogue number 199002) and pH 4.01 (potassium hydrogen phthalate, CertiPUR[®] from MERCK, catalogue number 199001) to ensure accurate readings. The reading of samples commenced immediately after calibration. Calibration was repeated after every 10 pH readings to reduce erroneous results. Similarly, an electrical conductivity meter (Consort C861) with a 0.001 $\mu\text{S cm}^{-1}$ resolution coupled with conductivity electrode was used. The EC meter was calibrated with EC 1.41 mS cm^{-1} calibration solution (potassium chloride solution, CertiPUR[®] from MERCK, catalogue number 1012030500) and the reading of samples commenced immediately. The calibration of the EC meter was also repeated every after 10 readings. All the EC readings were expressed in mS m^{-1} .

6.3 Results and discussion

6.3.1 pH changes of mixtures as influenced by leaching

pH is often called the master variable that vastly affects numerous essential chemical reactions and processes. It affects the rates of anion and cation exchange and attenuation, redox reactions, microbial activity, solution speciation of elements, surface charge characteristics as well as mineral precipitation and dissolution. Low pH increases the solubility of elements such as Mn, Al and Fe and induces the deficiency of Ca, Mg and P, but under alkaline conditions Cu, Fe, Zn, and Mn

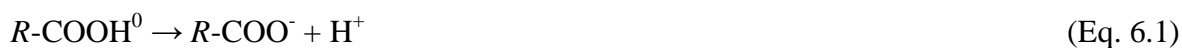
precipitate (Sparks, 2004 & Brady & Weil 2008). The effect of pH on surface charge characteristics indirectly affects anion and cation exchange and attenuation. Clay minerals carry a permanent negative charge that results from isomorphous substitution, for example, Si^+ is replaced by Al^{3+} (Mulder & Chresser, 1994). At this point cation retention becomes more pronounced at pH values greater than the point of zero charge (pzc). When the solution pH is lower than the pzc, the surface will exhibit a net positive charge and the surface affinity for anions increases (Prasad and Power, 1997, Essington, 2004, Brady and Weil, 2008).

Fine ash indicated a high pH value of 11.3 (indicative of P alkalinity) and this value was 1.2 units lower than pH 12.5 obtained by Mahlaba *et al.* (2011) in his characterization of Sasol fine ash. Previous analysis in 2008 of Sasol fine ash, gasification ash and sludge were characterized and had pH values of >12.0, 10.8 and 6.8 respectively. Gasification ash (mixture 11 - 100% gasification ash) exhibited a higher pH value (11.7) than in 2008. The high pH in both ashes was expected because they result from the combustion of lignite coals (low grade coals) that contain low sulphur and high Ca that subsequently maintains the pH at high values (> 12) (Haynes, 2009). The Ca in the ashes is a result of limestone (CaCO_3) that is added and undergoes calcination during coal gasification to retain S and CO_2 (Merrick, 1984). Mixing the gasification ash and fine ash did not influence the leachate pH of mixtures without sludge (mixtures 1 to 11) had pH values greater than 10. But the incorporation of sludge reduced the pore solution pH of the ashes, for example, mixture 14 (20% fine ash, 70% gasification ash and 10% sludge) had the lowest pH (8.3) after the first leaching cycle (Fig. 6.1, a).

Generally, the incorporation of sludge suddenly reduced the pH to a mean of 10 and a median of 9.8 (Fig.6, b). The frequency indicated that 45.1% of the mixtures had the pH falling in the range 9.80 ± 0.38 with 8.3% as coefficient of variation. Even after the tenth eluviation cycle mixtures without sludge retained pH values above 8.4 and the abrupt transition of pH from the mixtures without sludge (1 to 11) to treatments that received varying amounts of sludge (12 to 51) resulting from the addition of sludge was still distinct (Fig.6, c). Mixture 7 (40% fine ash, 60% gasification ash and 0% sludge) maintained the highest pH value (10.3) while mixture 49 (20% fine ash, 30% gasification ash and 50% sludge) showed the lowest pH (7.6). However, the overall pH mean was reduced to 8.2

and the median brought down to 8.0. At this stage the frequency indicated that 37.2% of the mixtures had the pH falling in the range 7.9 ± 0.31 with 8.0% as coefficient of variation (Fig.6, d).

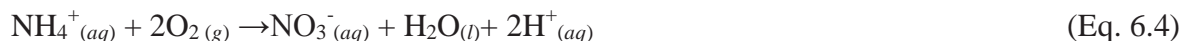
Subjecting the columns to more eluviation / leaching gradually decreased the pH of all mixtures (with and without sludge) with time. This was attributed to the removal of soluble alkalinity and various reactions possibly occurred resulting in the release of protons (H^+) into the solution. Generally, a decrease or increase in pH is the net effect of various reactions. Firstly, the biodegradation of sludge in the ash environment released dissolved organic carbon (DOC) that parted a tanned colour to the solutions. This was an indication that some of the decomposition products were polar and water soluble to some extent. It is reasonable to expect that, the DOC released also contained humified compounds such as fulvic acid (FA) and humic acid (HA) (Mulder & Cresser, 1994 & Singh & Agrawal, 2010). From literature FA is often isolated from sludge amended soil (Sposito *et al.*, 1978). Fulvic acid contains numerous of functional groups including carboxylic groups ($-COOH$, $pK_a = 4-6$). The greater solubility under alkaline conditions is caused by the deprotonation and ionisation of the various functional groups at pH conditions greater than their respective pK_a values. This makes the organic molecule more polar and thus water soluble. Carboxylic groups, for example, will be completely ionised (Eq. 6.1) at the pH measured for the various treatments (Essington, 2004 & Kleber & Johnson, 2010). The ionisation / deprotonation of these functional groups will obviously also contribute to the increase in proton activity in solution.



Secondly, the carbonation process produced protons. During this process CO_2 was liberated from the breakdown of the sludge and subsequently formed carbonic acid (H_2CO_3) with the solution through carbonation reaction. The dissociation /deprotonation of H_2CO_3 formed HCO_3^- and CO_3^{2-} increasing the aqueous proton concentration and activity (Eq. 6.2 & 6.3) (Essington, 2004 & Brady & Weil, 2008).



Thirdly, sludge generally contains bacteria that feature in nitrogen mineralization, the availability of organic matter and a reduced pH in mixtures with sludge favoured the nitrification process. The oxidation of NH_4 results in an increase in the concentration of NO_3^- and produced 2 moles of H^+ in the solution (Eq. 6.4) (Essington, 2004 & Brady & Weil, 2008).



Finally, Sasol coal ashes contain appreciable amounts of aluminium (Al) (aluminium is the second most abundant after silicon, 6.75%) iron and to a lesser extent manganese. In general when exposed to weathering these hydroxo cations first undergo hydrolysis and then precipitated. In the pH ranges of soil the net reaction involving the precipitation of these minerals are usually associated with the release of protons (H^+) into the solution (Essington, 2004, Brady & Weil, 2008). However, in alkaline environments trivalent hydroxo cations in solution often occur in anionic forms, for example, $\text{M}(\text{OH})_4^-$ and the mol fraction of $\text{Al}(\text{OH})_4^-$ at pH 9 is, for example, 0.82 and at pH 10 = 0.98. A balanced generic precipitation reaction of a metal hydroxide involving M^{3+} in the anionic hydrolysis form $\text{M}(\text{OH})_4^-$ actually shows a consumption of a proton (Eq. 6.5),



However, the preceding reaction involving the hydration and hydrolysis of a M^{3+} , liberated from the ash matrix to form $\text{M}(\text{OH})_4^-$, resulted in the generation of protons (Lindsay, 1979). It should be noted that these are elements in solution. It was also evident that increasing sludge from 10 to 50% after all the eluviation cycles (1 to 10) could not further reduce the pH because of the onset of some strong buffering reaction or reactions with high buffering capacity that occurred. The pH range was close to the pKa of $\text{NH}_4^+ / \text{NH}_3$ (9.2) therefore the transformation of ammonium to ammonia resulted in the release of protons into the solution buffering the pH in this range for the sludge amended treatments. The hydrolysis (Eq. 6.6) of silicon has a pKa of 9.71 and produces protons that add to the buffering capacity of the system.



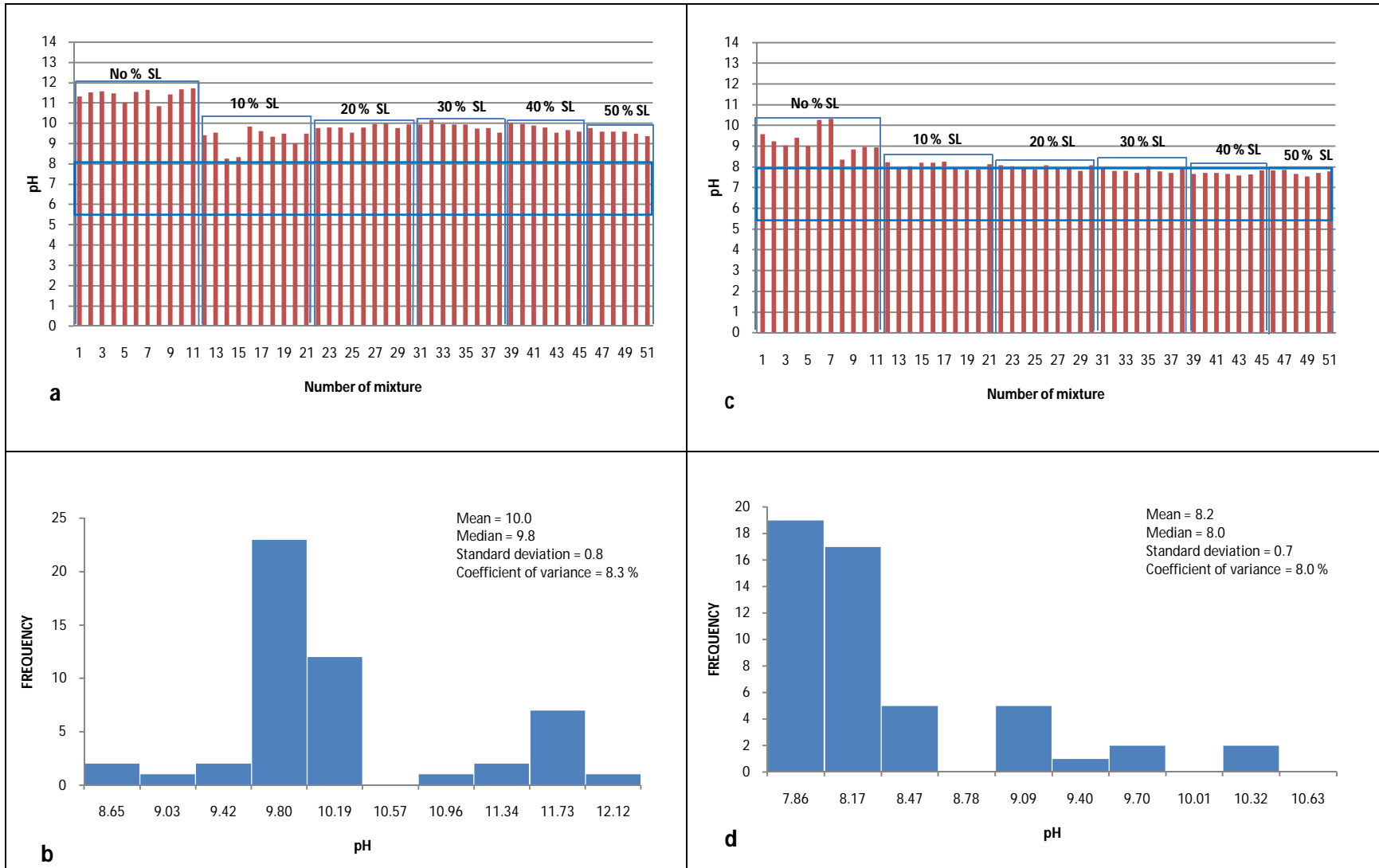


Fig.6. 1: a) pH of the pore solution upon sludge addition for the first eluviation cycle, b) frequency distribution of the pore solution pH for the first eluviation cycle, c) pH of the pore solution upon sludge addition for the tenth eluviation cycle, and d) frequency distribution of the pore solution pH for the tenth eluviation cycle. The SL in a and c means sludge. The gray shaded rectangles in a and c demarcate proposed optimum pH range suitable for plant growth.

6.3.2 Electrical Conductivity (EC) changes of mixtures as influenced by leaching

Salinity is defined as the concentration of dissolved mineral salts (Na^+ , K^+ , Ca^{2+} , Mg^{2+} , Cl^- , SO_4^{2-} , HCO_3^- , CO_3^{2-} , and NO_3^-) in a growth medium. Literature reveals that EC values greater than 400 mSm^{-1} denote saline conditions that can induce salt toxicity to most plants. An optimum EC suitable for most plants fall between 70 and 400 mSm^{-1} . However, some tolerant plants can survive at EC values greater than 1000 mSm^{-1} (Handrek, 1984, Essington, 2005 & Sparks, 2004). High salinity ($>400 \text{ mSm}^{-1}$) can limit the chemical suitability of the medium to support plants (Sparks, 2004). Calcium to S molar ratios of over 2.5 in the feedstock (coal) results in the ash containing not only CaSO_4 but also CaO (Anthony, 2003). Such basic coals also contain appreciable amounts of salts like Na^+ , K^+ , Ca^{2+} and Mg^{2+} that control salinity (Tsai, (1982).

Most of the salinity was contributed immensely by fine ash (580 mSm^{-1}) and followed closely by gasification ash (527 mSm^{-1}) (Fig.6.2, a). These EC values are greater than 400 mSm^{-1} therefore denote salt toxic conditions (saline) not suitable for the growth of most plants. This was expected because alkaline and unweathered ash deposits are generally saline with high levels of soluble salts and a high electrical conductivity (EC) of 1300 mSm^{-1} (Haynes, 2009). The high salinity in the Sasol ash could be attributed to the results from the interaction of the ash with saline brines (which has reported total dissolved solids content in the order of 8000 mg l^{-1}) in the form of slurry during hydraulic or fluid disposal (Mahlaba *et al.*, 2011). It was therefore expected that the salinity would gradually decrease as the content gradient for both ashes decreased from mixture 1 (100% fine ash) to 51 (50% sludge and 50% gasification ash) and salinity dilution effect caused by sludge in mixtures with sludge (mixtures 12 to 51 described in chapter 3). The addition of sludge generally increased the release of salts from all the mixtures with sludge after the first eluviation cycle for the pore solution (Fig.6.3, a). But had the least salts released due to the small amount of sludge (10%) added. Generally, the incorporation of sludge increased the salinity to a mean of 500 mSm^{-1} and a median of 526 mSm^{-1} for all mixtures with sludge. The frequency indicated that the EC for 41.2% of the mixtures ranged 563.4 ± 58.6 (with 19.0% as coefficient of variation) after the first eluviation cycle (Fig.6.3, b). The breakdown of sludge produced dissolved organic carbon (DOC). It was reasonable to expect that the tanned colour (observed in chapter 3 on the column set up) of the leachates indicated the presence of FA and HA and their conjugated bases humates and fulvates form complexes with metals through

chelation, this in turn, promoted the dissolution of metals from minerals (Mulder & Cresser, 1994). Dissolved organic carbon also contributed to EC due to its ionization caused by the oxidative breakdown. The increase in EC and concentrations of K^+ Ca^{2+} Mg^{2+} and Na^+ for the sludge treated mixtures were a contribution of these processes. The effect of abovementioned processes was evident throughout the study as a result mixtures with sludge maintained a higher salinity. After the 10th leaching the EC values of the treatments that did not receive sludge were below 200 $mS\ m^{-1}$, while some mixtures that received 10, 30, 40 and 50% sludge had EC values between 200 and 300 $mS\ m^{-1}$ (Fig.6.3 c). Even mixture 13 had an increased salinity. Leaching did decrease salinity as indicated by the decrease in EC over time and on average the EC was less than half than initial (Fig.6.2). The frequency distribution showed that the EC of 21.6% of the mixtures (some mixtures with 0 to 30% sludge) fell in the range 124.3 ± 36.3 with 40.7% as coefficient of variation after the tenth eluviation cycle (Fig.6.3, c and d). This EC range was within the optimum and acceptable EC range (70 to 400 mSm^{-1}) for good growth media. Only mixtures 40 and 43 that proved to be saline after the tenth eluviation cycle with EC values above 400 mSm^{-1} (Fig.6.3 C). The complexation of the salts by soluble ligands maintained a higher salinity even after the tenth eluviation cycle (Mulder & Cresser, 1994 & Li & Shuman 1997) (Fig.6.3 c). According to Handreck and Black (1984) and Brady and Weil, (2008) the most suitable EC range for plant growth falls between 70 and 400 mSm^{-1} . It was only mixtures 40 and 43 that had their EC beyond 400 mSm^{-1} after ten eluviation cycles.

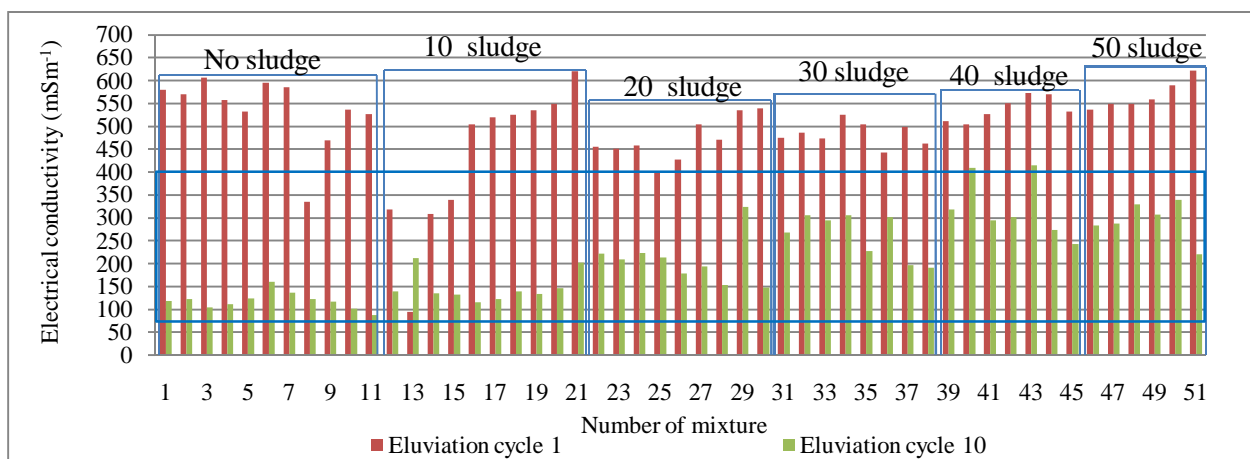


Fig.6. 2: Salinity comparison for the first and tenth eluviation cycles. The gray shaded rectangle demarcates proposed optimum salinity range for plant growth.

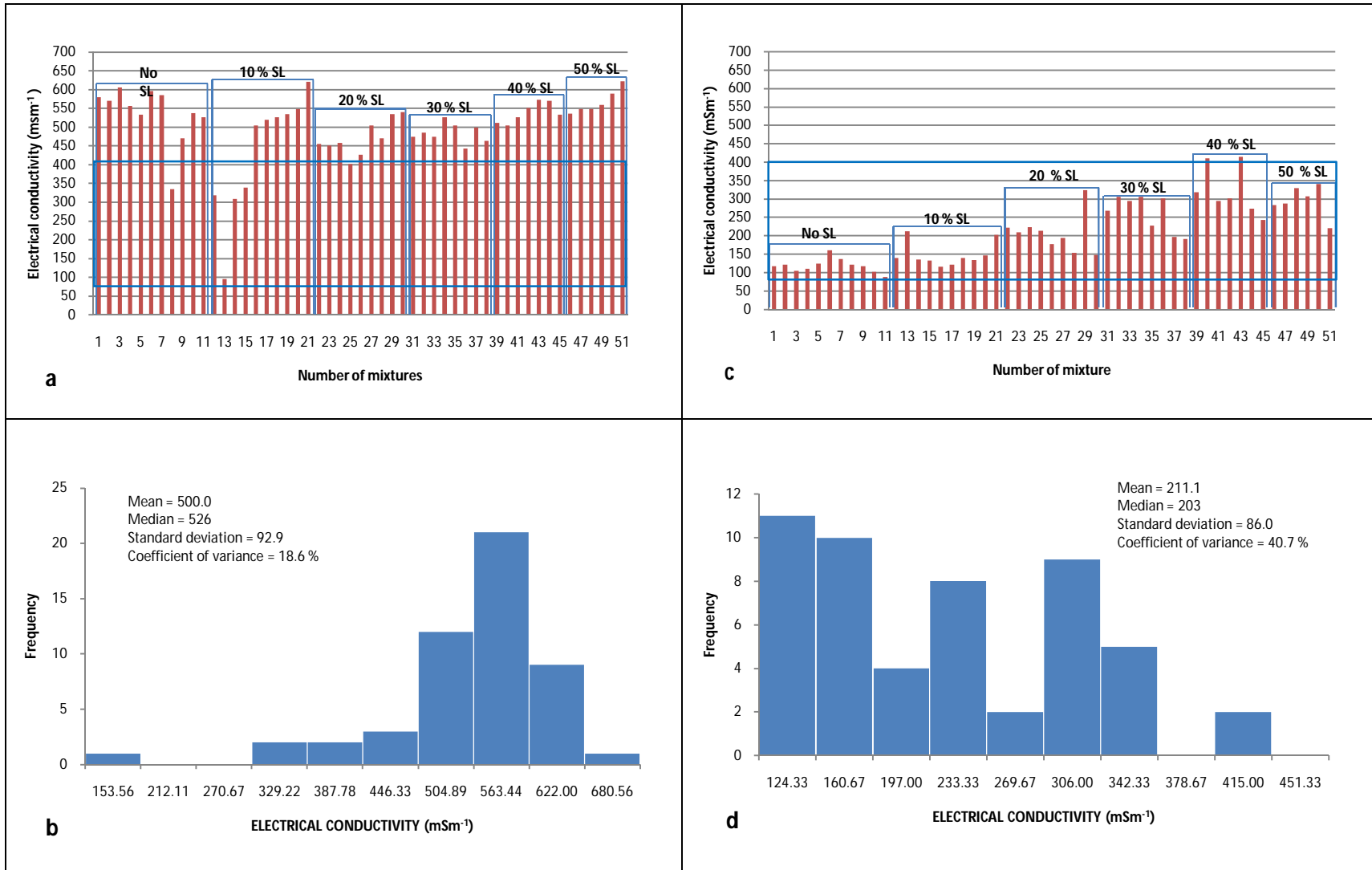


Fig.6. 3: a) Electrical conductivity of the pore solution upon sludge addition to the various treatment groups (with sludge increasing from 0 to 50%, fine ash decreasing and gasification ash increasing – illustrated in chapter 3) for the first eluviation cycle, b) frequency distribution of the pore solution electrical conductivity for the first eluviation cycle, c) Electrical conductivity of the pore solution upon sludge addition for the tenth eluviation cycle and d) frequency distribution of the pore solution electrical conductivity for the tenth eluviation cycle. The SL in a and c means sludge. The gray shaded rectangles in a and c demarcate proposed optimum EC range for plant growth.

6.3.3 Calcium content of Sasol sludge, fine and gasification ashes measured in 2006, 2007, 2008 and 2011

The calcium content had been measured over time for the Sasol sludge (in 2007, 2008 and 2011), fine ash (2006 and 2011) and gasification ash (in 2008 and 2011) by various laboratories (Fig 6.4). Statistically the Ca content of sludge (mean 0.6%) was found to be significantly lower at (a significance level of $\alpha = 5\%$) level than the Ca content of gasification ash (mean 6.8%) and fine ash (mean 5.1%). The Ca content of the fine ash was also significantly lower than that of the gasification ash at 5% level. The computed least significant difference (LSD) was 0.7 and the coefficient of variation (CV) was 15.0 %. The variability in Ca content as indicated by longer error bars was significantly higher in gasification ash (with 95% confidence interval of between 4.6 and 9.0%) than in fine ash (with 95% confidence interval of between 4.8 and 5. %) and had a minimum, maximum and median of 5.7%, 8.2% and 6.8% respectively. Fine ash had a narrower variability (with shorter error bars) and a minimum, maximum and median of 5.0%, 5.4% and 5.1% respectively. The high variability in particle size distribution (illustrated in chapter 4 Fig.4.1) of gasification ash (80% > 2 mm) could be the source of the variability in Ca content. Sludge had the lowest Ca content and variability (with shortest error bars and a 95% confidence interval between 0.5 and 0.7%) and a minimum, maximum and median of 0.5%, 0.7% and 0.63% respectively and a CV of 9.3%.

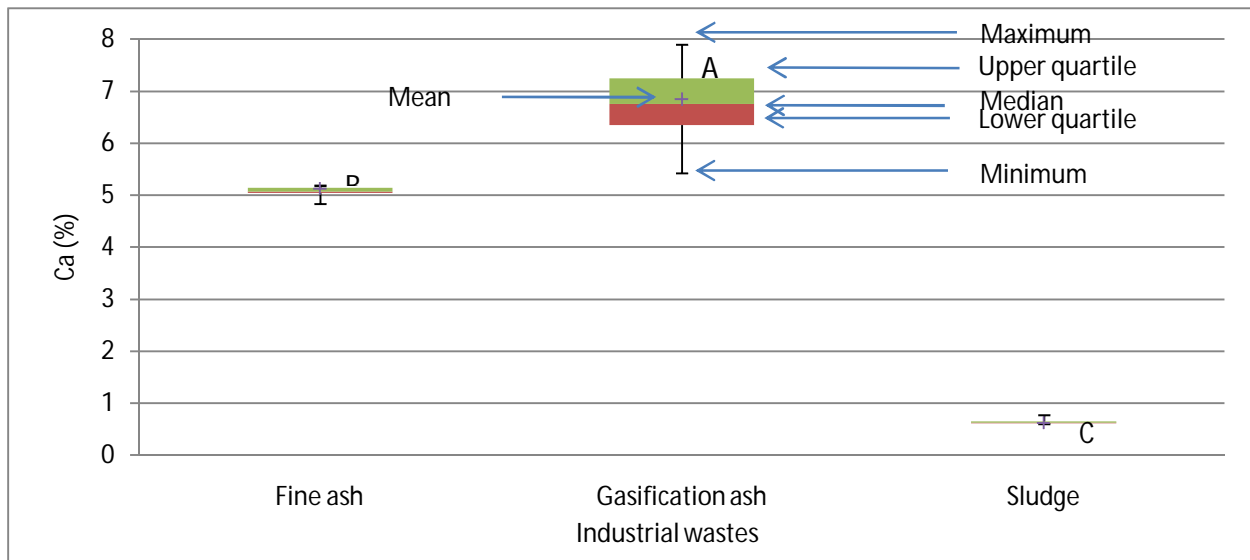


Fig.6. 4: The variation in calcium content of Sasol sludge, fine and gasification ashes based on analyses done in 2006, 2007, 2008 and 2011 (at least 1 sample per year). The method used was acid digestion using hydrofluoric acid (HF) acid and a mixture of perchloric acid (HClO_4) and nitric acid (HNO_3) (as indicated in section 6.2.2).

Table 6.3: The Ca content for the Sasol fine and gasification ashes as determined by X-ray Fluorescence Spectroscopy (XRF) measured in 2008 and 2011 by two laboratories.

Year	Ca (%) in gasification ash	Ca (%) in fine ash
2011	7.1	-
2011	7.3	5.7
2011	-	5.9
2008	5.2	-
<i>Mean</i>	6.6	5.8
<i>Standard deviation</i>	1.2	0.1
<i>Coefficient of Variation (%)</i>	18.1	2.3

X-ray Fluorescence Spectroscopy (XRF) was used in 2008 and 2011 to measure calcium oxide content in Sasol fine and gasification ashes (Table 6.3). The Ca content varied significantly over the two years in gasification ash with a standard deviation of 1.2 and a large CV of 18.1% confirming the variability. This variability was further confirmed by the wider 95% confidence interval (3.6 to 9.5%) provided by XRF method in gasification ash. The acid digestion method gave a narrower 95% confidence interval (4.6 to 9.0%) (Table 6.4). The variability of Ca for fine ash was narrow as indicated by the standard deviation of 0.1 and a low coefficient of variation of 2.3%. Again this was confirmed by both methods; XRF gave a narrower 95% confidence interval of 5.4 to 6.2% and acid digestion gave a 95% confidence interval of 4.8 to 5.5% (Table 6.4). Gasification ash showed a significantly higher Ca content with a mean of 9.2% compared to Ca content for fine ash with a mean of 8.1%.

In comparing the two methods (acid digestion and XRF) 95% confidence intervals were computed and the confidence intervals for both methods in fine ash overlapped (indicating a significant difference between the means obtained by the two methods) and in gasification ash the confidence intervals for acid digestion fitted into the XRF confidence intervals (indicating that there was no significant difference between the means obtained by the two methods (Table 6.4)

Table 6.4: Comparison of total Ca content determined using acid digestion and XRF in fine and gasification ashes based on 95 % confidence intervals

Ash material	Acid digestion					XRF				
	Mean	Lower limit	Upper limit	Stdev	CV (%)	Mean	Lower limit	Upper limit	Stdev	CV (%)
Fine	5.1	4.8	5.5	0.1	2.3	5.8	5.4	6.2	0.2	3.1
Gasification	6.8	4.6	9.0	1.2	18.1	6.6	3.6	9.5	1.0	15.0

Gasification ash at 95% had the confidence interval of between 4.6 and 9.0% and fine ash with

confidence interval of between 4.8 and 5.5% with the acid digestion method while with XRF method gasification ash at 95% had the confidence interval of between 3.6 and 9.5% and fine ash had confidence interval of between 5.4 and 6.2%.

6.3.4 Calcium content of mixtures

Ca was more abundant than other alkaline and alkaline earth metals followed by Mg, Na and K in all mixtures. However, in mineral soils this arrangement differs slightly, Ca still is more abundant but followed by K, Mg and Na (Essington, 2004). The Ca content of the sludge was significantly lower than that of gasification ash and fine ash (Table 6.2). It was therefore expected that with increasing sludge content the Ca content of the mixtures will decrease (Fig 6.5). Total elemental analysis was also performed on selected mixtures: that contained 100% fine ash (mixture 1), a combination of 50% fine and 50% gasification ash (mixture 6), 100% gasification ash (mixture 11), a combination of sludge, fine and gasification ash (mixture 26), a combination of 50% sludge and 50% fine ash (mixture 46) and a combination of 50% sludge and 50 % gasification ash (mixture 51). This was done to assess the variability and potential error that resides in calculating the elemental content by summing the fractional contribution of gasification ash, fine ash and sludge. The Ca content of a mixture, for example, was the measured Ca content of fine ash alone multiplied with the percent fractional contribution content of fine ash in the mixture. Similarly the measured Ca content of gasification ash alone was multiplied by the percent content of gasification ash in the mixture. The same procedure was followed to calculate the contribution of sludge to the Ca content in the mixture. The calculated Ca content of a mixture was then obtained by summing the three products.

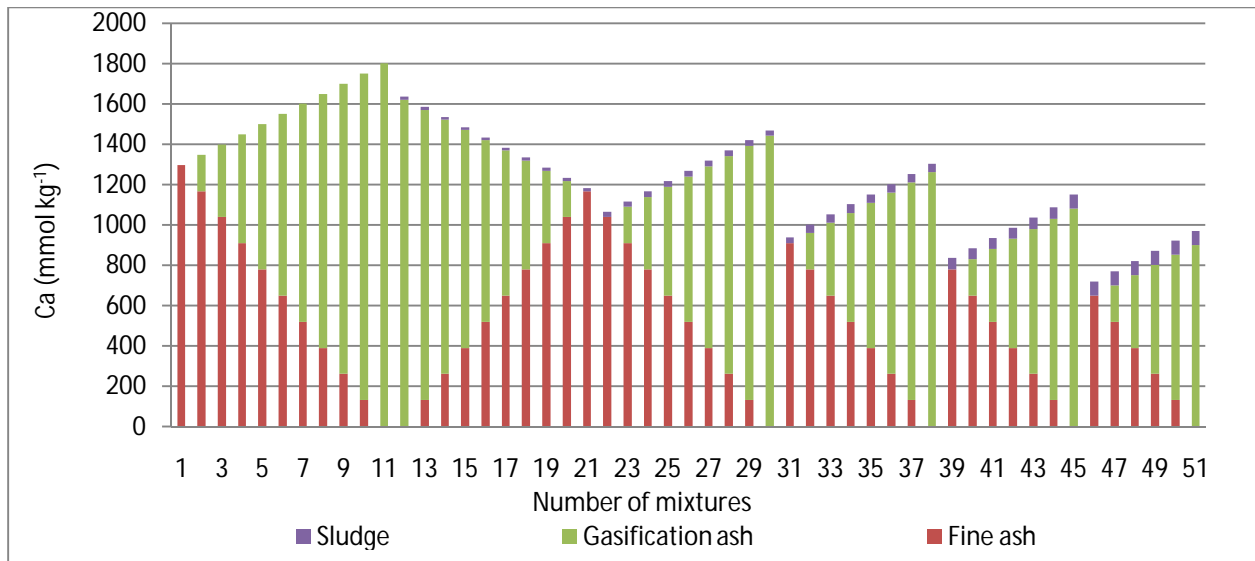


Fig.6. 5: Calculated Ca content of the mixtures based on the mean content depicted in Fig 6.3. of sludge, fine and gasification ash to total Ca content of mixtures

The approach followed was to establish a 95% confidence interval based on the measured data (Ca means in selected mixtures) and compared to the predicted Ca content of the mixtures in an attempt to establish some significant differences between the means. It was found that the calculated means for mixtures 1, 6, 11, 46 and 51 fell within the 95% confidence interval. However, the calculated mean ($1263.4 \text{ mmol kg}^{-1}$) for mixture 26 fell outside the confidence interval (upper limit $1251.2 \text{ mmol kg}^{-1}$ and lower limit $1153.2 \text{ mmol kg}^{-1}$) indicating to be significantly different from the measured mean ($1202.2 \text{ mmol kg}^{-1}$). Repopulating the data readjusted the confidence interval (upper limit $1322.7 \text{ mmol kg}^{-1}$ and lower limit $1204.0 \text{ mmol kg}^{-1}$) allowing the mean of the calculated values not to be significantly different. (Table 6.5) This statistical verification provided evidence that the means of calculated Ca values in the mixtures were not significantly different from the means of the measured Ca values.

Noticeably the measured Ca content of the gasification ash was more ($1802.3 \text{ mmol kg}^{-1}$) than for fine ash ($1283.3 \text{ mmol kg}^{-1}$) and sludge ($145.5 \text{ mmol kg}^{-1}$) (Table 6.3). These findings were similar in trend to results obtained in 2008 in the characterization of Sasol wastes; gasification ash had the highest Ca content ($1802.3 \text{ mmol kg}^{-1}$) than fine ash ($1283.3 \text{ mmol kg}^{-1}$) and sludge ($87.3 \text{ mmol kg}^{-1}$). Clearly the Ca content of the mixtures increased with increase in gasification ash (Fig 6.5). The determination of the specific sources of Ca in the Sasol ashes was beyond the

scope of this study, however, Mahlaba *et al.* (2011) found through X-ray Diffraction (XRD) that the secondary mineral, calcite (CaCO_3), was the most abundant (2.2-6.3%) Ca containing mineral and remained the main source of Ca followed by ettringite ($\text{Ca}_6\text{Al}_2(\text{SO}_4)_3(\text{OH})_{12}\cdot 26\text{H}_2\text{O}$) (0.8-4.5%).

Table 6.5: Measured and calculated means for Ca, in selected mixtures using microwave digestion method

Mixture Number	Measured Ca (mmol kg^{-1})	Calculated Ca (mmol kg^{-1})	Confidence interval at 95 % (mmol kg^{-1})		Standard deviation (mmol kg^{-1})	CV %
			Lower limit	Upper limit		
1	1283.3	1283.3	1166.1	1400.6	47.2	3.7
6	1465.5	1442.8	1375.2	1555.7	36.4	2.5
11	1802.3	1802.3	1281.0	2323.6	210	11.7
26	1203.2	1263.4	1322.7	1204.0	19.7	1.6
46	718.6	714.4	702.2	735.0	6.6	0.9
51	922.3	973.9	869.0	975.8	21.5	2.3
SL	145.5	145.5	-	-	12.4	18.1

Note: mixtures 1 (100% fine ash), 6 (50% fine ash and 50% gasification ash), 11 (100% gasification ash), 26 (40% fine ash, 40% sludge and 20% sludge), 46 (50% fine ash and 50% gasification ash) and 51 (50% gasification ash and 50% sludge) were exclusively analysed to enable the estimation of total elements of the other mixtures. SL means sludge.

6.3.5 Calcium leaching from mixtures

Amending gasification ash with sludge, and increasing its content in the mixtures, increased Ca released from the mixtures and therefore the net effect of sludge amendment was the increase in the soluble Ca of the mixture (Fig.6.6, a and b). As a result mixture 43 (40% gasification ash, 20% fine ash 40% sludge) released the most cumulative Ca ($52.6 \text{ mmol kg}^{-1}$) than any other mixture but with $> 400 \text{ mSm}^{-1}$ followed by mixtures 37, 40, 41, 44 and 48 (described in chapter 3) which also released more than 40 mmol kg^{-1} Ca and had salinity less than 400 mSm^{-1} . Based on the significantly higher Ca content of the gasification and fine ash, it is reasonable to expect that it was the source of Ca. Most of the Ca in all these mixtures eluviated from both fine and gasification ash than from sludge (Fig.6.5). Mixtures without sludge released the least Ca on average compared to all mixture group. Increasing sludge increased dissolved organic carbon (DOC) that enhanced the solubility of Ca from the solid phases (Li & Shuman, 1997). The addition of soluble organic ligands has been found to decrease the sorption of elements on the surfaces of clay minerals (Sposito *et al.*, 1982). Sludge contributes organic ligands that form

soluble complexes with the elements like Ca enhancing their leachability (Li & Shuman, 1997). Subjecting the mixtures to weathering (wetting and drying) and the formation of carbonic acid (resulting from the reaction of CO₂ and H₂O enhanced by microbial activities) increased the dissolution of calcite (CaCO₃) and ettringite in ash that led to an increase Ca release (Sparks, 2003 & Kolahchi & Jalali, 2007) by the dissociation of CaHCO₃ (from the CaCO₃) produced H⁺ which resulted in mineral weathering (Mengel *et al.*, 2001). Fine ash alone (mixture 1) released the least cumulative Ca (7.8 mmol kg⁻¹) than any other mixture due to the high pH that remained high even after the tenth eluviations cycle (Fig.6.1 c).

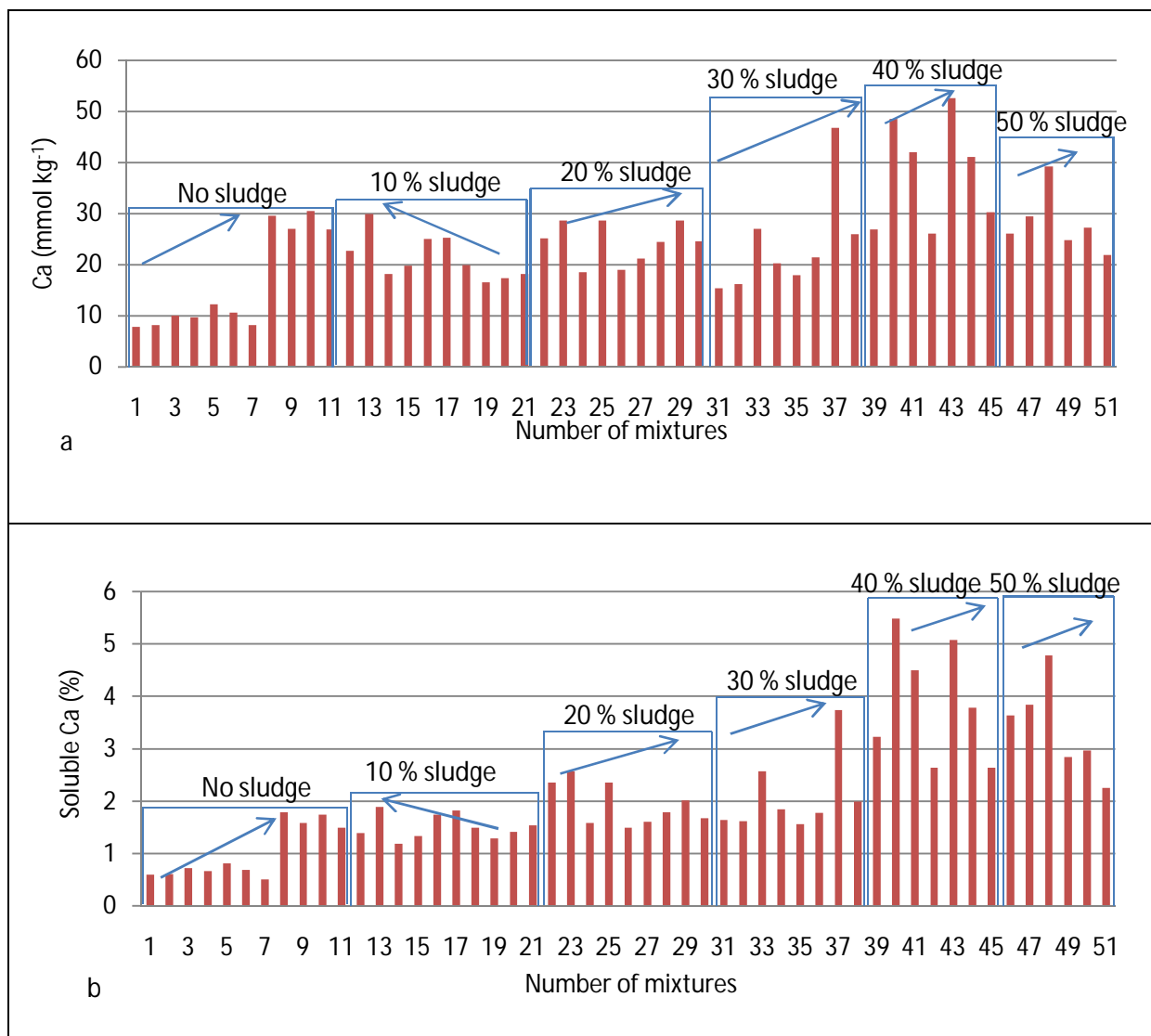


Fig.6. 6: a) Cumulative amount of soluble Ca (mmol kg⁻¹) released after 10 eluviations cycles and b) Cumulative soluble Ca (%) in mixtures released after 10 eluviations cycles. The arrows in a and b indicate the direction of increasing gasification ash content of each sludge treatment group.

The release of Ca should also be viewed in context of the other major cations and anions that potentially can play role in controlling the solubility. The solubility of Mg and P was favored over the solubility of Ca after the addition of sludge. This was revealed by the molar ratios of Ca:Mg and Ca:P in Fig. 6.7, a and d respectively. The molar ratio of Ca:Mg indicated that solid phases containing Ca were more soluble than solid phases containing Mg in the mixtures without sludge but the trend changed, the Mg solubility was favored over Ca solubility in mixtures with 10 to 50% sludge. The trend presented by molar ratio Ca:P was similar to the trend that was presented by the molar ratio Ca:Mg, Ca solubility was more than the solubility of P in mixtures without sludge and drastically dropped after the addition of sludge.

The trend presented by molar ratio Ca:K differed, K solubility was more than Ca solubility in mixtures without sludge. However, the liberation of Ca was favoured over that of K in mixtures with sludge. The solubility of Ca was favored in mixtures with 40% sludge and rapidly reduced in mixtures with 50% sludge favoring K. At this stage more K was complexed by soluble organic ligands improving its mobility. The trend presented by the molar ratio of Ca:Na was similar to the trend presented by the molar ratio of Ca:K. Sludge increased the solubility of Ca in mixtures with sludge (Fig.6.7, c).

The decrease of Ca release relative to that of Ca and P could be attributable to several factors. Ca could have been adsorbed by organic functional groups (from sludge) that increased the cation exchange capacity (CEC) from 5.5 to 19.0 cmolc kg⁻¹ (chapter 7 Fig. 7.1 a) The sorption of organic ligands on mineral surfaces creating new sorption surfaces for Ca could lower the Ca release (Li & Shuman, 1997). The increase in sludge content in the mixtures increased CEC that also slowed down the leaching of soluble Ca (Mulder & Cresser, 1994). This led to the displacement of other cations on the surfaces of clay minerals (present in Sasol fine and gasification ashes as characterized by Mahlaba et al., (2011) and Ginster & Matjie, 2005 & Matjie *et al.*, in chapter 2) like K, Mg and Na (with lower selectivity) by Ca; this subsequently reduced the amount of Ca available for leaching (Wang, Brusseau & Artiola *et al.*, 1997, Messenger, Menge, Amrhein & Faber 1997). A high pH and the presence of Ca favours the formation of soluble Ca-ligand complexes increasing the solubility of Ca shown by millimolar ratios of Ca:K and Ca:Na in mixtures with sludge (Mengel *et al* 1987). The more soluble P

exhibited by the molar ratio Ca:P could be attributable to the more soluble P contained in sludge in organic form.

Calcium is an essential element without which plants cannot complete their life cycle, irreplaceable by other elements, and directly involved in plant metabolism (Fageria *et al.*, 2002). This element therefore is indispensable in soil fertility and is required by plants in large quantities (Brady & Weil, 2008). An increase in soluble Ca as a result of sludge addition is arguably beneficial as the sludge has an indirect effect, that is, by the dissolution of solid phases. The soluble Ca released by mixtures without sludge and mixtures with 20 to 30 % sludge was quite low and need to be supplemented for the betterment of plant growth.

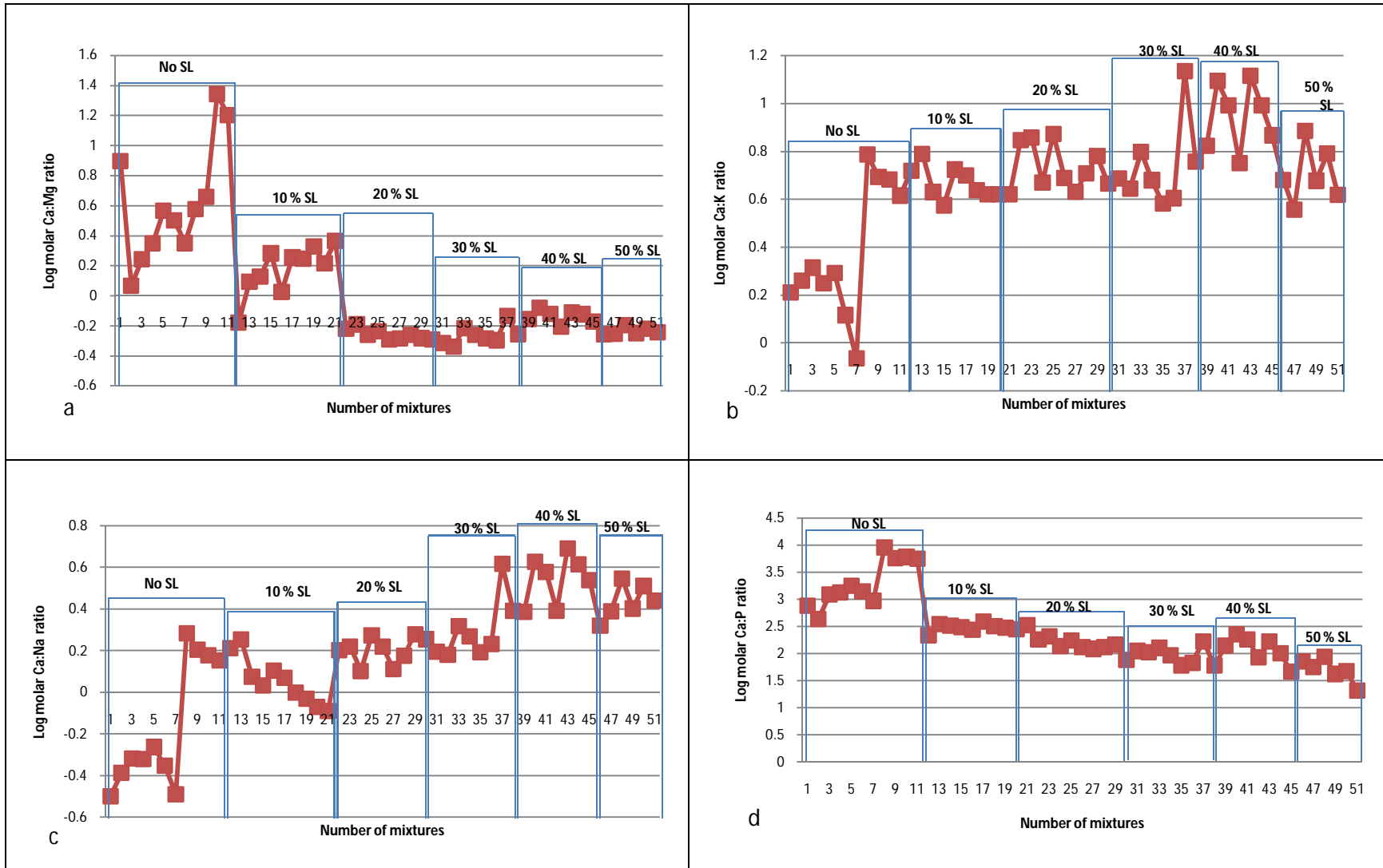


Fig.6. 7: a) Log molar Ca:Mg ratio based on the cumulative calcium and magnesium released after ten eluviation cycles, b) Log molar Ca:K ratio based on the cumulative calcium and potassium released after ten eluviation cycles, c) Log molar Ca:Na ratio based on the cumulative calcium and sodium released after ten eluviation cycles, and d) Log molar Ca:P ratio based on the cumulative calcium and phosphorus released after ten eluviation cycles. The SL in a, b, c and d means sludge.

6.3.6 Magnesium content of Sasol sludge, fine and gasification ashes measured in 2006, 2007, 2008 and 2011

Mg analysis of these industrial wastes over the five year period indicated that Mg content in sludge was significantly lower with a mean of 0.2% than the Mg content of fine (1.3%) and gasification (mean 1.4%) ashes at 5% level (Fig.6.8). However, fine and gasification ashes were not significantly different from each other at both 1 and 5% level. The least significant difference was 0.3% while the coefficient of variation was 23.0%. The variability in magnesium content of both fine and gasification ash were high (as indicated by the long error bars). This was due to the low Mg content which was obtained for the fine ash in 2006 and gasification ash in 2008 of 0.95 and 0.97% respectively compared to the higher Mg content (1.3 to 1.6%) measured in 2011. However, the Mg content of the fine ash was slightly more variable with a minimum, maximum and median of 0.95, 1.57 and 1.3% respectively than gasification ash with a minimum, maximum and median 1.0, 1.5 and 1.5% respectively. Sludge showed a narrower variability indicated by shorter error bars with minimum, maximum and median 0.1, 0.3 and 0.3% respectively.

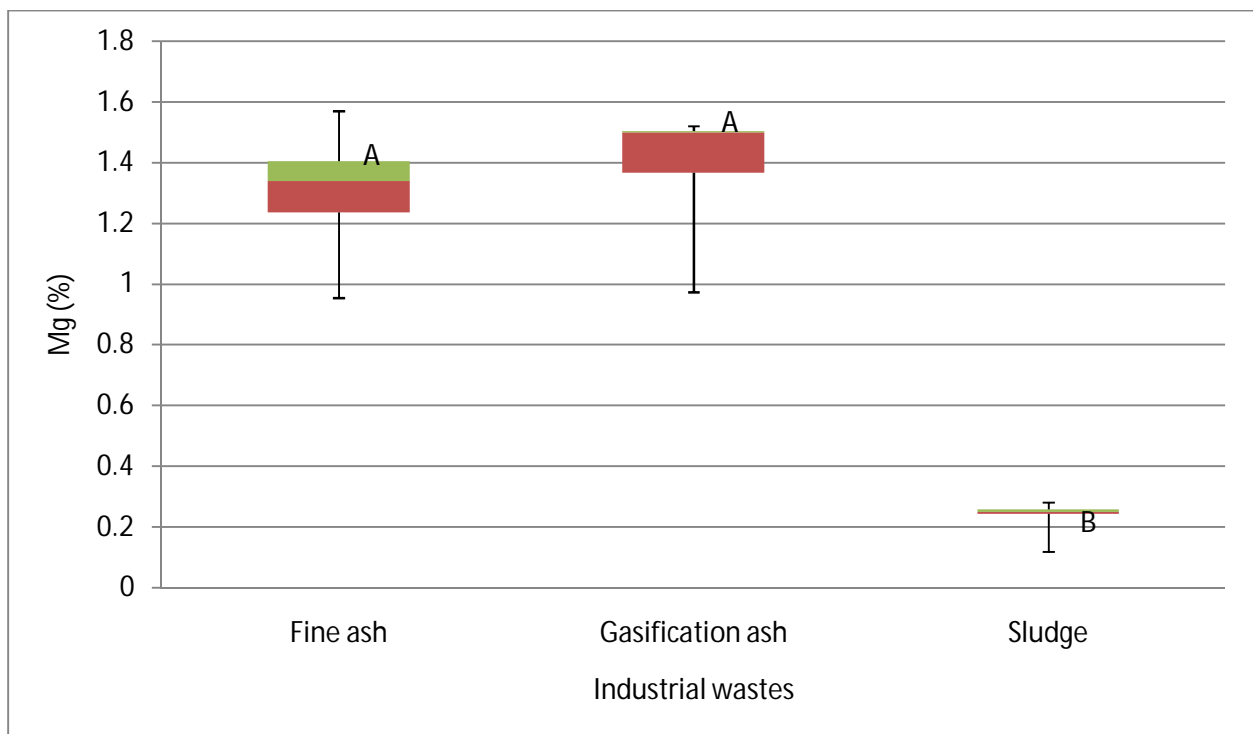


Fig.6. 8: The variation in magnesium content of the Sasol sludge, fine and gasification ashes based on analysis performed in 2006, 2007, 2008 and 2011 as determined by digestion method.

Table 6.6: Magnesium content in Sasol fine and gasification ashes as determined by X-ray Fluorescence Spectroscopy (XRF) measured in 2008 and 2011.

Year	Mg (%) in Gasification ash	Mg (%) in Fine ash
2011	1.5	-
2011	1.2	1.5
2011	1.5	0.8
2008	1.5	-
<i>Mean</i>	<i>1.4</i>	<i>1.1</i>
<i>Standard deviation</i>	<i>0.1</i>	<i>0.4</i>
<i>Coefficient of variation(%)</i>	<i>8.9</i>	<i>41.4</i>

Magnesium content analysed using X-ray Fluorescence Spectroscopy (XRF) in 2008 and 2011 indicated high variability in fine ash than in gasification ash (Table 6.6). Fine ash showed a higher coefficient of variation (41.4%) than gasification ash with a lower coefficient of variation (8.9%). Noticeably, the Mg content of gasification ash was higher (mean 1.4%) than in fine ash (1.1%). Sasol coal ashes contain periclase (MgO) (Mahlaba *et al.*, 2011) which could be higher in gasification ash than in fine ash. There was a significant difference in the Mg determined by the two methods (XRF and acid digestion) in gasification as indicated by the overlapping 95% confidence intervals. However, in fine ash the 95 % confidence interval given by acid digestion was narrower and fitted in the wider 95% confidence interval given by the XRF method (Table 6.7). This was an indication that there was no significant difference in the two methods in determining Mg in fine ash.

Table 6.7: Comparison of total Mg content determined using acid digestion and XRF in fine and gasification ashes based on 95% confidence intervals

Ash material	Acid digestion					XRF				
	Mean	Lower limit	Upper limit	Stdev	CV (%)	Mean	Lower limit	Upper limit	Stdev	CV (%)
Fine	1.3	0.8	1.9	0.3	19.6	1.2	0.3	2.6	0.5	41.4
Gasification	1.4	0.8	1.9	0.3	19.4	1.4	1.1	1.7	0.1	8.9

6.3.7 Magnesium content of mixtures

The Mg proved to be the second most abundant after Ca in all mixtures (Table 6.8). Similar to Ca content, Mg was more abundant in gasification ash ($619.9 \text{ mmol kg}^{-1}$) than in fine ash ($582.9 \text{ mmol kg}^{-1}$) and sludge ($107.7 \text{ mmol kg}^{-1}$). The Mg content in Sasol gasification and fine ashes were 0.97% and 0.95% respectively in 2008 showing to be significantly lower than the Mg content of gasification (1.51%) and fine ash (1.46%) of the current study. The Mg content of sludge was much lower compared to the Mg content of both fine and gasification ash. In both the current study and in 2008 the Mg content of sludge was 0.30 and 0.12% respectively. Evidently the contribution of gasification ash to Mg content was higher than the contribution of fine ash and sludge (Fig.6.9). In characterizing Sasol fine ash, Mahlaba *et al.* (2011) found that Mg was localized in periclase (MgO) that ranged between 0.3-1.3% in abundance. The abundance of MgO was much lower than Ca bearing minerals hence Ca content was higher than Mg content in the mixtures.

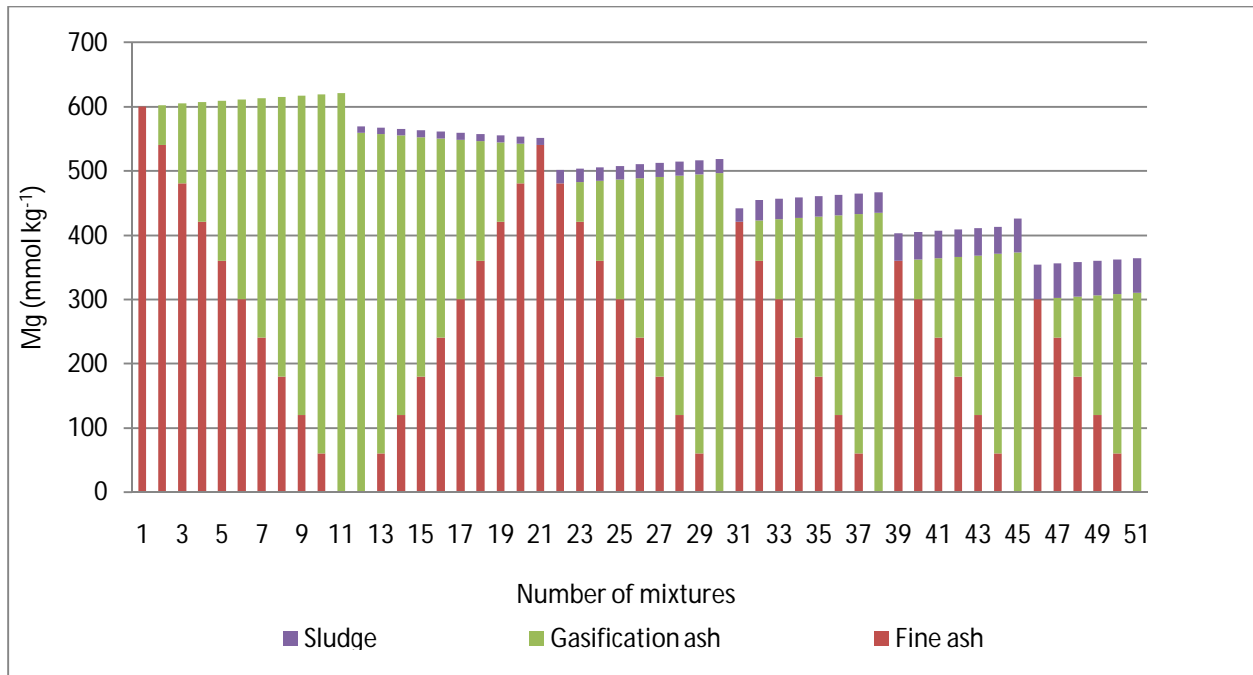


Fig.6. 9: Contribution of sludge, fine and gasification ash to Mg content of mixtures

Table 6.8: Measured and calculated means for Mg, in selected mixtures using microwave digestion method

Mixture Number	Measured Mg (mmol kg ⁻¹)	Calculated Mg (mmol kg ⁻¹)	Confidence interval at 95 % (mmol kg ⁻¹)		Standard deviation (mmol kg ⁻¹)	CV %
			Lower limit	Upper limit		
1	582.9	582.9	446.8	588.9	54.8	9.4
6	588.4	601.4	561.3	615.4	10.9	1.9
11	619.9	619.9	608.1	631.7	4.8	0.8
26	483.4	502.6	487.5	517.8	5.4	1.1
46	320.9	345.3	257.1	384.7	25.7	8.0
51	345.6	363.8	288.7	402.5	22.9	6.6
SL	107.7	107.7	-	-	7.2	6.7

Note: mixtures 1 (100% fine ash), 6 (50% fine ash and 50% gasification ash), 11 (100% gasification ash), 26 (40% fine ash, 40% sludge and 20 % sludge), 46 (50% fine ash and 50% gasification ash) and 51 (50% gasification ash and 50% sludge) were exclusively analysed to enable the estimation of total elements of the other mixtures. SL means sludge.

The Mg content measured in the selected mixtures (mixture 1, 6, 11, 26, 46 and 51) was compared to the calculated Mg content. This was made possible by calculating a 95% confidence interval based on the measured Mg values and the mean. The calculated means fitted well in the respective 95% confidence intervals. The calculated mean (502.6 mmol kg⁻¹) for mixture 26 was significantly different from the measured mean (483.4 mmol kg⁻¹) since it did not fit in the confidence interval (upper limit 497.0 and lower limit 469.9). Repopulating the data readjusted the confidence interval to an upper limit of 517.8 mmol kg⁻¹ and a lower limit 487.5 mmol kg⁻¹ that fitted the calculated mean (502.6 mmol kg⁻¹).

6.3.8 Magnesium leaching from mixtures

Cumulatively mixtures without sludge (mixtures 1 to 11) released the least Mg (1.0 to 7.8 mmol kg⁻¹) than any other group mixtures (Fig.6.10 a). Similarly the same mixtures (mixtures 1 to 11) released the least percent soluble Mg fraction (0.2 to 1.3%) than any other group mixture (Fig.6.10 b). Mixture 43 (with >400 mSm⁻¹) released the most Mg (68.0 mmol kg⁻¹) followed by mixtures 29, 37 40, 41, 44, 47 and 48 (with <400 mSm⁻¹) that released Mg above 50 mmol kg⁻¹. Fine ash (mixture 1) released the least Mg (1.0 mmol kg⁻¹) than any other mixture.

The release of Mg was further viewed in relation to other major cations and anions that potentially can play role in controlling the solubility. Magnesium solubility was less favoured over the solubility of K, Ca and Na in mixtures without sludge and this was indicated by millimolar ratios Mg:K, Ca:Mg and Mg:Na in Fig.6.11 a, Fig.6.7 a and Fig.6.11 b respectively. Adding sludge enhanced in solubilizing Mg containing solid phases and the solubility dominated over the solubility of K, Ca and Na containing solid phases (Fig.6.11 a, Fig.6.8 a and Fig.6.11 b). The addition of sludge further created new negatively charged adsorption sites for Mg reducing its solubility in mixtures without sludge, concurrently increasing the solubility of P in mixtures with sludge (Fig.6.11 c millimolar ratio Mg:P).

Magnesium generally increases the availability of other cations (with one positive charge) to plants by displacing them from the exchange site (Essington, 2004 & Maiti *et al.*, 1990). Magnesium is an essential plant nutrient required in large amounts by plants (Brady and Weil, 2008) thus high solubility of Mg containing minerals influenced by the addition of sludge and its release is desired in improving the fertility status of the mixtures. Mixtures without sludge (mixtures 1 to 11) and mixtures with 10% sludge may need to be supplemented with soluble Mg to fulfill plant requirements.

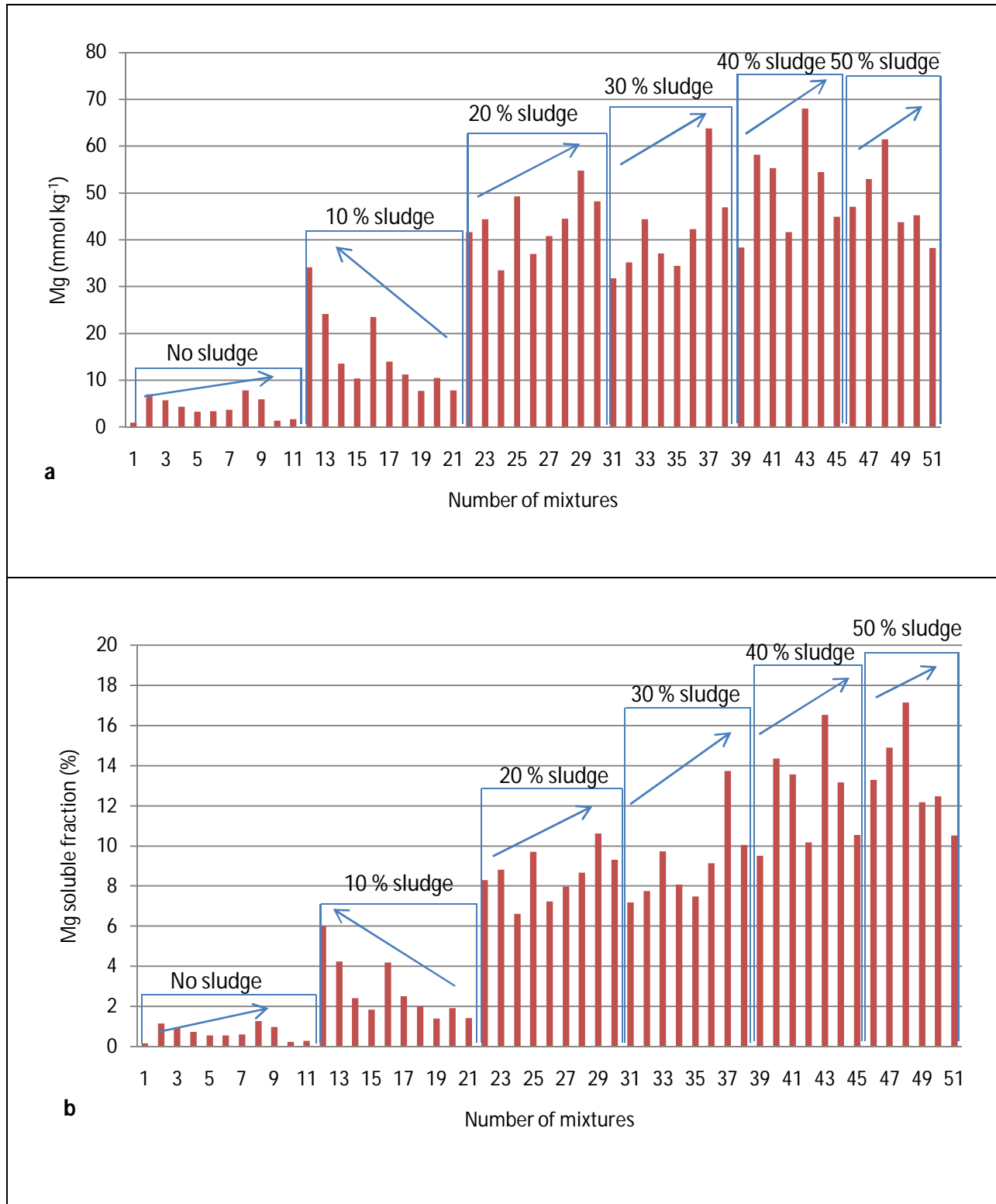


Fig.6. 10: a) Cumulative amount of Mg (mmol kg^{-1}) released after 10 eluviation cycles and b) Cumulative soluble Mg fraction (%) in mixtures released after 10 eluviation cycles. The arrows in a and b indicate the direction of increasing gasification ash content of each sludge treatment group.

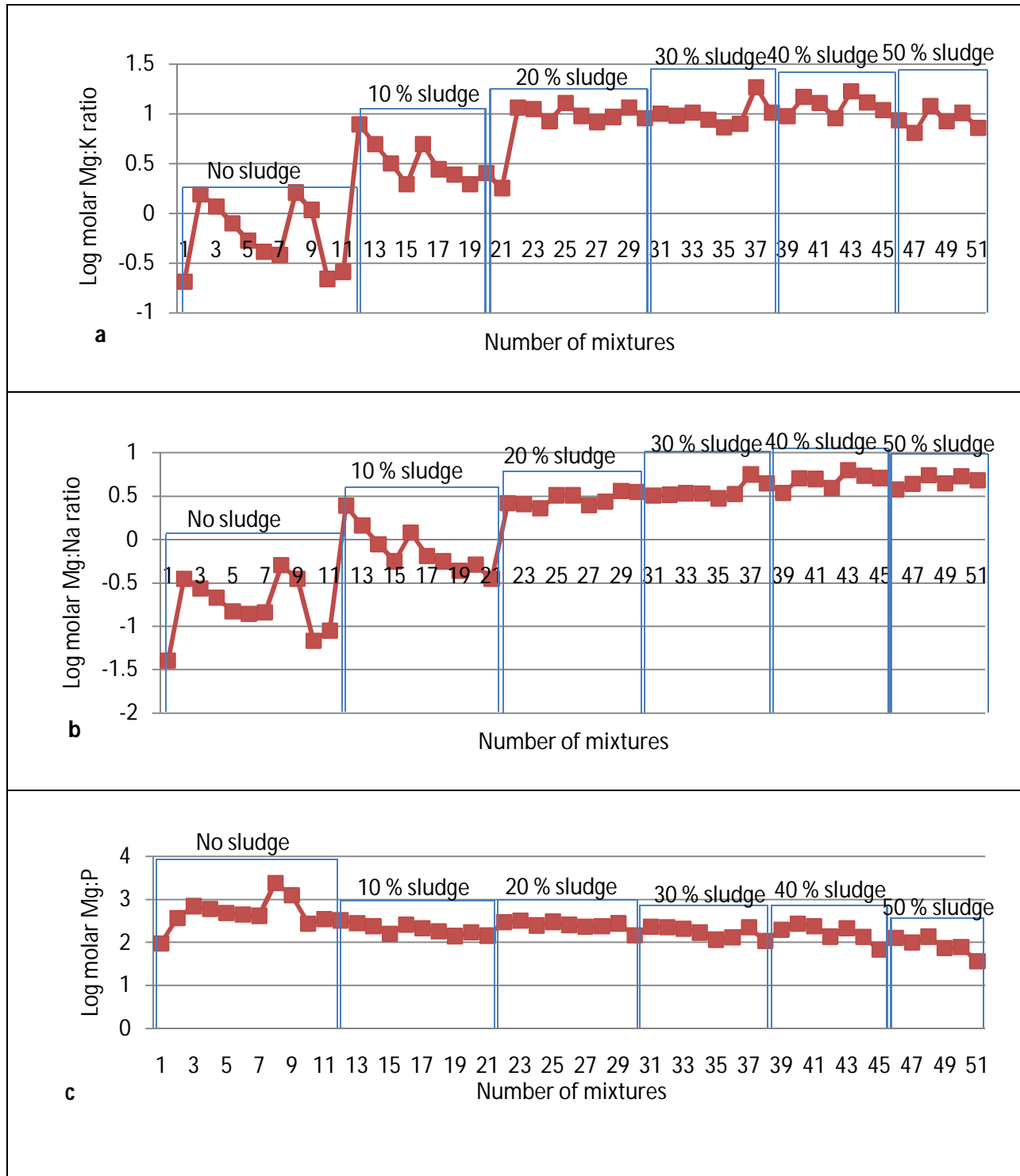


Fig.6. 11: a) Log molar Mg:K ratio based on the cumulative magnesium and potassium released after ten eluviation cycles, b) Log molar Mg:Na ratio based on the cumulative magnesium and sodium released after ten eluviation cycles and c) Log molar Mg:P ratio based on the cumulative magnesium and phosphorus released after ten eluviation cycles.

6.3.9 Potassium content of Sasol sludge, fine and gasification ashes measured in 2006, 2007, 2008 and 2011

Statistically there was no significant difference at both 1 and 5% level in K content amongst the means 0.2, 0.2 and 0.1% for sludge, fine and gasification ashes respectively (Fig.6.12). The least significant difference was calculated as 0.3. The coefficient of variation was very high (122.2%) due to the high variability in K content for gasification ash as indicated by longer error bars with minimum, maximum and median of 0.02, 0.9 and 0.02% respectively. Fine ash had the least variability in K content over the five year period with minimum, maximum and median of 0.02, 0.2 and 0.02% respectively. Potassium content in sludge varied slightly with minimum, maximum and median of 0.1, 0.3 and 0.4% respectively.

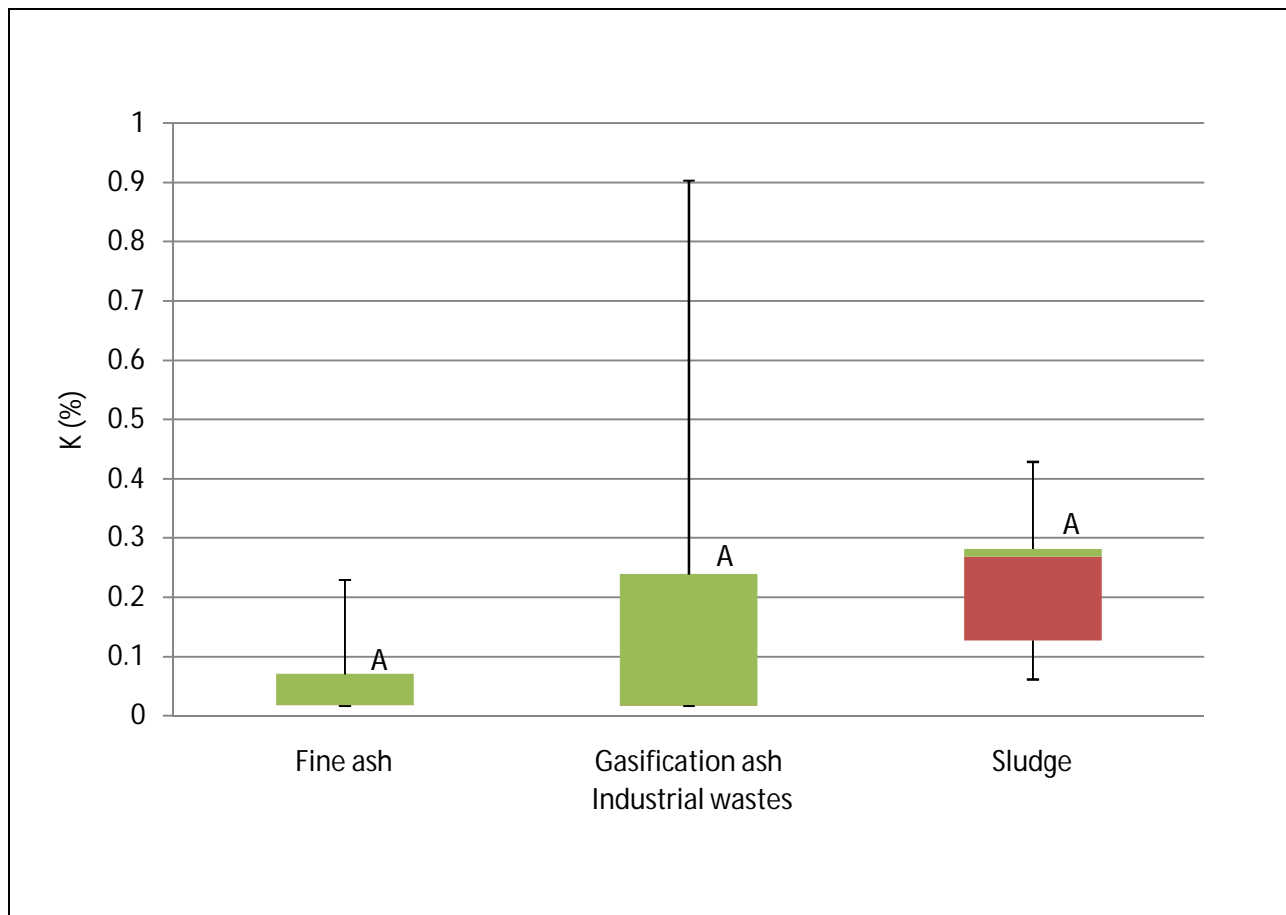


Fig.6. 12: Potassium content in Sasol sludge, fine and gasification ashes measured in 2006, 2007, 2008 and 2011 as determined by digestion method

Table 6.9: Potassium content in Sasol fine and gasification ashes as determined by X-ray Fluorescence Spectroscopy (XRF) measured in 2008 and 2011.

Year	K (%) in Gasification ash	K(%) in Fine ash
2011	0.5	-
2011	0.6	0.8
2011	0.5	0.8
2008	0.5	-
<i>Mean</i>	<i>0.6</i>	<i>0.8</i>
<i>Standard deviation</i>	<i>0.04</i>	<i>0.0</i>
<i>Coefficient of variation (%)</i>	<i>7.5</i>	<i>2.8</i>

Over the two years the K content in both fine and gasification ash differed, the means for gasification and fine ashes were 0.6 and 0.8% respectively (Table 6.9). However, the K content in gasification ash showed to be more variable over the two year period with a coefficient of variation of 7.5%. The K content in fine ash was less variable with a coefficient of variation of 2.8% and a standard deviation of 0. In determining K both methods (XRF and acid digestion) gave different results with 95% confidence interval indicating significant differences in the two methods in determining K for fine and gasification ashes (Table 6.10).

Table 6.10: Comparison of total K content determined using acid digestion and XRF in fine and gasification ashes based on 95% confidence intervals

Ash material	Acid digestion					XRF				
	Mean	Lower limit	Upper limit	Stdev	CV (%)	Mean	Lower limit	Upper limit	Stdev	CV (%)
Fine	0.1	-0.2	0.3	0.1	150.4	0.6	0.5	0.6	0.0	2.7
Gasification	0.2	-0.7	1.2	0.4	185.7	0.6	0.5	0.7	0.0	7.5

6.3.10 Potassium content in mixtures

Measured and calculated K content was less abundant than Ca, Mg and Na in the mixtures (Table 6.9) Fine and gasification ash total K content was 44.8 and 43.8 mmol kg⁻¹ respectively higher than the K content of sludge (26.5 mmol kg⁻¹). Therefore, fine ash contributed the most to K content in the mixtures followed by gasification ash and sludge respectively (Fig.6.13). The K content in sludge was low because most K compounds are water soluble and remain in the aqueous fraction during sludge dewatering (Rehcgil, 1995). While the K in both ash is located in the interior glassy matrix and in minerals present in ash (Jala & Goyal, 2006).

Table 6.11: Measured and calculated means for K, in selected mixtures using microwave digestion method

Mixture Number	Measured K (mmol kg ⁻¹)	Calculated K (mmol kg ⁻¹)	Confidence interval at 95 % (mmol kg ⁻¹)		Standard deviation (mmol kg ⁻¹)	CV %
			Lower limit	Upper limit		
1	44.8	44.8	42.5	47.1	0.9	2.1
6	47.1	44.3	43.9	44.7	0.5	1.1
11	43.8	43.8	42.2	45.4	0.6	1.5
26	42.5	40.7	37.4	47.5	2.0	4.8
46	66.5	35.7	32.4	38.9	2.5	3.8
51	68.2	35.2	32.0	38.4	8.2	12.1
SL	26.5	26.5	-	-	9.4	35.4

Note: mixtures 1 (100% fine ash), 6 (50% fine ash and 50% gasification ash), 11 (100% gasification ash), 26 (40% fine ash, 40% sludge and 20% sludge), 46 (50 % fine ash and 50% gasification ash) and 51 (50% gasification ash and 50% sludge) were exclusively analysed to enable the estimation of total elements of the other mixtures. SL means sludge.

To establish the significance level of the calculated means for the mixtures 1, 11, 26, 46 and 51 a 95% confidence interval was computed based on the measured means of the same mixtures (Table.6.11). The calculated means 44.8, 43.8 and 40.8 mmol kg⁻¹ for mixtures 1, 11 and 26 fitted into their respective confidence intervals 47.1 – 42.5, 45.4 – 42.2 and 47.5 – 37.4 mmol kg⁻¹. However, the calculated means 44.3, 35.7, 35.2 mmol kg⁻¹ for mixtures 6, 46 and 51 respectively could not fit in the corresponding confidence intervals showing to be significantly different from the measured means. Repopulating the measured data adjusted the confidence interval to 44.7 - 43.9, 38.9 – 32.4 and 38.4 – 32.0 mmol kg⁻¹ for mixtures 6, 46 and 51 allowing the calculated means to fit respectively.

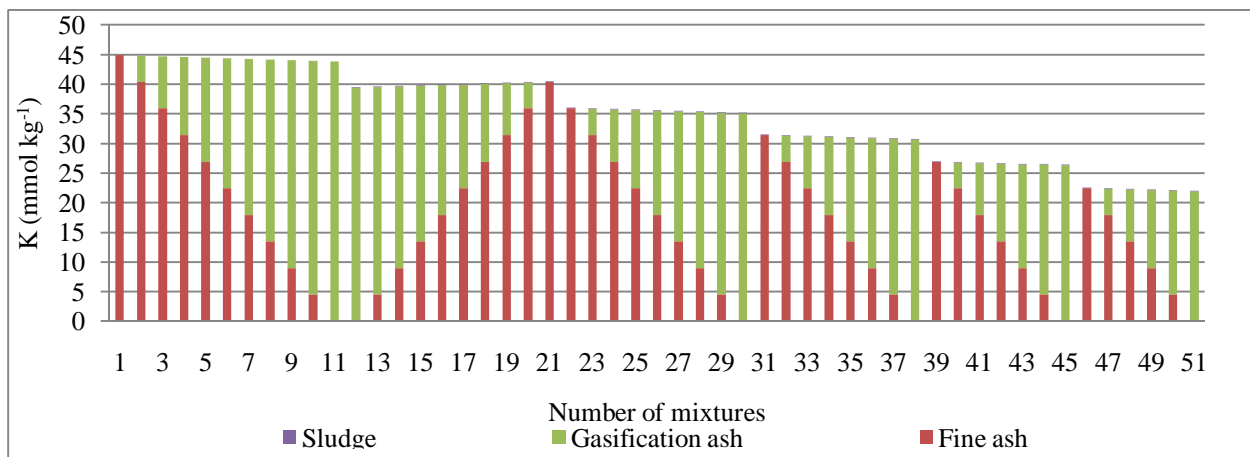


Fig.6. 13: Contribution of sludge, fine and gasification ash to total K content of mixtures

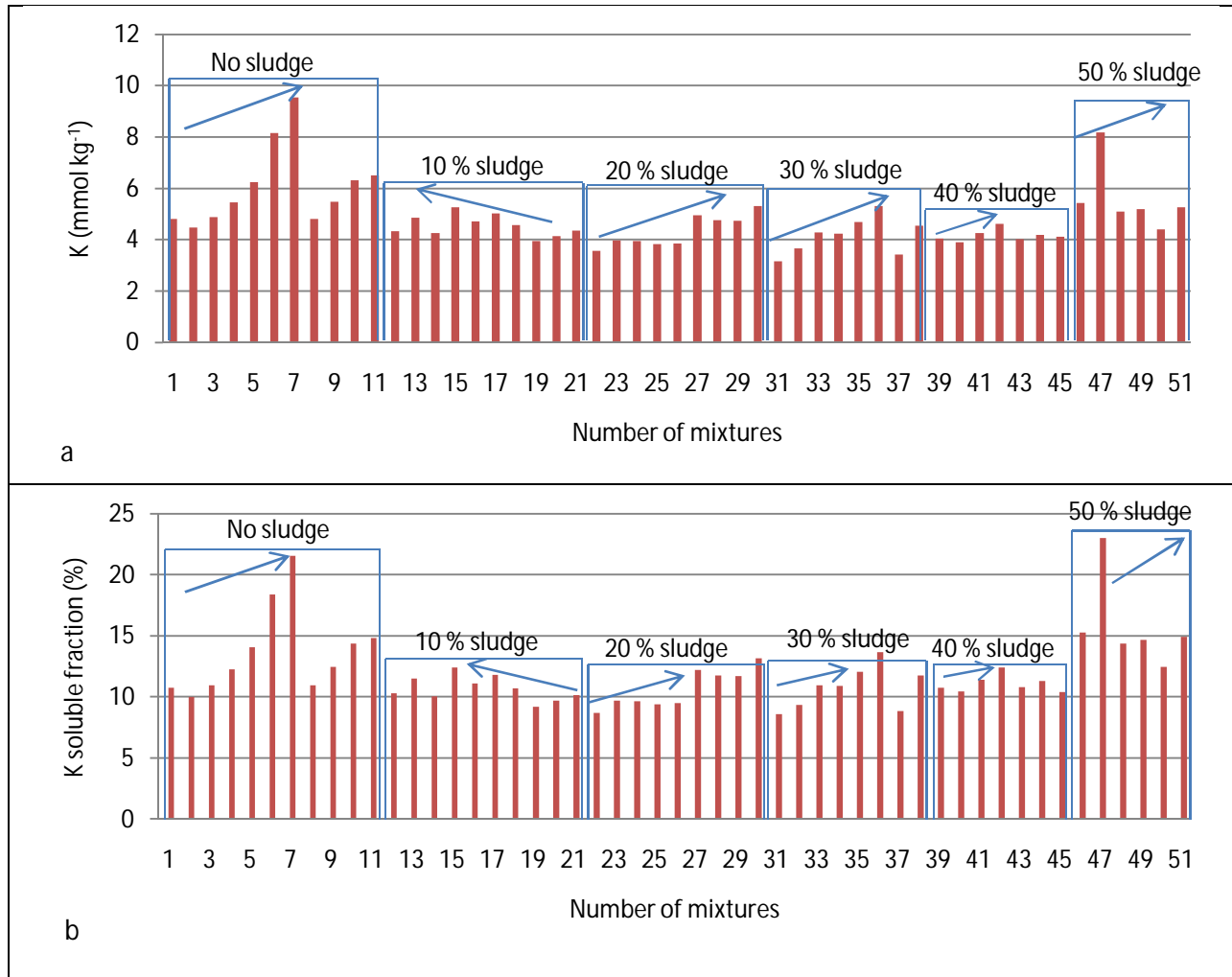


Fig.6. 14: a) Cumulative amount of K (mmol kg⁻¹) released after 10 eluviation cycles and b) Cumulative soluble K fraction (%) in mixtures released after 10 eluviation cycles. The arrows in a and b indicate the direction of increasing gasification ash content of each sludge treatment group.

6.3.11 Potassium leaching from mixtures

After the tenth eluviation cycle, cumulatively mixture 7 released the most K (9.5 mmol kg⁻¹) than any other mixture followed by mixtures 6 (8.2 mmol kg⁻¹) and 47 (8.2 mmol kg⁻¹). Both ashes remain as the main source of K. Mixture 31 released the least K (3.2 mmol kg⁻¹) (Fig.6.14 a). However, mixture 46 released the most soluble percent K fraction and mixture 19 released the least (Fig.6.14 b).

Potassium released was also compared to the release of other major nutrients. Potassium release was favoured over the solubility of Ca, Mg and P in mixtures without sludge as exposed by millimolar ratios Ca:K (Fig.6.8 b), Mg:K (Fig.6.12 a) and K:P (Fig.6.16 b). The same millimolar

ratios Ca:K, Mg:K and K:P showed that most of the soluble K was released from both fine and gasification ash than from sludge. Therefore, increasing sludge could not enhance K solubility which was continuously decreasing with decrease in both fine and gasification ash. New negative adsorption sites for K developed as a result of the organic matter from increasing K retention in the mixtures with sludge. The millimolar ratio K:Na indicated that Na solubility was favoured over the solubility of K in mixtures without sludge and in mixtures with 20 to 30% sludge. Increasing the sludge content of the mixtures from 40 to 50% solubilized most of the solid phases containing Na. The increase in Na concentration contributed to the replacement of K by Na from the exchange sites increasing K release (Fig.6.15 a).

The deficiency of potassium could result to a plant not completing its life cycle (Brady and Weil, 2008) therefore K released is essential for the improvement of soil fertility. Adding sludge increases the retention of K through adsorption, as such, mixtures with sludge require soluble K supplement.

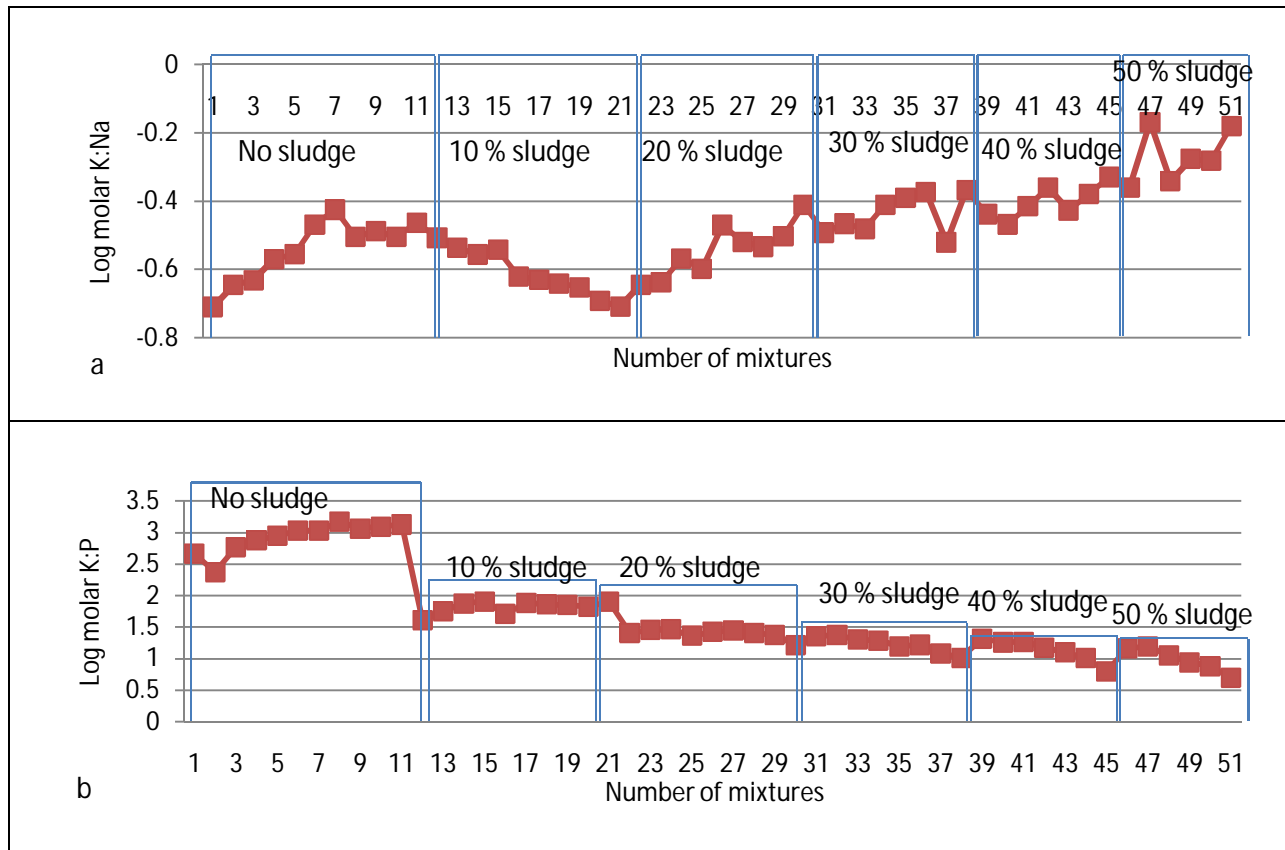


Fig.6. 15: a) Log molar K:Na ratio based on the cumulative potassium and sodium released after ten eluviation cycles and b) Log molar K:P ratio based on the cumulative potassium and phosphorus released after ten eluviation cycles

6.3.12 Sodium content of Sasol sludge, fine and gasification ashes measured in 2006, 2007, 2008 and 2011

The measured Na content (with a mean of 0.1%) in sludge was significantly different and lower than the Na content of both fine (with a mean of 0.3 %) and gasification ash (with a mean of 0.3%) over the five year period (Fig.6.16). However, the Na content in fine ash was not significantly different from the Na content of gasification ash. The calculated least significant difference was 0.09 and the coefficient of variation was slightly high (30.2%). The high coefficient of variation was due to the high variability in the Na content in fine ash as indicated by the long error bars having the minimum, maximum and median of 0.1, 0.4 and 0.4% respectively. Gasification ash had the lowest variability in Na content with minimum, maximum and median of 0.3, 0.4 and 0.3% respectively. Unexpectedly, Na content in sludge was more variable than in gasification ash this was because the measured Na content was high in 2007 (0.1%) and for two replications in 2008 (0.13 and 0.16%). The Na contents for some sludge replications were lower (0.05 to 0.1%) in 2008 and 2011 compared to 2007 and 2008 (for two replications).

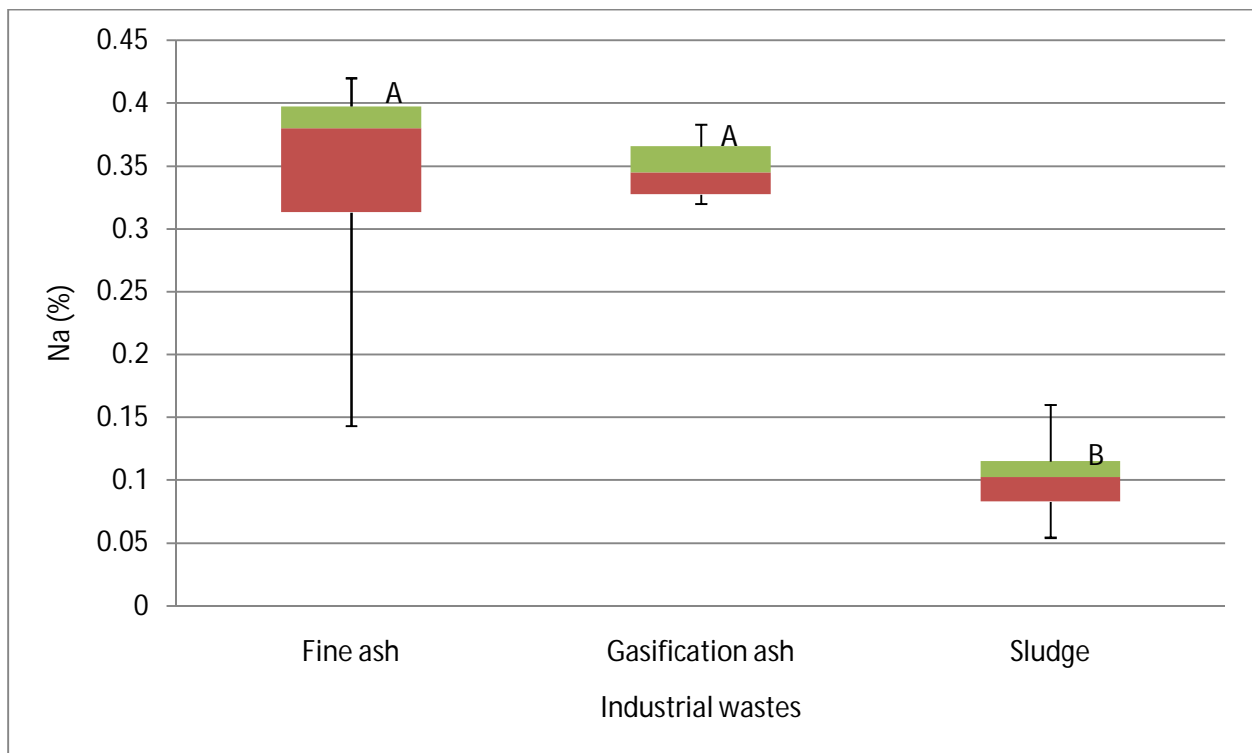


Fig.6. 16: Sodium content in Sasol sludge, fine and gasification ashes measured in 2006, 2007, 2008 and 2011 as determined by digestion method

Table 6.12: Sodium content in Sasol fine and gasification ashes as determined by X-ray Fluorescence Spectroscopy (XRF) measured in 2008 and 2011.

Year	Na (%) in Gasification ash	Na(%) in Fine ash
2011	0.3	-
2011	0.3	0.6
2011	0.4	3.2
2008	0.4	-
<i>Mean</i>	<i>0.4</i>	<i>1.9</i>
<i>Standard deviation</i>	<i>0.07</i>	<i>1.8</i>
<i>Coefficient of variation (%)</i>	<i>18.7</i>	<i>96.4</i>

The Na content was less variable in gasification ash with a coefficient of variation of 18.7% than fine ash with an extremely high coefficient of variation of 96.4% (Table 6.12). The high variability in the Na content for fine ash was because of the high Na content (4.48%) which was measured in 2011. However, the Na content in fine ash was higher (with a mean of 1.9%) than in gasification ash (with a mean of 0.4%). The 95% confidence intervals given by XRF for fine and gasification were wider than those given by acid digestion indicating no significant differences between the two methods in determining Na (Table 6.13).

Table 6.13: Comparison of total Na content determined using acid digestion and XRF in fine and gasification ashes based on 95 % confidence intervals

Ash material	Acid digestion					XRF				
	Mean	Lower limit	Upper limit	Stdev	CV (%)	Mean	Lower limit	Upper limit	Stdev	CV (%)
Fine	0.3	0.1	0.6	0.1	38.3	1.9	-3.7	7.5	1.8	96.4
Gasification	0.3	0.3	0.4	0.0	8.3	0.4	0.2	0.5	1.1	18.7

6.3.13 Sodium content of mixtures

Measured and calculated Na was the third abundant element after Ca and Mg in the mixtures (Table 6.14). Fine ash remained the main contributor of Na ($171.1 \text{ mmol kg}^{-1}$) in the mixtures followed by gasification ($146.4 \text{ mmol kg}^{-1}$) and sludge contributed the least ($37.8 \text{ mmol kg}^{-1}$) (Fig.6.17 and Table 6.12). The main sources of Na in ash are sodium silicate (Na_2SiO_3) and halite (NaCl) (Dijkistra *et al.*, 2006). Sasol fine ash as characterized by Mahlaba *et al.* (2011) was

found to contain analcime ($\text{NaAlSi}_2\text{O}_6 \cdot \text{H}_2\text{O}$) ranging between 0.5 to 1.6% as Na source and the percent Na_2O ranged between 0.98 to 3.51%. However, in 2008, gasification ash was found to contain more Na (0.38%) than fine ash (0.14%). Noticeably the Na content for fine ash (0.39%) of the current study was significantly above the Na content of fine ash obtained in 2008, while the Na content for gasification ash (0.34%) in the current study was found to be significantly low. However, fine ash remained the main contributor of Na than gasification ash and sludge in the current study (Fig.6.17).

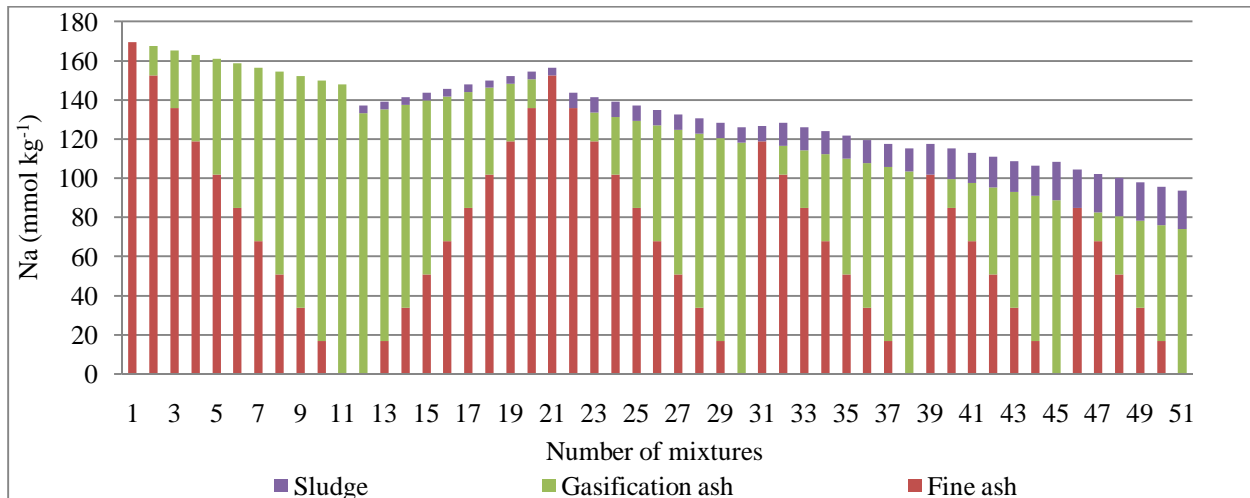


Fig.6. 17: Contribution of sludge, fine and gasification ash to total Na content of mixtures

Table 6.14: Measured and calculated means for Na, in selected mixtures using microwave digestion method

Mixture Number	Measured Na (mmol kg ⁻¹)	Calculated Na (mmol kg ⁻¹)	Confidence interval at 95 % (mmol kg ⁻¹)		Standard deviation (mmol kg ⁻¹)	CV % (mmol kg ⁻¹)
			Lower limit	Upper limit		
1	171.1	171.1	143.9	198.3	10.9	6.4
6	161.7	158.8	144.3	179.0	7.0	4.3
11	146.4	146.4	124.0	168.9	9.19	6.2
26	135.6	134.6	122.0	149.2	5.5	4.0
46	116.0	104.4	93.5	138.5	9.19	7.8
51	89.2	92.1	79.8	98.5	3.8	4.2
SL	37.8	37.8		-	12.6	33.4

Note: mixtures 1 (100% fine ash), 6 (50% fine ash and 50% gasification ash), 11 (100% gasification ash), 26 (40% fine ash, 40% sludge and 20% sludge), 46 (50% fine ash and 50% gasification ash) and 51 (50% gasification ash and 50% sludge) were exclusively analysed to enable the estimation of total elements of the other mixtures. SL means sludge.

To enable the estimation of Na content for the rest of the mixtures Na was measured in mixtures 1, 6, 11, 26, 46 and 51. The calculated Na contents were then compared to the measured Na mean values. To verify the significance of the calculated Na values a 95% confidence interval for each of the mixtures was calculated based on the measured Na means to fit in the means of the calculated values. It was found that the calculated means; 171.1, 158.8, 146.4, 134.6, 104.4 and 92.1 mmol kg⁻¹ for mixtures 1, 6, 11, 26, 46 and 51 fitted in the confidence intervals; 198.3 - 143.9, 179.0 - 144.3, 168.9 - 124.0, 149.2 - 122, 138.5 - 93.5 and 98.5 - 79.8 mmol kg⁻¹ respectively. This clearly showed that there was no significant difference between the measured means and calculated means.

6.3.14 Soluble sodium released

The release of Na was also viewed in relation to the other major nutrients. Evidently the release of Na was controlled by the concentration of other cations that also compete for the exchange sites, Ca being the most competitor. Calcium ions have a larger interaction with mineral surfaces than Na⁺ and Ca²⁺ forms monodentate inner sphere complex. Sodium ions have a weak interaction with the mineral surfaces forming outer sphere complexes (Rahnemaie *et al.*, 2006). This was evident from molar ratio Ca:Na (Fig.6.7 a), where Na released was favoured over Ca released in mixtures without sludge. Adding sludge reduced Na released through the development of new adsorption sites for Na further reducing the dissolution of less soluble Na containing mineral phases (Fig.6.18, a and b) (Dijkistra *et al.*, 2006).

Cumulatively mixture 7 released the most Na (25.4 mmol kg⁻¹) than any other mixture as the ashes remain as the main source of Na (they contain minerals with Na) and mixture 51 released the least Na (8.0 mmol kg⁻¹). Most mixtures without sludge (mixtures; 1, 3, 4, 5, 6 and 10) and mixtures that received 10 % sludge (mixtures; 17, 20 and 21) were capable of releasing Na above 20 mmol kg⁻¹ but less than 25 mmol kg⁻¹. Molar ratios; Ca:Na, Mg:Na and K:Na in Fig.6.7 a, Fig.6.11 b and Fig.6.15 a respectively indicated that solubility favoured Na over Ca, Mg and K in mixtures without sludge. The addition of sludge favours the solubility of Ca, Mg and K than Na in all mixtures with sludge.

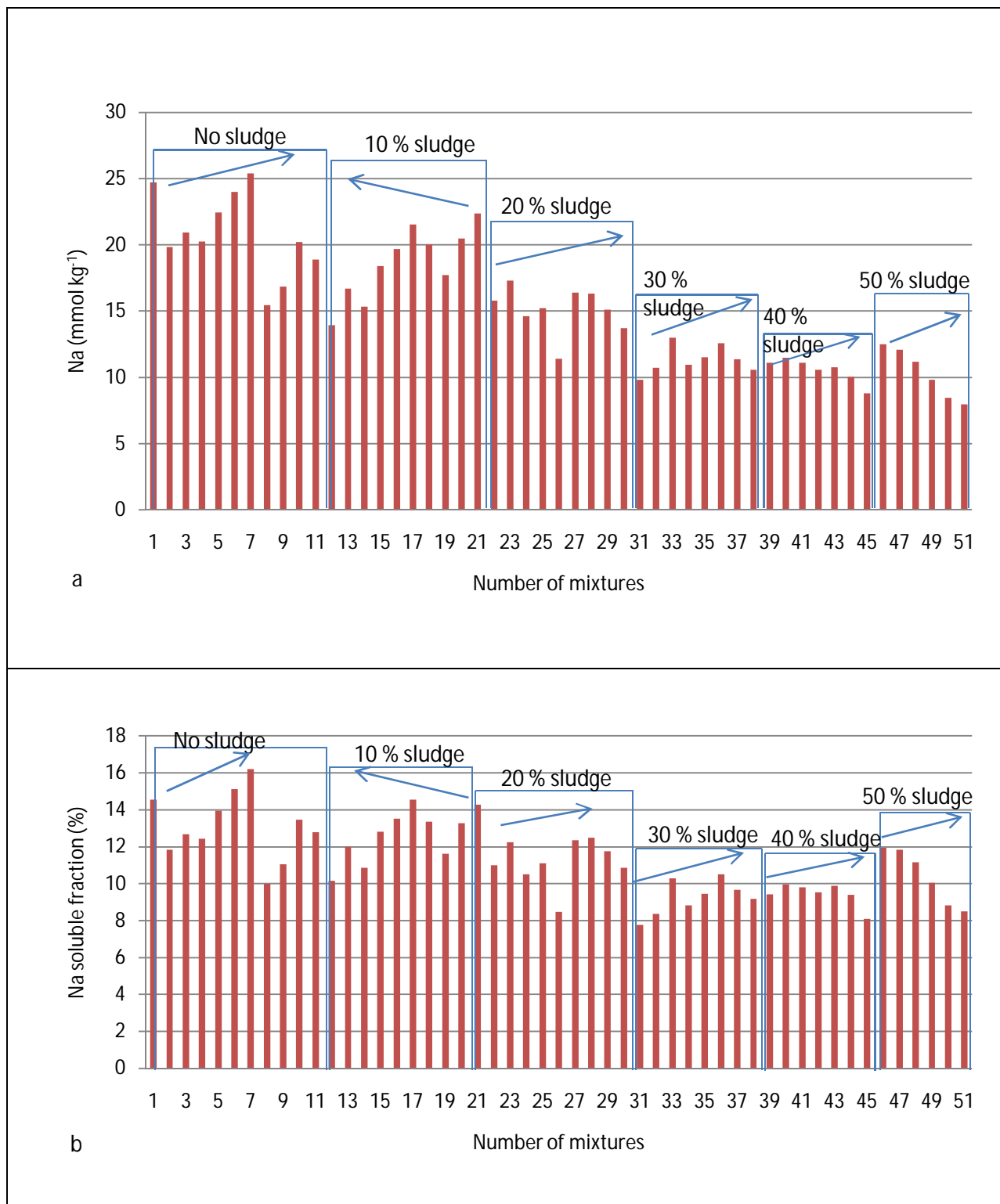


Fig.6. 18: a) Cumulative amount of Na (mmol kg⁻¹) released after 10 eluviation cycles and b) Cumulative soluble Na fraction (%) in mixtures released after 10 eluviation cycles. The arrows in a and b indicate the direction of increasing gasification ash content of each sludge treatment group.

6.3.15 Phosphorus content of Sasol sludge, fine and gasification ashes measured in 2006, 2007, 2008 and 2011

As expected the measured P in sludge was high (with a mean of 0.6%) and significantly different from the P content of both fine (with a mean of 0.3%) and gasification ashes (with a mean of 0.3%) at both 1 and 5% levels (Fig.6.19). But the P contents of both fine and gasification ashes were not significantly different from each other. The least significant difference was computed as 0.2 and the coefficient of variation was calculated as 28.8%. Gasification ash showed to have the least variability in P content as indicated by short error bars than fine ash and sludge. The P content in gasification ash had minimum, maximum and median of 0.3, 0.4 and 0.3% respectively while sludge had minimum, maximum and median of 0.4, 0.8 and 0.6% respectively. Fine ash had similar error bars as sludge with minimum, maximum and median of 0.2, 0.4 and 0.3% respectively.

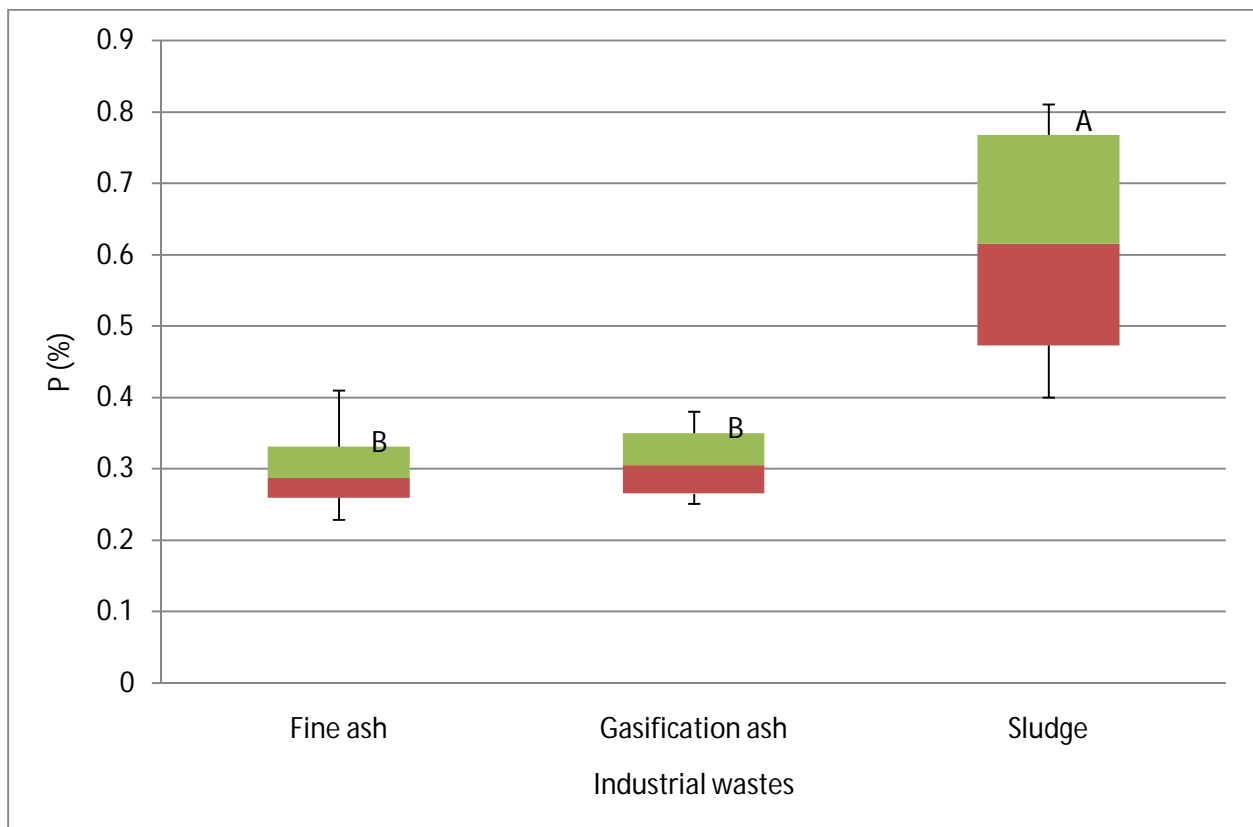


Fig.6. 19: Phosphorus content in Sasol sludge, fine and gasification ashes measured in 2006, 2007, 2008 and 2011 as determined by digestion method

Table 6.15: Phosphorus content in Sasol fine and gasification ashes as determined by X-ray Fluorescence Spectroscopy (XRF) measured in 2008 and 2011.

Year	P(%) in Gasification ash	P(%) in Fine ash
2011	0.5	-
2011	0.5	0.5
2011	0.5	0.6
2008	0.6	-
<i>Mean</i>	<i>0.5</i>	<i>0.6</i>
<i>Standard deviation</i>	<i>0.05</i>	<i>0.08</i>
<i>Coefficient of variation (%)</i>	<i>10.2</i>	<i>14.9</i>

The mean P content in gasification ash was 0.1 units lower than the P content on fine ash when averaged over a period of two years (Table 6.15). However, the variability in P content for fine ash was higher with a coefficient of variation of 14.9% than the variability P content in gasification ash with a coefficient of variation of 10.9%. In determining total P both methods (acid digestion and XRF) gave overlapping 95% confidence intervals for both fine and gasification ashes indicating significant differences in the two methods in determining P (Table 6.16)

Table 6.16: Comparison of total P content determined using acid digestion and XRF in fine and gasification ashes based on 95 % confidence intervals

Ash material	Acid digestion					XRF				
	Mean	Lower limit	Upper limit	Stdev	CV (%)	Mean	Lower limit	Upper limit	Stdev	CV (%)
Fine	0.3	0.1	0.4	0.1	25.5	0.5	0.3	0.8	0.1	14.9
Gasification	0.3	0.2	0.4	1.2	18.1	0.5	0.4	0.6	0.1	10.2

6.3.16 Phosphorus content in mixtures

Sludge contained the most measured P content ($149.6 \text{ mmol kg}^{-1}$) than fine ($106.0 \text{ mmol kg}^{-1}$) and gasification ashes ($106.5 \text{ mmol kg}^{-1}$) (Table 6.17). In 2008 the P content of Sasol sludge (0.45%), fine (0.23%) and gasification ash (0.25%) was significantly lower than the P content of sludge (0.46%), fine ash (0.32%) and gasification ash (0.33%) of the current study. The contribution of sludge to P content of the mixtures was therefore more evident in Fig.6.20. Most

of the P is contained in calcium compounds such as carbonate apatite ($\text{Ca}_5(\text{PO}_4)_3(\text{OH},\text{F},\text{Cl})$) in alkaline conditions like in coal ash (Brady and Weil, 2008).

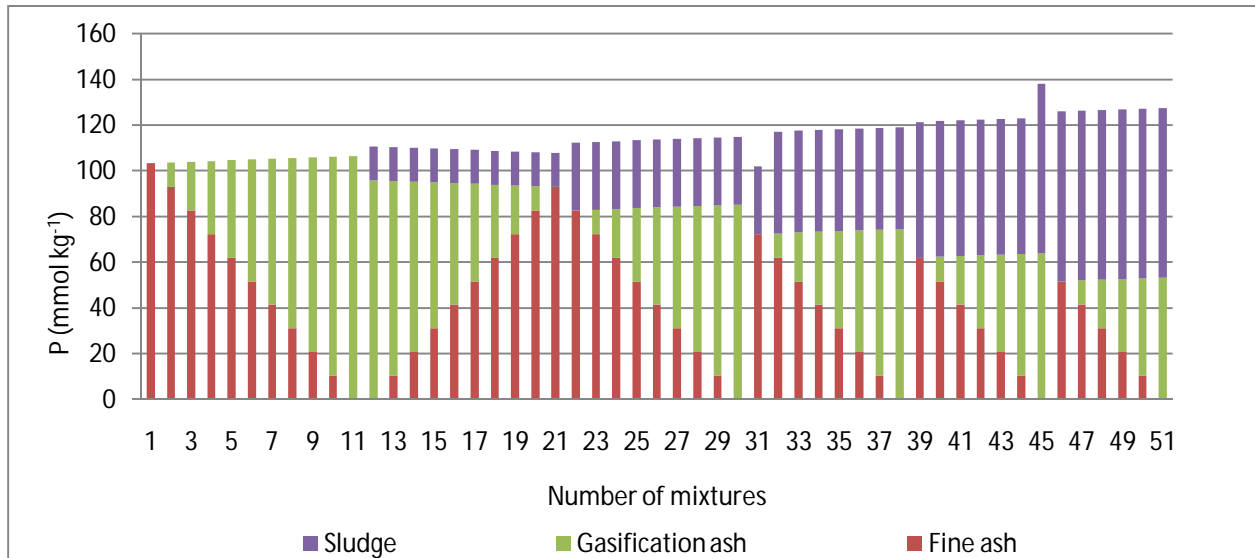


Fig. 6. 20: Contribution of sludge, fine and gasification ash to total P content of mixtures

Table 6.17: Measured and calculated means for P, in selected mixtures using microwave digestion method

Mixture Number	Measured P (mmol kg^{-1})	Calculated P (mmol kg^{-1})	Confidence interval at 95 % (mmol kg^{-1})		Standard deviation (mmol kg^{-1})	CV % (mmol kg^{-1})
			Lower limit	Upper limit		
1	106.0	106.0	47.6	164.4	23.5	22.2
6	135.6	106.3	17.5	253.7	47.6	35.1
11	106.5	106.5	61.9	151.2	18.0	16.9
26	113.0	114.9	78.3	147.7	14.0	12.4
46	102.2	127.8	71.9	132.6	12.2	12.0
51	99.0	128.1	119.2	136.9	10.4	10.5
SL	149.6	149.6	-	-	18.4	12.3

Note: mixtures 1 (100% fine ash), 6 (50% fine ash and 50% gasification ash), 11 (100% gasification ash), 26 (40% fine ash, 40% sludge and 20% gasification ash), 46 (50% fine ash and 50% gasification ash) and 51 (50% gasification ash and 50% sludge) were exclusively analysed to enable the estimation of total elements of the other mixtures. SL means sludge.

Based on measured P values for mixtures 1, 6, 11, 26, 46 and 51 a 95% confidence interval was calculated to verify the significance of the calculated P values. It was found that the calculated means for mixtures 1, 6, 11, 26, and 46 fitted well in the respective confidence intervals

indicating not to be significantly different from the measured means. However, the calculated mean ($128.1 \text{ mmol kg}^{-1}$) for mixture 51 did not fit in the confidence interval ($124.8 - 73.2 \text{ mmol kg}^{-1}$) showing to be significantly different from the measured mean ($99.0 \text{ mmol kg}^{-1}$). Repopulating the data readjusted the confidence interval to an upper limit of $136.9 \text{ mmol kg}^{-1}$ to a lower limit of $119.2 \text{ mmol kg}^{-1}$ that fitted the calculated mean ($128.1 \text{ mmol kg}^{-1}$).

6.3.17 Soluble phosphorus released

The release of P is generally controlled by pH and an increase in pH desorbs the P from the Ca-P compounds by increasing competition between hydroxyl ions and the adsorbed P (Jin *et al.*, 2006). The initial P release in ash is generally rapid until equilibrium is reached. Fast, intermediate and slow P released is attributed to; the dissolution of poorly crystalline metastable calcium phosphates converting to hydroxyapatite. A combination of desorption and diffusion-dissolution reactions control the initial fast and final slow release of P in ash (Shariatmadari *et al.*, 2006).

Cumulatively mixture 51 released the highest P (1.1 mmol kg^{-1}) followed by mixtures 45, 49, 50, 47, 48, 38 and 44 respectively with more than 0.4 mmol kg^{-1} . In these mixtures sludge remained as the main source of P. Mixture 21 (fine ash 90%, gasification ash 0% and sludge 10%) released the least P ($0.05 \text{ mmol kg}^{-1}$) amongst mixtures with sludge. Mixtures without sludge released the least P that ranged from 0.01 to $0.004 \text{ mmol kg}^{-1}$ (Fig.6.21 a). The same trend was also indicated in the release of soluble P fraction (%) in Fig.6.21 b where P released increased with increase in sludge. The increase in P release as influenced by sludge has been showed by millimolar ratios; K:P, Mg:P and Ca:P in Fig.6.15 b, Fig.6.11 c and Fig.6.7 d respectively. Humified compounds such as fulvic acid (FA) and humic acid (HA) resulted from the decomposition of sludge and contained functional groups (carboxyl and phenolic hydroxyl) that normally deprotonate at certain pH levels. In these mixtures the dissociation of the functional groups was possible because the pH ranged from 7.6 to 11.7 since at this pH ($\text{pH} > 3$) Ha and FA behave as negatively charged poly-electrolytes. The dissociation of carboxyl groups ($3 < \text{pH} < 9$) and phenolic hydroxyl groups ($\text{pH} > 9$) increased P release (Mulder & Cresser, 1994).

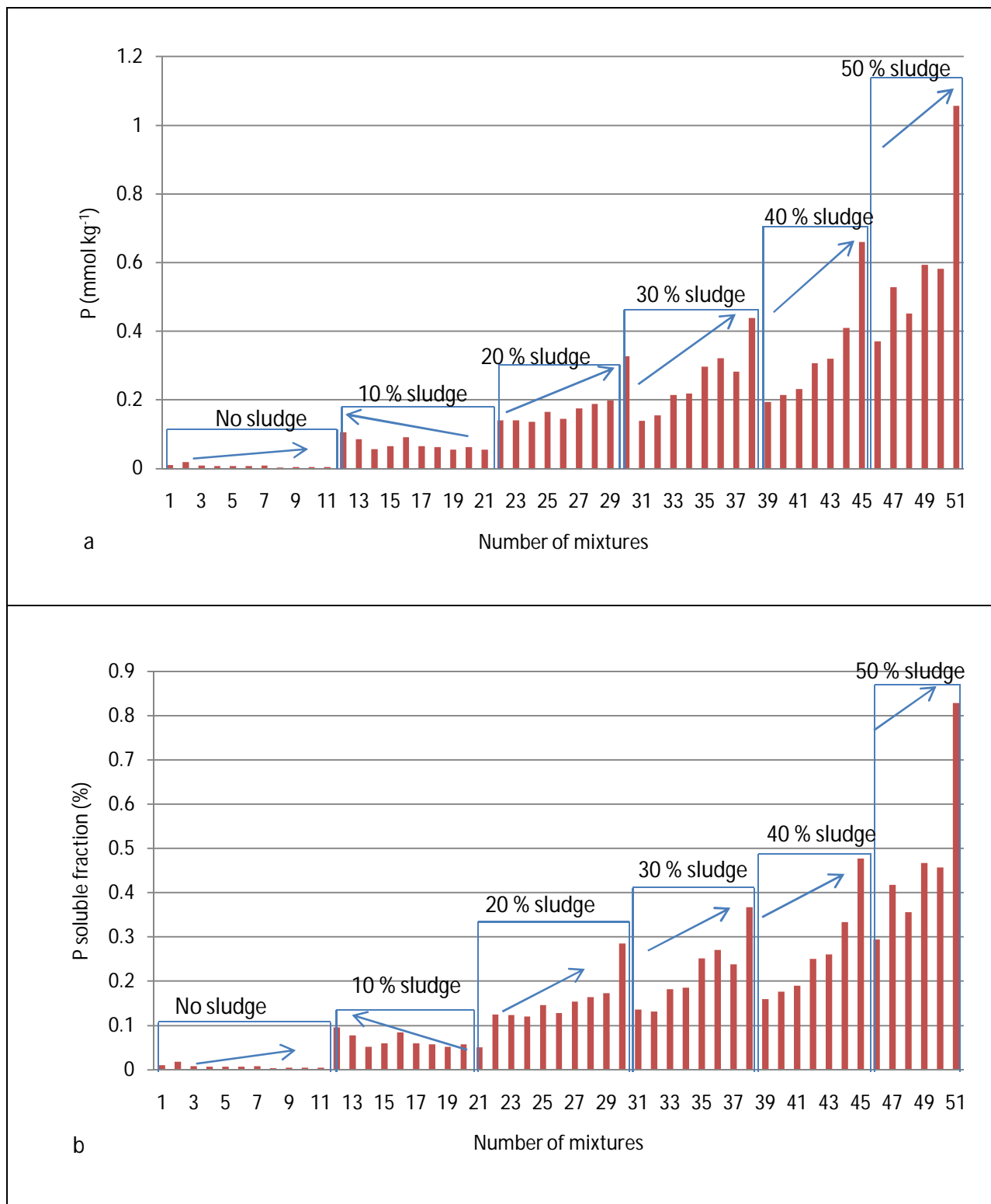


Fig.6. 21: a) Cumulative amount of P (mmol kg⁻¹) released after 10 eluviation cycles and b) Cumulative soluble P fraction (%) in mixtures released after 10 eluviation cycles. The arrows in a and b indicate the direction of increasing gasification ash content of each sludge treatment group.

6.3.18 Micronutrients

Essential micronutrients (Zn, Cu, Mn, Mo, Fe, Cl and B) described as trace elements and required by plants in extremely small quantities (Fageria *et al.* 2002, Gupta *et al.*, 2008 & Brady & Weil, 2008) were also determined in the leachates as soluble elements including; S, Al and Co. However, the discussion was limited to Zn, Cu, Mn, Mo, Fe and B, but it should be noted that total elemental analysis on fresh samples was done for Fe, Zn, Mn and Cu amongst the micronutrients (Table 6.18). The analysis was performed on selected mixtures (mixtures 1, 6, 11, 26, 46, 51 and sludge). The reason behind analyzing mixture 1 (fine ash), 11 (gasification ash) and sludge was to enable calculation of the total elements in the other mixtures. Mixtures 6 (50% fine ash and 50% gasification ash), 26 (40% fine ash, 40% gasification ash and 20% sludge), 46 (50% fine ash and 50% sludge) and 51 (50% gasification ash and 50% sludge) were included in the analysis for verification purposes. Generally, the total measured and calculated content of micronutrients in the mixtures were in the following order; Fe>Mn>Zn>Cu (Table 6.18). The percentage difference between the measured and calculated total elements was narrow and ranged between 0 to 23%.

6.3.19 Iron and manganese in mixtures

The trend in Fe and Mn indicated that fine ash had both elements in abundance compared to gasification ash and sludge (Table 6.18). Fine ash, gasification ash and sludge contained 2145.2, 515.7 and 109.2 mmol kg⁻¹ Fe respectively. With respect to Mn; fine ash, gasification ash and sludge contained 14.93, 5.10 and 1.49 mmol kg⁻¹ respectively. It was also evident in Fig.6.22, a and c that fine ash was the main contributor of both Fe and Mn in the mixtures while sludge contributed the least. In comparison with results obtained in 2008, fine ash contained less Fe (0.56%) than fine ash Fe content (12.0%) of the current study. Similarly, in 2008 fine ash contained less Mn (0.032%) than the Mn content (0.082 %) of the same material for the current study. Sasol fine ash contains magnetite (FeFe₂O₄), hematite (Fe₂O₃) and pyrrhotite (Fe₉S₁₀) that range from 0.1 to 14.1%, 0.75 to 2.0% and 0.3 to 0.8% respectively that remain as main sources of Fe (Mahlabane *et al.*, 2011). Manganese occurs in carbonates (rhodochrosite), silicates (rhodanate), simple oxides (manganite) and complex oxides (braunite) (Fageria *et al.* 2002) that may also be present in coal ash.

Table 6.18: Measured and calculated Cu, Mn, Zn and Fe in selected mixtures

Mix. No.	Meas. Cu	Calc. Cu	Meas. Mn	Calc. Mn	Meas. Zn	Calc. Zn	Meas. Fe	Calc. Fe
	mmol kg ⁻¹							
1	0.83	0.83	14.93	14.93	0.40	0.40	2145.22	2145.22
6	0.79	0.87	10.27	10.01	0.33	0.29	1328.68	1330.47
11	0.92	0.92	5.10	5.10	0.19	0.19	515.71	515.71
26	0.70	0.75	8.19	8.31	0.77	0.70	1077.98	1086.22
46	0.61	0.55	7.60	8.21	1.49	1.36	1088.73	1127.23
51	0.45	0.59	2.89	3.30	1.43	1.26	333.06	312.47
SL	0.27	0.27	1.49	1.49	2.32	2.32	109.23	109.23

Note: mixtures 1 (100% fine ash), 6 (50% fine ash and 50% gasification ash), 11 (100% gasification ash), 26 (40% fine ash, 40% sludge and 20% sludge), 46 (50% fine ash and 50% gasification ash) and 51 (50% gasification ash and 50% sludge) were exclusively analyzed to enable the estimation of total elements of the other mixtures

6.3.20 Soluble Fe and Mn

In both ashes it was expected that processes such as dissolution of the solid phases and desorption of Fe and Mn could occur as initiated by weathering, but seemingly they occurred at very slow rate in mixtures without sludge because the minerals containing Fe and Mn have limited solubility in nature (Essington, 2004). However, the addition of sludge liberated more of the Fe and Mn by increasing the solubility of the solid phases and through humic substances (Fig.6.22 b and d). Humified compounds such as fulvic acid (FA) and humic acid (HA) that result from the decomposition of organic matter contain functional groups (carboxyl and phenolic hydroxyl) that form complexes with metals through chelation, the chelation further promotes the dissolution of metals from the minerals (Mulder & Cresser, 1994). This was possible in the mixtures because pH ranged from 7.6 to 11.7 which is a parameter that determines the charge characteristics of the humic substances. At this pH (pH>3) Ha and FA behave as negatively charged poly-electrolytes due to the dissociation of carboxyl groups (3<pH<9) and phenolic hydroxyl groups (pH>9) (Mulder & Cresser, 1994).

Cumulatively, the contribution of sludge to the solubility of solid phases and subsequent release of Fe and Mn was more pronounced. Mixture 47 (40% fine ash, 10% gasification ash and 50% sludge) released the most Fe (0.04 mmol kg⁻¹) than any other mixture and mixture 21 (90% fine ash, 0% gasification ash and 10% sludge) released the least (0.2 μmol kg⁻¹). Mixture group

without sludge (mixture 1 to 11) and the group with 10% sludge (mixture 12 to 21) released the least Fe (0.2 to $0.9 \mu\text{mol kg}^{-1}$) compared to all other mixture groups that released Fe in the range between 2.0 to $40.0 \mu\text{mol kg}^{-1}$) (Fig.6.22 b). With Mn, mixtures without sludge and the mixture group with 10% sludge released the least Mn (5.9×10^{-4} mmol kg^{-1} to 1.2×10^{-3} mmol kg^{-1}) than any other mixture group, while mixture 43 (20% fine ash, 40 % gasification ash and 40% sludge) released the most Mn (0.013 mmol kg^{-1}) than any other mixture and mixture 1 (100% fine ash) released the least Mn (5.9×10^{-4} mmol kg^{-1}) (Fig.6.22 d).

Critical concentration ranges of available Fe and Mn for most plants are 2.5 - 5 mg kg^{-1} (as extracted by NH_4HCO_3 -DTPA and DTPA-TEA) and 4 - 8 mg kg^{-1} (as extracted by NH_4HCO_3 -DTPA and Mehlich-1, 2 and 3) respectively (Fageria, *et al.*, 2002). Seemingly the ranges 0.011 - 2.2 mg kg^{-1} (Fe) and 0.03 - 0.7 mg kg^{-1} (Mn) released from the mixtures were far below the critical concentrations in literature. According to Fageria, *et al.* (2002) pH influences both solubility and mobility of micronutrients. Iron solubility decreases approximately 1000 fold for each unit increase of pH in the range between 4 to 9. At this pH Fe^{2+} is oxidized to Fe^{3+} that precipitates. Manganese exists as Mn^{2+} and decreases approximately 100 fold for each unit increase in pH and increases the organic fraction of Mn. The high pH (7.6 to 11.7) in the mixtures could be the reason for the low soluble Fe and Mn. Both elements may therefore need to be supplemented in all the mixtures.

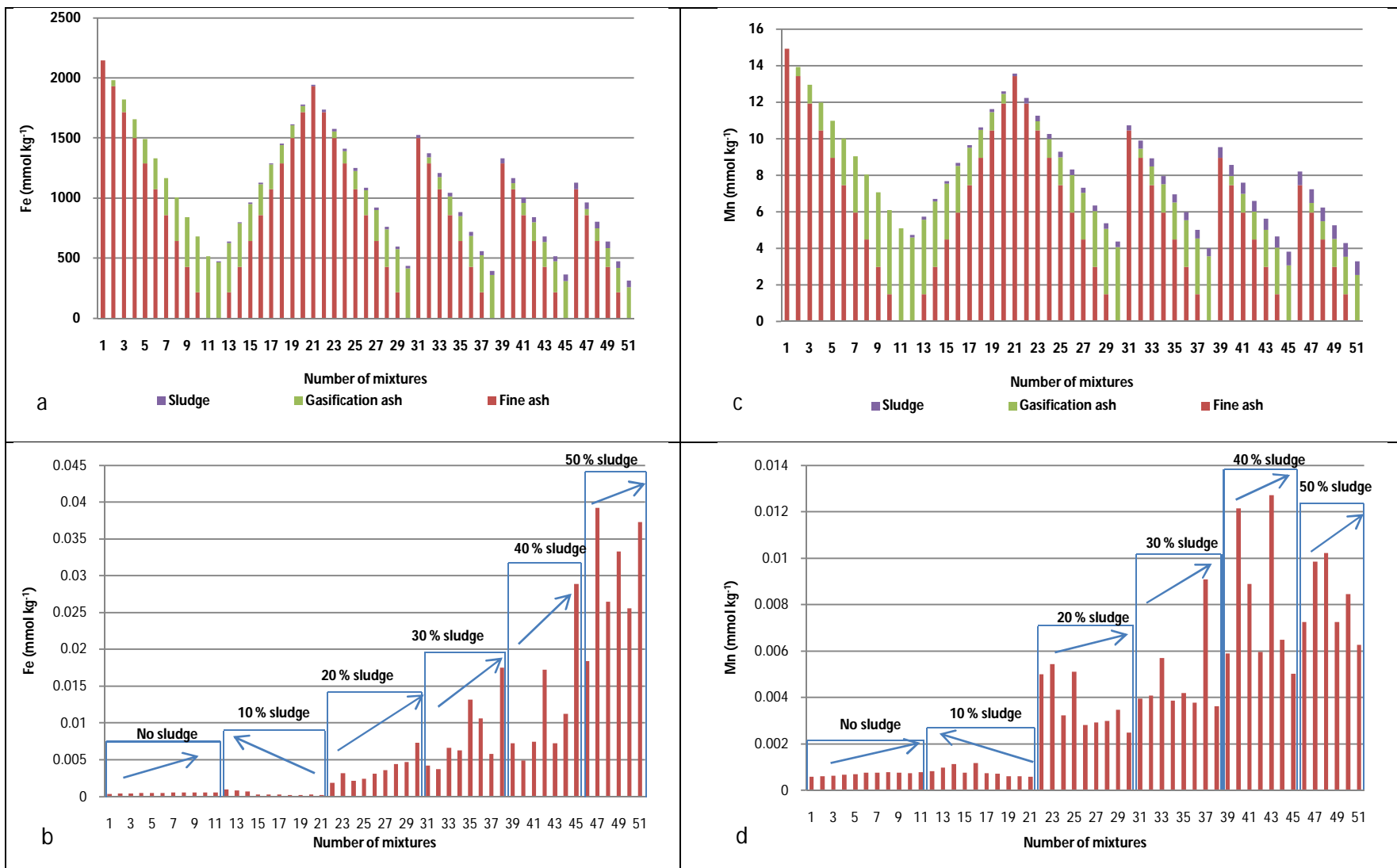


Fig.6. 22: a) Contribution of sludge, fine and gasification ash to total Fe content of mixtures, b) Cumulative amount of Fe (mmol kg⁻¹) released after 10 elutriation cycles, c) Contribution of sludge, fine and gasification ash to total Mn content of mixtures and d) Cumulative amount of Mn (mmol kg⁻¹) released after 10 elutriation cycles. The arrows in b and d indicate the direction of increasing gasification ash content of each sludge treatment group.

6.3.21 Zinc and copper

Measured and calculated Zn indicated to be more abundant in sludge (2.3 mmol kg^{-1}) than in fine ash (0.4 mmol kg^{-1}) and gasification ash ($0.19 \text{ mmol kg}^{-1}$) (Table 6.18). The dominance of sludge contribution to Zn content was evident in all mixtures with sludge; similarly the dominance of fine ash contribution to Zn content was clearly depicted in mixtures without sludge (Fig.6.23 a). However, in 2008 gasification ash dominated in Zn content ($3.36 \text{ mmol kg}^{-1}$) over fine ash ($0.31 \text{ mmol kg}^{-1}$ Zn) and sludge (1.7 mmol kg^{-1}). In the current study, Cu was more abundant in the ashes (0.9 mmol kg^{-1} Cu in gasification ash and 0.8 mmol kg^{-1} Cu in fine ash) than in sludge (0.3 mmol kg^{-1}) (Table 6.18). The dominance of both ashes in Cu contribution was evident in all mixtures and the minimal contribution of sludge to Cu in mixtures with sludge was clearly shown in Fig.6.23 c. Copper content in 2008 was dominant in gasification ash (3.9 mmol kg^{-1}) than in fine ash (0.3 mmol kg^{-1}) and sludge (1.6 mmol kg^{-1}). Generally, in alkaline conditions Zn and Cu are constituents of carbonates which are abundant in alkaline coal ashes (Fageria *et al.* 2002).

6.3.22 Solubility of zinc and copper in mixtures

Cumulatively, mixtures containing 50% sludge dominated in Zn released. Mixture 51 released the most zinc ($4.0 \text{ } \mu\text{mol kg}^{-1}$) compared to any other mixture and mixture 11 released the least ($0.2 \text{ } \mu\text{mol kg}^{-1}$) (Fig.6.23 b). Copper released after eluviation cycle 10 increased with increase in sludge and fine ash. Mixture 21 (90% fine ash, 0% gasification ash and 10% sludge) released the highest Cu ($1.0 \text{ } \mu\text{mol kg}^{-1}$) than any other mixture and mixture 5 (60% fine ash, 40% gasification ash and 0% sludge) released the least ($0.1 \text{ } \mu\text{mol kg}^{-1}$). Clearly most of the copper was released from both fine and gasification ashes than from sludge (Fig.6.23 c).

The generally low quantities of Zn and Cu released could result from the fact that Cu adsorption increases at pH 4 to 7 on exchange sites and occluded by hydroxides and oxides. pH levels above 6 generally induce hydrolysis of hydrated Cu which then increases its adsorption to clay minerals and organic matter (Fageria *et al.* 2002). Copper also precipitates as carbonate of hydroxides at higher pH and forms strong bonds with soil organic matter (Wei *et al.*, 2006). The adsorption of Zn on hydrous oxides of Al, Fe and Mn increases as pH increases above 5.5. But at pH above 7,

Zn solubility increases due to solubilization of organic matter (Fageria *et al.* 2002). The high pH (7.6 to 11.7) levels in the mixtures therefore favoured the precipitation of both Zn and Cu.

Zinc and Cu critical concentrations for most plants ranges from 0.25 to 10 mg kg⁻¹ (as extracted by NH₄HCO₃-DTPA, DTPA-TEA, Mehlich-1, 0.1 M HCl and 0.05 M HCl) and 0.1 to 10 mg kg⁻¹ (as extracted by NH₄HCO₃-DTPA, Mehlich-1 and 3, 0.05 M EDTA and 0.05 M HCl) respectively (Fageria, *et al.*, 2002). It was clear that the ranges 0.0008-0.06 mg kg⁻¹ Cu and 0.01-0.26 mg kg⁻¹ Zn released from the mixtures were below the critical concentrations presented by Fageria, *et al.* (2002). Both elements therefore need to be supplemented in all the mixtures. However, it should be noted that EDTA results will always be higher than results obtained with dionised water.

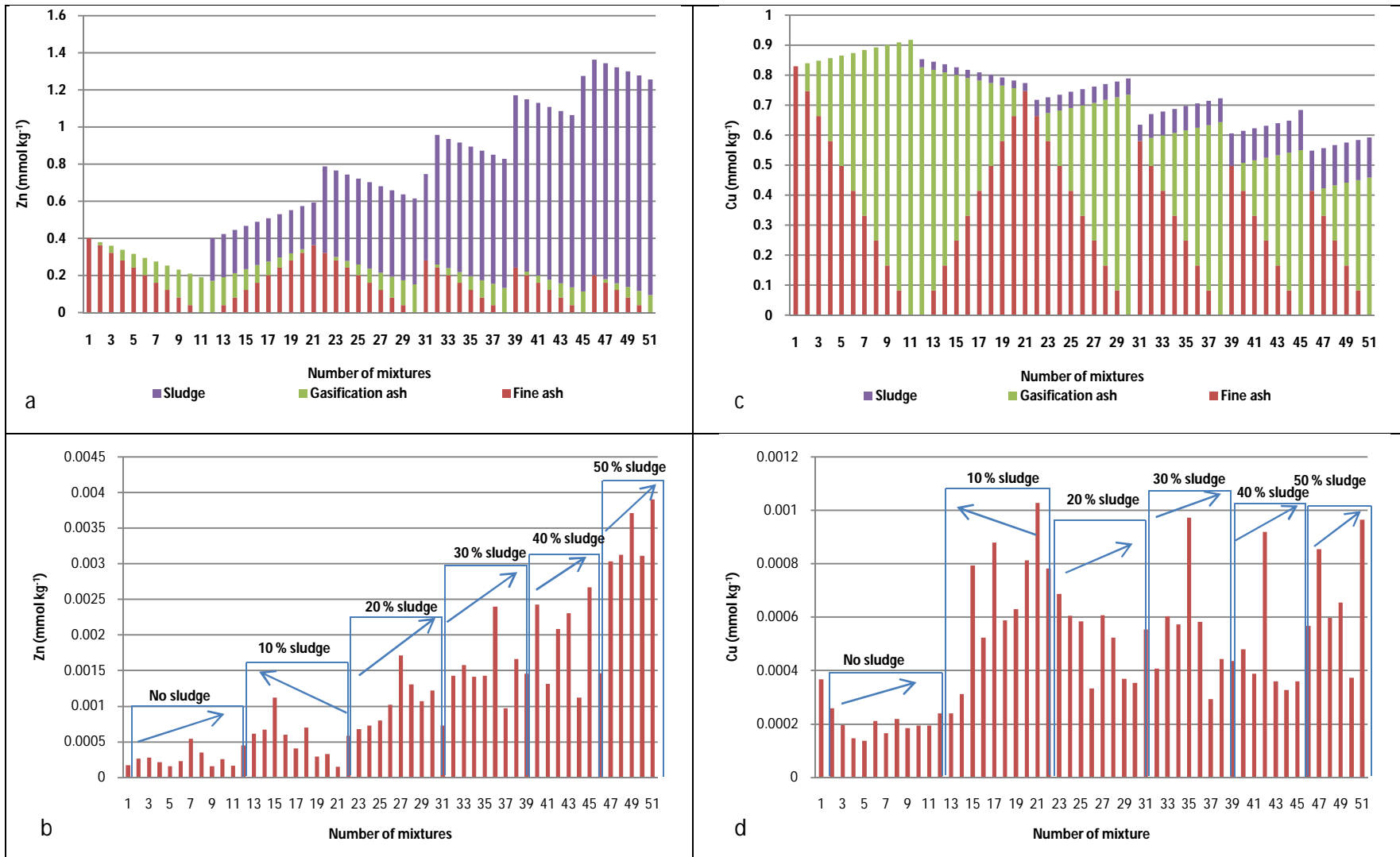


Fig.6. 23: a) Contribution of sludge, fine and gasification ash to total Zn content of mixtures, b) Cumulative amount of Zn (mmol kg⁻¹) released after 10 elutriation cycles, c) Contribution of sludge, fine and gasification ash to total Cu content of mixtures and d) Cumulative amount of Cu released after 10 elutriation cycles. The arrows in b and d indicate the direction of increasing gasification ash content of each sludge treatment group.

6.3.23 Boron and molybdenum in mixtures

During elemental analysis B and Mo were excluded, thus the following discussion was based on release only. After the first to the tenth eluviation cycles B increased with increase in sludge and fine ash. Group mixtures with 50% sludge dominated in B release. Cumulatively, the same trend was observed, mixture 46 (50% fine ash and 50% sludge) releasing the most B (5.6 mmol kg^{-1}) and mixture 7 (40% fine ash and 60% gasification ash) releasing the least (0.6 mmol kg^{-1}) (Fig.6.24, a and b). Cumulatively, Mo released increased with increase in sludge content. Mixture 49 (20% fine ash, 30 % gasification ash and 50% sludge) released the most Mo ($0.032 \text{ mmol kg}^{-1}$) and mixture 11 (100% gasification ash) released the least ($0.008 \text{ mmol kg}^{-1}$).

Boron in coal ash occurs in borax, Mg hydroxides and in Ca carbonates (Rahnemaie *et al.*, 2006) while Mo is a constituent of oxides, molybdates (Fageria *et al.* 2002). The dissolution of the solid phases containing B and Mo occurred at a very slow rate in mixtures without sludge, because the minerals containing them generally have a low solubility in nature (Essington, 2004). However, the addition of sludge liberated more of the B and Mo by increasing the solubility of the solid phases and through humic substances (Mulder & Cresser, 1994).

Boron and Mo released were in the range 6.5 to 60.4 mg kg^{-1} and 0.8 to 2.9 mg kg^{-1} far above the critical available concentration for B (0.1 - 2 mg kg^{-1} as extracted by hot water) and Mo (0.1 - 0.3 mg kg^{-1} as extracted by NH_4 -oxalate) in soils (Fageria *et al.* 2002) and such levels may induce toxicity to plants.

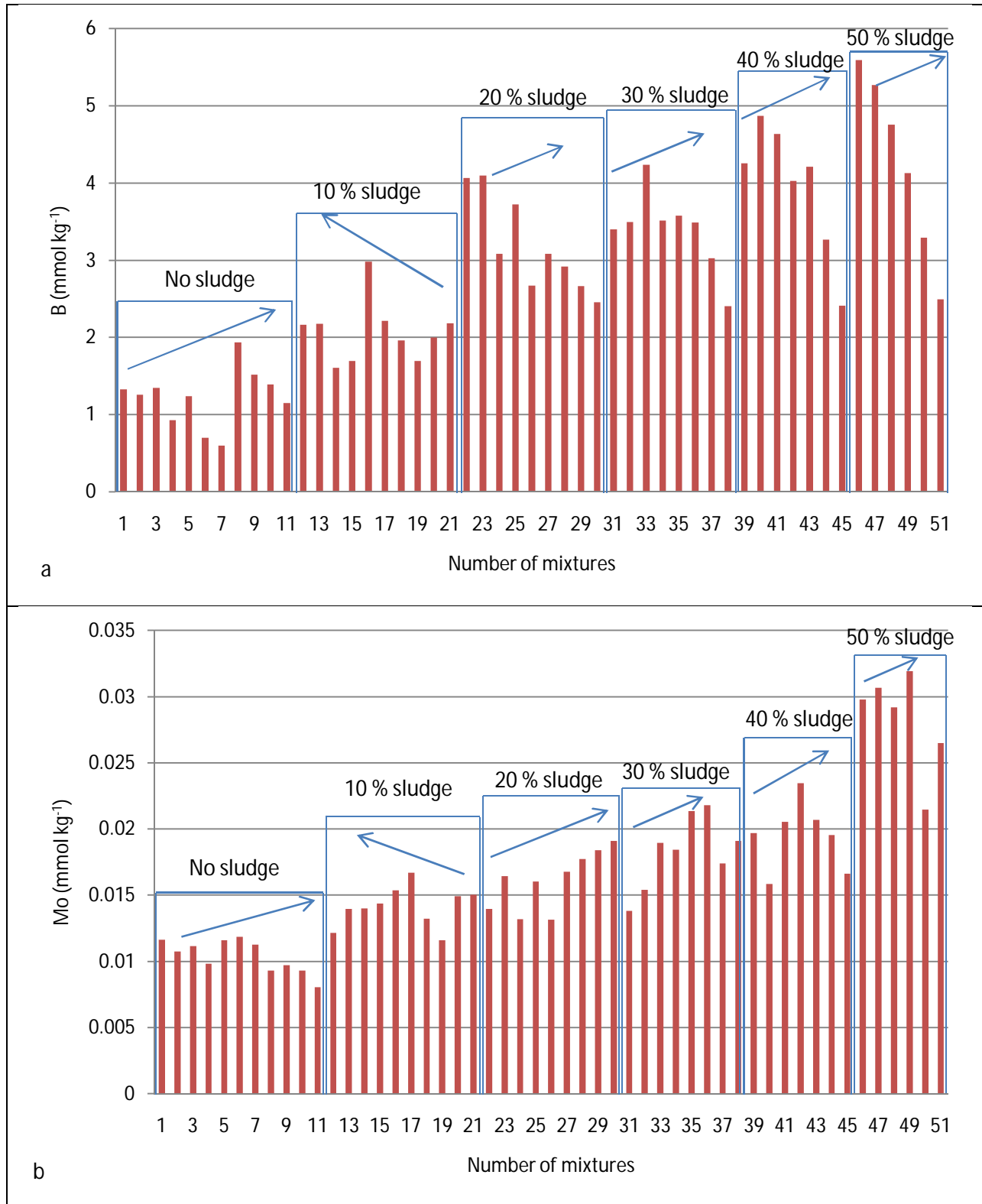


Fig.6. 24: a) Cumulative amount of B (mmol kg⁻¹) released after 10 eluviation cycles and b) Cumulative amount of Mo (mmol kg⁻¹) released after 10 eluviation cycles. The arrows in a and b indicate the direction of increasing gasification ash content of each sludge treatment group.

6.4 Conclusions

The main contributors to the high pH of the mixtures were fine and gasification ashes with pH values of 11.3 and 11.7 respectively, while sludge alone had a pH of 6.8. Wetting and drying cycles gradually reduced the pH for the mixtures. Initially (after the first eluviation cycle), the pH for the mixtures was between 8.3 to 11.7 and this dropped to between 7.6 to 10.3 after the tenth eluviation cycle. The incorporation of sludge in mixtures 12 to 51 (described in chapter 3) abruptly reduced pH while mixtures without sludge retained a pH above 8.4. As a result, mixture 7 (40% fine ash, 60% gasification ash and 0 % sludge) maintained the highest pH of 10.3 while mixture 49 (20% fine ash, 30% gasification ash and 50% sludge) showed the lowest pH value of 7.6. Mixtures 14 (20% fine ash, 70% gasification ash and 10% sludge), 19 (70% fine ash, 20 % gasification ash and 10% sludge), 20 (80% fine ash, 10% gasification ash and 10% sludge), 24 (60% fine ash, 20% gasification ash and 20% sludge), 25 (50% fine ash, 30% gasification ash and 20% sludge), 28 (20% fine ash, 60% gasification ash and 20% sludge), 29 (10% fine ash, 70% gasification ash and 20% sludge) and from 31 to 51 (with 30% sludge) maintained a pH of less than 8 but greater than 7.6 after ten eluviation cycles. All other mixtures had pH more than 8. The reduction in pH could be caused by the removal of soluble alkalinity and various reactions that released protons into the solution. In this case dissolved organic carbon upon degradation released fulvic and humic acids containing carboxylic groups that deprotonated and ionized under alkaline conditions. Other processes such as carbonation, hydrolysis, nitrification and precipitation released H^+ that reduced the pH. Clearly, the sludge reduced the pH in the ashes but not low enough to be accommodated in optimum pH range (5.5-7.5) for a functional growth medium.

In terms of salinity gasification ash with 527 mSm^{-1} EC and fine ash with 580 mSm^{-1} EC remained as the main contributors to the mixtures. The addition of sludge gradually decreased the salinity of all the mixtures to a mean of 500 mSm^{-1} after the first eluviation cycle. However, wetting and drying coupled with functional groups resulting from dissolved organic carbon that complexed the salts enhanced solubility and leaching of the salts reducing the salinity of the mixtures after the tenth eluviation cycle. Mixture 11 (100% gasification ash) retained the lowest EC (88 mSm^{-1}) and mixture 43 (20% fine ash, 40% gasification ash and 40% sludge) retained the highest EC of 415 mSm^{-1} . It was only mixtures 40 (50% fine ash, 10% gasification

ash and 40% sludge) and 43 (20% fine ash, 40% gasification ash and 40% sludge) that had their EC beyond the range (70 to 400 mSm⁻¹) suggested by Handreck and Black (1984) and Brady and Weil (2008) as optimum for plant growth after ten eluviation cycles.

Measured elements in all the mixtures in order of abundance were as follows; Ca>Mg>Na>P>K. Gasification ash remained the main contributor of Ca and Mg while fine ash contributed mostly K and Na. Sludge remained the main source of P as its contribution to these elements were in this order; P>Ca>Mg>Na>K. The release of each element was further viewed in relation to the release of other major elements. The solubility of Ca was favoured over the solubility of Mg and P in mixtures without sludge (mixtures 1 to 11) but the solubility of Na and K were favoured over the solubility of Ca in these mixtures giving a different order of abundance (Na>K>Ca>Mg>P). This indicated that solid phases containing Ca were more soluble than solid phases containing Mg and P but less soluble than solid phases containing Na and K. In mixtures with sludge (mixtures 12 to 51) Ca solubility was favoured over Na and K solubility but the solubility, of P and Mg were favoured over the solubility of Ca in these mixtures and the order of abundance was as follows; P>Mg>Ca>Na>K. Sludge increased the solubility of solid phases containing Ca more than the solid phases containing Na and K.

Mixture 43 (20% fine ash, 40% gasification ash and 40% sludge) released the highest Ca (52.6 mmol kg⁻¹) and Mg (68.0 mmol kg⁻¹), mixture 7 (40% fine ash, 60% gasification ash and 0% sludge) released the highest K (9.7 mmol kg⁻¹) and Na (25.4 mmol kg⁻¹) while mixture 51(0% fine ash, 50% gasification ash and 50 % sludge) released the highest P (1.1 mmol kg⁻¹). Generally it was clear that increasing sludge increased the solubility of most of the solid phases containing the elements but at different rates. Increasing sludge content in the mixtures increased P release overtime. A functional growth medium should be able to provide all the major elements in sufficient quantities and reduced quantities of Na (high concentrations are toxic to plants). Mixtures with 20 to 50% sludge (mixtures 22 to 51) are such desired functional growth media.

The order of abundance of measured trace elements contents in the mixtures was as follows; Fe>Mn>Cu>Zn. Gasification ash was the main contributor of Cu and Mn while fine ash contributed mostly Zn and Fe. Sludge contributed trace elements in this order; Fe>Mn>Zn>Cu.

Mixture 47 (40% fine ash, 10% gasification ash and 50% sludge) released more Fe ($0.04 \text{ mmol kg}^{-1}$) than any other mixture while mixture 43 (20% fine ash, 40% gasification ash and 40% sludge) released the most Mn ($0.01 \text{ mmol kg}^{-1}$). Mixture 51 (0% fine ash, 50% gasification ash and 50% sludge) released more Zn ($0.004 \text{ mmol kg}^{-1}$) than any other mixture, while mixture 21 (90% fine ash, 0% gasification ash and 10% sludge) released the most Cu ($0.001 \text{ mmol kg}^{-1}$). Boron (5.6 mmol kg^{-1}) was released the most by mixture 46 (50% fine ash, 0% gasification ash and 50% sludge), while mixture 49 (20% fine ash, 30% gasification ash and 50% sludge) released the highest Mo ($0.03 \text{ mmol kg}^{-1}$), more than any other mixture. It was evident that the solubility of Fe, Zn, B and Mo increased with increase in sludge and mixtures that supplied abundant plant available trace elements included mixtures from 22 to 51 (described in chapter 3).

CHAPTER 7: ASSESSING THE CATION EXCHANGE CAPACITY PROPERTIES OF THE VARIOUS MIXTURES

7.1 Introduction

The mineralogy of Sasol fine ash mainly consists of; amorphous phase (a phase with non fixed elemental proportions and has no ordered crystalline structure), mullite ($\text{Al}_6\text{Si}_2\text{O}_{13}$) and quartz (SiO_2) and gasification ash mainly consists of; SiO_2 , $\text{Al}_6\text{Si}_2\text{O}_{13}$ and anorthite ($\text{CaAl}_2\text{Si}_2\text{O}_8$) (Ginster & Matjie, 2005 & Matjie *et al.*, 2008, Mahlaba *et al.*, 2011). The fine particles result from fused clay minerals mainly comprising aluminium-silicate ($\text{AlO})_2\text{SiO}_3$) and Sasol fly ash is dominated by 59% of the silt-sized particles (Ahmaruzzaman, 2010 & Mahlaba *et al.*, 2011).

The SiO_2 and $\text{Al}_6\text{Si}_2\text{O}_{13}$ in ash provide a ready source of Al and Si and the ratio (Al/Si) of these elements is important for the development of cation exchange capacity (CEC). In this case a net negative charge can develop through isomorphous substitution where structural cations of higher valence replace cations of lower valence forming a permanent negative surface charge (Mulder & Cresser, 1994). The CEC in ash is a result of the formation of zeolites (crystalline aluminium-silicates) that consists of structure made of $[\text{SiO}_4]^{4-}$ and $[\text{AlO}_4]^{5-}$ tetrahedral linked by oxygen (O^{2-}) with lots of voids and spaces. The substitution of Si (IV) by Al (III) in the tetrahedra accounts for a negative charge of the structure which gives rise to high CEC (Querol, *et al.*, 2002). The development of zeolites depends on the dissolution of the Al-Si bearing mineral phases and a high Al/Si ratio results to a high CEC (Woolard *et al.*, 2000). Chemical weathering over time may induce alterations in the aluminium-silicate property to non-crystalline clay minerals and the formation of such minerals is generally indicated by an increase in CEC (Zevenbergen *et al.*, 1999). Gitari *et al.*, (2009) suggested that the increase in CEC is attributable to the Al-Si rich phases that form during mineral transformation.

Sasol biological sludge is an unavoidable byproduct of the aerobic activated biosolid treatment process and it contains 82% organic matter (OM) content (Sasol Synfuels, 2008). Organic matter increases CEC through its deprotonated functional groups carboxylic and phenolic groups that form during OM decomposition (Essington, 2004). Variable charges form with an increase in pH and ionic strength that allows the dissociation of H^+ from organic functional groups. Carboxyl and phenolic hydroxyl groups have a $\text{pK}_a < 5$ and deprotonate at pH values below their

respective pKa values (Sparks, 2003). Carboxyl and phenolic hydroxyl groups deprotonate at $3 < \text{pH} < 9$ and at $\text{pH} > 9$ respectively, increasing negative charges (Mulder and Cresser, 1994 & Sparks, 2003).

Basically, CEC is important for the retention of adequate quantities of plant available cations such as calcium (Ca), magnesium (Mg) and potassium (K) (Brady & Weil, 2008, Rashidi & Seilsepour, 2008 & Ross & Ketterings, 2011). It was envisaged that the incorporation of sludge will transform to humic compounds, (during OM decomposition) with functional groups capable of deprotonating under the alkaline conditions provided by the ash increasing the CEC. It was also expected that subjecting the ash to prolonged weathering will promote the dissolution of Al-Si bearing minerals and enhance the formation of secondary minerals with high and permanent CEC. The characteristics of ash and sludge provided the necessary motivation to measure the CEC of these materials.

Determination of CEC at pH 7.0 using ammonium acetate is a widely accepted and well adopted method that buffers the soil pH at pH 7.0. The principle behind this method is that the exchange sites are saturated with 1 M ammonium acetate (NH_4OAc) extracting cations, equilibrated overnight, reducing the 1 M NH_4OAc concentration in the pore spaces by washing the soil with 0.1 M NH_4OAc and replacement and leaching of exchangeable NH_4 with 1 M KCl (Jackson, 1958, Chapman, 1965 and Horneck *et al.*, 1989). The NH_4 is then determined by Kjeldahl procedure described by Bremner (1965). The disadvantage with this method is that it has the potential of over estimating the CEC of acid soils by buffering the pH and is not suitable for soils with $\text{pH} > 7.5$ containing significant amounts of calcite (CaCO_3). Under these conditions the extracting solution dissolves the CaCO_3 and reacts with NH_4OAc generating Ca^{2+} that competes with NH_4^+ for the exchange sites resulting in an under estimation of the CEC (Reiner, 2006 & Ross & Ketterings, 2011). In view of these disadvantages un-buffer methods without a conjugated basis of a weak organic acid with strong complexing ability have been developed. An example is the lithium chloride (LiCl) method.

The basic principle of this method as described by the Soil Science Society of South Africa, 1990 is that a 1 M LiCl solution is used as an extractant by saturating the exchange sites

simultaneously extracting the naturally existing cations. To reduce the 1 M LiCl concentration in the pore spaces 95% ethanol is used to wash the sample. The Li^+ that is adsorbed on the exchange sites is displaced with 1 M CaCl and further determined using Inductively Coupled Plasma Optical Emission Spectrometry (ICP-OES). The disadvantage is that Li at low electrolyte concentration increases electrostatic repulsion of soil components like sodium (Na), K and NH_4 (Ahmad & Mermut, 1996).

The hypothesis in this chapter was that the incorporated sludge in the mixtures and weathering induced by eluviation cycles will increase the CEC of the mixtures through the deprotonation of functional groups forming variable charges and formation of secondary minerals with permanent charges. It was also hypothesized that the pH 7.0 buffer method will give a higher CEC than the non-pH buffer methods. The aims of this study were to: 1) Determine the CEC of the leached and unweathered alkaline coal ash – sludge artificial growth media; 2) Compare buffered and unbuffered CEC methods to establish the most applicable method for determining CEC of these mixtures.

7.2 Materials and methods

7.2.1 Ammonium acetate procedure for the measurement of CEC for unleached and leached mixtures

Unleached material refers to unweathered alkaline coal ash – sludge mixtures and leached material refers to coal ash – sludge mixtures that have been subjected to wetting and drying cycles for a year.

Step 1: Following the ammonium acetate procedure as was described by Jackson (1958), 40 g of each mixture was replicated three times, transferred in preweighed 100 ml Schott bottles and then saturated with 80 ml of 1 M NH_4OAc . The purpose of saturating the sample is to ensure the exchange of the cations (Ca^{2+} , Mg^{2+} , and K^+) electrostatically adsorbed by negatively surface charges by ammonium (NH_4^+). After the addition of NH_4OAc , the sample was shaken on a reciprocal shaker for 60 min and then let to stand overnight for equilibration purposes. The equilibration allowed more time for the NH_4 to replace the cations. After equilibration the sample was centrifuged for 10 min and the resulting supernatant was filtered using a No. 2 Whatman filter paper with 110 mm diameter into a 250 ml volumetric flask. The samples were

again treated with a 1 M NH_4OA_c solution, shaken in the mechanical shaker for 30 min, centrifuged for 10 min and then filtered through a new Whatman filter paper into the same 250 ml volumetric flask. The flask was then filled to the mark with 1 M NH_4OA_c solution. The extract in the volumetric flask was filtered through a 0.45 μm membrane to reduce colloid interference and then analysed using an Inductively Coupled Plasma Optical Emission Spectrometry (ICP-OES) to determine the 1 M NH_4OA_c extractable cations. Because of the high concentration of soluble cations and a myriad of possible sources these cations extracted by the 1 M NH_4OA_c is only referred to as NH_4OA_c extractable cations.

Step 2: To reduce the 1 M NH_4OA_c concentration in the pore volume to about 0.1 M NH_4OA_c , the sample was washed with 80 ml of 0.1 M NH_4OA_c three times. This was done to reduce the carry over concentration of the NH_4OA_c . After each addition the sample was shaken with a reciprocal shaker for 30 min and centrifuged for 10 min. Afterwards the supernatant was filtered through a new No. 2 Whatman filter paper into a new 250 ml volumetric flask which was afterwards filled to the mark using the same 0.1 M NH_4OA_c . The extract in the volumetric flask was analyzed for NH_4^+ using the Kjeldahl procedure described by Bremner (1965). In order to calculate and correct later on for the amount of NH_4 in the entrained solution, it was important to determine the volume of the entrained solution after this step.

Step 3: The samples from step 2 were treated with 80 ml of 1 M KCl twice. After each addition, the sample was shaken with a reciprocal shaker for 30 min and centrifuged for 10 min. The supernatant was filtered through a new No. 2 Whatman filter paper into a new 250 ml volumetric flask which was further filled to the mark using the 1 M KCl solution. The extract in the volumetric flask was analyzed for NH_4^+ using the Kjeldahl procedure.

Step 4: These methods were developed for soil, a stable product subjected to millennia of weathering. It is not expected that the intensive leaching with extractants during the CEC determination will result in much further weathering of it. However, in the case of ash the extractants may induce weathering. This was a minus step (intended to remove naturally existing NH_4 in the mixtures) where 40 g of each fresh mixture was treated with 80 ml of 1 M KCl twice to leach out all the NH_4 that was naturally in the mixtures. This step was necessary to subtract

from the NH_4 obtained in step 3 all the NH_4 that was not added. After each addition, the sample was shaken with a reciprocal shaker for 30 min and centrifuged for 10 min. The supernatant was filtered through a new No. 2 Whatman filter paper into a new 250 ml volumetric flask which was further filled to the mark using the 1 M KCl solution. The extract in the volumetric flask was analyzed for NH_4^+ using the Kjeldahl procedure described.

Step 5: To determine NH_4^+ in the extracts from the 0.1 M NH_4OAc and 1 M KCl treatments, 10 ml was pipetted into separate distillation flasks and then added 10 ml de-ionized water in each flask increasing the contents to a final volume of 20 ml. In each flask 2.5 g of magnesium oxide (MgO) was added and immediately connected to a distiller and distilled to a final volume of 50 ml into a 50 ml conical flask containing 10 ml boric acid indicator. To determine NH_4^+ the Kjeldahl procedure described in chapter 5 was used. The CEC was calculated based on the dry mass of the mixtures.

7.2.2 Lithium chloride procedure for the measurement of CEC for leached mixtures

Step 1: 40 g of each mixture was replicated three times, transferred into preweighed 100 ml Schott bottles and then added 80 ml of 1 M LiCl solution. The saturated sample was shaken on a reciprocal shaker for 60 min and then let to stand overnight for equilibration purposes. After equilibration the sample was centrifuged for 10 min and the resulting supernatant was filtered using a No. 2 Whatman filter paper into a 250 ml volumetric flask. The samples were again treated with a 1 M LiCl solution, shaken on a reciprocal shaker for 30 min, centrifuged for 10 min and then filtered through a new Whatman filter paper into the same 250 ml volumetric flask. The flask was then filled to the mark with 1 M LiCl solution. The extract in the volumetric flask was filtered through a 0.45 μm membrane to reduce colloid interference and then analysed for Li using ICP-OES.

Step 2: The sample was again treated with a diluted 80 ml of 0.001 M LiCl three times. After each addition the sample was shaken with a reciprocal shaker for 30 min and centrifuged for 10 min, filtered the supernatant through a new No. 2 Whatman filter paper into a new preweighed 250 ml volumetric flask. The volumetric flask together with its contents was reweighed and recorded the mass. The extract in the volumetric flask was filtered through a 0.45 μm membrane

and then analyzed for Li using the ICP-OES. Before the next step the Schott bottles with the samples inside were reweighed and recorded the mass to enable final calculations.

Step 3: The same sample was treated with 80 ml of 1 M MgNO₃ three times. After each addition the sample was shaken with a reciprocal shaker for 30 min and centrifuged for 10 min, filtered the supernatant through a new No. 2 Whatman filter paper into a new preweighed 250 ml volumetric flask. The volumetric flask together with its contents was reweighed and recorded the mass. The extract in the volumetric flask was filtered through a 0.45 µm membrane to reduce colloid interference and then analysed using for Li using ICP-OES.

7.2.3 Potassium chloride (KCl) method for the measurement of CEC for leached mixtures

This method was similar to the LiCl method except that the 1 M LiCl was replaced with 1 M KCl and the 0.001 M LiCl was replaced with 0.001 M KCl.

Step 1: 40 g sample of each mixture replicated three times and transferred into preweighed 100 ml schott bottles and then added 80 ml of 1 M KCl. The saturated sample was shaken on a reciprocal shaker for 60 min and then let to stand overnight for equilibration purposes. After equilibration the sample was centrifuged for 10 min and the resulting supernatant was filtered using a No. 2 Whatman filter paper into a 250 ml volumetric flask. The samples were again treated with a 1 M KCl solution shaken on a reciprocal shaker for 30 min, centrifuged for 10 min and then filtered through a new Whatman filter paper into the same 250 ml volumetric flask. The flask was filled to the mark with 1 M KCl solution. The extract in the volumetric flask was filtered through a 0.45 µm membrane to reduce colloid interference and then analysed using for K using ICP-OES.

Step 2: The same sample was again treated with a diluted 80 ml of 0.001 M KCl three times. After each addition the sample was shaken with a reciprocal shaker for 30 min and centrifuged for 10 min, filtered the supernatant through a new No. 2 Whatman filter paper into a new preweighed 250 ml volumetric flask. The volumetric flask together with its contents was reweighed and recorded the mass. The extract in the volumetric flask was filtered through a 0.45

μm membrane and then analysed for K using the ICP-OES. Before the step 3 the Schott bottle with the sample inside was reweighed and recorded the mass to enable final calculations.

Step 3: The same sample was treated with 80 ml of 1 M MgNO_3 three times. After each addition the sample was shaken with a reciprocal shaker for 30 min and centrifuged for 10 min, filtered the supernatant through a new No. 2 Whatman filter paper into a new preweighed 250 ml volumetric flask. The volumetric flask together with its contents was reweighed and recorded the mass. The extract in the volumetric flask was filtered through a 0.45 μm membrane and then analysed for K using the ICP-OES.

The "minus step" for the lithium chloride and potassium chloride methods

The Li^+ and K^+ obtained using the ICP-OES in steps 2 for the lithium chloride and potassium chloride methods include Li^+ and K^+ naturally existing in the pore spaces and on the exchange sites of the sample. The ash is very weatherable and the process of leaching will result the release of Li and K from the ash matrix and can therefore not be referred to as "exchangeable" cations. Not all of the cations resided from the exchange complex. It was important to establish how much was released by this. Similarly, to correct or separate exchangeable K from K that was released from the ash as a result of weathering induced by the leaching with the LiCl solution and to correct or separate exchangeable Li from Li that was released from the ash as a result of weathering induced by the leaching with the KCl solution.

7.3 Results and discussion

7.3.1 Cation exchange capacity (CEC) determination of selected unleached and leached mixtures using ammonium acetate (NH_4OAc) procedure

The incorporation and increase in sludge content from 10 to 50% in mixtures 12 to 51 generally increased the CEC for these mixtures (Fig.7.1 a). The same trend was maintained even after 10 eluviation cycles (Fig.7.1 b). This phenomenon was expected because the decomposition of organic matter (OM) from sludge releases humified compounds such as humic acids (HA) and fulvic acids (FA) that contain functional groups especially carboxyl and phenolic hydroxyl groups (Mulder & Cresser, 1994, Sparks, 2003 & Essington, 2005). Humic acids are dissolved in the solution and will as much to CEC as dissolved anions like chloride and sulphate. It is the

humified solid phase organic material that formed as a result of sludge breakdown that will contribute to CEC. The contribution of these functional groups to CEC relies on their charge which also depends on their dissociation and ionisation.

Mixtures; 1 (with 100% fine ash), 6 (with 50% fine ash and 50% gasification ash) and 11 (with 100% gasification ash) was a group without sludge and maintained the lowest CEC of all the mixtures even after ten eluviation cycles. Mixture 11 maintained the lowest CEC mean ($2.4 \text{ cmol}_c \text{ kg}^{-1} \pm 0.1$) before and after ten eluviation cycles. However, after ten eluviation cycles mixture 30 (with 0% fine ash, 80% gasification ash and 20% sludge) had a CEC mean ($2.2 \text{ cmol}_c \text{ kg}^{-1}$) which was not significantly different from the CEC mean ($1.7 \text{ cmol}_c \text{ kg}^{-1}$) for mixture 11. This was an indication that sludge contributed very little. Mixture 48 (with 30% fine ash, 20% gasification ash and 50% sludge) had the highest averaged mean CEC ($19.04 \text{ cmol}_c \text{ kg}^{-1} \pm 1.1$) than any other mixture but this mean was not significantly different from the CEC means of 19.04, 18.2 and $17.9 \text{ cmol}_c \text{ kg}^{-1}$ for mixtures 46 (with 50% fine ash and 50% sludge), 51 (with 50% gasification ash and 50% sludge) and 39 (with 60% fine ash and 40% sludge) respectively (Fig.7.1 a). These CEC values could be comparable to CEC values of soils dominated by kaolinite (2 to $15 \text{ cmol}_c \text{ kg}^{-1}$) (Sparks, 2004). After ten eluviation cycles mixture 46 had the highest mean CEC ($4.5 \text{ cmol}_c \text{ kg}^{-1} \pm 0.3$ standard deviation) but was not significantly different from CEC means; 4.4 and $4.2 \text{ cmol}_c \text{ kg}^{-1}$ for mixtures 48 and 39 respectively. It should be noted that eluviation cycles drastically reduced the CEC of all the mixtures (Fig.7.2 b).

The general reduction in CEC in all the mixtures after the tenth eluviation cycle was due to acidification by the dissociation and ionisation of HA and FA produced during OM decomposition (Ross & Ketterings, 2011). Deprotonation increased the concentration of H^+ reducing the pH of the system that in turn limited the chances of developing negative charges thus reduced the CEC (Mulder and Cresser, 1994 & Sparks, 2003 & Essington 2005). Under alkaline conditions carboxyl and phenolic hydroxyl groups increase in solubility because of deprotonation and ionisation that occurs at pH conditions greater than their respective pKa values. This makes the organic molecule more polar and thus water soluble (Kleber & Johnson, 2010). The increase in solubility of the functional groups could also result in the reduction of CEC in the mixtures. It could be possible that most of the NH_4 leached over time. The fixation of NH_4 used to replace the

base cations naturally in the samples could result in the reduction of CEC (Tan, 1996). The fixation of NH_4 is result of aluminosilicate minerals which are dominant in the ash. It is possible that the ash release K as well and this also blocked adsorption sites (include minus data)

These results differed from findings by Zevebergen *et al.* (1999) who found that the CEC for fly ash weathered for 8 to 12 years was higher ($8.1 \text{ cmol}_c \text{ kg}^{-1}$) than the CEC for a fresh fly ash ($2.9 \text{ cmol}_c \text{ kg}^{-1}$). This author used NH_4OA_c method and did not apply sludge. The CEC results for the fresh fly ash ($2.9 \text{ cmol}_c \text{ kg}^{-1}$) by Zevebergen *et al.* (1999) could only be comparable to the CEC for leached fine ash of the current study with a CEC of $2.98 \text{ cmol}_c \text{ kg}^{-1}$. The fresh fine ash of the current study had a higher CEC ($6.98 \text{ cmol}_c \text{ kg}^{-1}$) compared to the CEC of the fly ash by Zevebergen *et al.* (1999). The reason they gave for the high CEC in weathered fly ash was that weathering reactions rapidly modified the surface of the glass matrix they also observed higher levels of Al_{ox} and Si_{ox} . This was an indication that there was formation of non-crystalline hydrous aluminosilicates that provided new phases for cation exchange. This phenomenon was expected in the mixtures but could not occur because wetting and drying cycles took only a year.

Unfortunately, no work has been published dealing with the characterization of Sasol fine and gasification ashes including the CEC parameter. However, work that was done by Woolard *et al.* (2002) in characterizing South African fresh fly ash reveal that it has a CEC of $2.1 \text{ cmol}_c \text{ kg}^{-1}$. Weathered data for the mixtures without sludge (especially fine ash) was in similar order for the current study. These authors used sodium acetate as a saturating solution, washed the sample with ethanol and used ammonium acetate as a displacing solution. This CEC value could be exaggerated because fly ash generally contains substantial amounts of sodium. Cation exchange capacity values determined using ammonium acetate in fresh fly ash ranging from 0.05 to $7.9 \text{ cmol}_c \text{ kg}^{-1}$ appear in the literature (Querol, *et al.*, 2002, Veeresh, *et al.*, 2003, Gupta & Sinha, 2006 & Nur Hanani *et al.*, 2010). However an inference to both fine and gasification ash can be made since Sasol fine ash is a combination of approximately 83% power station fly ash and 17% made up of both gasification ash and bottom ash fines with particles less than $250 \mu\text{m}$ (Mahlaba, *et al.*, 2011). It can be concluded that the CEC for both fine and gasification ashes fell within the range stated by literature.

7.3.2 Statistical comparison of CEC (NH_4OA_c) of unleached and leached mixtures

Statistically, there was a no significant difference between the CEC means of the unleached and leached mixtures. Some unleached mixtures showed CEC means which were not significantly different from CEC means of the same or different leached mixtures. The results suggest that the CEC of mixtures unamended with sludge did not change. This was an indication that weathering reactions could not effectively or significantly increase the CEC of such mixtures. For example, unleached mixture 11 (with 100% gasification ash) had a mean CEC ($2.4 \text{ cmol}_c \text{ kg}^{-1}$) which was not significantly different from the CEC mean ($1.7 \text{ cmol}_c \text{ kg}^{-1}$) of the same mixture but leached. The CEC of the unleached mixture 11 was also not significantly different from the CEC means of leached mixtures; 6, 12, 17, 30, 38, 21 and 26 (described in chapter 3). The interaction indicated that the time frame of 1 year was too short to cause measurable and statistically significant differences between the CEC's of unleached and leached mixtures without sludge. The silica base cations that were needed to accumulate and involved in the formation of secondary minerals were leached (McBride, 1994).

There is evidence that the sludge in the mixtures added NH_4 that increased the CEC in the unleached mixtures. Ammonium determined by the minus step increased with increase in sludge content (Table 7.3). In the first step NH_4 was able to replace cations from mineral surfaces (Table 7.3). Interestingly, the concentrations of these cations (Ca, K, Mg, and Na) replaced by NH_4 in this step (for unleached mixtures) were lower than the concentrations of cumulative cations obtained in ten eluviation cycles (chapter 6) confirming that weathering did occur.

Table 7.1: Cations replaced by NH₄ in step 1 and NH₄ replaced by K in the minus step.

Mixtures	Ca(mmol kg ⁻¹)	K(mmol kg ⁻¹)	Mg(mmol kg ⁻¹)	Na(mmol kg ⁻¹)	NH ₄ (mmol kg ⁻¹)
1	33.9	1.3	7.7	1.6	1.7
6	30.1	1.0	6.0	6.4	1.2
11	24.1	0.6	2.7	2.0	1.0
12	26.6	1.5	4.3	4.2	9.2
17	27.0	1.6	6.3	7.0	9.3
21	28.9	1.8	7.5	2.1	9.3
22	25.6	2.2	7.5	2.2	17.2
26	25.0	2.1	6.5	7.1	15.4
30	21.0	1.8	4.3	4.3	16.0
31	22.6	2.6	7.3	2.3	23.9
35	27.5	3.1	7.2	8.9	23.1
38	21.6	3.5	6.7	6.0	23.7
39	19.8	3.0	7.0	8.9	29.9
42	20.3	2.9	6.0	7.4	29.9
45	15.3	2.6	4.3	5.1	30.2
46	20.2	3.9	10.6	9.7	32.0
48	18.6	3.5	6.7	8.4	34.2
51	16.3	3.1	4.9	6.2	36.2

7.3.3 Cation exchange capacity (KCl) of leached mixtures

The CEC(KCl) and the CEC (LiCl) methods were used for comparison purposes since the CEC (NH₄OA_c) method could be interfered by NH₄ from sludge hence exaggerating the CEC at the end. The same general trend were seen for CEC(KCl) as in CEC(NH₄OA_c). However, the CEC values in general were lower. To evaluate the effectiveness of CEC (KCl) method in determining CEC in leached material, mixtures; 1, 6, 11, 23, 37, 46 and 51 (described in chapter 3) were used. Even with this method CEC increased with increase in sludge content (Fig.7.1 d). Similarly, the mean CEC (KCl) for mixture 46 (6.1 cmol_c kg⁻¹) was as well significantly different from any other CEC mean of any other mixture. As expected mixture 6 had the lowest CEC mean (1.5 cmol_c kg⁻¹) than any other mixture but this was not significantly different from the mean CEC of 1.7 cmol_c kg⁻¹ shown by mixture 11. Mixtures 23 and 51 with CEC means; 3.8 and 4.2 respectively were not significantly different from each other.

7.3.4 Cation exchange capacity (LiCl) of leached mixtures

This method was applied on leached material for mixtures; 1, 6, 11, 23 (with 70% fine ash, 10% gasification ash and 20% sludge), 37 (with 10% fine ash, 60% gasification ash and 30% sludge), 46 and 51. It was evident that CEC increased with increase in sludge content (Fig.7.1c). The

CEC (LiCl) method also indicated that mixture 46 had the highest CEC. Statistically, mixture 46 was significantly different from any other mixture and had the highest CEC mean ($6.8 \text{ cmol}_c \text{ kg}^{-1}$). The high CEC in mixture 46 was a major contribution of the 50% sludge (Table 7.3) content and a minor contribution of the 50% fine ash content. Mixtures 23, 37 and 51 with CEC means; 3.2, 3.8 and $4.8 \text{ cmol}_c \text{ kg}^{-1}$ respectively were not significantly different from each other but were significantly different and lower than the CEC mean given by mixture 46. Mixture 6 had the lowest CEC ($0.6 \text{ cmol}_c \text{ kg}^{-1}$) than any other mixture but was not significantly different from the CEC; 1.2 and $1.1 \text{ cmol}_c \text{ kg}^{-1}$ that were shown by mixtures 1 and 11 respectively. It was expected that the CEC would be low because these mixtures (1, 6 and 11) contained no sludge.

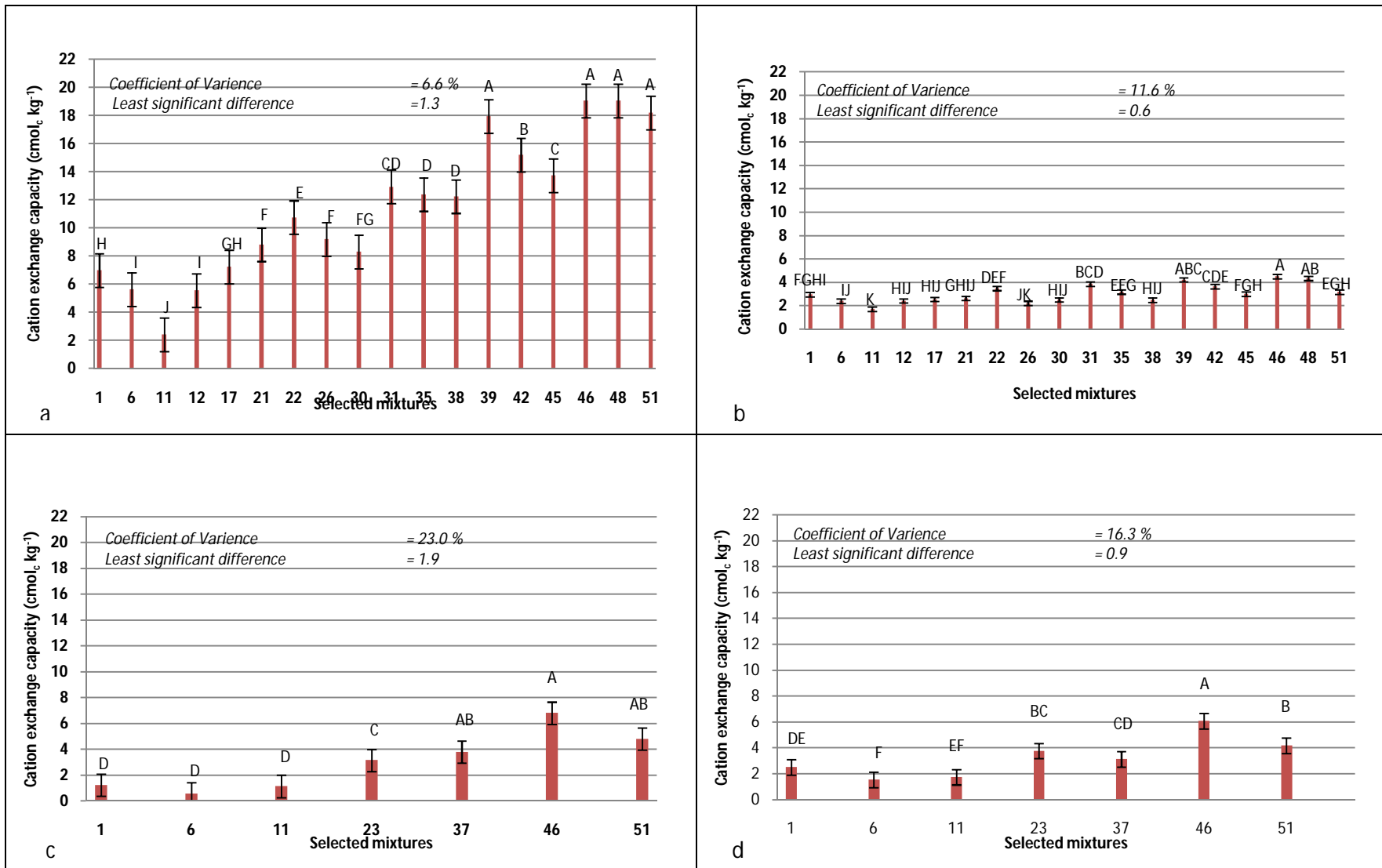


Fig.7. 1: a) Cation exchange capacity means for selected unleached mixtures determined by ammonium acetate (NH_4OAc) procedure, b) Cation exchange capacity means for selected leached mixtures determined by NH_4OAc procedure, c) Cation exchange capacity of leached mixtures determined by lithium chloride (LiCl) method and d) cation exchange capacity of leached mixtures determined by potassium chloride (KCl) method. Means with the same letter are not significantly different from each other and means with different letters are significantly different from each other.

7.3.5 Statistical comparison CEC (NH₄OA_c), CEC (LiCl) and CEC (KCl) procedures

The comparison of these procedures was based on their efficiency in determining CEC in leached material for mixtures; 1, 6, 11, 46, and 51 (Fig.7.2). Statistically the CEC (KCl) were lower from CEC(NH₄OA_c) and CEC(LiCl). Both the NH₄OA_c and LiCl methods showed CEC means that were higher (than those given by KCl) but not significantly different from each other. The least significant difference was 0.38 and coefficient of variance (CV) of 15.6%.

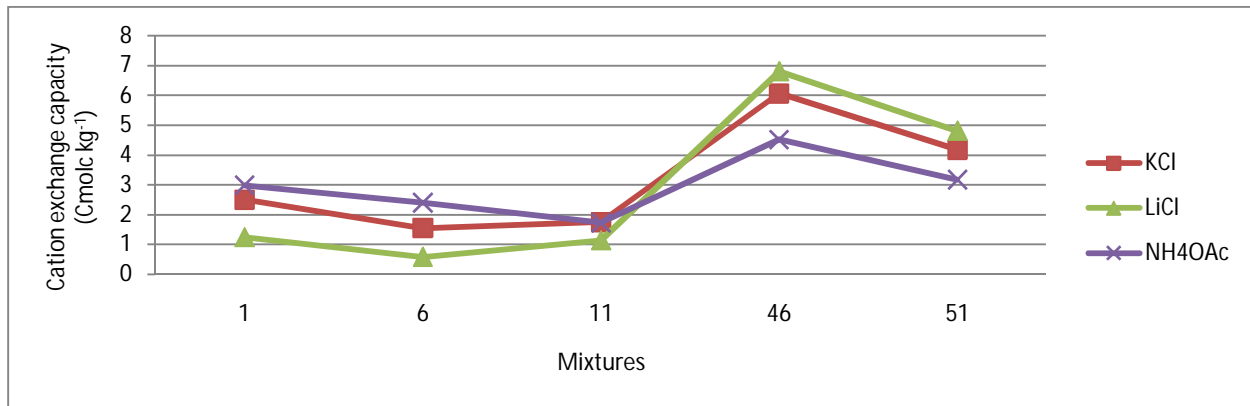


Fig.7. 2: Comparison of the CEC of selected leached mixtures as measured by NH₄OA_c, LiCl and KCl methods

For example, mixtures without sludge; 1, 6 and 11 for the LiCl, KCl and NH₄OA_c with CEC means of 1.2, 1.5, and 1.7 cmol_c kg⁻¹ respectively were not significantly different from each other. Mixture 46 (NH₄OA_c method), 51 (LiCl method) and 51 (KCl method) with CEC means; 4.5, 4.8 and 4.2 cmol_c kg⁻¹ respectively were also not significantly different from each other.

Each method had disadvantages in measuring CEC in coal ash-sludge mixtures because these methods are standard for soils. The NH₄OA_c method had the possibility of overestimating the CEC of mixtures with sludge and underestimating the CEC for mixtures without sludge. The sludge in the mixtures acted as a source of nutrients particularly nitrogen (N-7.9%). Therefore, it was evident that using NH₄OA_c as a saturating solution increased the N content of the mixtures and eventually increased the concentration of NH₄ displaced by KCl overestimating the CEC (the minus step revealed it Table 7.3). In mixtures without sludge the NH₄OA_c method underestimated the CEC. Under alkaline conditions the NH₄OA_c reacted and dissolved the CaCO₃ contained in the ash generating Ca²⁺ that further competed with NH₄⁺ for the exchange sites

leading to an under estimation of the CEC (Reiner, 2006 & Ross & Ketterings, 2011). Both fine and gasification ashes contained significant amounts of K (fine ash = 1.3 and gasification ash = 0.6 mmol kg⁻¹ shown in Table 7.3) and Li (fine ash = 0.2 and gasification ash = 0.1 mmol kg⁻¹). However, the ICP has a narrow range for Li and that it also dispersed the mixtures. The leaching could have induced more weathering and released K and Li from the ash, which can interfere with the method and resulting in high background concentrations. Similarly, saturation the mixtures with KCl increased the concentration of K displaced by MgNO₃ thus over estimating the CEC. Dispersion of samples occurred during step 2 (samples treated with 0.001 M LiCl and 0.001 M KCl) of both the LiCl and KCl methods increasing colloidal particles in the filtered supernatant that could interfere with readings given by the ICP-OES.

Reference samples of kaolinite and illite were included in the analysis to test the reliability of the methods. In the literature the CEC for kaolinite is narrower (2 and 15 cmol_c kg⁻¹) than the CEC for illite that range between 10 and 40 cmol_c kg⁻¹ (Sparks, 2003 & Essington, 2005). For kaolinite the CEC measured by all the methods fell within the range reported in literature (2 – 15 cmol_c kg⁻¹) (Table 7.4). However, the NH₄OA_c method measured the highest CEC (8.7 cmol_c kg⁻¹) and the KCl method measured the least (3.2 cmol_c kg⁻¹). The LiCl method measured the highest CEC in illite (18.1 cmol_c kg⁻¹) and KCl method measured the lowest (7.8 cmol_c kg⁻¹). The CEC measured by both NH₄OA_c and LiCl methods fell within the CEC range (10 – 40 cmol_c kg⁻¹) for illite while the CEC measured by KCl (7.8 cmol_c kg⁻¹) fell below the this range. Based on the CEC determined in kaolinite all the three methods can be used to determine CEC in coal ash-sludge mixtures. But the KCl method may not be an appropriate technique because it under estimated the CEC of illite and it is possible that it can also under estimate the CEC in coal ash-sludge mixtures. According to Tan (1996) the under estimation of CEC by the KCl method could result from the fixation of K by the clay minerals especially illite. Illite is a 2:1 clay mineral that has K⁺ as the predominant interlayer ion along with divalent ions such as Ca²⁺ and Mg²⁺ and NH₄⁺ can also occur (Sparks, 2003). Therefore, the fixation of K is the result of entrapment of K⁺ ions between the layers (Sharma *et al.*, 2010). The entrapped K⁺ can be displaced by Ca²⁺ and Mg²⁺ ions that expand the layers but cannot be effectively displaced by NH₄⁺ because it collapses mineral. However, potassium on the edge-interlayer sites can easily be replaced by

NH_4^+ . Hydrated Mg^{2+} and Ca^{2+} are not selectively sorbed by these sites thus they are not effective in replacing the K^+ (Sawhney, 1972 & Tan, 1996).

Table 7.2: Comparing mean CEC of the reference material (kaolinite and illite) included determined by the NH_4OA_c , LiCl and KCl procedures to that reported in literature.

Sample	Methods			From literature ($\text{cmol}_c \text{kg}^{-1}$)
	NH_4OA_c ($\text{cmol}_c \text{kg}^{-1}$)	LiCl ($\text{cmol}_c \text{kg}^{-1}$)	KCl ($\text{cmol}_c \text{kg}^{-1}$)	
Kaolinite	8.67 ± 0.69	5.48 ± 0.3	3.18 ± 0.54	2 – 15 (Sparks, 2004)
Illite	11.83 ± 1.36	18.05 ± 1.6	7.77 ± 0.22	10 – 40 (Sparks, 2004)

A t-test was computed for statistical inference of the differences CEC's. For kaolinite the calculated t values were 5.7 (comparing CEC means for KCl and LiCl methods), 18.5 (comparing CEC means for LiCl and NH_4OA_c methods) and 17.6 (comparing CEC means for KCl and NH_4OA_c methods). It was found that $t > t_{\text{critical}}$ (4.3) at 95% probability and thus the means were significantly different from each other meaning that the methods did not give the same results. For illite the calculated t values were 5.2 (comparing CEC means for KCl and LiCl methods), 6.9 (comparing CEC means for LiCl and NH_4OA_c methods) and 81.5 (comparing CEC means for KCl and NH_4OA_c methods). It was found that $t > t_{\text{critical}}$ (4.3) at 95% probability and thus the means were significantly different from each other and the conclusion was that the procedures give different results. The chemical component of the sample to be analysed must be known in advance to aid in the selection of one of the methods to analyse CEC. This is because a material may release an element that can interfere with the element being used to determine the CEC when the material is subjected to intense weathering.

7.3.6 The contribution of sludge, fine and gasification ashes to cation exchange capacity of the mixtures

Cation exchange capacity generally increased with increase in sludge content of the selected mixtures (Fig.7.1 a, b, c and d) as indicated by all the CEC methods used. To verify sludge and fine ash effects on CEC, mixtures; 1, 21, 22, 31, 39 and 46 were selected (Fig.7.3 a). The fine ash content of these mixtures was decreasing from 100 to 50%, gasification ash content maintained at 0% and sludge content increased from 0 to 50%. The CEC means for each mixture obtained from both unleached and leached material were plotted against sludge increase (Fig.7.3 a). The effects of sludge and gasification ash to CEC were assessed by selecting mixtures; 11,

12, 30, 38, 45 and 51 that had 0% fine ash content, decreasing gasification ash content (100 to 50%) and increasing sludge content (0 to 50%)(Fig.7.3 b). Similarly, the CEC means for each mixture obtained from both unleached and leached material were plotted against sludge increase (Fig.7.3 b). In both situations it was clear that increasing sludge content in the mixtures gradually increased CEC. A reduction in either fine and or gasification ash content did not counter the CEC increasing trend associated with increasing sludge amendment. The CEC rate of increase for unleached material increased following the incorporation and increase in sludge content. However, weathering reactions reduced the CEC rate of increase in leached material for both situations (Fig.7.3 a & b).

The unleached mixtures had pH values that ranged between 8.3 to 11.7 way above pKa 4-6 for carboxyl and phenolic hydroxyl groups from sludge. Such pH values allowed deprotonation of the functional groups creating negative charges thus rapidly increased CEC (Sparks, 2003). The reduction in pH over time limited the rate of deprotonation and ionization of the functional groups hence reduced the CEC in the leached mixtures.

To assess the contribution of fine and gasification ash mixtures without sludge; 1, 6 and 11 were selected. In these mixtures fine ash content decreased from 100 to 0% and gasification ash content increased from 0 to 100%. The CEC means for each mixture obtained from both unleached and leached material were plotted against gasification ash increase (Fig.7.3 c). It was evident that CEC increased with increase in fine ash for both leached and unleached material. Sasol fine and gasification ashes are generally low in organic matter content but contain numerous minerals that can contribute to CEC. Mahlaba *et al.* (2011) characterized weathered coal fine ash and found that it contained minerals such as; mullite ($\text{Al}_6\text{Si}_2\text{O}_{13}$), quartz (SiO_2), calcite (CaO_3), periclase (MgO), magnetite (FeFe_2O_4), hematite (Fe_2O_3), ettringite ($\text{Ca}_6\text{Al}_2(\text{SO}_4)_3(\text{OH})_{12}.26\text{H}_2\text{O}$), sillimanite (Al_2SiO_5), pyrrhotite (Fe_9S_{10}), and analcime ($\text{NaAlSi}_2\text{O}_6.\text{H}_2\text{O}$) that in combination can significantly contribute to CEC by weathering and form minerals with charges.

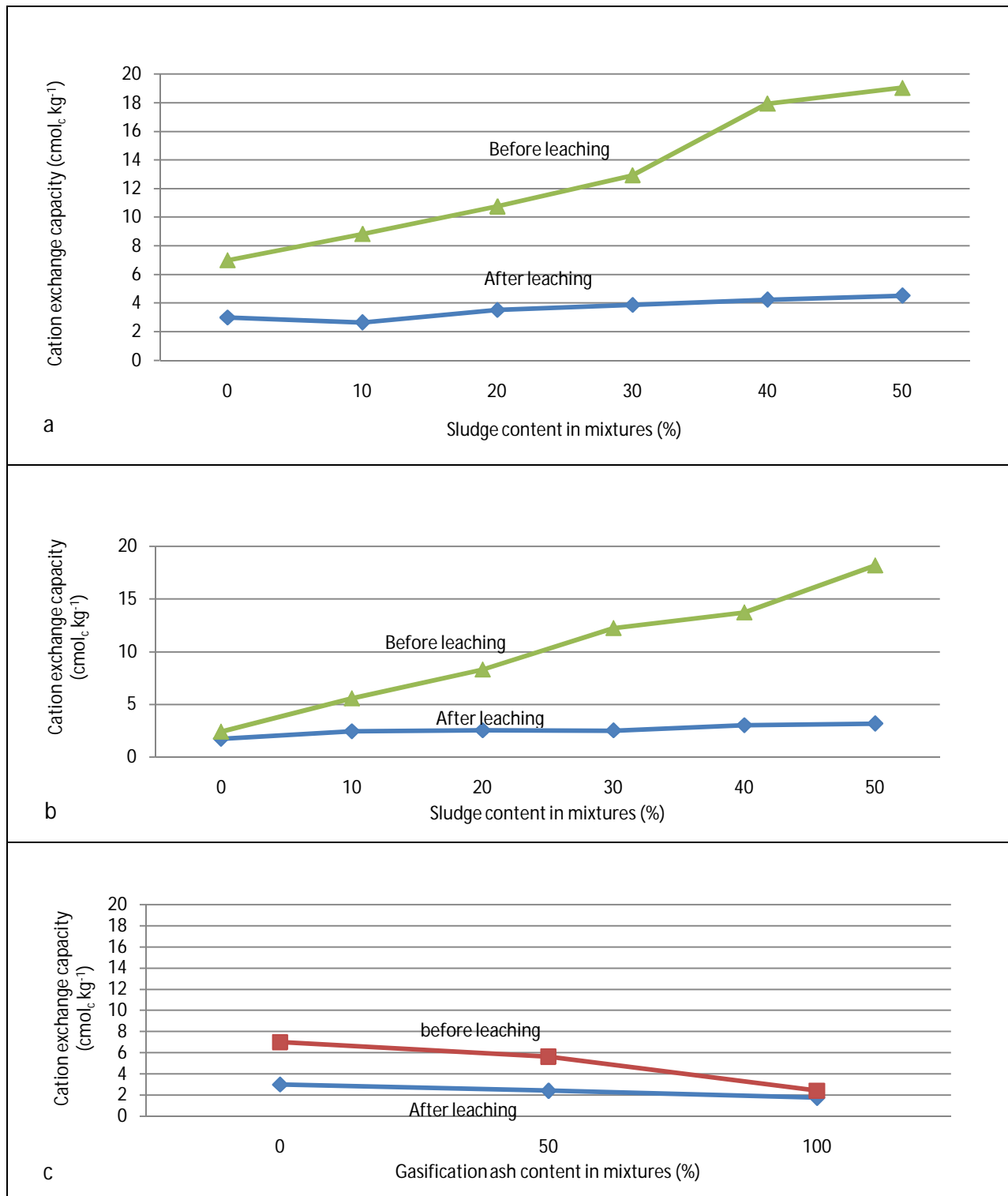


Fig. 7. 3: a) Sludge and fine ash contribution to CEC for selected mixtures (1, 21, 22, 31, 39 and 46) with sludge content increasing (0 to 50%), fine ash decreasing (100 to 50%), gasification ash content 0%, b) Sludge and gasification ash contribution to CEC for selected mixtures (11, 12, 30, 38, 45 and 51) with sludge content increasing and c) fine and gasification ash contribution to CEC for selected mixtures (1, 6 and 11) without sludge.

7.4 Conclusions

The mean cation exchange capacities; 17.9, 19.04, 19.05 and 18.2 $\text{cmol}_c \text{kg}^{-1}$ for unleached mixtures; 39(60% fine ash, 0% gasification ash and 40% sludge), 46 (50% fine ash, 0% gasification ash and 50% sludge), 48(30% fine ash, 20% gasification ash and 50% sludge) and 51(0% fine ash, 50% gasification ash and 50% sludge) respectively were not statistically different from each other but more than those of any other non-leached mixtures when determined using the NH_4OA_c method and mixture 11(0% fine ash, 100% gasification ash and 0% sludge) had the lowest (2.4 $\text{cmol}_c \text{kg}^{-1}$). Mixture 46 retained the highest mean cation exchange capacities; 4.5, 6.8 and 6.1 as determined by the NH_4OA_c , LiCl and KCl methods respectively. Mixture 11 had the lowest mean CEC (1.7) of any other mixture determined by the NH_4OA_c method for the leached material, while mixture 6 (50% fine ash, 50% gasification ash and 0% sludge) retained the lowest mean cation exchange capacities (mean CEC of 0.6 and 1.5 $\text{cmol}_c \text{kg}^{-1}$ for the LiCl and KCl methods respectively) of any other mixture.

In the determination of CEC for coal ash-sludge mixtures (leached or non-leached), caution should be taken that the concentration of LiCl and KCl should be $> 0.001 M$ in step two to avoid dispersion and $< 0.1 M$ to effectively reduce the $1 M$ concentration in the pore spaces. Any LiCl and KCl concentration $\geq 0.1 M$ in the second step increases the concentration of the carry over that needs to be subtracted from the last step of the method. The dispersion can increase colloidal particles that may interfere with the background of the element in the ICP-OES resulting in erroneous data or under estimating CEC (making filtration more difficult). Sludge in the mixtures has the potential of increasing the concentration of NH_4^+ added by the saturating solution when using the NH_4OA_c method hence, overestimating CEC. The NH_4OA_c method in mixtures without sludge could underestimate the CEC because the ash contains CaCO_3 that reacts with the NH_4OA_c generating Ca_2^+ that competes with the NH_4 for the exchange sites.

CHAPTER 8: GENERAL DISCUSSION

Based on particle size distribution gasification ash was found to be macroporous and dominated by particle sizes greater than 1mm in diameter as a result mixtures with 50 to 100% gasification content were dominated by particle sizes greater than 8mm. Therefore, increasing gasification ash content reduced the water holding capacities of mixtures like; 11(0% fine ash, 100% gasification ash and 0% sludge), 12 (0% fine ash, 90% gasification ash and 10% sludge), 30 (0% fine ash, 80% gasification ash and 20% sludge), 38 (0% fine ash, 70% gasification ash and 30% sludge), 45 (0% fine ash, 60% gasification ash and 40% sludge) and 51(0% fine ash, 50% gasification ash and 50% sludge) when compared to mixtures with 50 to 100% fine ash content such as; 22 (80% fine ash, 0% gasification ash and 20% sludge), 31(70% fine ash, 0% gasification ash and 30% sludge), 39 (60% fine ash, 0% gasification ash and 40% sludge), and 46 (50% fine ash, 0% gasification ash and 50% sludge). However, the incorporation of sludge at from 10 to 50% in mixtures such as; 12, 30, 38, 45, and 51 significantly increased their water holding capacities when compared to mixtures with the same content of gasification ash (50 to 100%) but without sludge (mixtures 6 to 11 described in chapter 3) for the first eluviation cycle. But continuous weathering reduced the water holding capacities of these mixtures (mixtures; 12, 30, 38, 45, and 51) to even below capacities shown by mixtures with 50 to 100% gasification ash and without sludge (mixtures 6 to 11).

Fine ash was found to be dominated by particle sizes between 100 to 250 μm in diameter and this particle size range dominated in mixtures with 50 to 100% fine ash content. This particle size range together with the incorporation of sludge from 20 to 50% increased the water holding capacity of mixtures; 22, 31, 39 and 46 for the first eluviation cycle. However, the water holding capacities of these mixtures were drastically reduced by weathering after the the tenth eluviation cycle to levels similar to mixtures 1 to 5 with 50 to 100% fine ash content but without sludge (described in chapter 3). Mixtures 31 and 39 maintained the highest water holding capacity (0.65 kg kg^{-1}) than any other mixture for the tenth eluviation cycle followed by mixtures; 24 (60% fine ash, 20% gasification ash and 20% sludge), 32 (60% fine ash, 10% gasification ash and 30% sludge), 40 (50% fine ash, 10% gasification ash and 40% sludge) and 46 with 0.52 , 0.60 , 0.62 and 0.63 kg kg^{-1} respectively.

The pozzolanic properties of fine ash and the hydration of minerals present in mixtures with 50 to 100% fine ash content and without sludge increased the water holding capacity and this was evident by the swelling of the mixtures 1 (100% fine ash, 0% gasification ash and 0% sludge) and 2 (90% fine ash, 10% gasification ash and 0% sludge). Such mixtures are not likely to provide plant available water and aeration required by essential processes such as nitrogen mineralization. Only mixtures with 50 to 90% gasification ash can actually provide the necessary aeration and plant available water.

The addition of sludge reduced the pH and salinity of all mixtures with 20 to 50% sludge and increased N mineralization. The resultant lower pH range (7.6-10.3) and salinity (88-415 mSm^{-1}) provided a conducive environment for the oxidation of NO_2^- to NO_3^- . The NO_3^- and NH_4^+ species were mostly contributed by sludge while fine ash contributed more to the NO_2^- species. The production of NO_2^- by fine ash was because of the NH_3 purposely added by Sasol to remove fly ash from the processing plant that was converted to NO_2^- and the oxidation rate of this species to NO_3^- was minimal due to the extreme conditions caused by high pH (8.3-11.7) and salinity (622 mSm^{-1}). The extreme conditions caused by high pH and salinity of mixtures with 0 and 10% sludge negatively affected the nitrifying bacteria (*Nitrobacter*) as a result only NH_4^+ and NO_2^- species were detected in mixtures without sludge. Mixtures 35 (30% fine ash, 40% gasification ash and 30% sludge), 42 (30% fine ash, 30% gasification ash and 40% sludge), 46, 48 (30% fine ash, 20% gasification ash and 50% sludge) and 51 exhibited the most amounts of NH_4^+ and NO_3^- species and lower NO_2^- compared to all other mixtures. Mixture 48 had the most mineralized total inorganic N (24.4 mg kg^{-1}) compared to all mixtures and in all eluviation cycles, while mixture 12 exhibited the lowest (10.5 mg kg^{-1}). It was clear that the reduction of pH and salinity enhanced the N mineralization process in mixtures with sludge.

Fine and gasification ashes contributed to the high pH, with initial pH values of 11.3 and 11.7 respectively. The pH values for mixtures without sludge ranged between 10.8 and 11.7 for the first eluviation cycle and reduced to between 8.4 and 10.3 for the tenth eluviation cycle due to carbonation process. While the pH values for mixtures with sludge ranged between 8.3 and 10.2 for the first eluviation cycle and reduced to the range 7.6 to 8.2 for the tenth eluviation cycle. Mixture 7 (40% fine ash, 60% gasification ash and 0% sludge) maintained the highest pH of 10.3

while mixture 49 (20% fine ash, 30% gasification ash and 50% sludge) showed the lowest pH (7.6) for the tenth eluviation cycle. The pH was reduced by dissolved organic carbon upon degradation of sludge released fulvic and humic acids containing carboxylic groups that deprotonated and ionized under alkaline conditions. Other processes such as carbonation, hydrolysis and nitrification released H^+ that reduced the pH. As a result mixtures; 14 (20% fine ash, 70% gasification ash and 10% sludge), 19 (70% fine ash, 20% gasification ash and 10% sludge), 20 (80% fine ash, 10% gasification ash and 10% sludge), 24 (60% fine ash, 20% gasification ash and 20% sludge), 25 (50% fine ash, 30% gasification ash and 20% sludge), 28 (20% fine ash, 60% gasification ash and 20% sludge), 29 (10% fine ash, 70% gasification ash and 20% sludge) and from 31 to 51 (with 30% sludge) retained a pH of less than 8 but greater than 7.6 after ten eluviation cycles while, all other mixtures had pH more than 8. Clearly, the sludge reduced the pH in the ashes but not low enough to be accommodated in optimum pH range (5.5-7.5) for a functional growth medium.

Gasification and fine ashes also contributed to high salinity, with EC of 527 mSm^{-1} and 580 mSm^{-1} respectively. The EC values for mixtures without sludge ranged between 335 and 606 mSm^{-1} for the first eluviation cycle and reduced to the range 102 to 160 mSm^{-1} for the tenth eluviation cycle. While the EC values for mixtures with sludge ranged between 95 to 622 mSm^{-1} for the first eluviation cycle and reduced to the range 116 to 415 mSm^{-1} for the tenth eluviation cycle. Weathering coupled with functional groups resulting from dissolved organic carbon that complexed the salts enhanced solubility and leaching of the salts reducing the salinity of the mixtures for the tenth eluviation cycle. Mixture 11 exhibited the lowest EC (88 mSm^{-1}) and mixture 43 (20% fine ash, 40% gasification ash and 40% sludge) maintained the highest EC of 415 mSm^{-1} for the tenth eluviation cycle. It was only mixtures 40 and 43 that had their EC beyond the range (70 to 400 mSm^{-1}) suggested by Handreck and Black (1984) and Brady and Weil (2008) as optimum for plant growth after ten eluviation cycles.

Gasification ash remained the main contributor of Ca and Mg while fine ash contributed K and Na mostly. The order of abundance of these elements in the mixtures was as follows; $Ca > Mg > Na > P > K$. Sludge remained the main source of P as its contribution to these elements were in this order; $P > Ca > Mg > Na > K$. The solubility of Ca was favoured over the solubility of

Mg and P in mixtures without sludge (mixtures 1 to 11 described in chapter 3) but the solubility of Na and K were favoured over the solubility of Ca in these mixtures giving a different order of abundance as follows; Na>K>Ca>Mg>P. In mixtures with sludge (mixtures 12 to 51 described in chapter 3) Ca solubility was favoured over Na and K solubility but the solubility of P and Mg were favoured over the solubility of Ca in these mixtures and the order of abundance was as follows; P>Mg>Ca>Na>K. Mixture 43 released the highest Ca ($52.6 \text{ mmol kg}^{-1}$) and Mg ($68.0 \text{ mmol kg}^{-1}$), mixture 7 released the highest K (9.7 mmol kg^{-1}) and Na ($25.4 \text{ mmol kg}^{-1}$) while mixture 51 released the highest P (1.1 mmol kg^{-1}). Generally it was clear that increasing sludge increased the solubility of most of the solid phases containing the elements but at different rates. Increasing sludge content in the mixtures increased P release overtime. A functional growth medium should be able to provide all the major elements in sufficient quantities and reduced quantities of Na (high concentrations are toxic to plants). Mixtures with 20 to 50% sludge (mixtures 22 to 51) are such desired functional growth media.

Gasification ash was the main contributor of Cu and Mn while fine ash contributed mostly Zn and Fe. The order of abundance of measured trace elements contents in the mixtures was as follows; Fe>Mn>Cu>Zn. Sludge contributed trace elements in this order; Fe>Mn>Zn>Cu. Mixture 47 (40 % fine ash, 10 % gasification ash and 50 % sludge) released the highest Fe ($0.04 \text{ mmol kg}^{-1}$) than any other mixture while mixture 43 released the most Mn ($0.01 \text{ mmol kg}^{-1}$). Mixture 51 released the highest Zn ($0.004 \text{ mmol kg}^{-1}$) than any other mixture while mixture 21 (90 % fine ash, 0% gasification ash and 10% sludge) released the most Cu ($0.001 \text{ mmol kg}^{-1}$). Boron (5.6 mmol kg^{-1}) was released the most by mixture 46 while mixture 49 (20% fine ash, 30% gasification ash and 50% sludge) released the highest Mo ($0.03 \text{ mmol kg}^{-1}$) than any other mixture. It was evident that the solubility of Fe, Zn, B and Mo increased with increase in sludge content of the mixtures. It was evident that the solubility of Fe, Zn, B and Mo increased with increase in sludge and mixtures that supplied abundant plant available trace elements included mixtures from 22 to 51 (described in chapter 3).

The addition of sludge generally increased the CEC of the mixtures. When using the NH_4OA_c method the CEC means; 17.9, 19.04, 19.05 and $18.2 \text{ cmol}_c \text{ kg}^{-1}$ for unleached mixtures with 40 to 50 % sludge; 39, 46, 48 and 51 respectively were not statistically different from each other

and higher when compared to those of any other non-leached mixtures. Mixture 11 exhibited the lowest CEC mean ($2.4 \text{ cmol}_c \text{ kg}^{-1}$). Within leached mixtures mixture 46 maintained the highest CEC means; 4.5, 6.8 and $6.1 \text{ cmol}_c \text{ kg}^{-1}$ corresponding to NH_4OAc , LiCl and KCl methods respectively. Mixture 11 showed the lowest CEC mean ($1.7 \text{ cmol}_c \text{ kg}^{-1}$) than any other leached mixture when determined by the NH_4OAc method and mixture 6 (50% fine ash, 50% gasification ash and 0% sludge) exhibited the lowest CEC means; 0.6 and $1.5 \text{ cmol}_c \text{ kg}^{-1}$ corresponding to LiCl and KCl methods respectively than any other leached mixture. When statistically comparing these methods they did not give significantly different results for the leached mixtures as was expected. Though the methods were did not differ in their results but the LiCl remained as the best method in the determination of CEC in all the mixtures since the ashes contained abundant K and NH_4^+ that affected the KCL and NH_4OAc methods.

CHAPTER 9: CONCLUSIONS AND RECOMMENDATIONS

9.1 Conclusions

A good growth medium should have: 20% of its particle size distribution between 100 and 250 μm to provide a good balance between airfilled porosity and supply readily available water; be able to provide plant available inorganic N (NH_4^+ and NO_3^-) and reduced supply of NO_2^- toxic to plants; with pH ranging between 5.5 and 8.0 to supply adequate macro and macronutrients; have a salinity of less than 400 mSm^{-1} ; have high CEC to enhance availability of nutrients to plants and reduce their leaching; and provide plant available macro and micronutrients and reduced release of Na which is toxic to plants.

Physically, the incorporation of fine ash and sludge generally increased the water holding capacities of the mixtures by providing at least 20% particle size between 100 and 250 μm . But continuous weathering reduced the water holding capacities of all mixtures. As expected the sludge incorporated moderated the extreme conditions of the mixtures by reducing the pH of the mixtures to between 7.6 and 8.2 and salinity to less than 400 mSm^{-1} . The reduction in pH and salinity enhanced N mineralization and the release of both macro and micronutrients.

In terms of macronutrients gasification ash remained the main contributor of Ca and Mg while fine ash contributed K and Na mostly. Sludge remained the main source of P. In terms of micronutrients gasification ash was the main contributor of Cu and Mn while fine ash contributed mostly Zn and Fe. Sludge contributed mostly Fe.

The addition of sludge generally increased the CEC of the mixtures. It was worth noting that statistically the methods did not give significantly different results as was expected. But the LiCl remained as the best method in the determination of CEC in all the mixtures since the ashes contained abundant K and NH_4^+ that affected the KCL and NH_4OAc methods.

In conclusion the main objective was achieved since mixtures: 31, 35, 39, 42, 43, 46, 47, 48, 49 and 51 appeared to be the best growth media since they provided available water, adequate aeration, high CEC, sufficient plant available nutrients reduced salinity and optimum pH levels.

9.2 Recommendations

- A thorough mineralogical characterization of the ashes is necessary to aid in explaining their behaviour when used as artificial growth media and when subjected to weathering.
- Redox status of the mixtures needs to be determined to help explain the species of elements likely to be released.
- Alkalinity measurement in the mixtures needs to be carried out to quantify bases.
- The dissolution/solubility kinetics of the various minerals needs to be determined to help explain the concentration levels of the elements in the leachates/solutions.
- The adsorption and desorption reactions of essential plant nutrients need to be determined using modeling techniques.
- The next phase should include direct evaluation using plants. There is a need to match vegetation to the growing media and climate/water balance and carry out bio assays to validate the laboratory findings.
- Characterisation of the dissolved organic compounds in the sludge treated mixtures.

10. References

- ADRES, N.F. & FRANCISCO, M.S., 2008. Effects of sewage sludge application on heavy metal leaching from mine tailings impoundments. *Bioresource Technology* 99, 7521 – 7530.
- AGBENIN, J.O. & YAKUBU, S., 2006. Potassium-Calcium and potassium-magnesium exchange equilibria in an acid savanna soil from northern Nigeria. *Geoderma* 136, 542-554.
- AHMARUZZAMAN, M., 2010. A review on the utilization of fly ash. *Progress in Energy and Combustion Science* 36, 327–363.
- AKAY, O. & FOX, G.A., 2007. Experimental investigation of direct connectivity between macropores and subsurface drains during infiltration. *Soil Science Society of America Journal* 71, 1600-1606.
- ANNANDALE, J.G., SMITH, H.J.C., TRUTER, W.F. & HERBERT, M., 2004. The rehabilitation of coarse ash dump: Investigating opportunities to co-dispose Sasol waste materials with coarse ash and negate the need for expensive soil covers. *Department of Plant Production and Fractal Forest AFRICA CC, University of Pretoria*.
- ANTHONY, E.J., BERRY, E.E., BLONDIN, J., BULEWCZ, E.M. & BURWELL, S., 2003. Advance ash management technologies for CFBC ash. *Waste Management* 23, 503-516.
- ASOKAN, P., SAXENAA, M. & ASOLEKARB, S.R., 2005. Coal combustion residues: Environmental implications and recycling potentials. *Resources, Conservation and Recycling* 43, 239-262.
- BENDZ, D., TÜCHSEN, P.L. & CHRISTENSEN, T.H., 2007. The dissolution kinetics of major elements in municipal solid waste incineration bottom ash particles. *Journal of Contaminant Hydrology* 94, 178-194.
- BENITO, M., MASAGUER, A., DE ANTONIO, R., AND MOLINER, A., 2005. Use of pruning waste compost as a component in soilless growing media. *Bioresource Technology* 96, 597-603.
- BI, E., SCHMIDT, T.C., & HADERLEIN, S.B., 2010. Practical issues relating to soil column chromatography for sorption parameter determination. *Chemosphere* 80, 787-793.
- BRADY, N.C. & WEIL, R.R., 2008. Factors controlling rates of decomposition and mineralization. pp503 - 692. *In: The nature and properties of soils, 14th edn, Prentice Hall Inc., Upper Saddle River, New Jersey.*

- BREMNER, J.M., 1965. Total nitrogen. P 1149-1237. *In: methods and soil analysis part 2. Chemical and microbiological properties*, Agronomy 9, Inc. Madison, Wisconsin, USA.
- BROMLY, M., HINZ, C. & AYLMOORE, L.A.G., 2007. Relation of dispersivity to properties of Homogeneous saturated repacked soil columns. *European Journal of Soil Science* 58, 293–301.
- BROWN, G.E., FOSTER, A.L. & OSTERGREN, J.D., 1999. Mineral surfaces and bioavailability of heavy metals: A molecular-scale perspective. *Proceedings of the National Academy Science USA* 96, 3388-3395.
- CANFIELD, D.E., GLAZER, A.N. & FALKOWSKI, P.G., 2010. The Evolution and Future of Earth's Nitrogen Cycle. *Science* 330, 192-196
- CARLSON, C.L. & ADRIANO, D.C., 1993. Environmental impacts of coal combustion residues. *Journal of Environmental Quality* 22, 227-247.
- CHARBENEAU, R.J., 2000. Groundwater Hydraulics and Pollutant Transport. p 593. Prentice Hall, USA.
- CHATTERJEE, N.N., 1940. Sulphur in coal. pp 523-534. Department of Geology, Calcutta University, USA.
- CHAPMAN, H.D., 1965. Cation exchange capacity. *In: Methods of soil analysis – chemical and microbiological properties*. *Agronomy* 9, 891-901.
- CHENG, C.M., 2005. Leaching of coal combustion products: field and laboratory studies. PhD thesis. The Ohio State University, USA.
- CHU, Y.J., JIN, Y., BAUMANN, T., YATES, M.V., 2003. Effect of soil properties on saturated and unsaturated virus transport through columns. *Journal of Environmental Quality* 32, 2017–2025.
- CORTIS, A. & BERKOWITZ, B., 2004. Anomalous transport in “classical” soil and sand columns. *Soil Science Society of America Journal* 68, 1539–1548.
- DEENIK, J., 2006. Nitrogen mineralization potential in important agricultural soils of hawai‘i. *Soil and Crop Management* 15, 1-5.
- DERMATAS, D. & MENG, X., 2003. Utilization of fly ash for tabilization/solidification of heavy metal contaminated soils. *Engineering geology* 70, 377-394.
- DIJKSTRA, J.J., VAN DER SLOOT, H.A. & COMANS, R.N.J., 2006. The leaching of

- major and trace elements from MSWI bottom ash as a function of pH and time. *Applied Geochemistry* 21, 335-351.
- DINÇER, A.R., & KARGI, F., 2000. Kinetics of sequential nitrification and denitrification process. *Enzyme and Microbial Technology* 27, 37-42.
- EDMUNDS, W.E., 2002. Coal in Pennsylvania. Commonwealth of Pennsylvania department of conservation and natural resources. Educational Series 7. pp 1-29.
- ESSINGTON, M.E., 2004. Organic matter in soils. pp 129-180. *In: Soil and water chemistry: An integrative approach.* CRC Press LLC, 200 N.W. Corporate Blvd., Boca Raton, Florida.
- FAGERIA, N.K., BALIGAR, V.C. & CLARK, R.B., 2002. Micronutrients in crop production. *Agronomy* 77, 185-268
- FANG, M., WONG, M.H., & WONG, J.W.C., 1999. Digestion activity of thermophilic bacteria isolated from ash-amended sewage sludge compost. *Water, Air, and soil pollution* 126, 1-21.
- GINSTER, M. & MATJIE, R.H., 2005. Beneficial Utilization of Sasol Coal gasification ash. *Submitted for consideration in the 2005 World of coal ash, April 11-15, 2005, Lexington, Kentucky, USA.*
- GITARI, M.W., FATOBA, O.O., NYAMHINGURA, A., PATRIK, L.F., VADAPALLI, V.R.k, NEL, J., OCTOBER, A., DLAMINI, L., GERHAR, G. & DU TOIT, R., 2009. Chemical weathering in a dry ash dump: An insight from physicochemical and mineralogical analysis of drilled cores. *Submitted for consideration in the World of Coal ash Conference (WOCA) May 4-7, Lexington, Kentucky, USA.*
- GOSS, M.J., EHLERS, W. & UNC, A., 2010. The role of lysimeters in the development of our understanding of processes in the vadose zone relevant to contamination of ground water aquifers. *Physics and Chemistry of the Earth* 2-14.
- GRAY, N.F., 1990. Nutrient removal. p 153-168. *In: Activated sludge theory and practice.* Oxford University Press.
- GUPTA, U.C., KENING, W. & SIYUAN, L., 2008. Micronutrients in soils, crops, and livestock. *Earth Science Frontiers* 15, 110-125.
- GUPTA, A.K. & SINHA, S. 2006. Role of *Brassica juncea* (L) Czern. (var Vaibhav) in the phytoextraction of Ni from soil amended with fly ash: Selection of extractant for metal bioavailability. *Journal of Hazardous Materials* B135, 371-378.

- HANDRECK, K.A. & BLACK, N.D., (1984). Choosing materials for potting mixes. P 102-123.
In: Growing media for ornamental plants and Turf. New South Wales University Press, Australia.
- HANSEN, L., 2010. Quantifying the reduction in hydraulic conductivity of disturbed soil columns as a function of the salinity and sodicity of applied water. BSc. Theses, University of Queensland, Australia.
- HANSEN, J.B., HOLM, P.E., HANSEN, E.A. & HJELMAR, O., 2000. Use of Lysimeters for Characterisation of Leaching from Soil and Mainly Inorganic Waste Materials. *Nordtest Technical Report 473, Nordtest Project no. 1949–00*. Danish Hydraulic Institute and The Royal Veterinary and Agricultural University of Denmark, Hørsholm, Denmark.
- HAYNES, R.J., 2009. Reclamation and revegetation of fly ash disposal sites – challenges and research needs. University of Queensland, Australia. *Journal of environmental management* 90, 43-53.
- HERSELMAN, J.E., WADE, P.W., STEYN, C.E. & SNYMAN, H.G., 2005. International approach to sludge disposal. pp 9-14. In: an evaluation of dedicated land disposal practices for sewage sludge. WRC Report No. 1209/1/05. *Water Research Commission*, South Africa.
- HODGSON, D.R. & HOLLIDAY, R., 1966. The agronomic properties of pulverized fuel ash. *Chemistry and Industry*. 20, 785-790.
- HORNECK, D.A., HART, J.M., TOPPER, K. & KOESPELL, B., 1989. Methods of Soil Analysis used in the soil testing laboratory at Oregon State University. Ag. Expt. Station SM 89:4.
- HUANG, P.M., ZHOU, J.M., XIE, J.C. & WANG, M.K., 2005. Potassium in soils. *Encyclopedia of Soils in the Environment* pp303-314.
- HUO-YAN, W., JIAN-MIN, Z., CHANG-WEN, D. & XIAO-QIN, C. 2010. Potassium fractions in soils as affected by monoculcium phosphate, ammonium sulfate, and potassium chloride application. *Pedosphere* 20, 368-377.
- HUTCHISON, J., SEAMAN, J., ABURIME, S. & RADCLIFFE, D., 2003. Chromate transport and retention in variably saturated soil columns. *Vadose Zone Journal* 2, 702–714.
- Ilg, K., 2007. Comparing unsaturated colloid transport through columns with differing sampling systems. *Soil Science Society of America Journal* 71, 298–305.

- IYER, R., 2002. The surface chemistry of leaching coal fly ash. Department of chemical engineering, University of Queensland. *Journal of Hazardous Materials* B93, 321-329.
- JACKSON, M.L., 1958. Cation exchange determination for soils. pp 57-70. In: Soil chemical analysis. Constable and LTD. University of Wisconsin Madison, USA.
- JALA, S. & GOYAL, D., 2006. Fly ash as a soil ameliorant for improving crop production-a review. *Biosource Technology* 97, 1136-1147.
- JALALI, M. & MOHARRAMI, S., 2007. Competitive adsorption of trace elements in calcareous soils of western Iran. *Geodema* 140, 156-163.
- JANKOWSKI, J., WARD, C.R., FRENCH, D. & GROVES, S., 2006. Mobility of trace elements from selected Australian fly ashes and its potential impact on aquatic ecosystems. *Australia, Fuel volume* 85, 243-256.
- JAYASINGHE, G. Y., TOKASHIKI, Y., KITOU, M. & KINJO, K., 2009. Coal fly ash-based synthetic aggregates as potential alternative container substrates for ornamentals. *Journal of Plant Nutrition and Soil Science* 000, 1-9.
- JIN, X., WANG, S., PANG, Y. & WU, F.C., 2006. Phosphorus fractions and the effect of pH on the phosphorus release of the sediments from different trophic areas in Taihu Lake, China. *Environmental pollution* 139, 288-295.
- JUNKINS, R., DEENY, K. & ECKHOFF, T., 1983. The activated sludge process: Fundamentals of operation. *Butterworth publishers, Roy F. Weston, Inc.* 53, 68 & 71.
- KATALAMBULA, H. & GUPTA, R., 2009. Low-grade coals: a review of some prospective upgrading technologies. *Energy and Fuels* 23, 3392-3405.
- KEEN, G.A. & PROSSER, J. I., 1987. Interrelationship between pH and surface growth of nitro bacter. *Soil Biology and Biochemistry.* 19, 665-6-672.
- KIEBER, R.J., LONG, M. S. & WILLEY, J.D., 2005. Factors Influencing Nitrogen Speciation in Coastal Rainwater. *Journal of Atmospheric Chemistry* 52, 81-99.
- KLEBER, M. & JOHNSON, M.G., 2010. Advances in Understanding the Molecular Structure of Soil Organic Matter : Implications for Interactions in the Environment. *Advances in Agronomy*, 106, 77 - 142.
- KOLAHCHI, Z. & JALALI, M., 2007. Effect of water quality on the leaching of potassium from sandy soil. *Journal of Arid Environments* 68, 624-639.
- KOPSICK, D.A. & ANGINO, E.E., 1981. Effect of leachate solutions from fly and bottom ash

- on ground water quality. Department of Geology, University of Kansas, Lawrence, KS 66044 (USA). *Journal of Hydrology* 54, 341-356.
- KOPTTKE, P.M., SO, H.B. & MENZIES, N.W., 2006. Effect of ionic strength and clay mineralogy on Na-Ca exchange and the SAR-ESP relationship. *European Journal of Soil Science* 57, 626-633.
- KUMP, L.R., BRANTLEY, S.L. & ARTHUR, M.A., 2000. chemical weathering, atmospheric CO₂, and climate. *Annual Reviews of Earth Planet Science* 28, 611-67.
- LAL, R. & SHUKLA, M.K., 2004. Basic definitions and concepts: Soil components and phases. pp. 15-25. *In: Principles of Soil physics*. Marcel Dekker, Inc. USA.
- LAMY, E., LASSABATERE, L., BECHET, B. & ANDRIEU, H., 2009. Modeling the influence of an artificial macropore in sandy columns on flow and solute transfer. *Journal of Hydrology* 376, 392-402.
- LEIJ, F.J. & VAN GENUCHTEN, M.T., 2002. Solute transport. p 189-248. *In: Warrick, A.W. (Ed.), Soil Physics Companion*. CRC Press, Boca Raton, FL.
- LEWIS, J. & SJOSTRÖM, J., 2010. Optimizing the experimental design of soil columns in saturated and unsaturated transport experiments. *Journal of Contaminant Hydrology* 2-13.
- LI, Z. & SHUMAN, L.M., 1997. Mobility of Zn, Cd and Pb in soils as affected by poultry litter extract-1 leaching in soils. *Environmental pollution* 95, 219-226.
- LINDSAY, W.L. 1979. Chemical equilibria in soils. John Wiley & Sons, New York.
- LOUBSER, M. & VERRYIN, S., 2008. Combining XRF and XRD analyses and sample preparation to solve mineralogical problems. *South African Journal of Geology* 111, 229-238.
- MAGESAN, G.N., VOGELER, I., CLOTHIER, B.E., GREEN, S.R. & LEE, R., 2003. Solute movement through an allophanic soil. *Journal of Environmental Quality* 32, 2325-2333.
- MAHLABA, J.S., KEARSLY, E.P. & KRUGER, R.A., 2011. Physical, chemical and mineralogical characterisation of hydraulically disposed fine coal ash from SASOL Synfuels. *Fuel* 90, 2491-2500.
- MAHMOOD-UL-HASSAN, M., AKHTAR, M.S. & NABI, G. 2008. Boron and zinc transport Through intact columns of calcareous soils. *Pedosphere* 18, 524-532.
- MAITI, S.S., MUKHOPADHYAY, M., GUPTA, S.K. & BARNEJEE, S.K., 1990. Evaluation of

- fly ash as a useful material in agriculture. *Journal of Indian Society of Soil Science* 38, 342-344
- MALI, N., URBANC, J. & LEIS, A., 2007. Tracing of water movement through the unsaturated zone of a coarse gravel aquifer by means of dye and deuterated water. *Environmental Geology* 51, 1401–1412.
- MARX, C.J., ALEXANDER, W.V., JOHANNES, W.G. & STEINBACH-KANE, S., 2004. A technical and financial review of sewage sludge treatment technologies. *Water Research Commission*. Report No. 1240/1/04.
- MATJIE, R.H., LI, Z., WARD, C.R. & FRENCH, D., (2008). Chemical composition of glass and crystalline phases in coarse coal gasification ash. *Fuel* 87, 857-869.
- MATSCHEI, T., LOTHENBACH, B. & GLASSER F.P., 2007. Thermodynamic properties of portlandcement hydrates in the system CaO–Al₂O₃–SiO₂–CaSO₄–CaCO₃–H₂O. *Cement Concrete Resource* 37, 1379–410.
- M_CBRIDE, 1994. Secondary mineral formation. pp218-222. In: Environmental chemistry of soils. Oxford University Press, Inc. USA.
- M_CCONNELL, D., 1998. Weathering and Soils. Natural Science Geology. University of Akron. pp 1-8.
- MICHEL, K., HERRMANN, S., LUDWIG, B., 2010. Modeling chemical and biological reactions during unsaturated flow in silty arable soils. *Geoderma* 156, 293-301.
- MENGEL, K., KIRKBY, E.A., KOSEGARTEN, H. & APPEL, T., 2001. Calcium. p.455-480. In: Principles of plant nutrition. 5th edn, Kluwer Academic Publishers, Netherlands. plants. *New phytologist*. 141, 1-26.
- MERRICK, D., 1984. Coal combustion and conversion technology. p 46, 101, 102, 103, 125, 325 & 328. National Coal Board, Coal Research Establishment, Stoke Orchard Cheltenham. Machmillan publishers.
- MIKKELSEN, R., 2010. Soil and fertilizer magnesium. *Better Crops* 94, 26-28.
- MOLDES, A., CENDON Y. & BARRAL M.T., 2007. Evaluation of municipal solid waste compost as a plant growing media component, by applying mixture design. *Bioresource Technology* 98, 3069-3075.
- MØRKVED, P.T., DÖRSCH, P. & BAKKEN, L.R., 2007. The NO₂ product of nitrification and its dependence on long-term changes in soil pH. *Soil Biology and Biochemistry* 39, 2048-2057.

- MULDER, J. & CRESSER, M.S., 1994 (EDs). Soil and soil solution chemistry. p 108 – 131.
In: Biogeochemistry of Small Catchment: a tool for Environmental research. John Willey & Sons Ltd.
- MURASHKINA, M.A., SOUTHARD, R.J. & PETTYGROVE, G.S., 2007. Silt and fine sand fractions dominate K fixation in soils derived from granite alluvium of the San Joaquin Valley, California. *Geoderma* 141, 283-293.
- NUR HANANI, M., CHE FAUZIAH, I., SAMSURI, A.W. & ZAUYAH, S., 2010. Formulation of coal fly ash and sewage sludge mixtures to reduce impacts on the environment when used as soil ameliorant for acidic tropical soils. *Malaysian Journal of Soil Science* 14, 53-70.
- OSWALD, S., KINZELBACH, W., GREINER, A. & BRIX, G., 1997. Observation of flow and Transport processes in artificial porous media via magnetic resonance imaging in three dimensions. *Geoderma* 80, 417–429.
- PELTOVUORI, T., UUSITALO, R. & KAUPPILA, T., 2002. Phosphorus reserves and apparent phosphorus saturation in four weekly developed cultivated pedons. *Geoderma* 110, 35-47.
- PIETRI, J.C.A. & BROOKES, P.C., 2008. Nitrogen mineralization along a pH gradient of a silty loam UK soil. *Soil Biology and Biochemistry* 40, 797-802.
- PIZZEGHELLO, D., BERTI, A., NARDI, S. & MORARI, F., 2011. Phosphorus forms and P-sorption properties in three alkaline soils after long-term mineral and manure applications in north-eastern Italy. *Agriculture Systems and Environment* 141, 58–66.
- PLUMMER, M.A., HULL, L.C. & FOX, D.T., 2004. Transport of carbon-14 in a large unsaturated soil column. *Vadose Zone Journal* 3, 109–121.
- POWELSON, D.K. & MILLS, A.L., 2001. Transport of Escherichia coli in sand columns with constant and changing water contents. *Journal of Environmental Quality* 30, 238–245.
- PRASAD R. & POWER J.K., 1997. Soil Fertility Management for Suitable Agriculture. *Lewis Publishers*. Pp 95, 100, 101.
- QADIR, M., NOBLE, A.D., OSTER, J.D., SCHUBERT, S. & GHAFOR, A., 2005. Driving forces for sodium removal during phytoremediation of calcareous sodic and saline-sodic soils: a review. *Soil Use and management* 21, 173-180.
- QUEROL, X., MORENO, N., UMANA, J.C., ALASTUEY, A., HERNANDEZ, E., LOPEZ-

- SOLER, A. & PLANA, F., 2002. Synthesis of zeolites from coal fly ash: an overview. *International Journal of Coal Geology* 50, 413-423.
- RADCLIFFE, DE & ŠIMŮNEK, J., 2010. Soil solid phase *In: Soil physics with hydrous, modeling and applications*. p 1-3. CRC Press, Taylor and Francis Group, USA.
- RAHMATULLA & MENGEL, K., 2000. Potassium release from mineral structures by H⁺ ion resin. *Geoderma* 96, 291-305.
- RAHNEMAIE, R., HIEMSTRA, T., & VAN RIEMSDIJK, W.H., 2006. Inner and outer sphere complexation of ions at the goethite-solution interface. *Journal of Colloid and Interface Science* 297, 379-388.
- RASHIDI, M. & SEILSEPOUR, M., 2008. Modeling of soil cation exchange capacity based on soil organic carbon. *ARPN Journal of Agricultural and Biological Science* 3, 41-45.
- RECHCIGL, E.J., 1995. Soil amendments and environmental quality. p 327. Lewis publishers. Department of Biotechnology and environmental sciences, Thapar Institute of engineering and Technology, Deemed University, Patiala 147004, Punjab, India. *Biosource Technology* 97.
- REDDY, K.R., D NGELO, E.M. & HARRIS, W.G., 2000. Biogeochemistry of wet lands. PP 89-119. *In: CRC Press Handbook of Soil Science*. University of Florida, USA.
- REINER, D., 2006. Problems in CEC determination of calcareous clayey sediments using the ammonium acetate method. *Journal of plant nutrition and soil science* 169, 330-334.
- REYNOLDS, K., KRUGER, R. & RETHMAN, N., 2000. The manufacture and evaluation of an artificial soil (SLASH) prepared from fly ash and sewage sludge. pp 1-8. *In: International ash utilization symposium, Center for Applied Energy Research, University of Kentucky, USA.*
- ROSS, D.S. & KETTERINGS, Q., 2011. Recommended methods for determining cation exchange capacity. Pp 62-67. *In: Recommended soil testing procedures for the Northeastern United States. Cooperative Bulletin, No. 493, USA.*
- RYAN, B., 1997. a review of sulphur in coal: with specific reference to the telkwa deposit, north-western british columbia. *Geological Fieldwork* 29, 1-22.
- SAIKIA, N., KATO, S. & KOJIMA, T., 2006. Compositions and leaching behaviours of combustion residues. *Fuel* 85, 264-267
- SAWHNEY, B.L., 1972. Selective sorption and fixation of cations by clay minerals: a review.

- Clays and Clay Minerals* 20, 93-100.
- SCHWAB, A.P., ZHU, D.S. & BANKS, M.K., 2008. Influence of organic acids on the transport of heavy metals in soil. *Chemosphere* 72, 986-994.
- SENTENAC, P., LYNCH, R. & BOLTON, M., 2001. Measurement of the side-wall boundary effect in soil columns using fibre-optics sensing. *International Journal of Physical Modelling in Geotechnics* 4, 35–41.
- SERNA, M.D. & POMARES, F., 1992. Nitrogen mineralization of sludge amended soil. *Bioresource Technology* 39, 285-290.
- SHAMMAS, N.K., 1986. Interaction of temperature, pH and biomass on the nitrification process. *Journal (WaterPollution Control Federation)* 58, 1.
- SHAN, Y., YANG, L., YAN, T. & WANG, J., 2005. Downward movement of phosphorus in paddy soil installed in large-scale monolith lysimeters. *Agriculture, Ecosystems and Environment* 111, 270-278.
- SHARIATMADARI, H., SHIRVANI, M. & JAFARI, A., 2006. Phosphorus release kinetics and availability in calcareous soils of selected arid and semiarid toposequences. *Geoderma* 132, 261–272.
- SHARMA, A., JALALI, V.K. & ARORA, S., 2010. Non-exchangeable potassium release and its removal in foot-hill soils of North-West Himalayas. *Catena* 82, 112-117.
- SIERRA, J., 2002. Nitrogen mineralization and nitrification in a tropical soil: effects of fluctuating temperature conditions. *Soil Biology and Biochemistry* 34, 1219-1226.
- SIMONSSON, M., HILLIER, S. & ÖRBORN, I., 2009. Changes in clay minerals and potassium fixation capacity as a result of release and fixation of potassium in long-term field experiments. *Geoderma* 151, 109-120.
- SINGH, N., KLOEPPEL, H. & KLEIN, W., 2002. Movement of metolachlor and terbuthylazine in core and packed columns. *Chemosphere* 47, 409-415.
- SINGH, R.P. & AGRAWAL, M., 2008. Potential benefits and risks of land application of sewage sludge. *Wastes Management* 28, 347-358.
- SINGH, D., McLAREN, R.G. & CAMERON, K.C., 2006. Zinc sorption-desorption by soils: effect of concentration and length of contact period. *Geoderma* 137, 117-125.
- SMITH, K.A. & MULLINS, C.E., 1991. Soil analysis: Physical methods. Pp 284-286. Marcel

- Dekker, Inc. United States of America.
- SNYMAN, H.G. & VAN DER WAALS, J.E., 2004. Sludge disposal in South Africa. p 1. *In:* and field scale evaluation of agricultural use of sewage sludge. *Water Research Commission*, South Africa.
- SNYMAN, H.G., & HERSELMAN, J.E. 2009. Guidelines for the utilization and disposal of wastewater sludge: Selection of management options. *Water Research Commission*. Report TT262/09,
- SOIL SCIENCE SOCIETY OF SOUTH AFRICA, 1990. Handbook of standard soil testing methods for advisory purposes. *The non-affiliated soil analysis work committee*. ISBN0620148004.
- SPOSITO, G., SCHAUMBERG, G.D., PERKINS, T.G., AND HOLTZCLAW, K.M., 1978. Investigation of Fulvic Acid Extracted from Sewage Sludge Using Carbon- 13 and Proton NMR Spectroscopy. *Environmental Science & Technology*, 12 (8), 932 – 934.
- SPARKS, D.L., 2003. Sorption phenomena on soils. pp 133 – 183. *In:* Environmental soil chemistry, 2nd edn, Elsevier Science, United States of America.
- STEINER, L.D., BIDWELL, V.J., DI, H.J., CAMERON, K.C. & NORTHCOTT, G.L., 2010. Transport and modeling of estrogenic hormones in a dairy farm effluent through undisturbed soil lysimeters. *Environmental Science of Technology* 44, 2341-2347.
- TAN, K.H., 2005. Determination of soil nitrogen. pp 138-258. *In:* Soil sampling, preparation, and analysis. 2nd Ed. Taylor and Francis, USA.
- TAN, K.H., 1996. Cation exchange capacity determination. pp 114-134. *In:* Soil sampling, preparation and analysis. Marcel Dekker, Inc. New York, USA.
- TISHMACK, J.K. & BURNS, P.E., (2004) The chemistry and mineralogy of coal and coal combustion products. in *Energy, Waste and the Environment: A Geochemical Perspective*; Giere, R.; Stille P. Eds.; Special Publications 236; Geological Society: London, UK, 223-246.
- TORIDE, N., INOUE, M. & LEIJ, F.J., 2003. Hydrodynamic dispersion in an unsaturated dune sand. *Soil Science Society of America Journal* 67, 703–712.
- TRIVEDI, A. & SUD, V. K., 2002. Grain characteristics and engineering properties of coal ash. *C_ Springer-Verlag . Granular Matter* 4, 93–101.
- TSAI, S. C., 1982. Fundamentals of coal beneficiation and utilization. *Coal Science and*

- technology 2. *Elsevier Scientific Publishing Company* 17.
- VAN DER SLOOT, HA, ZONDERHUIS, J. & VAN STIGT, C.A., 1981. Trace elements in coal and ash. *Energiespectrum* 5, 150-162.
- VEERESH, H., TRIPATHY, S., CHAUDHURI, D., GHOSH, B.C., HART, B.R. & POWELL, M.A., 2002. Changes in physical and chemical properties of three soil types in India as a result of amendment with fly ash and sewage sludge. *Environmental Geology* 43, 513-520.
- VERNIMMEN, R.R.E., VERHOEF, H.A., VERSTRATEN, J.M., BRUINJZEEL, L.A., KLOMP, N.S., ZOOMER, H.R. & WARTENBERGH, P.E., 2007. Nitrogen mineralization, nitrification and denitrification potential in contrasting low land rain forest types in Central Kalimantan, Indonesia. *Soil Biology and Biochemistry* 39, 2992-3003.
- VOEGELIN, A., BARMETTLER, K. & KRETZSCHMAR, R., 2003. Heavy metal release from contaminated soils: comparison of leaching and batch extraction results. *Journal of Environmental Quality* 32, 865-875.
- VOGELER, I., 2001. Copper and calcium transport through an unsaturated soil column. *Journal of Environmental Quality* 30, 927-933.
- WANG, M., 1997. Land application of sewage sludge in China. *The Science of the Total Environment* 197, 149-160.
- WANG, L.K. & WANG, M.H.S., 1992. Handbook of Industrial waste treatment. p 2 & 8. Marcel Dekker, inc. Volume 1.
- WANG, T., LI, M. & TENG, S., 2009. Bridging the gap between batch and column experiments: a case study of Cs adsorption on granite. *Journal of Hazardous Materials* 161, 409-415.
- WEI, X., HAO, M., SHAO, M. & GALE, W.J., 2006. Changes in soil properties and the availability of soil micronutrients after 18 years of cropping and fertilization. *Soil and Tillage Research* 91, 120-130.
- WHITE, J.G. & ZASOSKI, R.J., 1999. Mapping soil micronutrients. *Field Crops Research* 60, 11-26.
- WONG, J.W.C., 1995. The production of artificial soil mix from coal fly ash and sewage sludge. *Environmental Technology* 16, 741-751.
- WONG, J.W.C., & SU, D.C., 1997. Reutilization of coal fly ash and sewage sludge as an

- artificial soil-mix: effects of preincubation on soil pyhysico-chemical properties. *Biosource technology* 59, 97-102.
- WOOLARD, C.D., STRONG, J. & ERASMUS, C.R., 2002. Evaluation of the use of modified coal ash as apotential sorbent for organic waste streams. *Applied Geochemistry* 17, 1159-1164.
- YUAN, Y.Z., SHENG, C.F., HUI, Z.D., QIONG, Z. & SHENG, C.G., 2008. Soil inorganic nitrogen and microbial biomass carbon and nitrogen under pine plantations in Zhanggutai sandy soil. *Pedosphere* 18, 775-784.
- ZEVENBERGEN, C., BRADLY, J.P., VAN REEUWIJK, L.P. SHYAM, A.K., HJELMAR, O. & COMANS, R.J.N., 1999. Clay formation and metal fixation during weathering of coal fly ash. *Environmental Science and Technology* 33, 3405-3409.
- ZHAO, L.Y.L., SCHULIN, R. & NOWACK, B., 2009. Cu and Zn mobilization in soil columns percolated by different irrigation solutions. *Environmental pollution* 157, 823-833.

11 Appendices

Appendix A: Pore solution pH

Mixture	Eluv. cycle 1	Eluv. cycle 2	Eluv. cycle 3	Eluv. cycle 4	Eluv. cycle 5	Eluv. cycle 6	Eluv. cycle 7	Eluv. cycle 8	Eluv. cycle 9	Eluv. cycle 10
1	11.32	10.31	10.44	10.31	10.9	7.94	9.2	7.68	9.16	9.59
2	11.52	10.31	10.13	10.07	10.55	7.82	8.34	7.68	9.33	9.23
3	11.58	9.4	9.91	10.02	10.25	7.92	9.12	7.76	9.34	9.04
4	11.47	9.41	10.69	10.91	10.85	7.79	7.72	7.68	9.58	9.42
5	11.01	8.96	9.88	9.91	10.21	7.83	7.63	7.81	9.26	9.01
6	11.55	10.16	11.2	11.48	11.1	7.82	7.88	7.68	10.65	10.26
7	11.64	11.13	11.3	11.47	11.32	7.82	7.97	7.76	10.57	10.32
8	10.84	8	8.99	9.07	9.14	7.65	7.7	7.6	8.78	8.35
9	11.43	10.47	9.64	9.57	9.98	7.9	8.92	7.68	9.01	8.84
10	11.67	10.31	9.71	9.66	10.06	7.57	7.55	8.87	9.15	8.96
11	11.73	10.97	10.11	10.03	10.28	8.05	9.79	7.52	9.45	8.95
12	9.42	8.61	8.88	8.75	8.74	7.99	7.8	7.95	7.96	8.22
13	9.55	8.38	8.87	8.87	8.87	7.82	7.72	7.76	8.06	7.94
14	8.26	8.11	9.11	8.83	9.13	7.8	7.72	7.63	7.96	8.03
15	8.34	7.83	9.22	9.16	9.14	7.82	8.7	7.7	8.53	8.21
16	9.83	8	8.56	8.58	8.55	7.99	7.68	7.75	8.03	8.2
17	9.62	7.77	8.56	8.45	8.58	7.89	7.7	7.74	7.88	8.26
18	9.35	8.1	8.45	8.55	8.82	7.89	7.68	7.75	7.56	7.94
19	9.5	8.02	8.25	8.41	8.79	8.41	7.72	7.78	7.86	7.87
20	9	8.02	8.51	8.25	8.79	8	7.63	7.7	7.88	7.88
21	9.49	8.18	8.72	8.88	8.84	7.78	7.63	7.67	7.97	8.12
22	9.76	8.02	8.3	8.41	8.28	7.73	7.63	7.82	7.88	8.08
23	9.79	8	8.47	8.45	7.44	7.82	7.63	7.77	7.93	8.04
24	9.79	7.89	8.42	8.46	8.55	8.24	8.19	8.08	7.62	7.98
25	9.54	8.09	8.47	8.53	6.95	7.65	7.72	7.75	7.8	7.89
26	9.79	8.03	8.56	8.58	8.55	6.66	7.73	7.75	7.87	8.08
27	9.96	8.08	8.56	8.6	8.55	8.24	8.34	8.18	8.31	7.96
28	9.98	7.84	8.64	8.68	8.63	8.35	8.32	7.65	7.88	7.96
29	9.76	8.18	8.66	8.67	8.63	8.24	7.72	7.81	7.88	7.8
30	9.93	8.02	8.86	8.82	8.78	8.3	8.29	8.27	7.95	8.07
31	9.93	7.73	8.4	8.5	8.6	8.34	8.3	8.33	8.32	7.95
32	10.18	8.04	8.38	8.58	8.63	8.46	8.59	8.21	8.39	7.8
33	9.96	7.89	8.47	8.75	8.72	8.48	8.47	7.64	7.74	7.81
34	9.93	7.92	8.47	8.67	8.74	8.49	8.48	8.34	8.41	7.71
35	9.93	8.96	8.64	8.82	8.85	8.57	8.79	8.36	8.66	8.04
36	9.75	7.82	8.69	8.82	8.83	8.54	8.55	8.38	8.66	7.79
37	9.76	8.21	8.75	7.74	7.7	7.89	7.7	7.68	7.71	7.71
38	9.54	8.35	8.86	8.82	8.79	8.5	8.33	7.52	7.82	7.99
39	10.01	8.6	8.47	8.62	8.63	8.61	8.34	7.58	7.57	7.67
40	9.96	8.48	8.5	6.92	7.6	7.91	7.72	7.76	7.52	7.71
41	9.88	7.93	8.56	8.77	6.95	7.63	7.55	7.67	7.7	7.71
42	9.8	7.89	8.62	8.78	8.87	8.69	8.65	7.48	7.64	7.66
43	9.55	8.33	8.67	7.4	7.72	7.9	7.72	7.74	7.61	7.59
44	9.67	8.1	8.74	8.63	7.79	7.87	7.7	7.76	7.4	7.63
45	9.59	8.27	8.81	8.89	8.55	7.9	7.93	7.93	7.54	7.83
46	9.76	8.38	8.64	8.72	8.87	8.66	8.64	8.39	7.49	7.83
47	9.59	7.85	8.25	8.58	8.72	8.53	8.47	8.54	7.71	7.85
48	9.58	7.98	8.37	8.67	8.51	7.56	7.46	7.73	7.47	7.66
49	9.59	8.2	8.3	8.63	8.69	8.5	8.64	8.34	7.5	7.55
50	9.49	8.21	8.39	8.61	8.73	8.69	8.39	7.98	7.42	7.71
51	9.36	7.87	7.99	8.53	8.72	8.74	8.71	8.56	8.74	7.79

Appendix B: Pore solution electrical conductivity (EC) in mSm^{-1}

Mixture	Eluv. cycle 1	Eluv. cycle 2	Eluv. cycle 3	Eluv. cycle 4	Eluv. cycle 5	Eluv. cycle 6	Eluv. cycle 7	Eluv. cycle 8	Eluv. cycle 9	Eluv. cycle 10
1	580	505	366	318	282	134	138	106	100	118
2	570	504	411	354	272	127	145	98	112	122
3	606	509	401	320	249	111	123	99	92	105
4	557	492	332	269	227	105	115	92	102	111
5	533	477	328	293	223	127	123	113	102	124
6	596	350	281	259	197	98	114	95	97	160
7	585	325	261	241	210	95	114	76	97	137
8	335	446	336	289	223	117	121	114	99	122
9	470	427	362	307	221	103	125	104	90.4	117
10	537	378	335	254	174	85	107	84	75	102
11	527	435	309	186	145	78	95	71	60	88
12	319	605	531	423	305	146	166	120	101	140
13	95	633	486	426	293	158	174	163	129	212
14	309	557	425	353	246	135	172	145	108	135
15	339	487	429	319	226	140	153	144	107	132
16	505	580	503	403	298	167	192	138	118	116
17	520	516	490	389	303	194	204	174	133	122
18	526	336	312	297	239	197	207	165	155	139
19	535	359	325	303	243	173	173	155	131	134
20	549	488	446	366	283	133	191	165	147	146
21	621	361	458	302	265	158	212	159	140	203
22	455	672	677	702	606	425	424	308	253	222
23	451	602	636	630	617	335	381	291	224	209
24	458	550	482	631	509	368	348	250	241	224
25	402	622	467	535	566	396	384	248	214	214
26	427	681	599	587	483	335	389	256	247	178
27	504	741	643	583	466	133	289	235	184	194
28	471	678	818	667	501	249	257	256	209	154
29	535	903	717	579	432	259	368	252	191	324
30	540	865	770	552	358	193	172	128	148	148
31	475	580	753	723	657	397	338	254	255	268
32	486	499	742	775	687	396	331	295	230	306
33	474	545	815	736	586	333	331	391	332	294
34	526	614	875	878	730	337	376	288	243	306
35	505	653	1107	920	721	341	311	260	206	227
36	443	708	1015	813	622	284	312	228	178	302
37	499	711	1000	915	681	322	279	239	221	197
38	463	868	960	764	601	359	341	377	258	191
39	511	544	752	821	725	408	403	523	383	319
40	504	542	923	925	756	428	419	351	349	410
41	527	580	815	793	868	415	444	364	312	294
42	551	589	935	848	749	366	365	518	330	302
43	573	563	932	858	617	316	338	275	231	415
44	570	637	903	829	799	411	432	370	298	274
45	533	717	916	832	664	345	315	255	248	243
46	536	238	622	805	697	350	373	260	435	284
47	549	844	744	602	543	253	242	249	338	287
48	549	604	901	818	708	507	465	342	255	329
49	559	500	847	806	715	423	346	323	373	307
50	590	640	751	760	623	321	346	296	266	340
51	622	723	528	497	445	270	282	204	157	220

Appendix C: Measured total elements from MINTEK in fine ash (FA), gasification ash (GA) and sludge (SL) using acid digestion

Mixtures	Reps	Cu (ppm)	Mn (ppm)	Zn (ppm)	Mg (%)	Ca (%)	Fe (%)	P(%)	N (%)	K (%)	Na (%)
FA	1	56	838	27.5	1.57	5.36	12	0.305	2.7123	0.01765	0.37
FA	2	51	830	25	1.35	5.06	12	0.27	4.0609	0.0171	0.39
FA	3	48	774	25	1.33	5.01	11.9	0.41	2.9467	0.0178	0.42
FA50%GA50 %	1	55	549	19	1.41	5.81	7.45	0.58	5.2948	0.0184	0.36
FA50%GA50 %	2	50	561	19	1.46	6.04	7.31	0.39	3.9595	0.0186	0.39
FA50%GA50 %	3	48	573	24	1.42	5.77	7.455	0.29	4.5789	0.0182	0.365
GA	1	65	290	16	1.52	8.17	2.92	0.34	6.264	0.0169	0.33
GA	2	59	274	10	1.5	6.56	2.83	0.27	2.8771	0.0171	0.32
GA	3	51	277	11	1.5	6.94	2.88	0.38	3.3438	0.0174	0.36
FA40%GA40%SL20%	1	43	486	53	1.17	4.75	5.99	0.4	9.8399	0.016	0.3
FA40%GA40%SL20%	2	43.5	454	49.5	1.19	4.8	6.155	0.325	7.08105	0.0163	0.31
FA40%GA40%SL20%	3	46	427.5	50	1.165	4.905	5.905	0.325	1.1823	0.375	0.325
FA50%SL50%	1	47	420	100	0.83	2.87	6.16	0.29	2.0767	0.27	0.29
FA50%SL50%	2	33	420	100	0.71	2.91	6.02	0.3	3.8165	0.26	0.26
FA50%SL50%	3	36	412	93	0.8	2.86	6.07	0.36	4.8036	0.25	0.25
GA50%SL50%	1	30	161	95	0.78	3.62	1.86	0.27	8.9584	0.29	0.21
GA50%SL50%	2	28	157	90	0.85	3.79	1.78	0.32	9.8416	0.23	0.195
GA50%SL50%	3	28	159	96	0.89	3.68	1.94	0.33	6.9969	0.28	0.21
SL	1	29	161	99	0.26	0.62	0.6	0.4	5.9584	0.12	0.0962
SL	2	12	54	173	0.28	0.63	0.59	0.48	8.1896	0.13	0.11
SL	3	13.5	56	168	0.245	0.5	0.615	0.51	8.16865	0.0618	0.0543

Appendix D: Total cumulative soluble elements measured using ICP-OES in mixtures for all 10 eluviation cycles

Mixture	Ca mmol kg ⁻¹	Cu mmol kg ⁻¹	Fe mmol kg ⁻¹	K mmol kg ⁻¹	Mg mmol kg ⁻¹	Mn mmol kg ⁻¹	Na mmol kg ⁻¹	P mmol kg ⁻¹	Zn mmol kg ⁻¹
1	7.8060	0.0004	0.0004	4.8087	0.9919	0.0006	24.6897	0.0104	0.0002
2	8.1490	0.0003	0.0004	4.4760	6.9701	0.0006	19.8204	0.0190	0.0003
3	10.0784	0.0002	0.0004	4.8843	5.7425	0.0006	20.9455	0.0083	0.0003
4	9.6932	0.0001	0.0005	5.4503	4.3449	0.0007	20.2649	0.0072	0.0002
5	12.2579	0.0001	0.0005	6.2407	3.3251	0.0007	22.4576	0.0069	0.0002
6	10.6593	0.0002	0.0005	8.1559	3.3461	0.0008	23.9983	0.0076	0.0002
7	8.2095	0.0002	0.0005	9.5356	3.6612	0.0008	25.3891	0.0088	0.0006
8	29.5518	0.0002	0.0006	4.8209	7.8070	0.0008	15.4367	0.0033	0.0004
9	27.0021	0.0002	0.0005	5.4760	5.9381	0.0008	16.8466	0.0047	0.0002
10	30.4592	0.0002	0.0005	6.3106	1.3830	0.0007	20.2098	0.0051	0.0003
11	26.8558	0.0002	0.0006	6.5022	1.6808	0.0008	18.8935	0.0049	0.0002
12	22.6861	0.0002	0.0009	4.3261	34.1464	0.0008	13.9323	0.1054	0.0005
13	29.9250	0.0002	0.0009	4.8471	24.1297	0.0010	16.7079	0.0857	0.0006
14	18.2036	0.0003	0.0007	4.2585	13.5624	0.0011	15.3399	0.0566	0.0007
15	19.7985	0.0008	0.0003	5.2658	10.3249	0.0008	18.3980	0.0654	0.0011
16	25.0143	0.0005	0.0003	4.7150	23.5449	0.0012	19.6904	0.0917	0.0006
17	25.2106	0.0009	0.0003	5.0341	13.9890	0.0008	21.5164	0.0656	0.0004
18	19.9113	0.0006	0.0002	4.5722	11.2375	0.0007	20.0312	0.0627	0.0007
19	16.4921	0.0006	0.0002	3.9379	7.7588	0.0006	17.6981	0.0556	0.0003
20	17.3789	0.0008	0.0003	4.1518	10.5319	0.0006	20.4814	0.0620	0.0003
21	18.2060	0.0010	0.0002	4.3628	7.8534	0.0006	22.3534	0.0546	0.0002
22	25.1530	0.0008	0.0019	3.5742	41.6879	0.0050	15.7962	0.1398	0.0006
23	28.6469	0.0007	0.0032	3.9783	44.3898	0.0054	17.3006	0.1398	0.0007
24	18.5004	0.0006	0.0021	3.9534	33.5109	0.0032	14.6307	0.1357	0.0007
25	28.6074	0.0006	0.0024	3.8310	49.2721	0.0051	15.2291	0.1649	0.0008
26	18.9340	0.0003	0.0031	3.8645	36.9345	0.0028	11.4130	0.1454	0.0010
27	21.2327	0.0006	0.0036	4.9599	40.8249	0.0029	16.4055	0.1758	0.0017
28	24.4149	0.0005	0.0044	4.7680	44.5508	0.0030	16.3095	0.1881	0.0013
29	28.6317	0.0004	0.0047	4.7437	54.8229	0.0035	15.0943	0.1986	0.0011
30	24.6137	0.0004	0.0073	5.3147	48.1938	0.0025	13.6926	0.3274	0.0012
31	15.3847	0.0006	0.0042	3.1560	31.7401	0.0039	9.8192	0.1389	0.0007
32	16.2019	0.0004	0.0037	3.6653	35.1804	0.0041	10.7307	0.1547	0.0014
33	26.9659	0.0006	0.0066	4.2845	44.4135	0.0057	12.9906	0.2140	0.0016
34	20.3186	0.0006	0.0063	4.2468	37.0575	0.0039	10.9439	0.2189	0.0014
35	17.9292	0.0010	0.0132	4.6873	34.4285	0.0042	11.5263	0.2974	0.0014
36	21.4116	0.0006	0.0106	5.3163	42.3056	0.0038	12.5686	0.3207	0.0024
37	46.8447	0.0003	0.0058	3.4205	63.8068	0.0091	11.3501	0.2823	0.0010
38	25.9789	0.0004	0.0175	4.5379	46.9731	0.0036	10.5724	0.4380	0.0017
39	26.9304	0.0004	0.0072	4.0387	38.3111	0.0059	11.0843	0.1938	0.0015
40	48.5279	0.0005	0.0049	3.9034	58.1855	0.0122	11.4782	0.2149	0.0024
41	41.9942	0.0004	0.0075	4.2638	55.2771	0.0089	11.0996	0.2316	0.0013
42	26.0284	0.0009	0.0172	4.6123	41.6713	0.0060	10.5840	0.3066	0.0021
43	52.5558	0.0004	0.0072	4.0158	68.0054	0.0127	10.7409	0.3200	0.0023
44	41.1304	0.0003	0.0113	4.1790	54.4596	0.0065	10.0263	0.4101	0.0011
45	30.3292	0.0004	0.0289	4.1110	44.9439	0.0050	8.7818	0.6600	0.0027
46	26.1032	0.0006	0.0184	5.4416	46.9974	0.0073	12.4823	0.3706	0.0015
47	29.5110	0.0009	0.0392	8.1936	53.0028	0.0099	12.0956	0.5282	0.0030
48	39.2006	0.0006	0.0265	5.0918	61.4238	0.0102	11.1673	0.4512	0.0031
49	24.7601	0.0007	0.0333	5.1982	43.8102	0.0073	9.8222	0.5931	0.0037
50	27.2636	0.0004	0.0255	4.4057	45.2009	0.0084	8.4366	0.5815	0.0031
51	21.8647	0.0010	0.0373	5.2589	38.2857	0.0063	7.9605	1.0574	0.0039

Appendix E: Total inorganic N in pore solution for ten eluviation cycles

Selected mixtures	Ammonium – N mg kg ⁻¹	Nitrate – N mg kg ⁻¹	Nitrite - N mg kg ⁻¹
1	4.79	0.00	9.43
6	4.10	0.00	8.12
11	3.60	0.00	7.11
12	3.98	0.00	6.50
17	4.57	0.00	8.14
21	5.25	0.00	9.24
22	5.88	1.12	7.63
26	5.06	0.49	6.93
30	4.51	2.32	4.16
31	6.66	4.66	3.76
35	5.78	8.53	2.25
38	5.17	3.33	4.12
39	7.59	4.48	5.85
42	6.73	8.48	4.59
45	5.83	4.03	6.10
46	8.76	7.65	5.03
48	7.76	8.56	8.06
51	6.76	6.67	1.91

Appendix F: CEC determination in leached and fresh mixtures using KCl, LiCl and NH₄OAc methods

Mixture	Replication	KCl on leached material	LiCl on leached material	Mixture	Replication	NH ₄ OAc leached material	NH ₄ OAc fresh material
		cmol _c kg ⁻¹	cmol _c kg ⁻¹			cmol _c kg ⁻¹	cmol _c kg ⁻¹
1	1	2.37	1.13	1	1	2.65	5.91
	2	2.46	1.27		2	3.28	7.40
	3	2.68	1.30		3	3.02	7.64
6	1	1.12	0.54	6	1	1.88	5.39
	2	1.92	0.45		2	2.58	5.51
	3	1.59	0.74		3	2.74	5.97
11	1	1.76	1.14	11	1	1.33	2.43
	2	1.78	1.19		2	2.15	2.27
	3	1.70	1.09		3	1.70	2.49
23	1	3.64	3.56	12	1	2.67	5.49
	2	3.87	4.10		2	2.30	5.57
	3	3.79	1.79		3	2.32	5.59
37	1	2.99	3.84	17	1	2.28	6.97
	2	3.22	5.44		2	2.66	7.89
	3	3.20	2.10		3	2.74	6.86
46	1	6.29	6.14	21	1	2.74	8.01
	2	6.26	6.62		2	3.54	9.19
	3	5.65	7.66		3	1.65	9.23
51	1	4.81	2.57	22	1	3.69	10.37
	2	3.97	7.11		2	3.32	11.11
	3	3.76	4.76		3	3.49	10.75
POA	1	2.16	4.19	26	1	2.05	8.18
	2	2.12	4.31		2	2.20	9.80
	3	2.06	4.39		3	2.42	9.62
NOA	1	1.23	3.49	30	1	2.63	8.99
	2	1.27	3.08		2	2.20	8.31
	3	0.98	3.15		3	2.73	7.60
KIOLINITE	1	2.83	5.65	31	1	3.51	13.96
	2	3.61	5.14		2	4.29	11.31
	3	3.09	5.65		3	3.78	13.50
ILLITE	1	8.99	19.38	35	1	2.98	12.89
	2	8.34	18.74		2	3.32	11.03
	3	5.99	16.04		3	3.30	13.22
				38	1	2.52	12.29
					2	2.58	11.60
					3	2.42	12.83
				39	1	4.13	16.92
					2	4.46	18.79
					3	4.12	18.09
				42	1	3.78	15.27
					2	3.37	15.15
					3	3.86	15.18
				45	1	3.09	13.40
					2	2.70	13.18
					3	3.25	14.62
				46	1	4.19	19.63
					2	4.64	19.28
					3	4.74	18.20
				48	1	4.56	19.40
					2	4.46	19.91
					3	4.06	17.83

Appendix F(continued)

Mixture	Replication	KCl on leached material	LiCl on leached material	Mixture	Replication	NH ₄ OA _e leached material	NH ₄ OA _e fresh material
				51	1	3.57	17.85
					2	3.11	18.36
					3	2.85	18.36
				POA	1	5.88	
					2	5.77	
					3	5.77	
				NOA	1	4.70	
					2	4.81	
					3	4.78	
				KAOLINITE	1	8.91	
					2	8.63	
					3	8.46	
				ILLITE	1	11.69	
					2	12.43	
					3	11.38	

Appendix G: ICP – OES theoretical and actual analytical ranges for each element and wavelengths used in the CEC analysis (Essington, 2004)

Element	Theoretical Wavelength (nm)	Theoretical Analytical ranges (mg L ⁻¹)	Actual Wavelengths (nm)	Actual Analytical ranges (mg L ⁻¹)
Li	670.8	0.0 – 3.0	670.8	0.0 – 10
K	766.5	0.4 – 100	766.5	0.0 – 150

MERCK chemicals used, their grades, concentrations and traceability in the determination of CEC

Chemical	Grade	Concentration/quantity	Catalog number
Li (standard)	CertiPUR [®]	1000 mg L ⁻¹	170223
K (standard)	CertiPUR [®]	1000 mg L ⁻¹	170230
Lithium Chloride (LiCl)	GR for analysis ACS, Reag. Ph Eur	0.1 kg	105679
Potassium Chloride (KCl)	GR for analysis ACS, Reag. Ph Eur	0.5 kg	104933
Magnesium Nitrate (MgNO ₃)	GR for analysis ACS, Reag. Ph Eur	0.5 kg	105853